AD-A135 244 MEASUREMENT OF SPINAL LOADS IN TWO MODIFIED ANTHROPOMORPHIC DUMMIES(U) SIMULA INC TEMPE AZ D H LAANANEN ET AL. 05 MAY 82 TR-82405 DAMD17-81-C-1175 1/2

UNCLASSIFIED F/G 5/5 NL

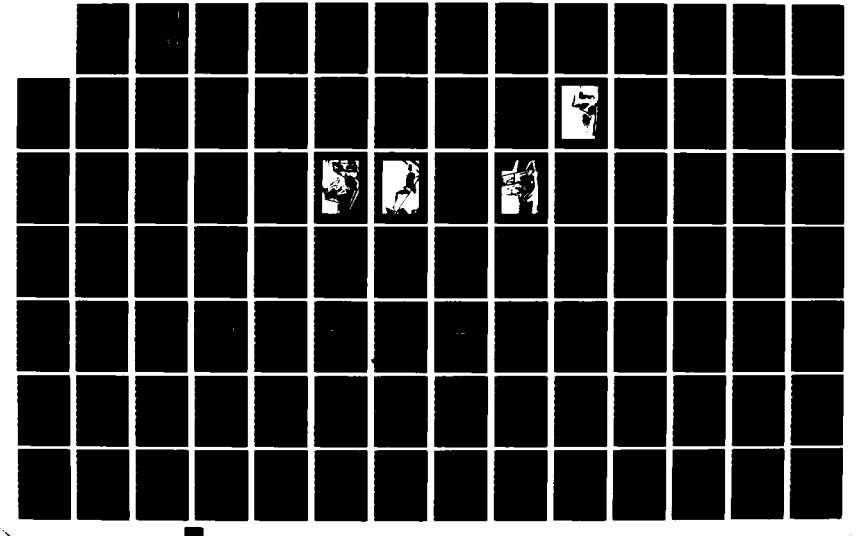

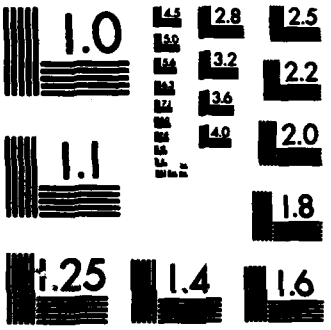

MICROCOPY RESOLUTION TEST CHART
NATIONAL BUREAU OF STANDARDS-1963-A

PHOTOGRAPH THIS SHEET

DTIC ACCESSION NUMBER

A135 244

LEVEL

II

INVENTORY

I

Rpt. No. TR-82405, Final 5 May '82

DOCUMENT IDENTIFICATION

Contract DAMD17-81-C-1175

DISTRIBUTION STATEMENT A

Approved for public release;
Distribution Unlimited

DISTRIBUTION STATEMENT

ACCESSION FOR	
NTIS GRA&I	☒
DTIC TAB	☐
UNANNOUNCED	☐
JUSTIFICATION	
BY	
DISTRIBUTION /	
AVAILABILITY CODES	
DIST	AVAIL AND/OR SPECIAL
A/1	

DISTRIBUTION STAMP

DTIC
ELECTE
DEC 1 1983
D

DATE ACCESSIONED

83 12 01 034

DATE RECEIVED IN DTIC

PHOTOGRAPH THIS SHEET AND RETURN TO DTIC-DDA-2

DOCUMENT PROCESSING SHEET

DTIC FORM OCT 79 70A

A135244

MEASUREMENT OF SPINAL LOADS IN TWO MODIFIED ANTHROPOMORPHIC DUMMIES

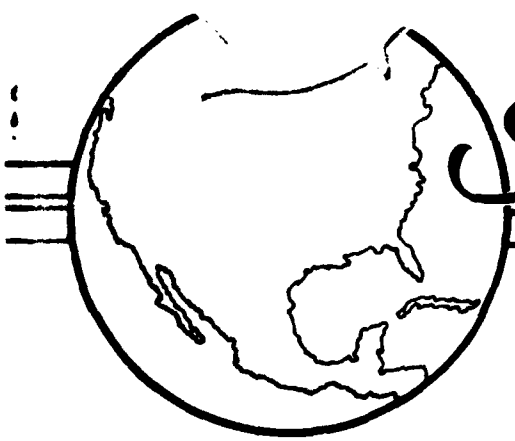

Simula Inc.

2223 SOUTH 48TH STREET
TEMPE, ARIZONA 85282
TELEPHONE (602) 894-2396

E-21

TR 82405

MEASUREMENT OF SPINAL LOADS IN TWO MODIFIED ANTHROPOMORPHIC DUMMIES

Contract DAMD17-81-C-1175
Final Report

David H. Laananen
and
Joseph W. Coltman

Prepared for:

U.S. Army Aeromedical Research Laboratory
Fort Rucker, Alabama 36362

Simula Inc.
2223 S. 48th Street
Tempe, Arizona 85282

May 5, 1982

CONTENTS

LIST OF ILLUSTRATIONS

LIST OF ILLUSTRATIONS (CONTD)

LIST OF ILLUSTRATIONS (CONTD)

1.0 INTRODUCTION

The new generation of U.S. Army helicopters possesses unprecedented crashworthiness, as pointed out in Reference 1. These aircraft are equipped with many crashworthy features, including seats designed to provide both efficient restraint in all loading directions and energy-absorbing stroke in the vertical, or $+G_z$, direction. The seats are designed to comply with existing criteria that were developed and documented in 1971 (References 2, 3, and 4). Although these seats are far superior to any prior systems, there are several areas of uncertainty in the design criteria that require additional research to enable further progress to be made in the hardware.

First, knowledge concerning human tolerance to $+G_z$ acceleration is extremely limited. In fact, little new information concerning human tolerance to acceleration in this direction has been developed in many years. Although extensive effort has been expended on the critical areas of human head and neck response (U.S. Navy) and the effects of restraint system variables on acceleration loads in the longitudinal, $-G_x$, and lateral, G_y, directions (U.S. Air Force), essentially no effort has been directed in this other very critical direction. The need for additional knowledge of $+G_z$ response is affirmed when it is considered that aircraft occupants can withstand the full 95th-percentile survivable crash acceleration conditions in the lateral and longitudinal directions with no energy absorption, only proper restraint (a complex problem when related to the head), but cannot tolerate the 95th-percentile vertical crash pulse without energy absorption.

The last program of significance to investigate the variables associated with vertical ($+G_z$) acceleration of aircraft occupants was sponsored by the U.S. Army Air Mobility Research and Development Laboratory, Fort Eustis, Virginia, (now the Applied Technology Laboratory) in 1969 and 1970. The results of this program are presented in Reference 5. The goal of this earlier program was to

evaluate the meager information available and to develop achievable criteria to guide the design of crashworthy crewseats for U.S. Army aviation. This task was accomplished, and the resulting criteria have now been in existence for the past ten years.

Techniques used for the design and evaluation of energy-absorbing seating systems are explained in detail in References 1, 2, 4, and 6; however, in summary, the Eiband human tolerance data with upper level ejection seat criteria superimposed (as presented in the Aircraft Crash Survival Design Guide, Reference 7) was taken as the upper limit of tolerable acceleration in the $+G_z$ direction. Tests and analyses were then conducted to establish the force level necessary on the vertical energy-absorption system to limit the acceleration excursions of the seat pan to magnitudes of less than 23 G for time durations in excess of 0.006 sec as directed by the tolerance data. The test results indicated that if the energy-absorbing mechanism were set for stroking at a force computed using a 14.5-G load factor, the desired result could be achieved. Test data supporting the conclusions of this analysis are presented in Reference 5.

In seat tests conducted during the ensuing years, a characteristic seat pan z-axis deceleration response was observed. In this characteristic curve, the seat pan deceleration rises sharply during the onset of the input pulse, then drops rapidly, sometimes passing through zero. It then rises sharply and forms a secondary spike before damping out around the load factor used in the design of the energy-absorbing system. In most of the tests conducted during the time period between 1971 (when the criteria were established) and the present, the secondary spikes have exceeded the criteria limit of 23 G and have been a source of concern. One question of concern is whether the secondary spike is a natural response of the seat and occupant spring-mass system, or if it is caused by some external source. Also, it is not known whether the acceleration spike is hazardous to the seat occupant.

The need for answering these questions was confirmed in August 1978, durirg qualification testing of the U.S. Army's Black Hawk helicopter crewseat, when the secondary acceleration spike once again exceeded the criteria limits. At that time it was decided to research the data available and to attempt, through analysis, to determine whether the secondary spike did, in fact, increase the hazard to the occupant. The results of this analysis indicated that the secondary spike is a natural response of the seating system and, in itself, does not increase the hazard to the occupant. However, the analysis also indicated that the crash pulse might be hazardous to the occupant at times other than during the secondary spike. It was further concluded that the criterion as it now exists is not sufficiently comprehensive, and that additional research should be immediately initiated to both establish the effects of system variables upon seat and occupant response and expand knowledge in the area of human tolerance to decelerative loading in the $+G_z$ direction. These additional data constitute a necessary prerequisite to establishing a more comprehensive set of criteria controlling the design of crashworthy crewseats. Under the leadership of the U.S. Army Applied Technology Laboratory at Fort Eustis, Virginia, (ATL) and the U.S. Army Aeromedical Research Laboratory at Fort Rucker, Alabama, (USAARL) a multiservice effort was initiated with goals of performing the research necessary in these areas. The research efforts were designed to provide at least a minimum level of needed information in each area and to meet the following objectives:

- Establish the sensitivity of seat and occupant response to system variables.
- Determine the effect on system performance of the type of dummy being used for testing and establish an appropriate standardized dummy for seat system eavluation.
- Investigate the performance of the seat with an occupant more nearly representative of the operational occupant than are anthropomorphic dummies. Cadavers were to be used for this investigation.
- Establish, through dynamic testing, additional information concerning human tolerance to accelerative loads in the $+G_z$ direction.

1.1 SENSITIVITY TESTING AND ANALYSIS

In July 1979, the U.S. Army Applied Technology Laboratory, Fort Eustis, Virginia, initiated a contract with Simula Inc. to conduct a program for development of design criteria for more effective use of stroking distance in energy-absorbing seats. As part of this effort, a matrix of dynamic tests was performed by the Federal Aviation Administration Civil Aeromedical Institute (CAMI), the Naval Air Development Center (NADC), and Simula Inc. Variables that are being investigated through analysis and testing include the shape, magnitude, and rate of onset of the input deceleration pulse; the velocity change; the type and size of the anthropomorphic dummy; the energy absorber limit load; the seat weight; the cushion characteristics; the seat orientation; and the structural spring rate of the seat. Testing has been accomplished using a UH-60A Black Hawk crewseat, which was inspected and overhauled as necessary during the test series to enable successful and repeatable results to be obtained.

CAMI conducted 23 tests with a rigid seat for evaluation and comparison of existing anthropomorphic dummies and 27 tests with the Black Hawk seat for investigation of the effects of the other variables. In order to examine the effects of different test facility types and input deceleration pulse shapes, NADC conducted nine tests and Simula Inc., three.

1.2 CADAVER TESTING AND ANALYSIS

Related to the energy absorber criteria research program, testing has been conducted at Wayne State University with human cadavers in a Black Hawk crewseat, as described in Reference 8. That program has been supported by Simula Inc. under a contract with the U.S. Army Applied Technology Laboratory. The primary objectives have been to determine a threshold deceleration tolerance of cadavers and relate this threshold to the U.S. Army aviator population; also to investigate whether the secondary acceleration peak

observed in tests of energy-absorbing seats exists when the seat is occupied by a human subject, and if so, to determine whether it presents a hazard to Army aviators.

The first phase of the cadaver testing program consisted of nine tests divided into two series. The first series consisted of a maximum of two dynamic tests with each cadaver. Both tests used a combined-loading mode with the seat pitched forward relative to the impact vector, first 17 degrees and then 34 degrees (orienting the seat back at 4 degrees and 21 degrees relative to the impact vector, respectively) and a 14.5-G energy absorber limit load. The tests resulted in two cadavers successfully passing the first test orientation, but receiving vertebral fractures at the 34-degree pitch; two other cadavers received fractures in the first test. For the remaining three tests in that first phase of the program, 11.5-G energy absorbers were used, with the seat in the more severe test orientation with 34-degree pitch. The second phase of the program, which has just started in 1982, includes six tests with the 34-degree orientation, the first three of which will utilize 8.5-G energy absorbers. Two tests have been completed in this phase with one vertebral fracture occurring. Details of the tests in this part of the overall program are described by King and Levine in Reference 8. It should be emphasized that bone strength for living humans, especially the aviator population, is significantly higher than for the cadaver population tested. Determination of the bone strength relationship between the cadaver and aviator populations, supported by recent operational experience with energy-absorbing seats, will justify use of a higher limit load than the threshold determined in this program.

1.3 STANDARDIZATION OF DUMMIES

Because the Part 572 anthropomorphic dummy is the only truly standardized test device, it was selected for use in most of the sensitivity testing. However, all anthropomorphic dummies developed

in recent years, including the Part 572 model, have been designed for automotive uses and utilize civilian anthropometric data. The objective for this design has been to provide repeatable bending of the neck and lumbar spine in $-G_x$ impact, as well as realistic body compliance under restraint system elements. Should a new dummy be developed for military aircraft seat testing, it would be most desirable to use characteristics of military aircrewmen and optimize spinal response for axial deflection in addition to bending. Under the leadership of the U.S. Army Aeromedical Research Laboratory (USAARL), a committee was formed to develop a specification for body dimensions, joint locations, and inertial properties of military aircrewmen. Membership included representatives of the U.S. Army, Navy, and Air Force, and various civilian organizations. The group agreed that a standard representation for a 50th-percentile male aircrewmember would be developed in the relaxed seated position, with head oriented in the Frankfort plane. During the work of this committee, which was carried out in 1981, the U.S. Air Force drawing board manikin, in the 50th-percentile male size, served as the basis for the development of a set of dimensions and inertial properties. These properties, described in Reference 9, should prove useful both in development of an improved test dummy and in use of mathematical models of the aircraft seat occupant. One area which will require additional work for development of future antropomorphic dummies is in identifying dynamic response of the human body to $+G_z$ loading. Hopefully, analysis of the data from the cadaver testing program will supply the needed information.

1.4 GOALS OF MODIFIED ANTHROPOMORPHIC DUMMY PROGRAM

Analyses of the data from the sensitivity testing program demonstrated that the current criterion for seat evaluation based on seat pan acceleration is not sufficiently sensitive or repeatable to provide a measure of hazard to the occupant. Spinal forces and moments, which are the vertebral injury causing mechanisms, need to be measured directly during the test. Therefore, a dummy

to be used in aircraft seat testing should include capability for measurement of such loads.

The program described herein has been conducted to assess the feasibility of using a modified Part 572 dummy to measure spinal loads and moments. The program has consisted of the three following tasks, which are described in greater detail in the subsequent chapters:

- Modification of anthropomorphic dummies for measurement of spinal loads and moments.
- Repeat of four dummy tests from the Sensitivity Testing and Analysis Program at CAMI with instrumented dummies.
- Testing with a modified dummy at Wayne State University under conditions similar to the cadaver tests previously conducted.

2.0 ANTHROPOMORPHIC DUMMY MODIFICATION

None of the existing anthropomorphic dummies has been designed for vertical impact, particularly with respect to the spinal column, which is a critical region for human tolerance. At present, the reinforced rubber cylinder used as the lumbar spine in the Part 572 dummy is the best available choice. It permits more consistent positioning than the steel ball-and-socket configuration used in some earlier dummies, and it is standardized among like dummies. Instability in the earlier type could affect response of the upper torso with concomitant penalties on test repeatability. Another advantage of the Part 572 dummy for seat testing is a humanlike pelvic structure, which should result in load distribution on the cushion close to that for a human. Secondly, if the results of tests conducted at different facilities are to be compared, standardization of dummies and test procedures is mandatory, and the Part 572 dummy is the only existing standard device.

To develop and apply a meaningful criterion for prediction of lumbar injury requires that the forces transmitted through the lumbar spine be measured dynamically during testing. The FAA Civil Aeromedical Institute (CAMI) made available two six-axis femur load cells that were developed at Wayne State University. These load cells contain four axial and four transverse beams that are instrumented with foil-type strain gages. With axial, shear, and bending load capabilities of 6750 lb, 3375 lb, and 3100, in.-lb, respectively, this device has the capacity for measurement of lumbar loads.

2.1 DUMMY SELECTION

Two dummies were selected for modification to include one of the load cells at the lower end of the lumbar spine. An Alderson 50th-percentile dummy (S/N 870) conforming to Part 572 specifications (Reference 10) was made available by CAMI. For the 95th-percentile device, the dummy most nearly resembling the Part 572

device was selected, an Alderson VIP-95, with a pelvic structure and lumbar region of Part 572 configuration and with an elastomeric spine. The dummy (S/N 133) is jointly owned by USAARL and CAMI.

Although loads and moments in the lumbar spine are of primary interest, measurement of forces and moments in the cervical spine are also of interest. First, based on cadaver testing, tolerable limits for both shear and bending of the neck have been developed. Installation of one of the six-axis load cells in the dummy neck segment was planned in order to provide forces and moments for direct comparison with these values. Such data should be particularly useful in evaluation of various helmets, whose weight may increase the potential for neck injury. A second reason for measuring neck loads would be to obtain a greater understanding of overall occupant response to loads transmitted by the seat. Such information would assist in validation of both simple and complex mathematical models of seat/occupant response.

Unfortunately, the Part 572 dummy (50th-percentile) does not have sufficient space available at either end of the neck segment to install a 2.5-in.-long load cell without significantly altering the head-neck length. The VIP-95 dummy, on the other hand, has a tubular steel section in the lower end of the neck. Adapters were designed to allow replacement of this element by a load cell.

2.2 DESIGN OF MODIFICATIONS

The lumbar spine of the Part 572 anthropomorphic dummy consists of a 5-3/8-in. long x 2-7/8-in. diameter butyl rubber cylinder. A steel plate, 1/2 in. thick, is molded into each end of the cylinder for attachment between the pelvic and thoracic segments of the dummy. A steel cable is passed axially through the cylinder to support the end plates and to provide additional stiffness to the rubber column. Figure 1 shows the lumbar spine (Item A) mounted on the pelvis.

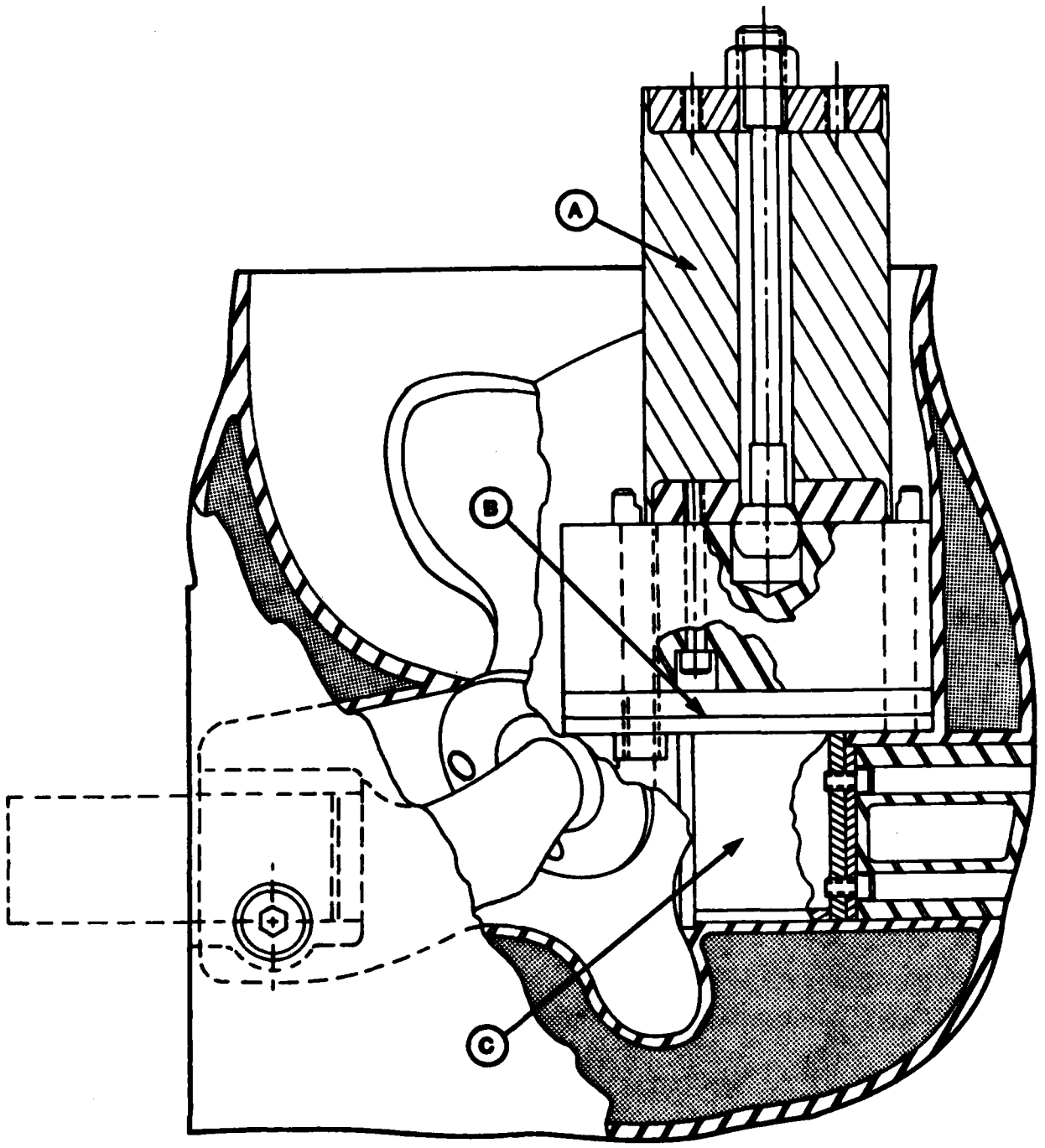

Figure 1. Part 572 pelvic segment with lumbar spine in place.

The load cells installed in the dummies are cylindrical in shape, approximately 2 in. in diameter and 2.5 in. in length. For installation of the load cell beneath the lumbar spine, a circular hole was cut in the aluminum plate to which the lumbar assembly is bolted. This plate is indicated as B in Figure 1. The cup-shaped housing shown as Item 1 in Figure 2 was designed to attach to the plate B and penetrate into the pelvic accelerometer cavity C. The lower end of the transducer was then screwed to the housing and to an adapter plate (Item 2 in Figure 2), which permitted attachment of the upper end of the transducer to the lumbar assembly. The assembly is illustrated in Figure 3. The Part 572 specification requires a dummy seated height of 35.7 in., and this dimension can be achieved by inserting spacers between the cup-shaped housing and the pelvis.

Whereas the Part 572 dummy uses a butyl rubber cylinder similar to the lumbar segment for the neck, the VIP-95 dummy has a rubber segment supported on top of a flanged steel tube. This steel section is then bolted to the thoracic segment. For installation of the transducer, this steel section of the neck was replaced by the load cell with specially designed end fittings. The lower adapter plate, show as Item 4 in Figure 2, is wedge shaped to yield the correct angle between the neck and thorax. The Item 3 plate is attached by three screws to the upper end of the load cell, and the Item 5 plate attached this assembly to the rubber neck segment. The neck transducer assembly is illustrated in Figure 3.

The test programs conducted with the two modified dummies are described in the following two chapters.

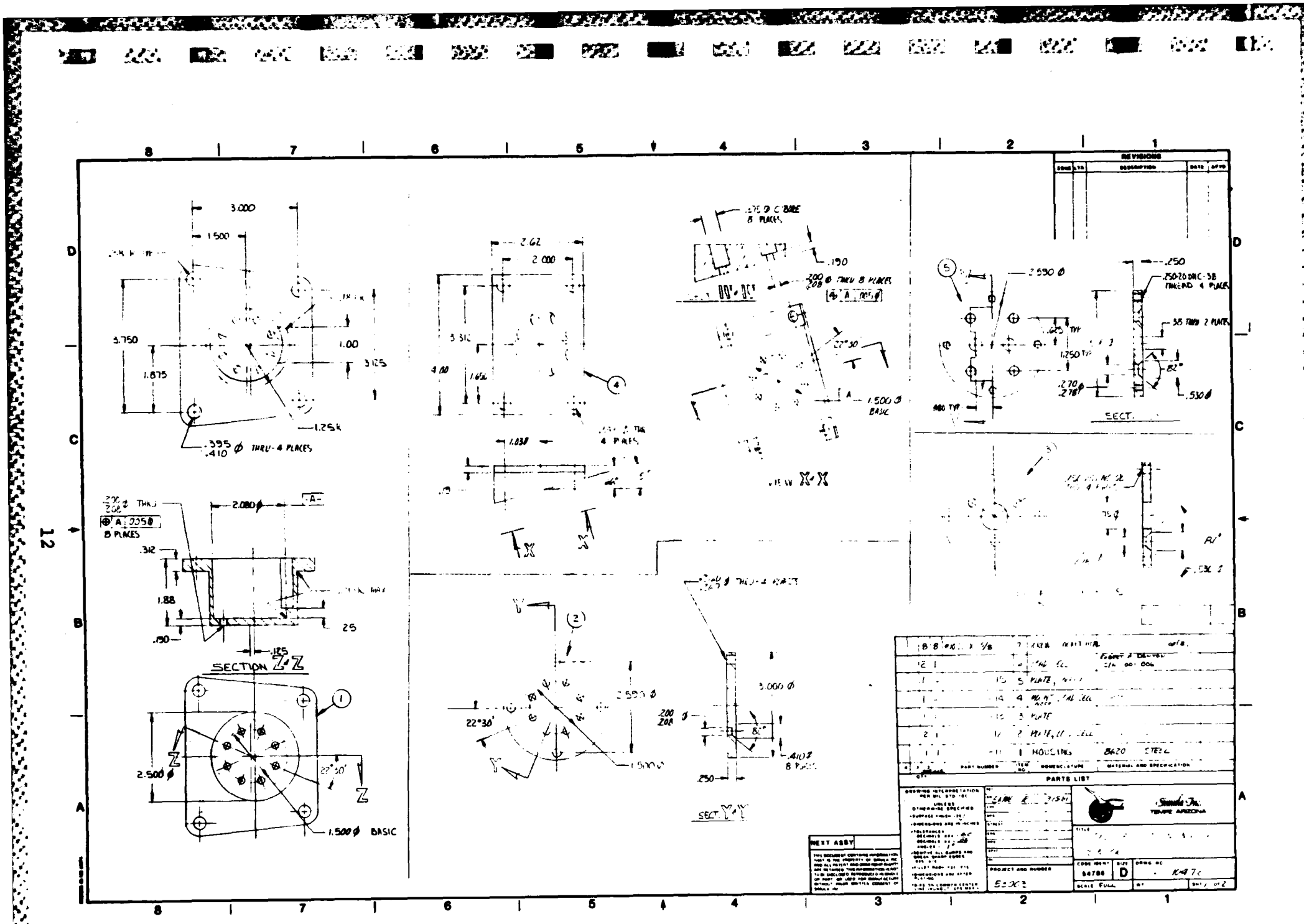

Figure 2. Load cell adapter details.

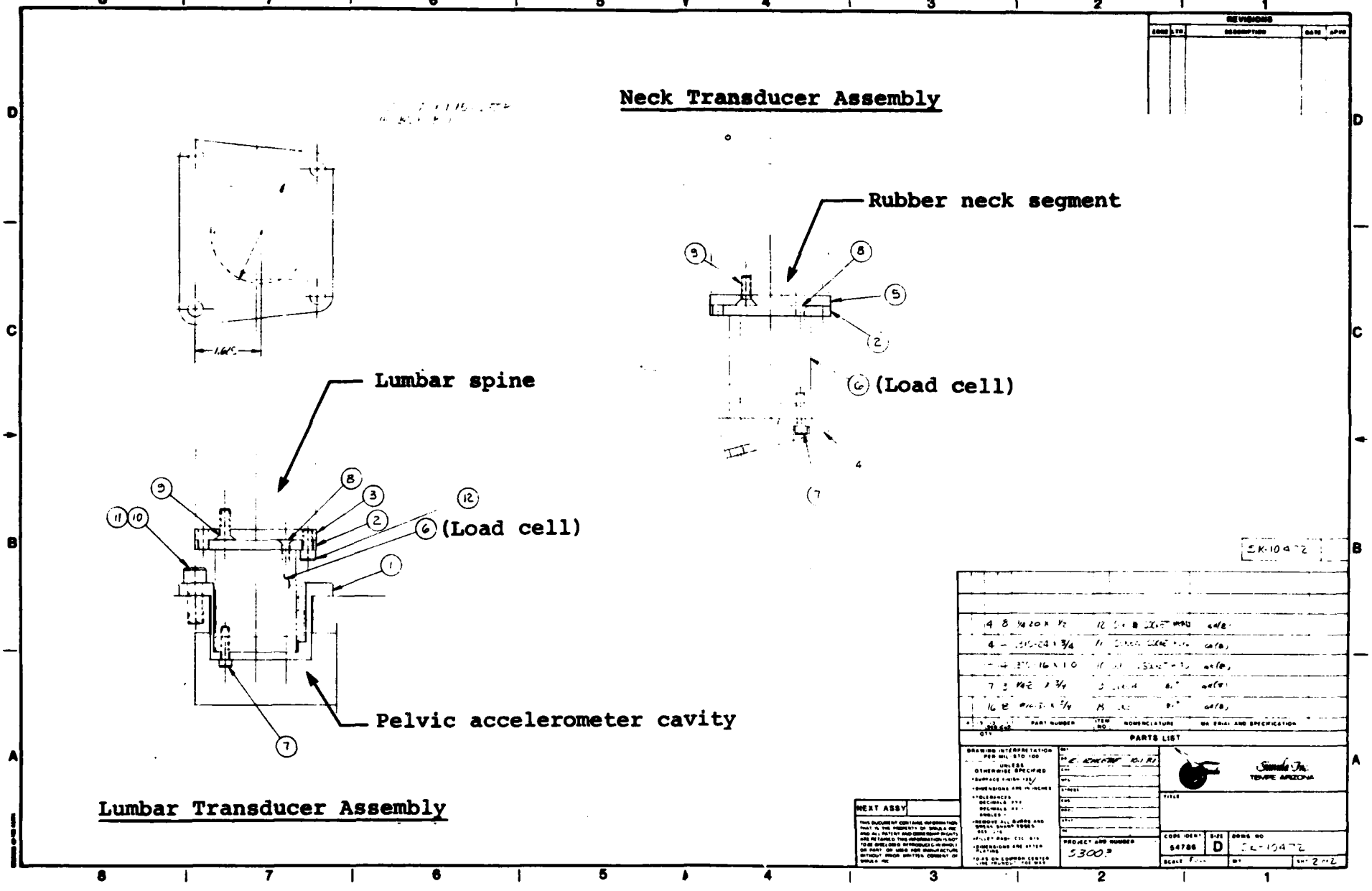

Figure 3. Transducer assemblies.

3.0 TESTING AT THE CIVIL AEROMEDICAL INSTITUTE

Five tests were conducted at the Federal Aviation Administration Civil Aeromedical Institute (CAMI) in Oklahoma City using the instrumented dummies. Two of the tests used a rigid seat, while three others used an energy-absorbing helicopter seat, as described below.

3.1 RIGID SEAT TESTING

One dynamic test was conducted with each of the dummies in a rigid seat whose seat pan and back formed a right angle with respect to each other, as shown in Figure 4. No cushions were used, and the plywood seat pan was supported by a six-axis load cell. The four-point restraint system used automotive-type nylon webbing. In order to impose a vertical ($+G_z$) acceleration on the dummy, the vertical (z) axis of the seat was aligned with the velocity vector, in other words, horizontal for the sled impact. For the test with the Part 572 dummy (CAMI Test A81-121), the sled deceleration is shown in Figure 5, and the deceleration for the test with the VIP-95 dummy (CAMI Test A81-122) was nearly identical. All recorded data from these two tests are presented in Appendix A, but the significant spinal forces and moments are shown here in Figures 6 through 11.

3.2 TESTS WITH ENERGY-ABSORBING HELICOPTER SEATS

Three tests were conducted at CAMI using a UH-60A Black Hawk crewseat, which has energy absorption capability in the vertical direction. Two test conditions were used, as described below.

3.2.1 Vertical Testing

Both dummies were tested on the CAMI sled under simulated vertical impact conditions. For these tests, the seat z-axis was pitched forward 17 degrees from the plane of the sled, as shown in Figure 12. The first 13 degrees of pitch was provided to align the

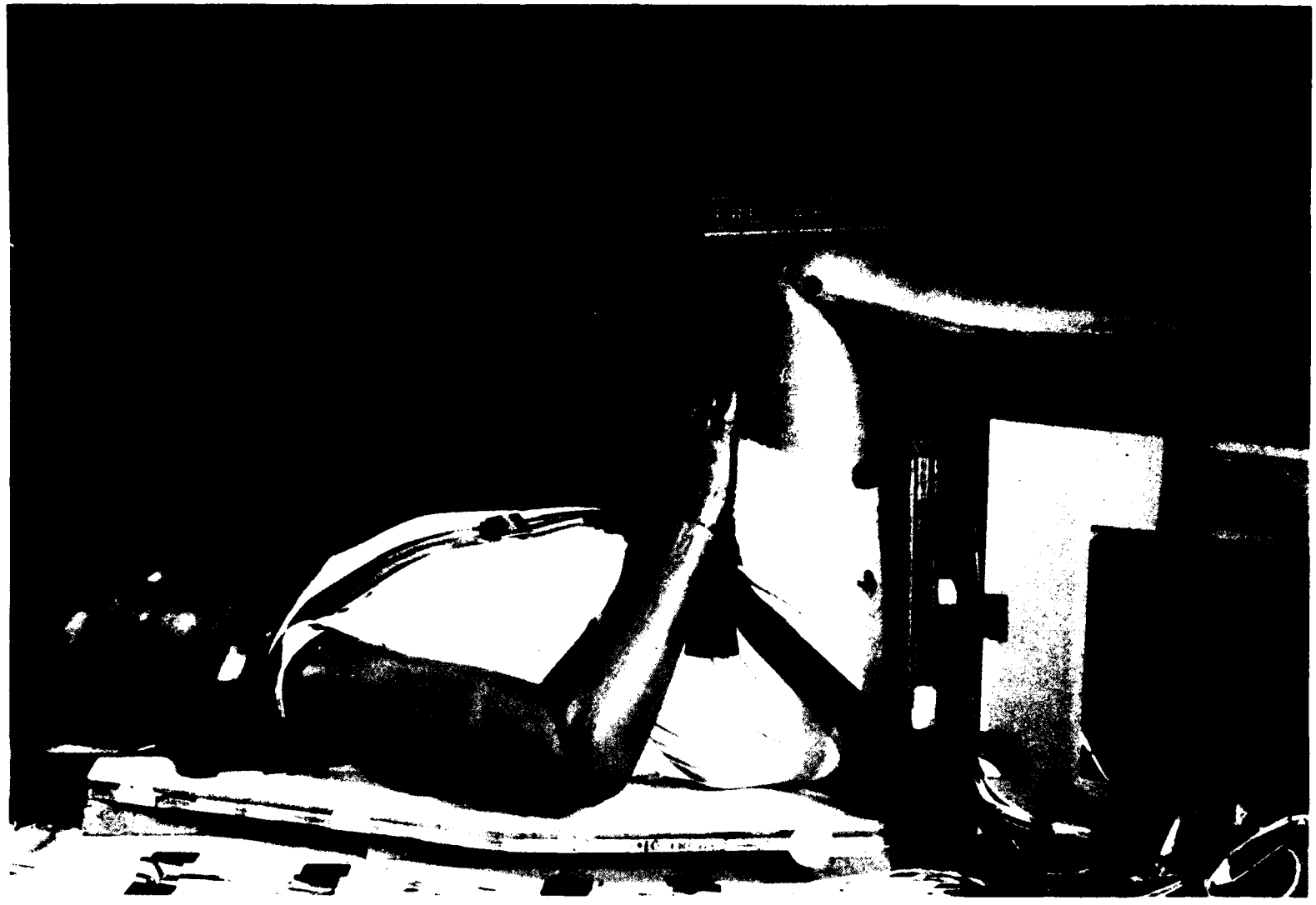

Figure 4. CAMI rigid seat (with VIP-95 dummy in place).

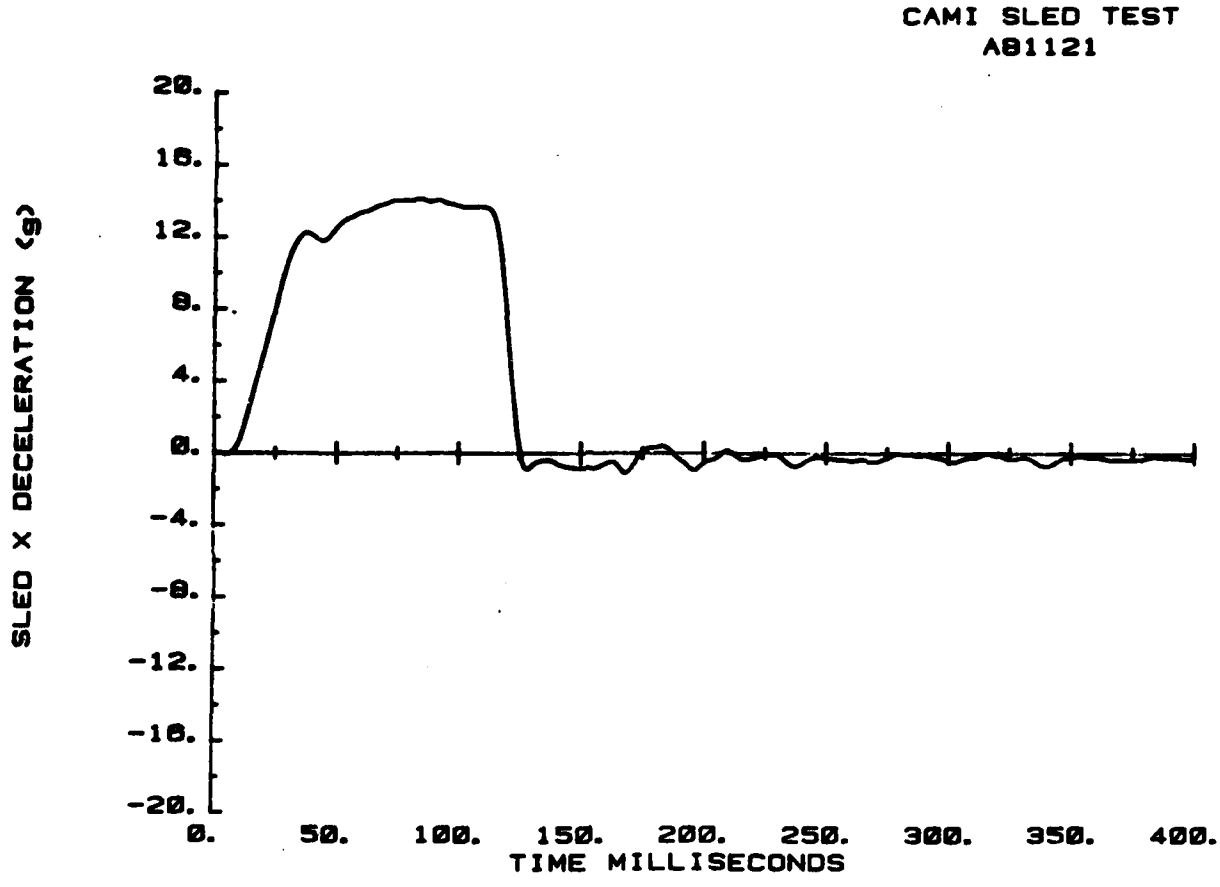

Figure 5. Sled deceleration for CAMI rigid seat test of Part 572 dummy.

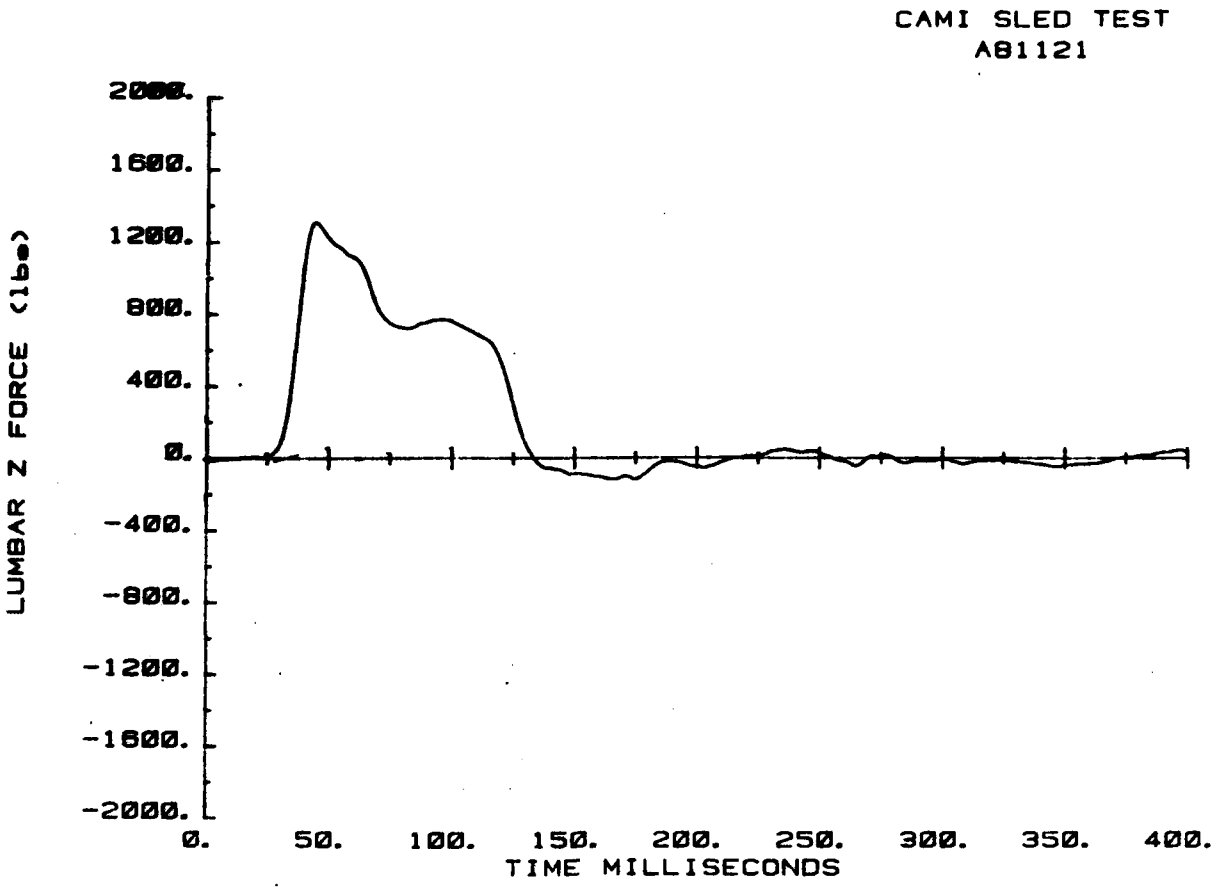

Figure 6. Lumbar axial force, Part 572 dummy, rigid seat.

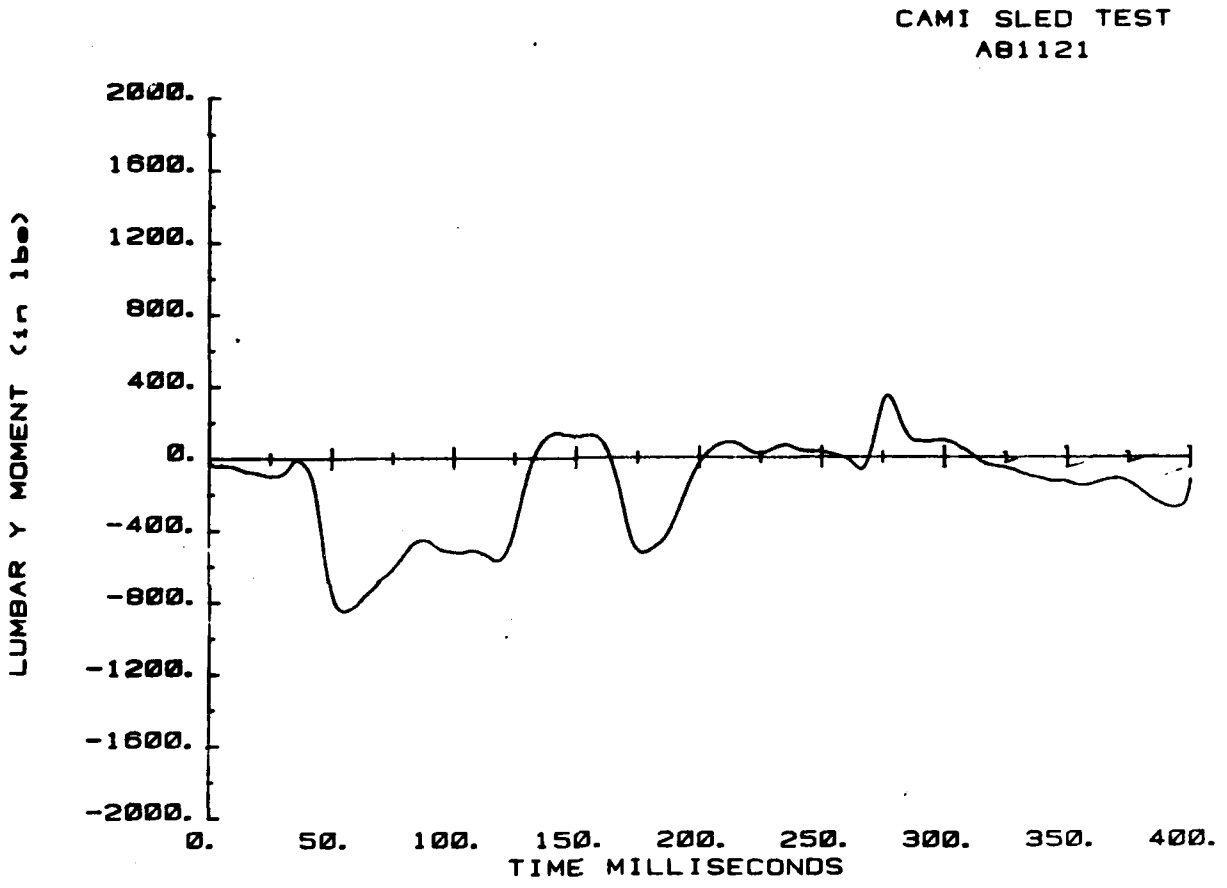

Figure 7. Lumbar y-moment, Part 572 dummy, rigid seat.

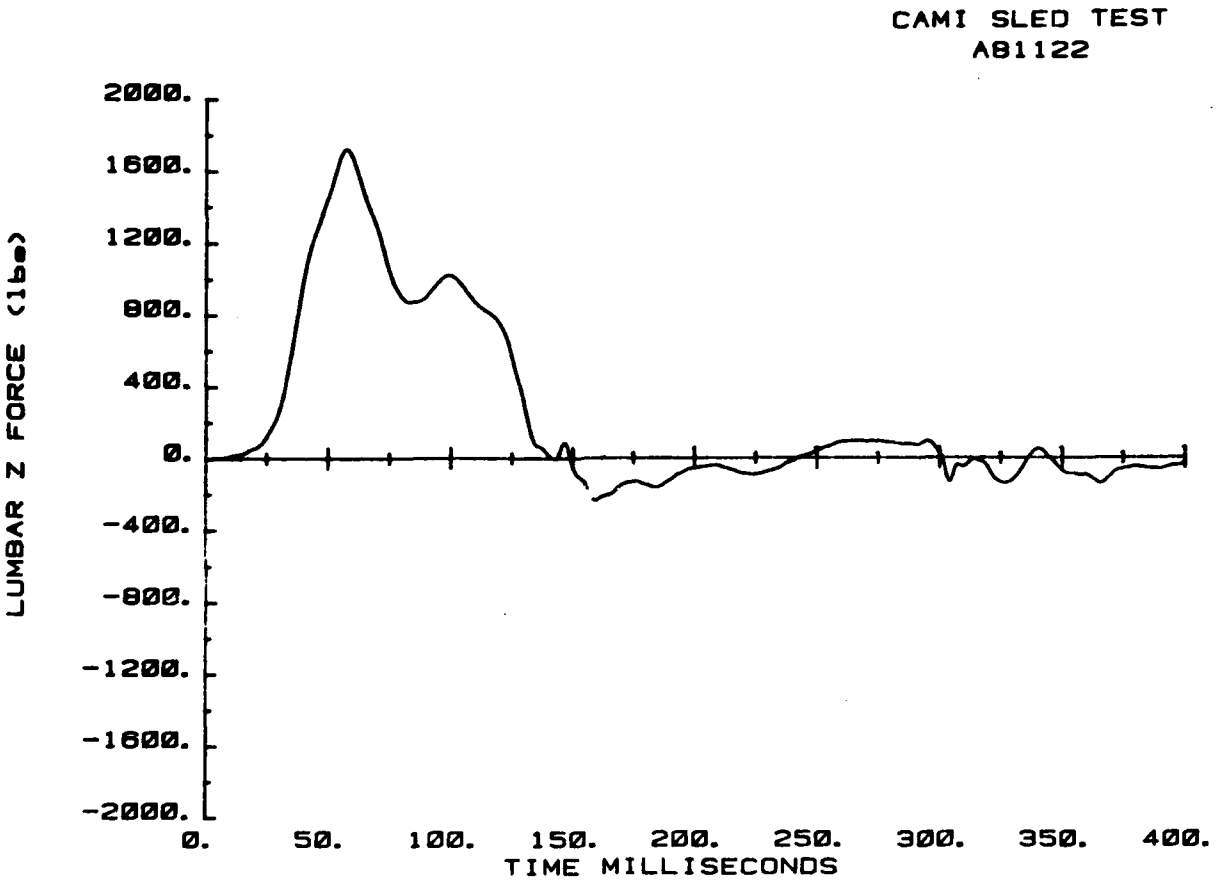

Figure 8. Lumbar axial force, VIP-95 dummy, rigid seat.

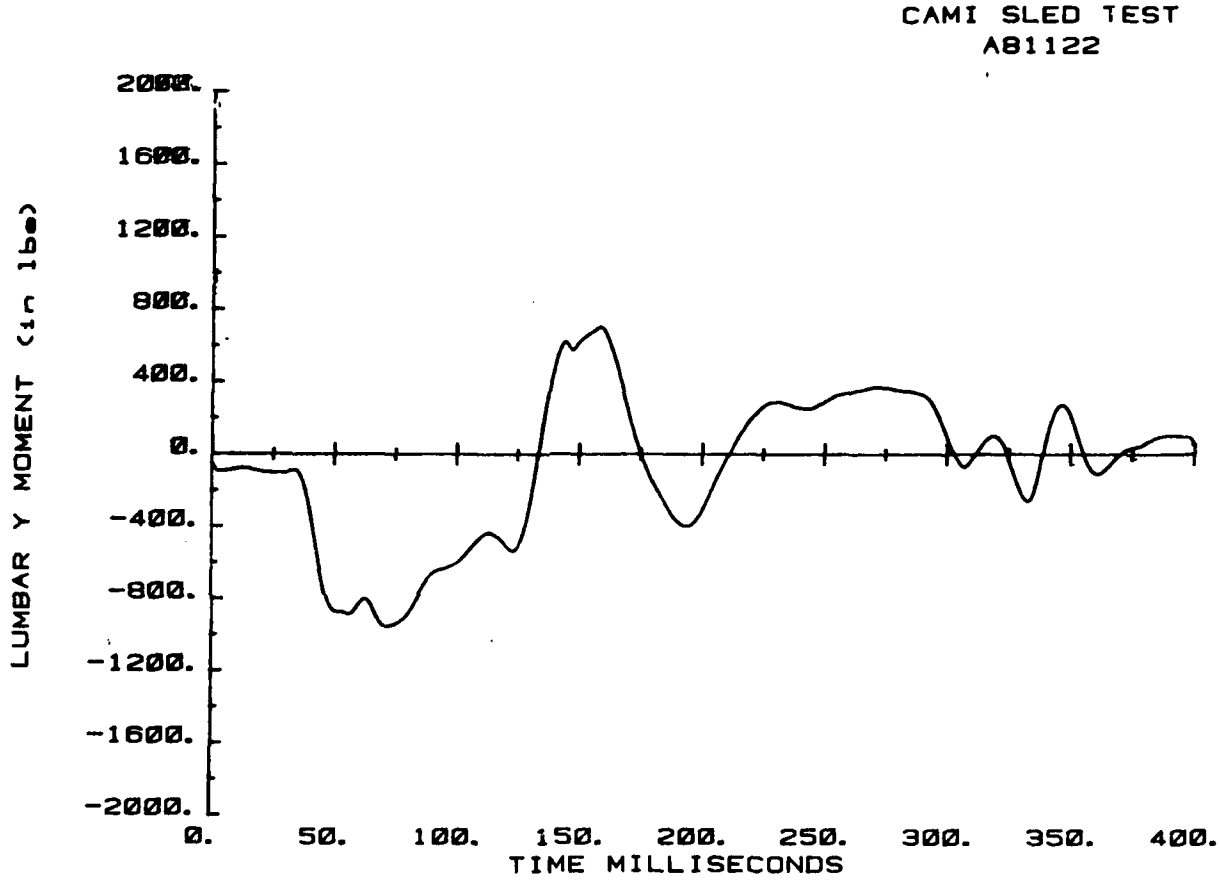

Figure 9. Lumbar y-moment, VIP-95 dummy, rigid seat.

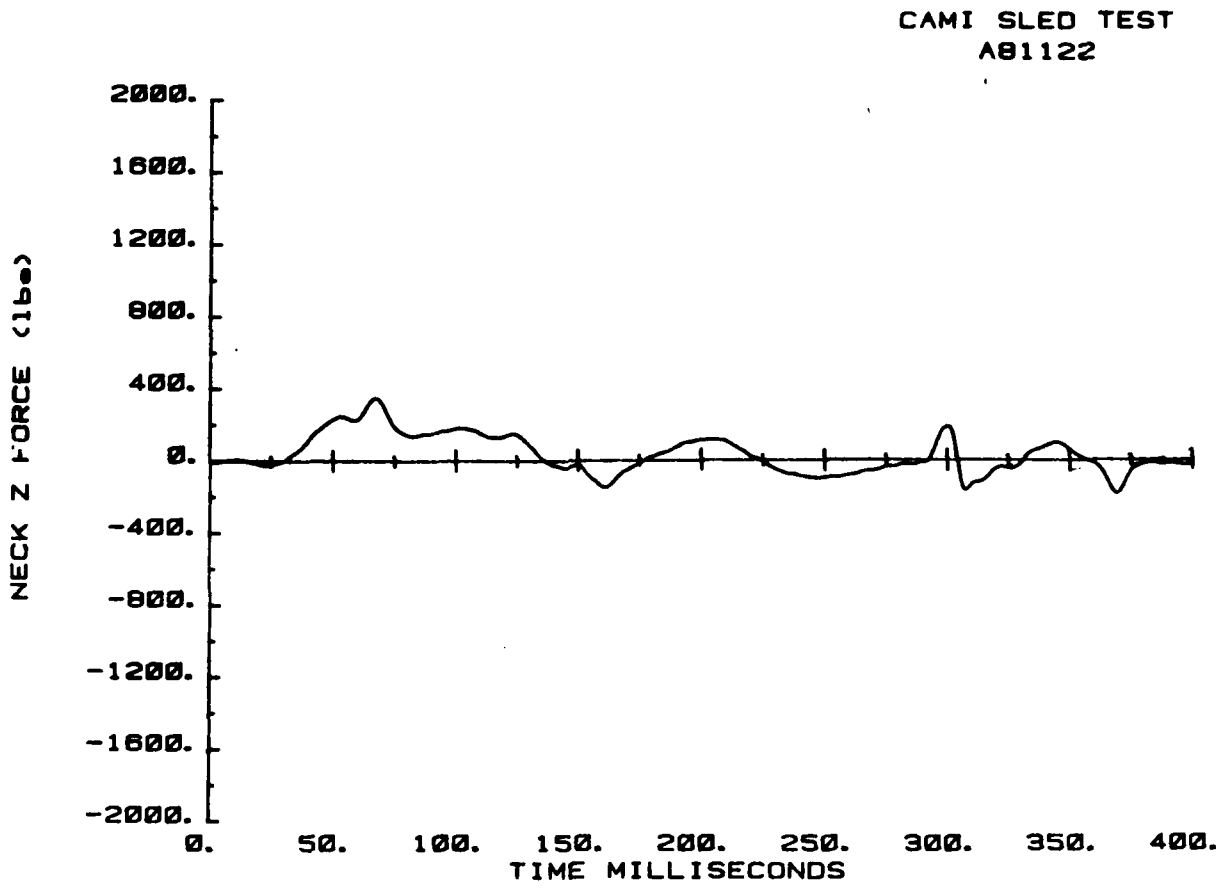

Figure 10. Neck axial force, VIP-95 dummy, rigid seat.

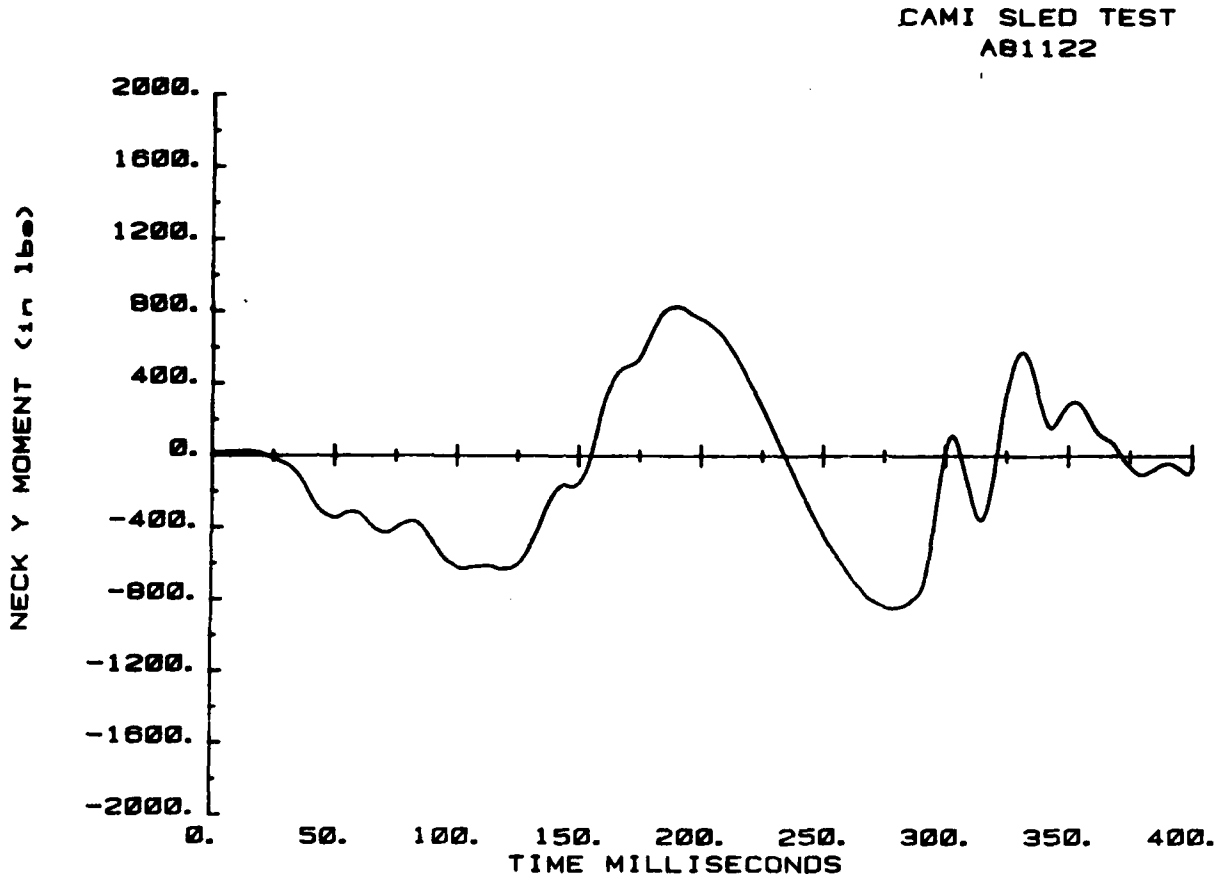

Figure 11. Neck y-moment, VIP-95 dummy, rigid seat.

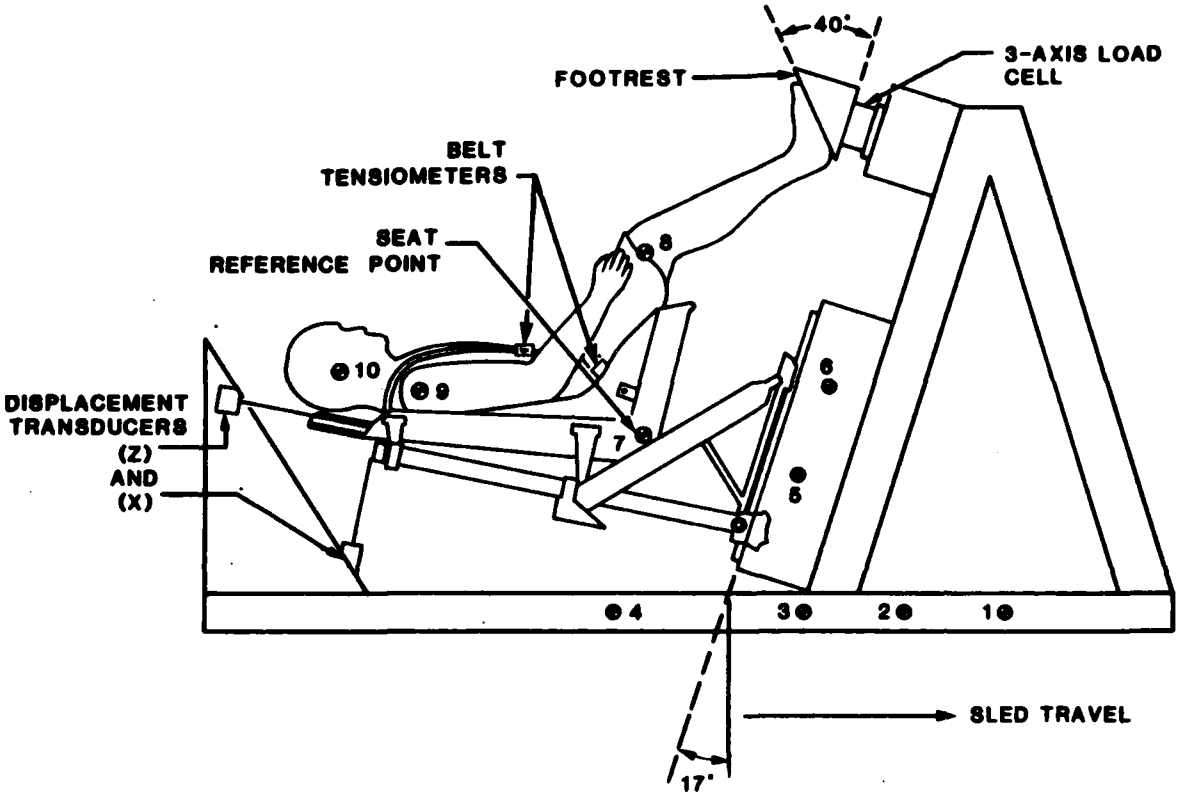

Figure 12. Test configuration for CAMI tests with energy-absorbing seats.

back tangent line with the horizontal surface of the sled (parallel to the velocity vector), in order to eliminate initial extension of the elastomeric spine that would be caused by a downward-oriented seat back angle. The additional 4 degrees of pitch was added to approximately counteract the one G of gravity that reduces the overturning moment on the dummy during seat stroking. Since during most of the tests the energy-absorbing mechanism on the seat is set to stroke at 14.5 G, the angle of the resultant deceleration was determined as the angle whose tangent is 1 divided by 14.5 equals 0.069, or 4 degrees. Therefore, under stroking loads, the overturning moment on the dummy should be approximately corrected for gravity, and the response should be similar to that for a seat in an upward-oriented position during vertical impact.

Pretest views of the dummy positioned in the seat are presented in Figures 13 and 14, where the fixture simulating the aircraft floor can be seen. (The Black Hawk helicopter has a well beneath each crewseat to permit additional stroke, so that a minimum of 12 in. and a maximum of 17 in.can be attained, depending on the seat's vertical adjustment position.) For all tests the seat was locked in the top adjustment position. Energy absorbers and the seat bottom cushion were replaced for each test. The dummy was flexed forward at the waist for positioning in the seat, and its lower torso was pushed firmly against the back cushion. The five-point restraint system was installed, and the lap belt was tightened. With the inertia reel unlocked, the shoulder harness was tightened using its adjusters. The inertia reel was then locked, and, using a torque wrench, an 80-in.-lb preload was applied to the reel. The dummy's feet were taped to the footrest, which was supported on a six-axis load cell.

The specified impact conditions included a 42-ft/sec velocity change, and an input deceleration pulse with a 42-G peak and a rate of onset of 1,050 G/sec (shown in Figure 15). A posttest view of the sled is shown in Figure 16, where the wires of the decelerating mechanism can be seen.

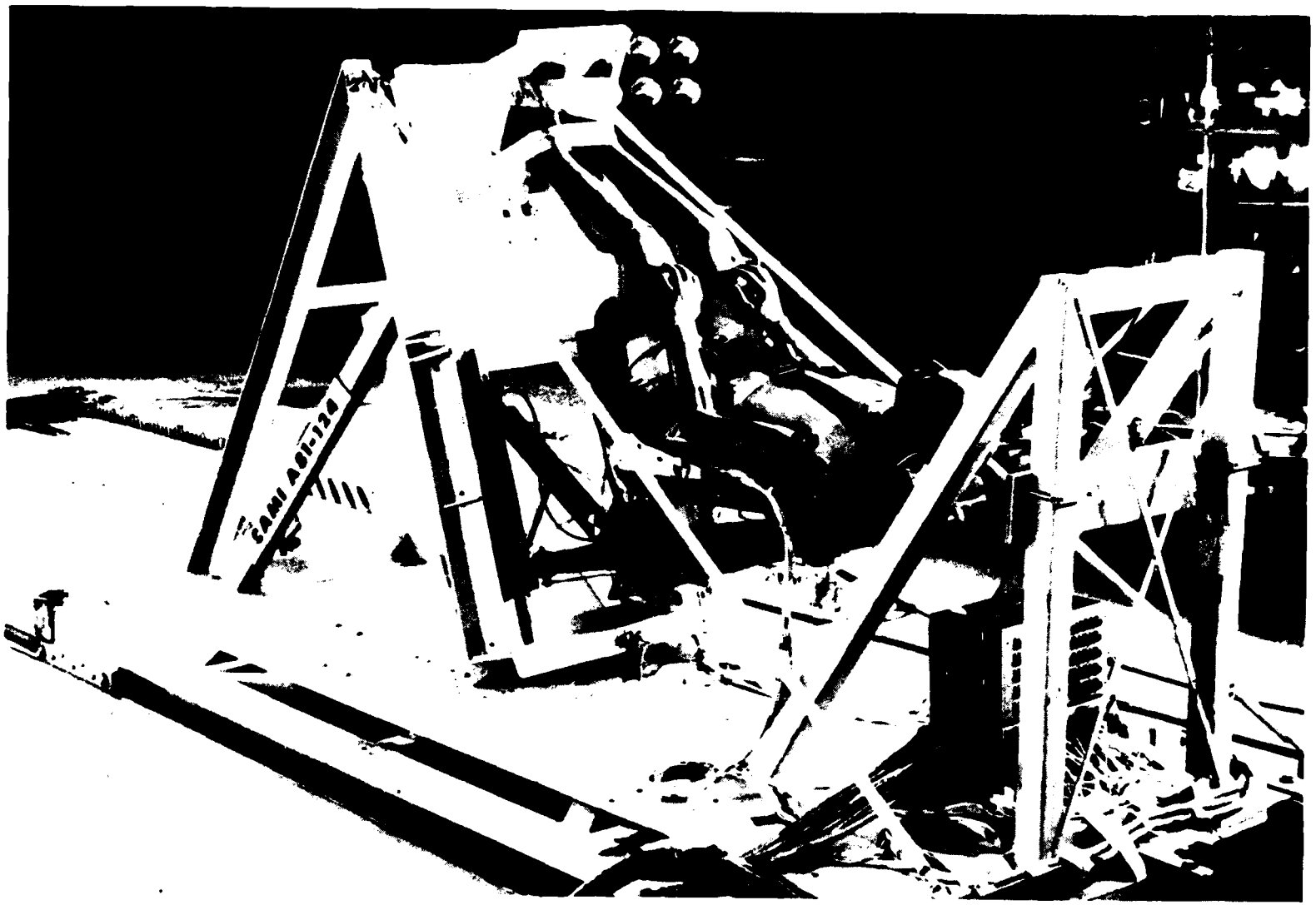

Figure 13. Part 572 dummy positioned in UH-60A Black Hawk crewseat prior to CAMI test.

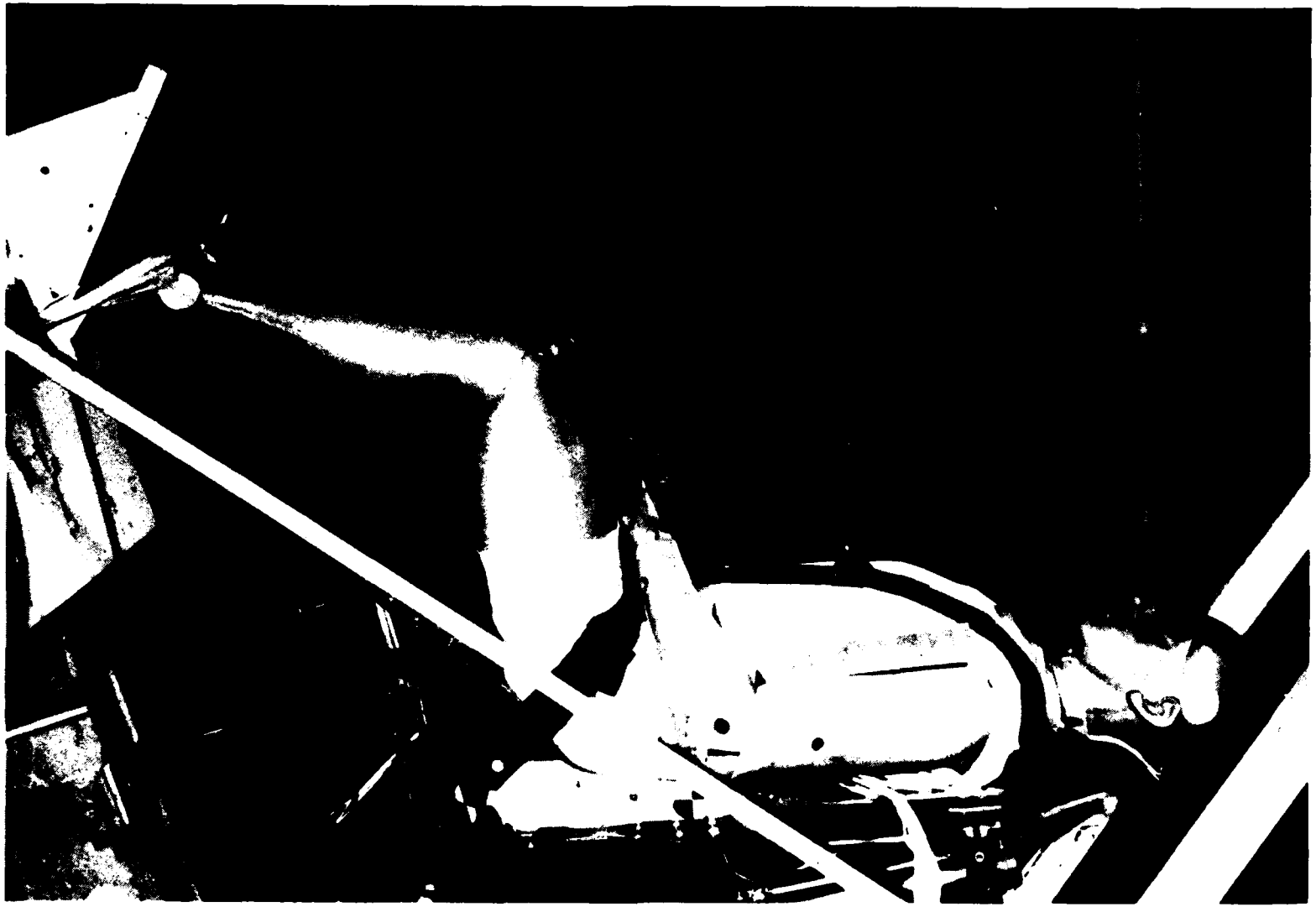

Figure 14. VIP-95 positioned in UH-60A Black Hawk crewseat prior to CAMI test.

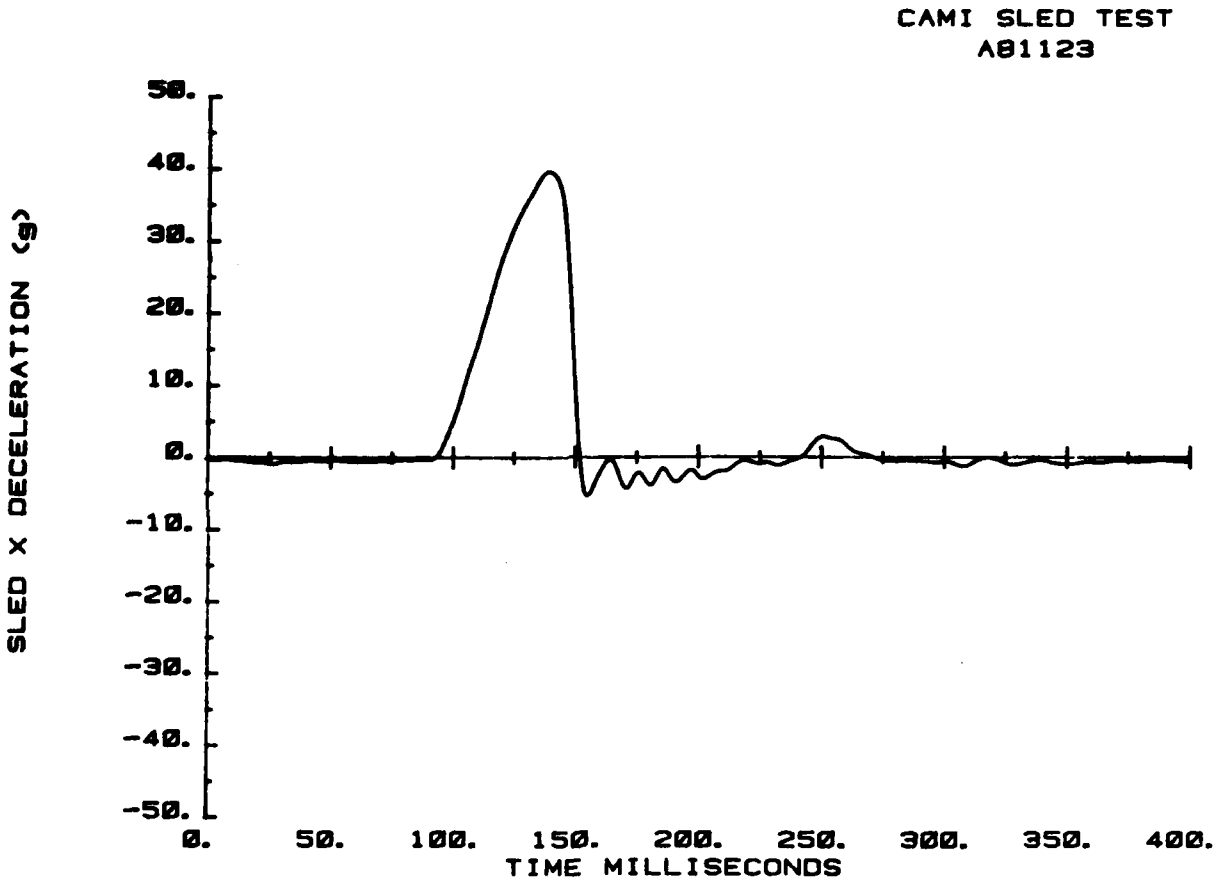

Figure 15. Sled deceleration for CAMI tests with energy-absorbing seat, vertical mode.

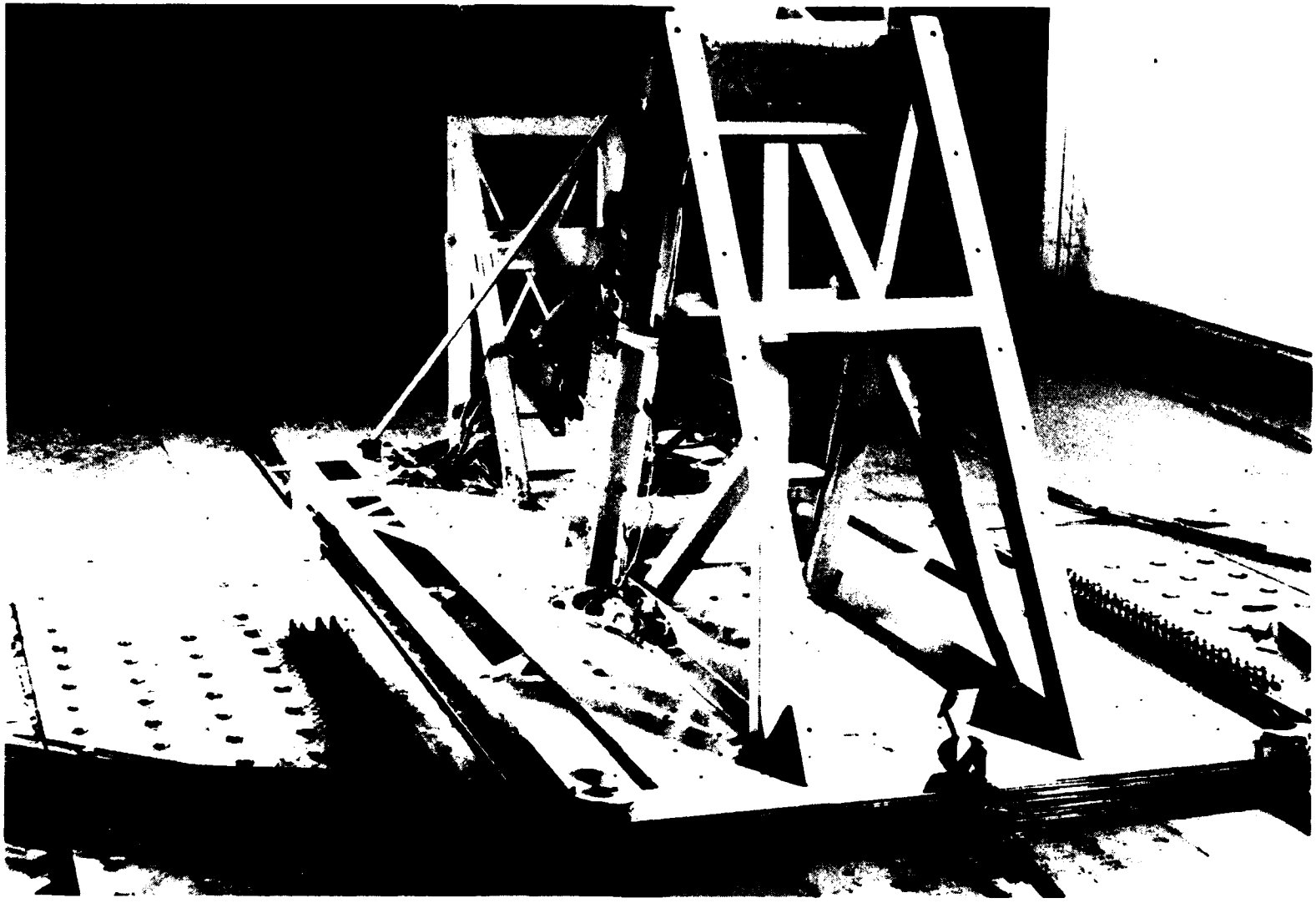

Figure 16. CAMI sled following test with energy-absorbing seat, vertical mode.

Accelerations were measured in the dummy pelvis, chest, and head, and on the seat. Forces were measured in the energy absorbers and the footrest, as well as in the spinal load cells. Seat stroke was also measured with a displacement transducer.

The significant spinal force and moment components are presented in Figures 17 through 22, along with vertical seat pan accelerations, which are used in the present criteria. Complete sets of plotted data are presented in Appendix B.

3.2.2 Combined Loading Test

One test was conducted using the Part 572 dummy with the seat pitched 17-degrees further forward on the sled and rolled 10 degrees to the right. A 50-ft/sec velocity change and 48-G input deceleration (Figure 23) were used, so that this test resembled Test Number 1 of MIL-S-58095(AV) (Reference 4), except for the additional four degrees pitch to approximately account for the difference in direction in conducting the tests on a horizontal sled. Significant lumbar forces and moments and seat pan vertical acceleration are presented in Figures 24 through 28, and complete data sets are presented in Appendix C.

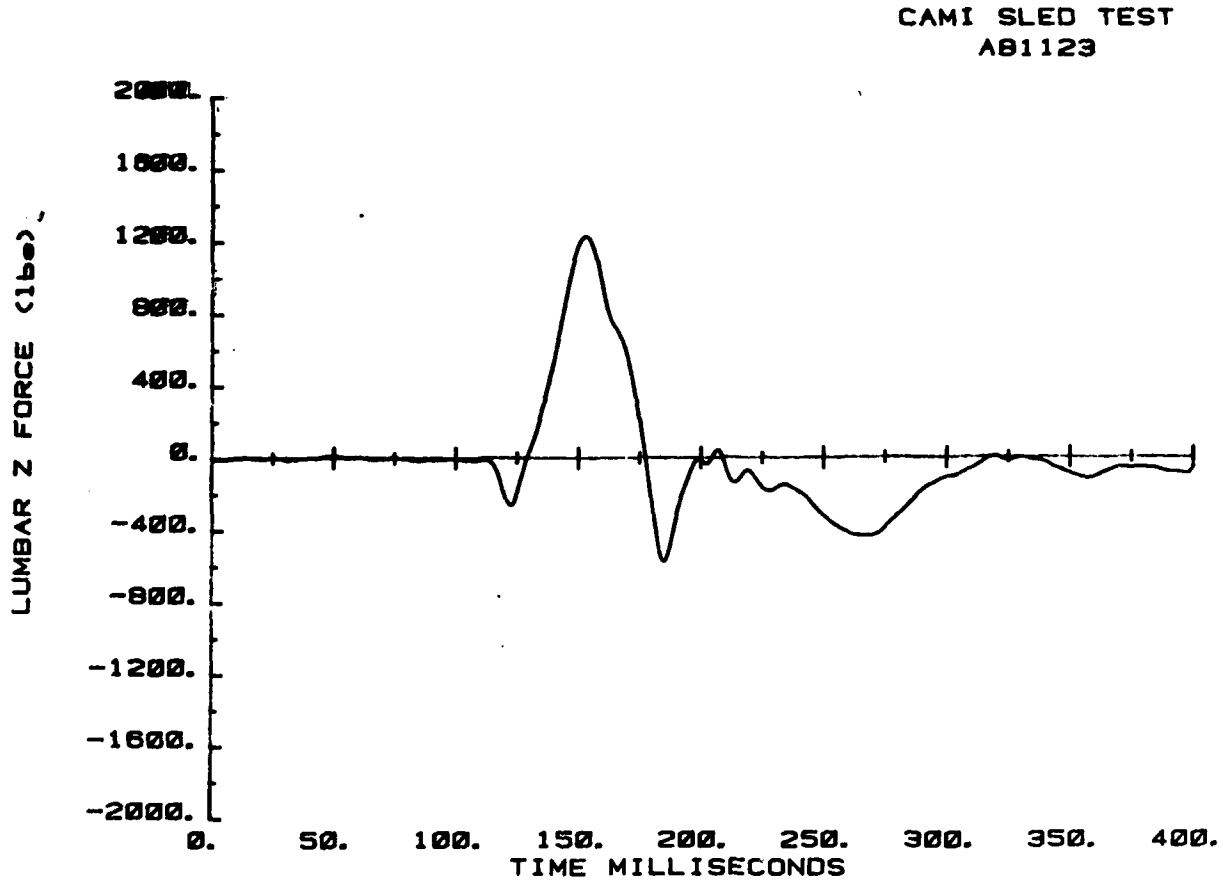

Figure 17. Axial force in lumbar spine, VIP-95 dummy, vertical test.

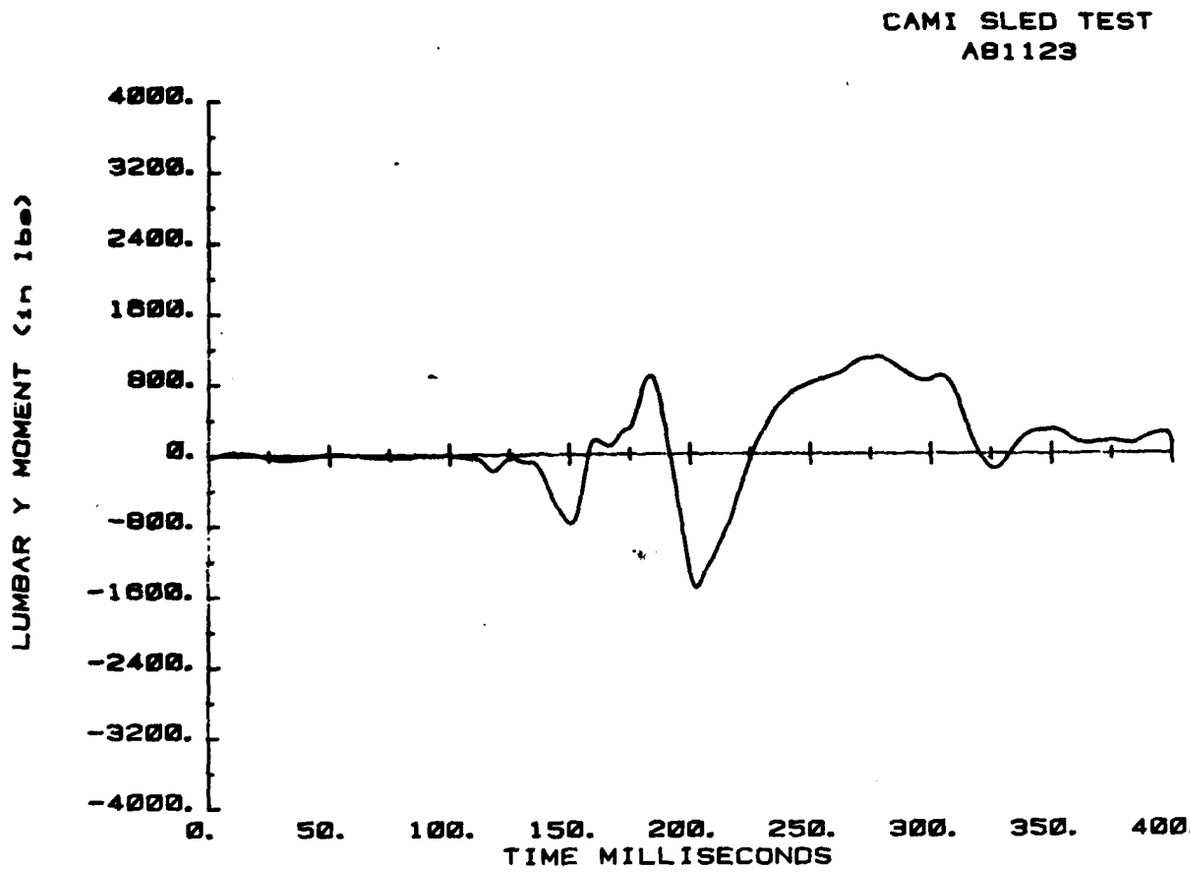

Figure 18. Moment (y-component) in lumbar spine, VIP-95 dummy, vertical test.

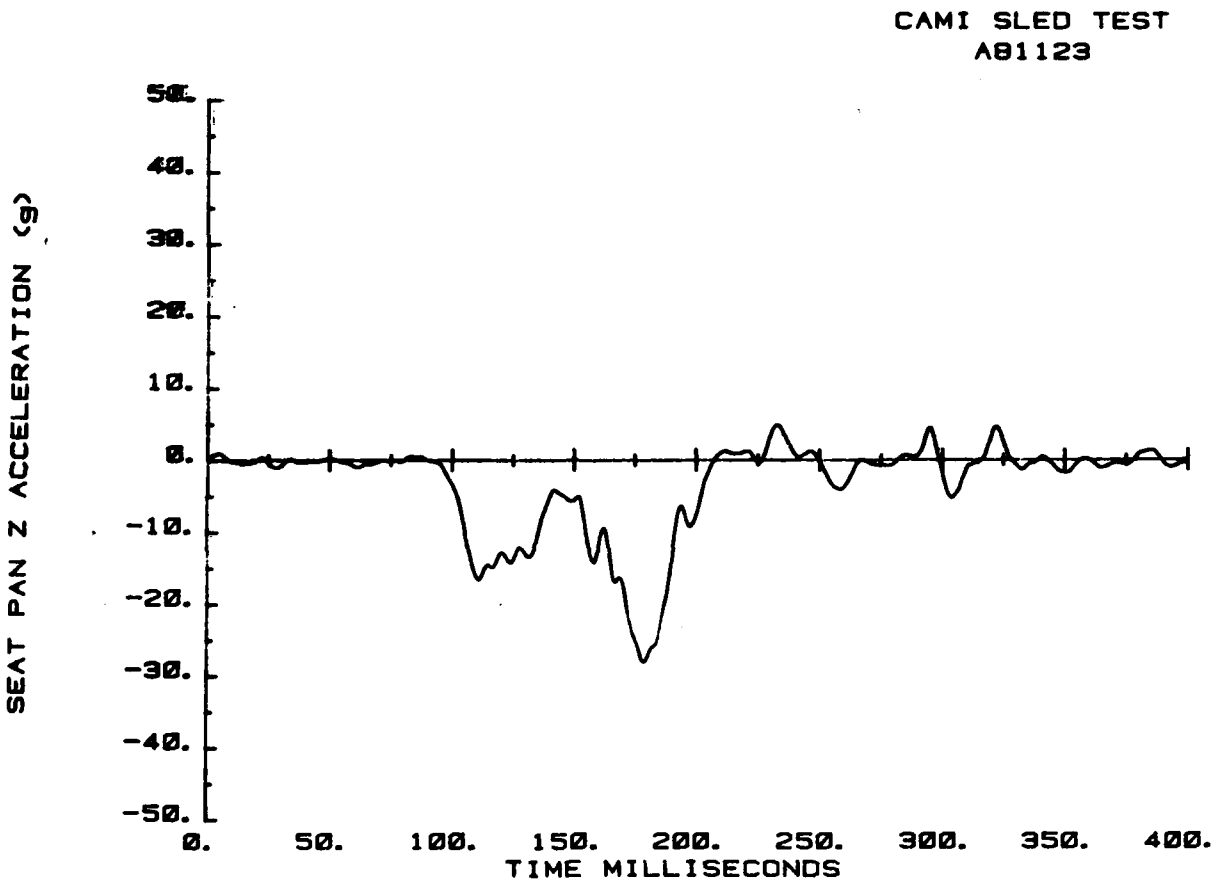

Figure 19. Seat pan vertical acceleration, VIP-95 dummy, vertical test.

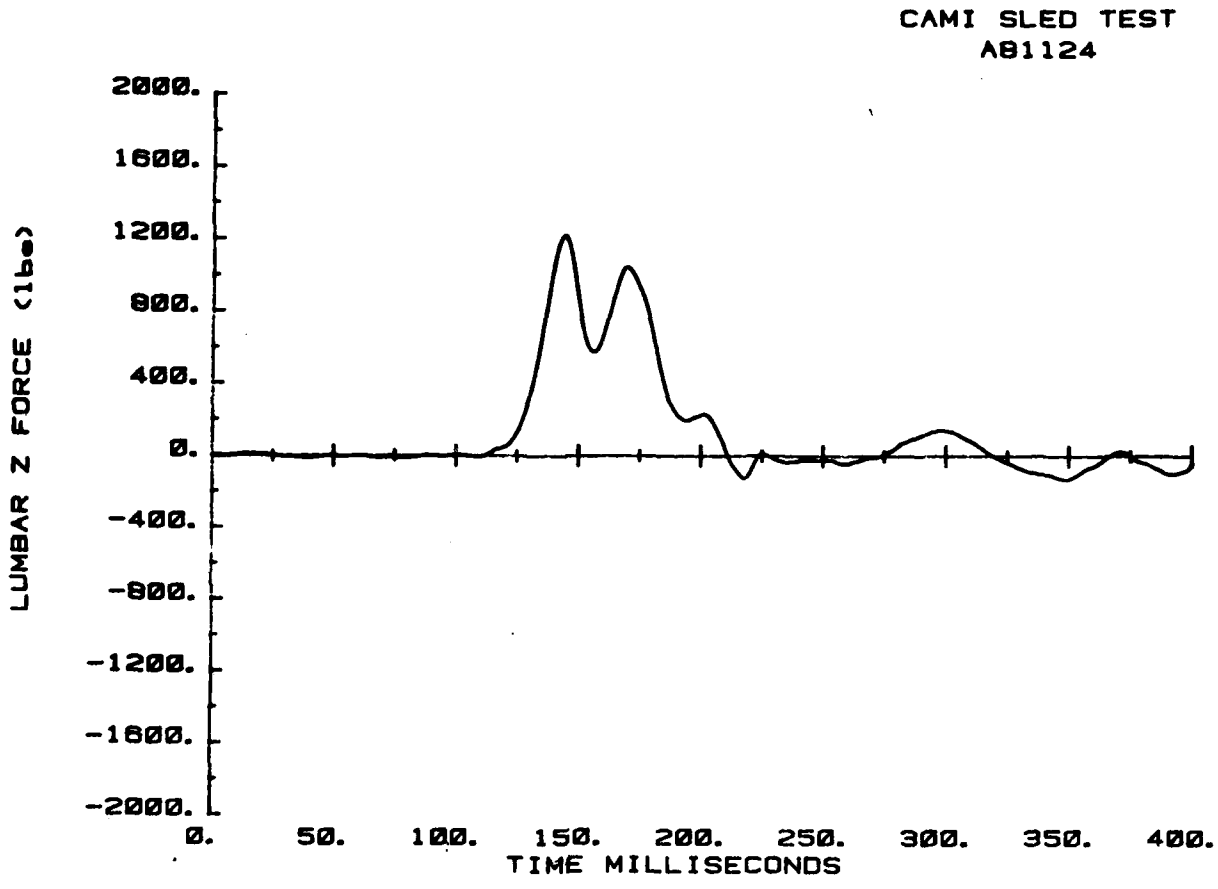

Figure 20. Axial force in lumbar spine, Part 572 dummy, vertical test.

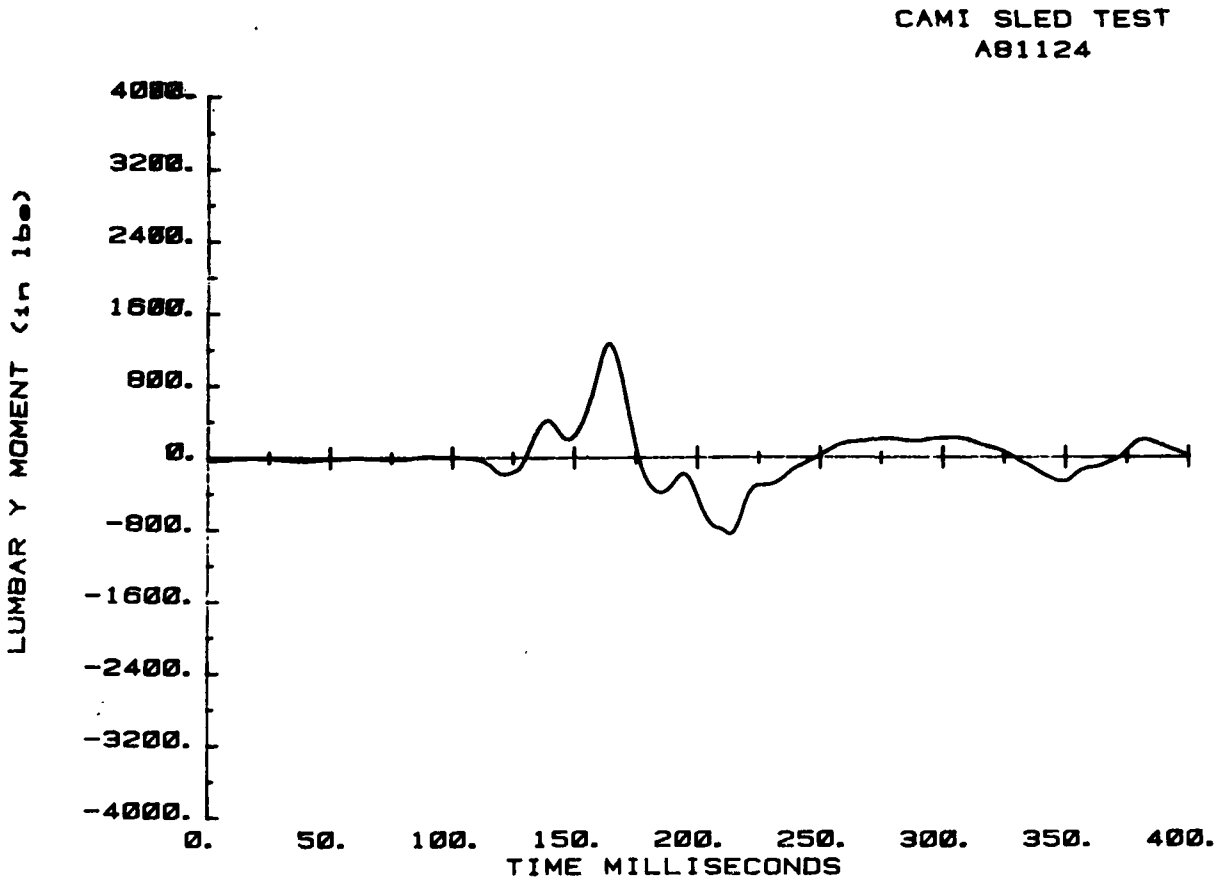

Figure 21. Moment (y-component) in lumbar spine, Part 572 dummy, vertical test.

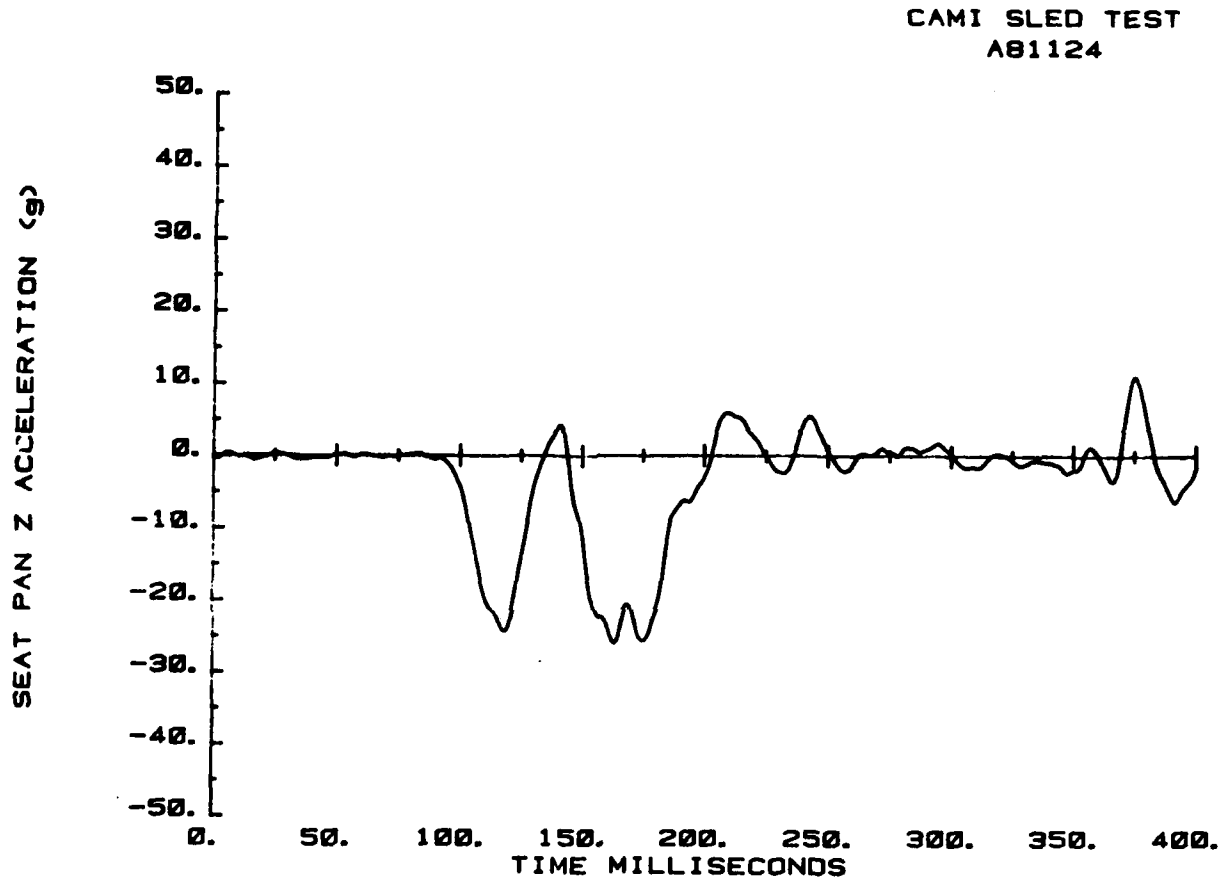

Figure 22. Seat pan vertical acceleration, Part 572 dummy, vertical test.

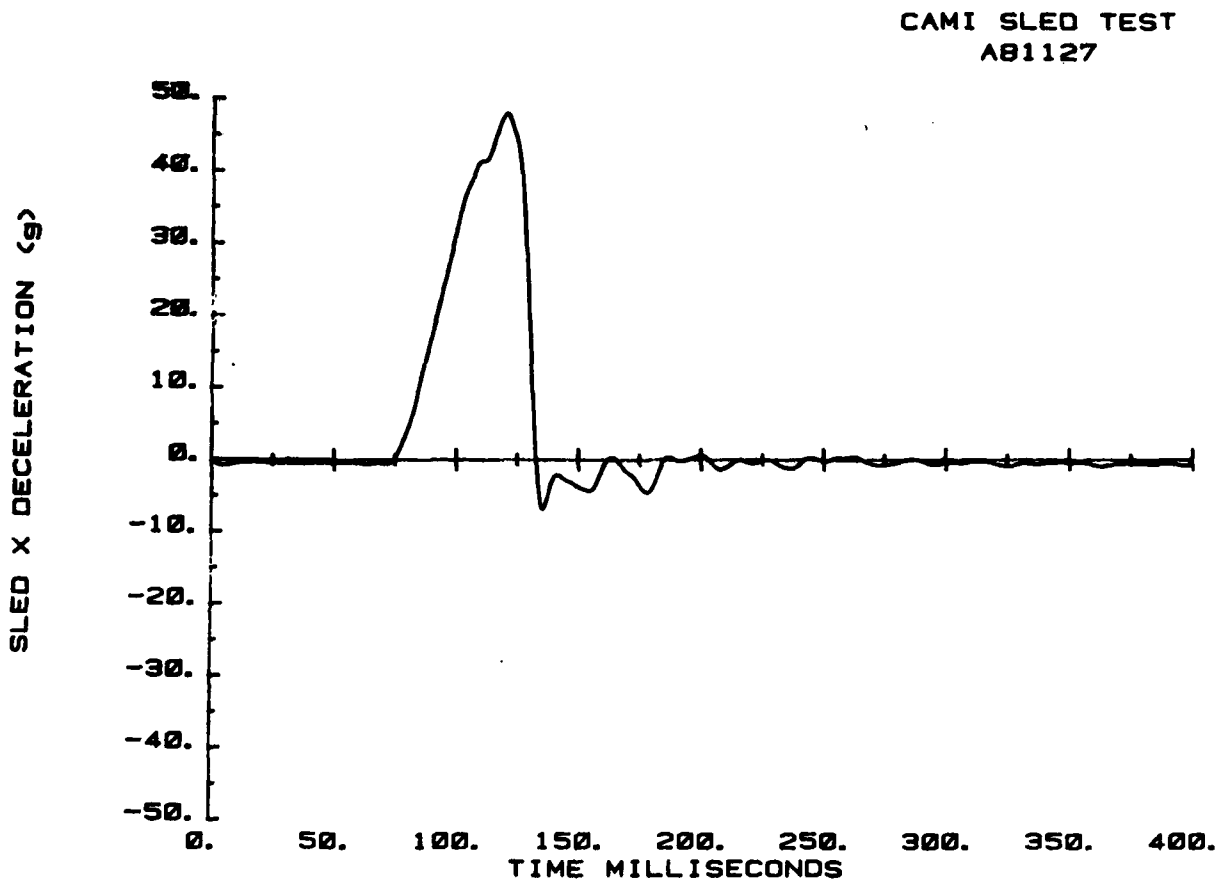

Figure 23. Sled deceleration for CAMI test with energy-absorbing seat, combined mode.

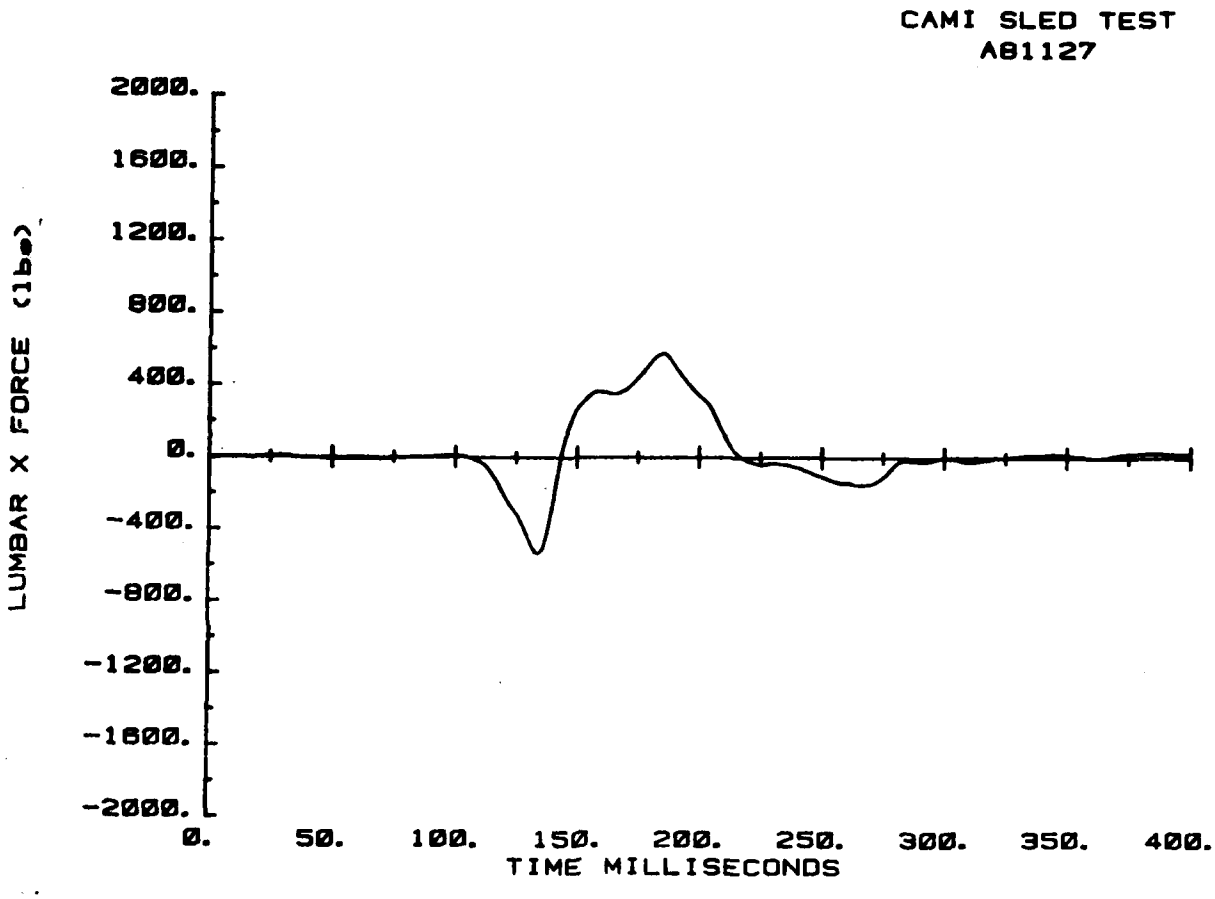

Figure 24. X-force in lumbar spine, Part 572 dummy, combined test.

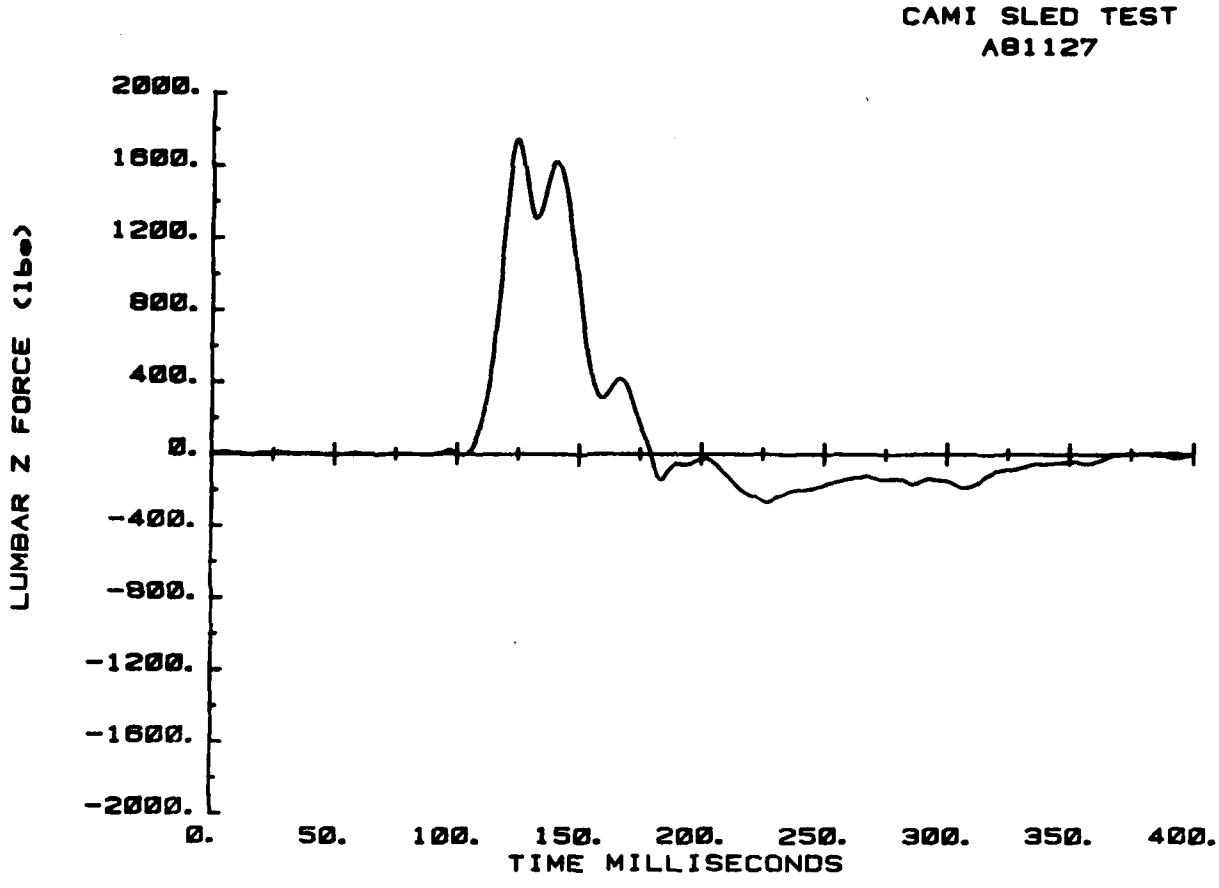

Figure 25. Axial force in lumbar spine, Part 572 dummy, combined test.

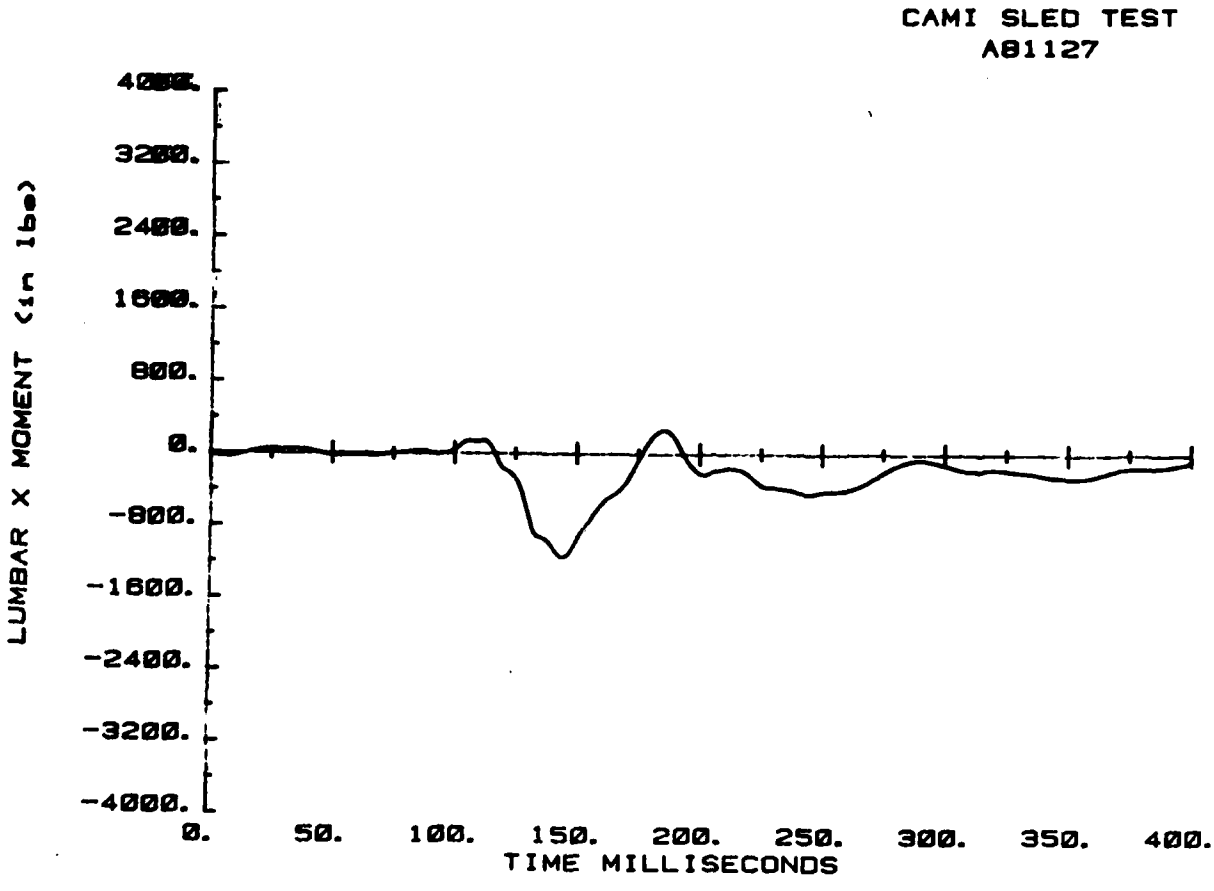

Figure 26. X-moment in lumbar spine, Part 572 dummy, combined test.

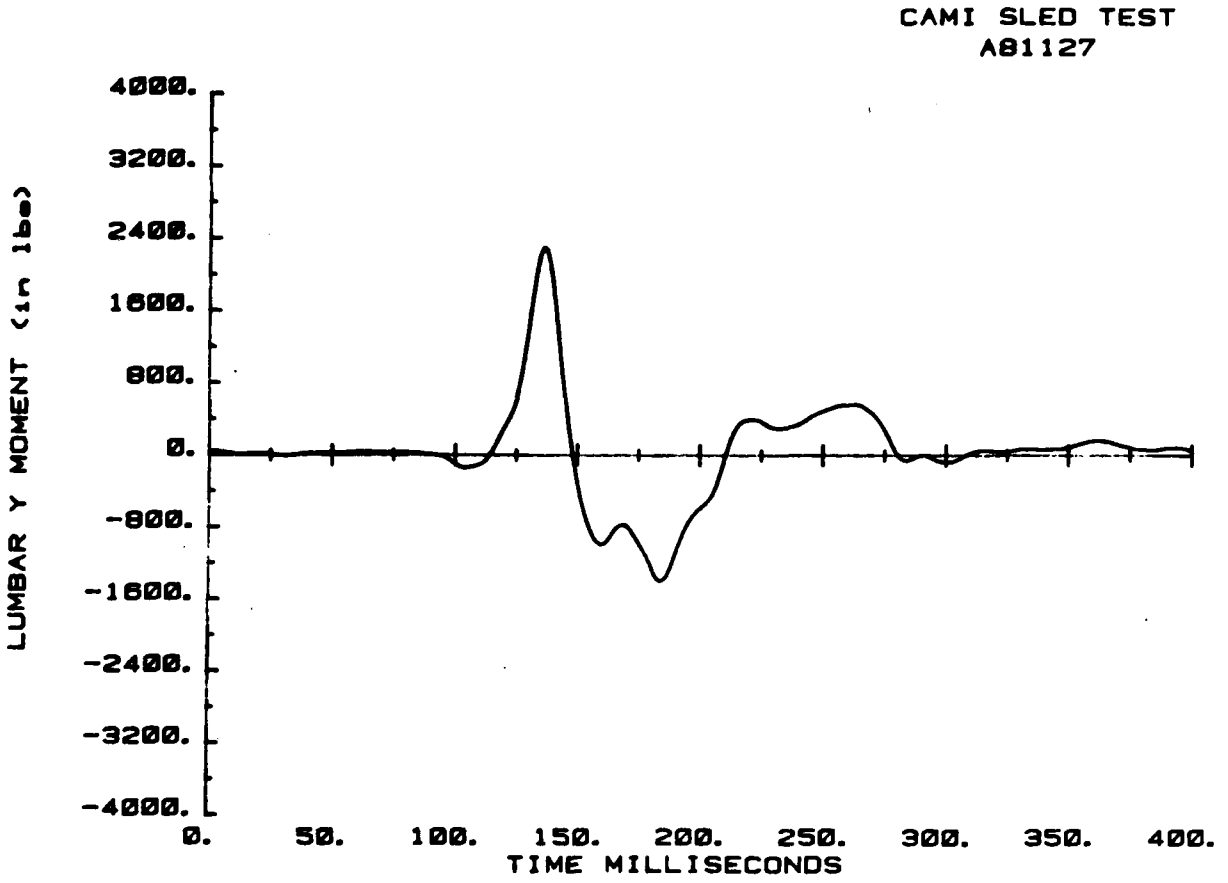

Figure 27. Y-moment in lumbar spine, Part 572 dummy, combined test.

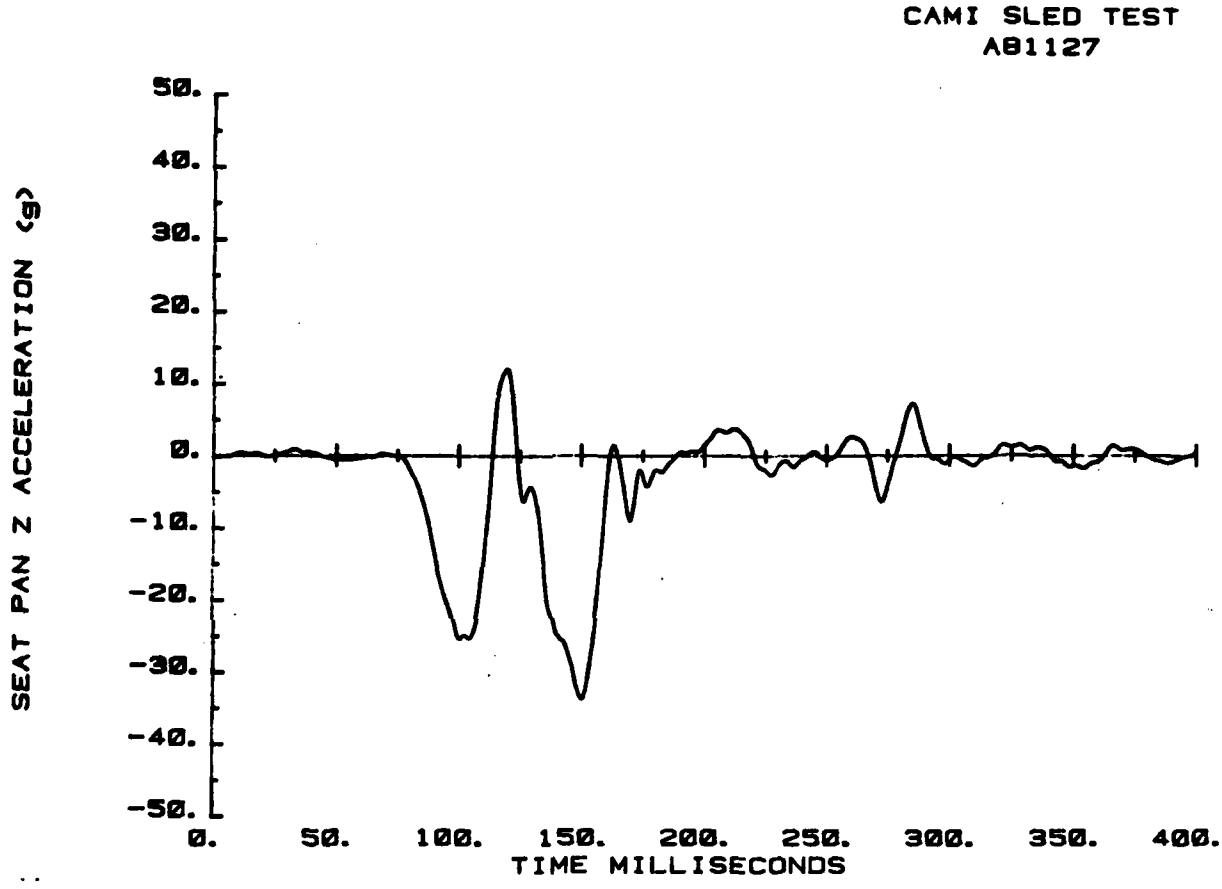

Figure 28. Vertical seat pan acceleration, Part 572 dummy, combined test.

4.0 TESTING AT WAYNE STATE UNIVERSITY

As discussed in the Introduction, a series of tests are being conducted to establish decelerative spinal fracture loads for occupants of energy-absorbing seats. In order to provide data for a comparison of cadaver and dummy response, five tests were conducted at Wayne State University with the instrumented Part 572 dummy under conditions similar to those used in the cadaver test series. Both vertical and combined mode tests were conducted. Three tests used 14.5-G energy absorbers, and two tests, specially designed 11.5-G devices, which were also used during the first phase of the cadaver test program. Results of comparable cadaver and dummy tests are shown in Table 2. Resultant peak body accelerations are presented for comparison because the accelerometer orientation in the cadaver does not necessarily correspond to the standard dummy coordinate system. The Dynamic Response Index (DRI), which is computed from the response of a single-degree-of-freedom damped, spring-mass model of the human torso, using seat acceleration as input, is also presented for these tests. The DRI has been correlated to ejection seat injury (References 11 and 12). Although it is not being proposed as an absolute measure of injury for the helicopter seat, its ability to integrate the input response waveform is considered meaningful.

Required seat stroke values presented in Tables 1 and 2 indicate that, in general, the Part 572 dummy requires slightly less stroke distance than does the cadaver. The seat pan vertical accelerations, presented in Figures 29 and 30 for the vertical and combined tests, respectively, show that the interaction between the Part 572 dummy and seat pan is very similar to the response measured with human cadavers. The comparison between body accelerations for the dummy and cadaver does not show a good correlation. Results of this limited comparison seem to indicate that seat performance criteria based on seat pan acceleration may not be as sensitive to occupant type as a criterion based on body segment acceleration. However, it may also indicate that injury mechanisms within

TABLE 1. COMPARISON OF SEAT AND OCCUPANT RESPONSE FOR DUMMIES AND CADAVERS

	Seat Stroke (in.)	Peak Acceleration (G)					Duration of Seat Pan z Acceleration at 23 G (sec)	DRI
		Seat Pan x	Seat Pan z	Pelvis Resultant	Chest Resultant	Head Resultant		
Dummy, Vertical	6.3	15.3	28.9	40.3	43.4	41.7	0.011	18.4
Cadaver, Vertical	7.6	17.5	26.5	33.9	N/A	49.7	0.004	21.8
Dummy, Combined	4.5	27.8	23.9	35.2	31.6	46.9	0.004	17.8
Cadaver, Combined	4.5	37.3	25.4	22.8	N/A	59.6	0.004	22.2
	5.5	40.5	21.0	44.4*	N/A	97.3*	0.	19.3

*Impact between mouth-mount accelerometer and thigh.

TABLE 2. COMPARISON OF SEAT STROKE FOR CADAVERS AND DUMMIES IN THE UH-60A CREWSEAT

Test Description	Cadaver Tests		Dummy Tests 50th% Hybrid II	
	Occupant Weight (lb)	Seat Stroke (in.)	Occupant Weight (lb)	Seat Stroke (in.)
14.5-G E/A, Vertical Orientation, 42-45 G Peak Input Acceleration	166	7.6	164	6.3
	160	7.4	164	7.0
	140	7.1		
	148	7.1		
14.5-G E/A, Combined Orientation, 42-45 G Peak Input Acceleration	166	5.5	164	4.5
	140	4.5		
11.5-G E/A, Combined Orientation, 42-45 G Peak Input Acceleration	218	9.4	164	6.5
	141	7.0		
	160	9.0		
8.5-G E/A, Combined Orientation, 42-45 G Peak Input Acceleration	200	13.1		
	143	9.7		

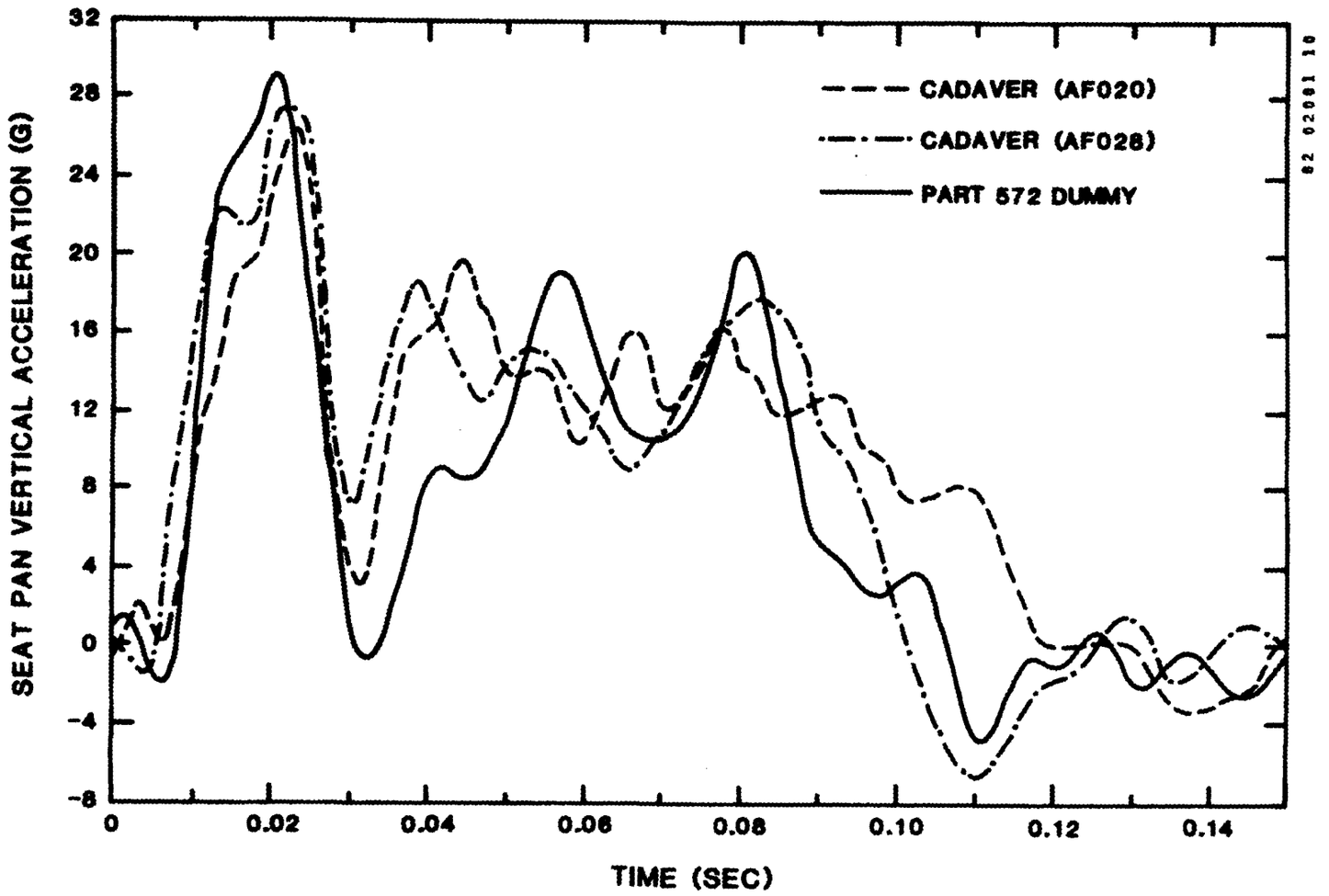

Figure 29. Seat pan vertical acceleration for a Part 572 dummy and two cadavers measured in vertical mode tests with 14.5-G energy absorbers.

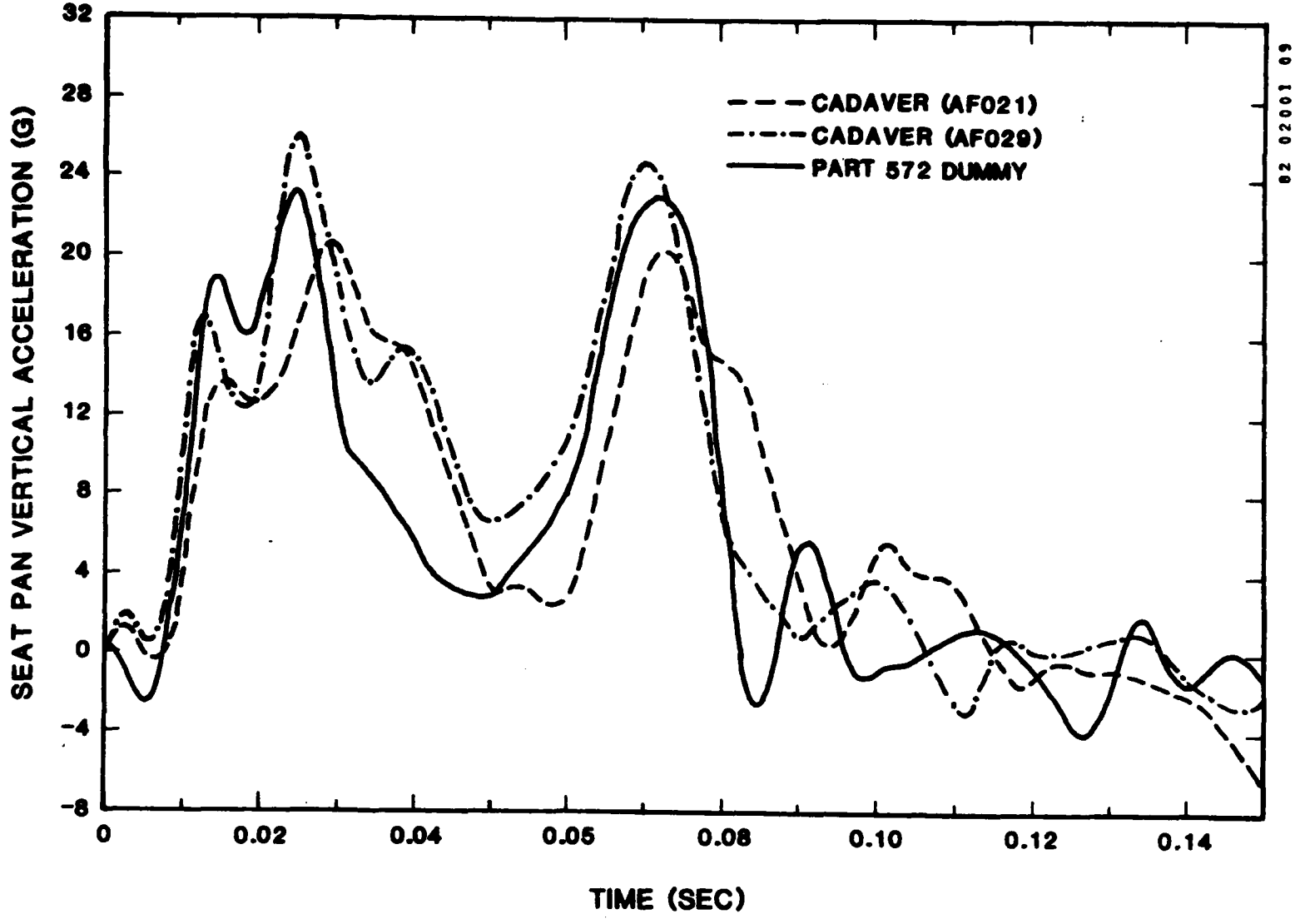

Figure 30. Seat pan vertical acceleration for a Part 572 dummy and two cadavers measured in combined mode tests with 14.5-G energy absorbers.

the body, e.g., spinal deformation, cannot be reliably predicted from seat pan acceleration, as internal body response can vary significantly for various occupant types with similar inputs from the seats.

5.0 DISCUSSION OF RESULTS

A question of interest concerning use of the dummies modified as described in Chapter 2 is whether their response characteristics were altered. Therefore, data from the tests described in this report were compared with results of earlier tests conducted under similar conditions using dummies of the same design as part of the program described in Section 1.1. Data from the rigid seat tests do not exhibit any differences in accelerations or forces measured before and after installation of the transducers. However, a trend was observed in the data from the tests that used the energy-absorbing seat. In these tests, for which the input deceleration was approximately three times higher than for the rigid seat tests, the vertical energy-absorbing system on the seat attenuated the z-components of dummy accelerations to the same order as those measured in the rigid seat tests, but the x-components were significantly higher. For both dummies, the x-component of chest acceleration was higher after installation of the lumbar load cell, indicating a possible alteration of torso flexural characteristics. Comparisons of these chest x-accelerations are presented in Figures 31 and 32 for the Part 572 dummy in the vertical and combined tests, respectively, and in Figure 33 for the VIP-95 dummy. In each of these plots, the high positive acceleration corresponds to maximum dummy forward displacement relative to the seat.

The x-component of head acceleration appeared different in the Part 572 combined test and the VIP-95 vertical test, as shown in Figures 34 and 35, respectively. For the latter dummy it is not known whether the change in head acceleration resulted from the modification to the neck or from the change in input from the chest. However, as shown in Figures 36 and 37, respectively, the z-component of head acceleration did not change for the Part 572 dummy, in which the neck was not modified, whereas for the VIP-95 a significant change did occur. Therefore, it is quite likely that some alteration of neck response characteristics was produced. The moment-rotation characteristics for the VIP-95 neck were measured

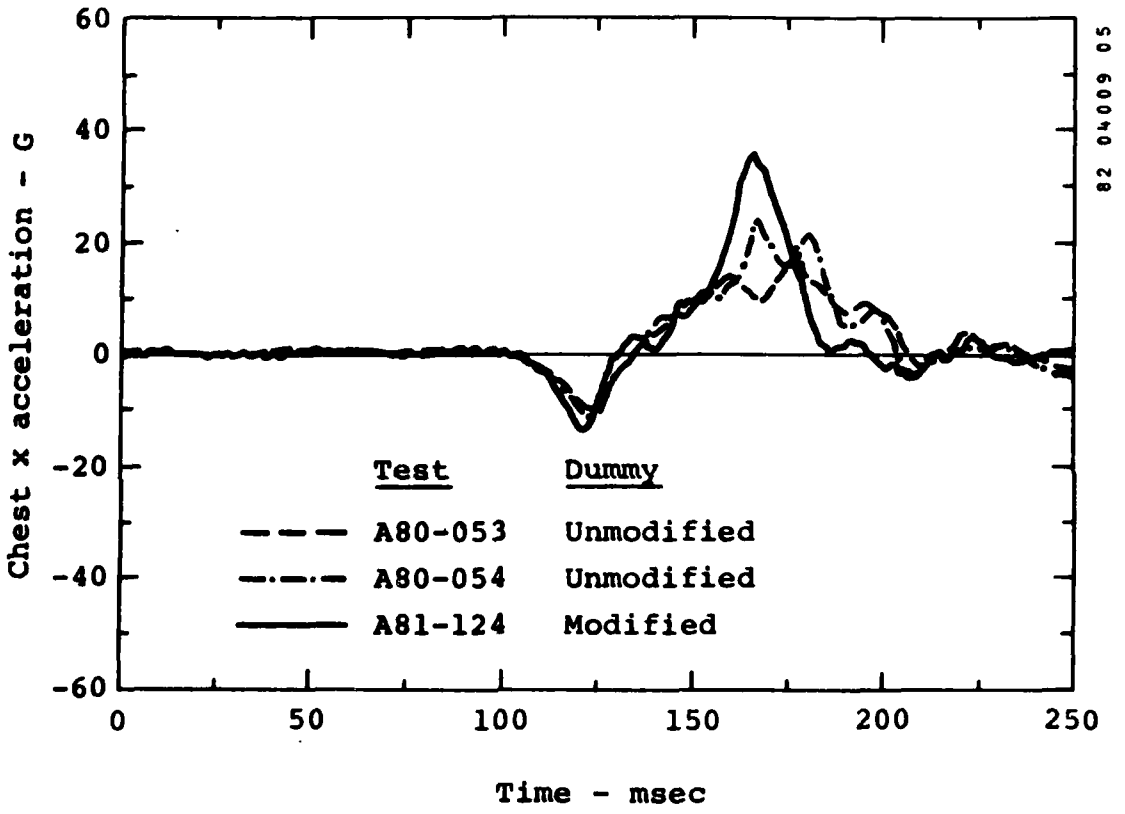

Figure 31. X-component of chest acceleration, Part 572 dummy, 42-ft/sec, 41-G vertical test.

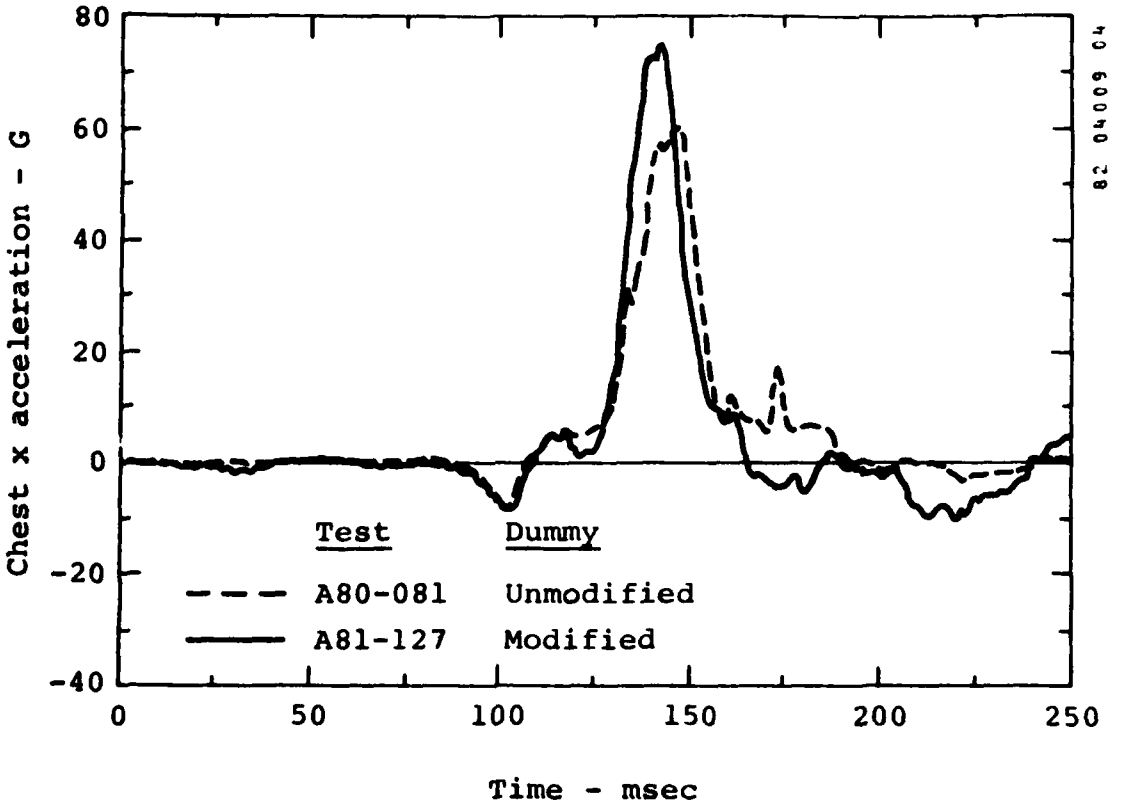

Figure 32. X-component of chest acceleration, Part 572 dummy, 50-ft/sec, 47-G combined test.

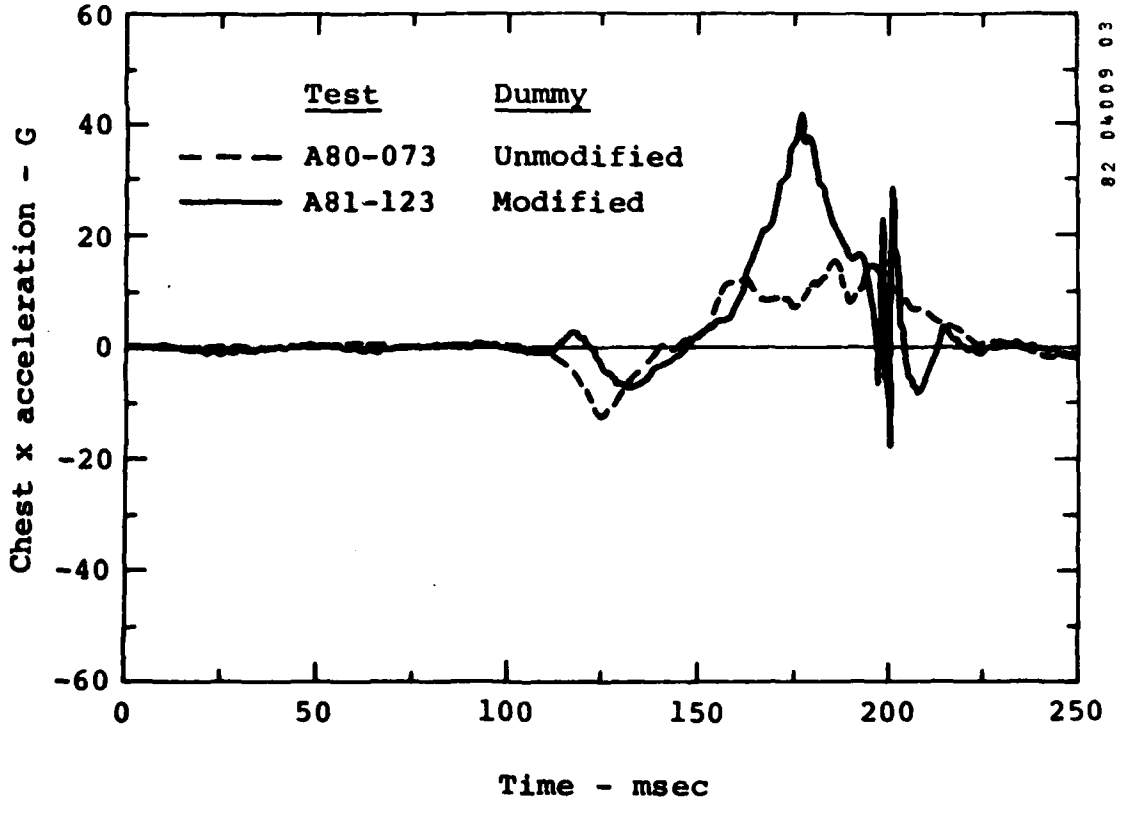

Figure 33. X-component of chest acceleration, VIP-95 dummy, 42-ft/sec, 40-G vertical test.

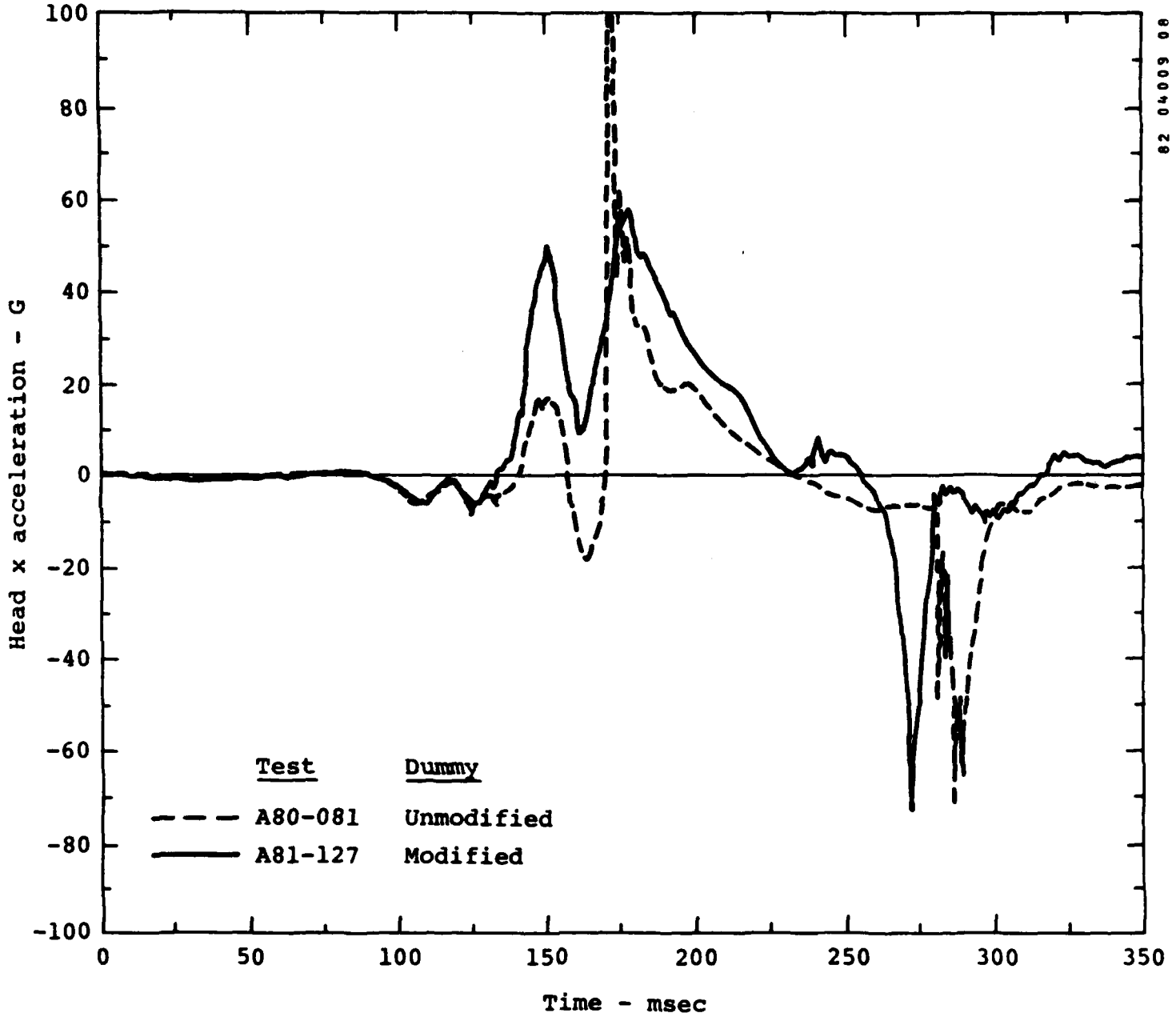

Figure 34. X-component of head acceleration, Part 572 dummy, 50-ft/sec, 47-G combined test.

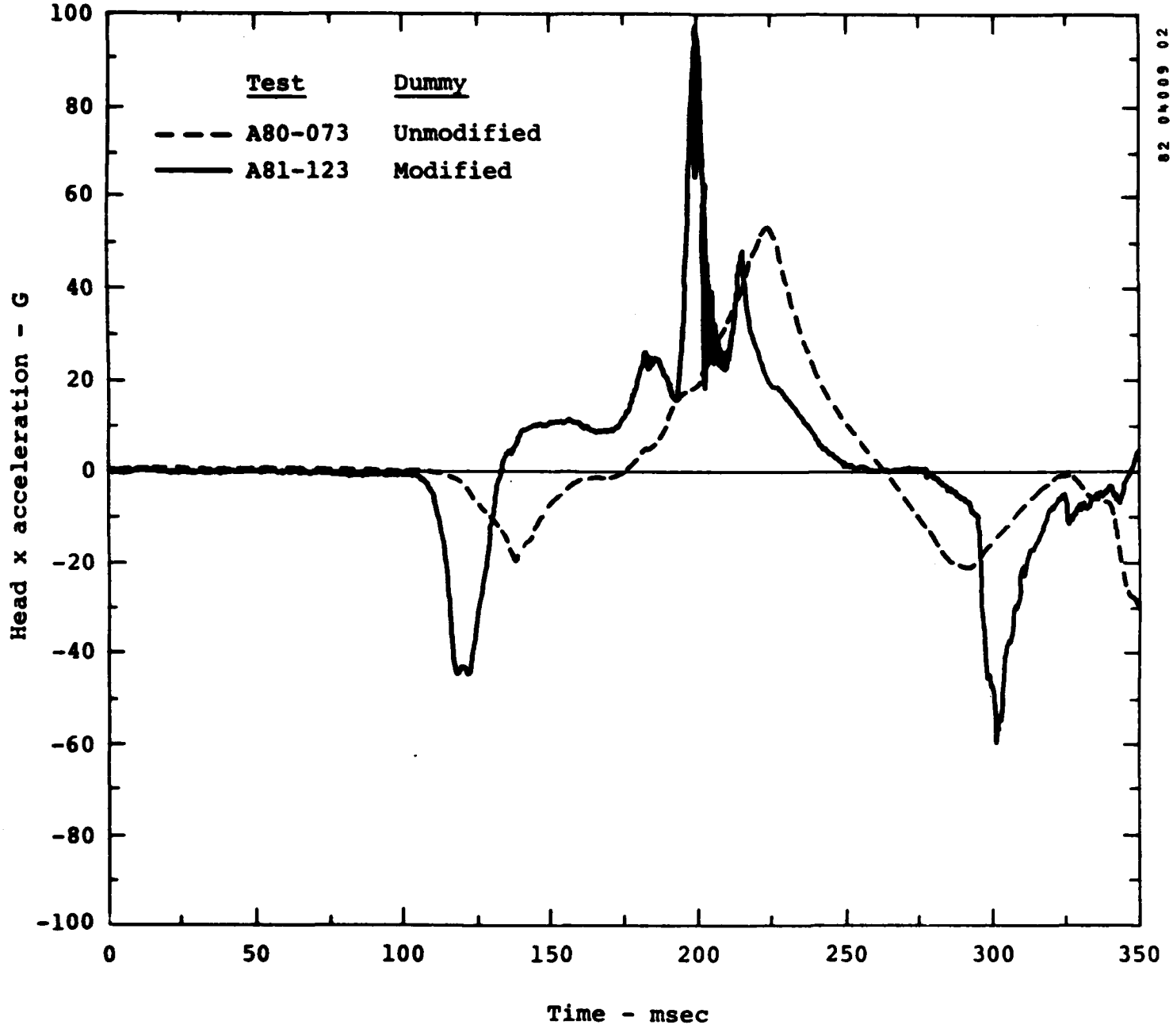

Figure 35. X-component of head acceleration, VIP-95 dummy, 42-ft/sec, 40-G vertical test.

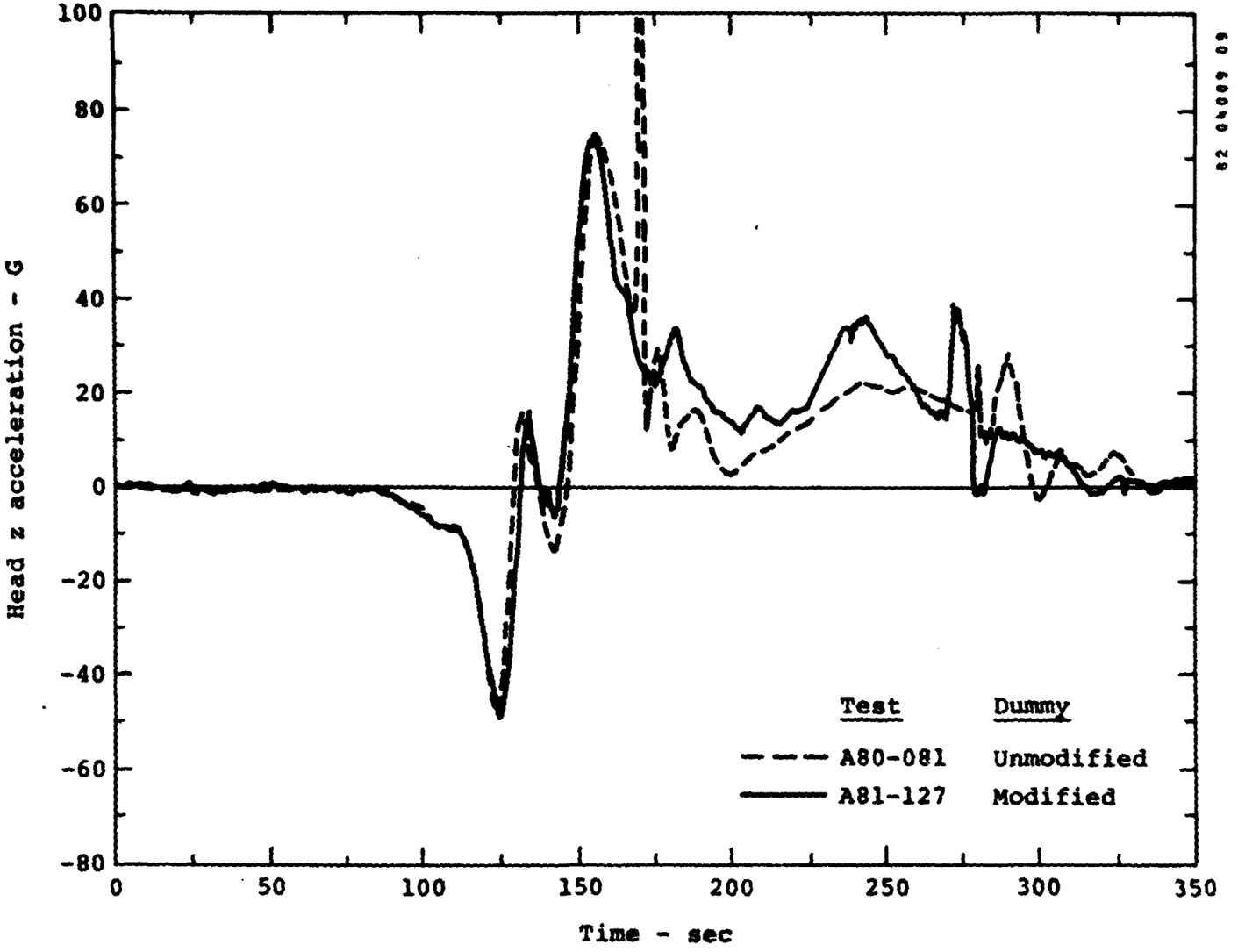

Figure 36. Z-component of head acceleration, Part 572 dummy, 50-ft/sec, 47-G combined test.

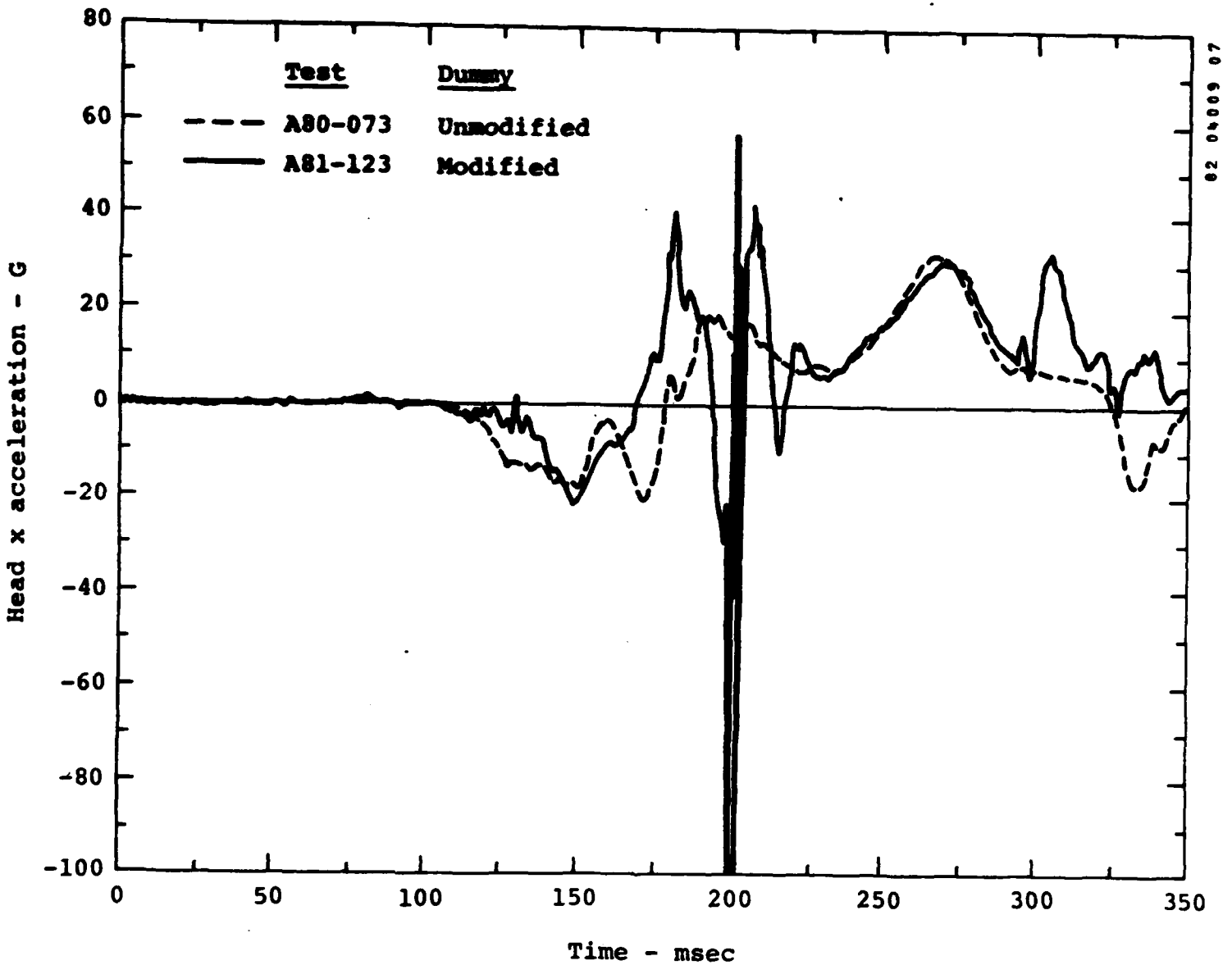

Figure 37. Z-component of head acceleration, VIP-95 dummy, 42-ft/sec, 40-G vertical test.

statically at CAMI, and the results are compared in Figure 38 with a flexion response envelope which was proposed in Reference 13 as a result of human volunteer and cadaver tests. It appears that the dummy neck response characteristics provide an adequate human simulation.

In the 40-G vertical test with the VIP-95 dummy the load cell installed in the neck measured a maximum shear force in the x-direction of approximately 800 lb. Reference 13 reported measuring shear forces of 357 and 437 lb without damage in dynamic tests of two cadavers. Also, in the same 40-G dummy test, the neck load cell measured maximum bending moments (y-axis) of approximately 900 in.-lb in extension and in excess of 2000 in.-lb in flexion. Reference 13 suggests tolerable levels of 504 in.-lb in extension and 1,680 in.-lb in flexion, measured with respect to the occipital condyles. For direct comparison with those values, the moments measured in the dummy near the base of the neck would have to be reduced to account for the difference in moment arm.

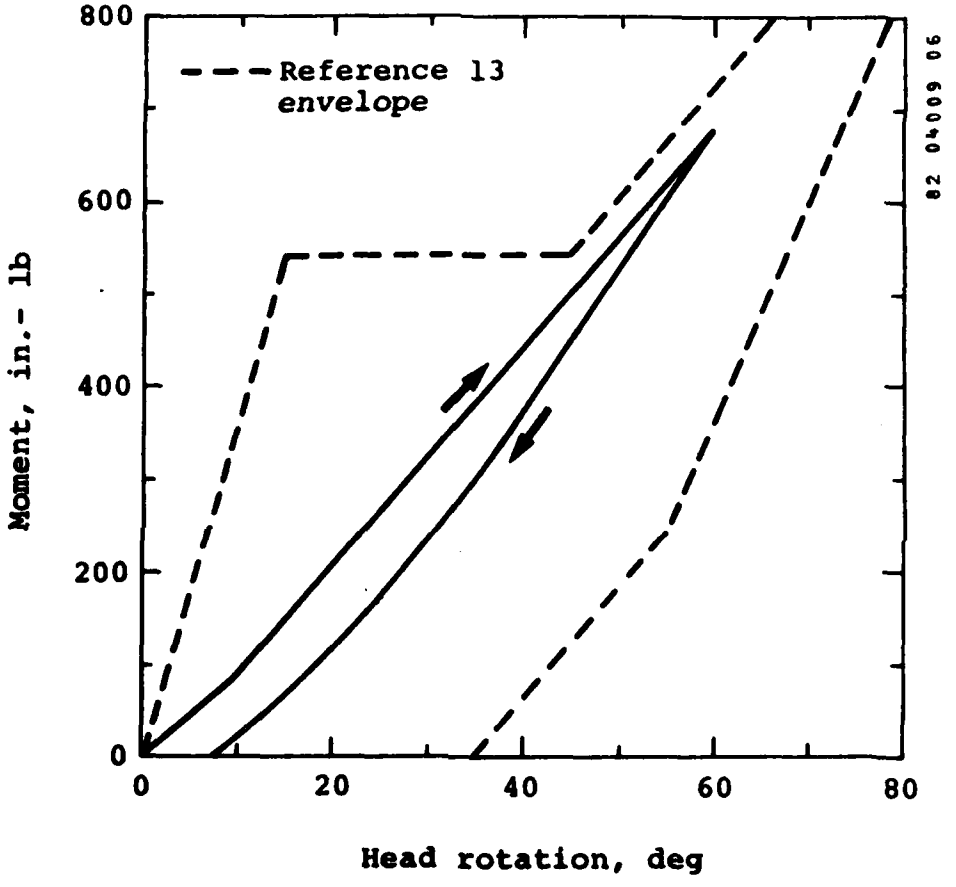

Figure 38. Response of VIP-95 neck compared with proposed flexion response envelope of Reference 13.

6.0 CONCLUSIONS

The results of this program indicate that forces and moments in the spine of an anthropomorphic dummy of Part 572 or similar design can be measured with a rather simple modification. However, for use of these measurements as predictors of vertebral injury, they must be correlated to fractures in the human spine. Tolerable levels of shear force and bending moment for the neck have been proposed in Reference 13, but a detailed comparison of dummy and cadaver head-neck anthropometry is required to relate the load cell measurements to these levels.

The modifications made to the dummies in this program appear to have altered the x-direction dynamic response of the upper torso and, in the case of the VIP-95, the head. The change in response was observed only in the energy-absorbing seat tests, where the peak chest acceleration reached 20 G and higher, and probably resulted from an altered natural frequency for torso bending due to installation of the load cell and adapters. In any future design of a standardized transducer installation, the dynamic response characteristics of the torso should be considered. Because the neck modification was simpler, merely replacing a stiff steel section with the load cell, a change in neck response characteristics appears less likely, but this should be verified.

7.0 ACKNOWLEDGMENTS

This program was conducted under Contract DAMD17-81-C-1175 with the U.S. Army Aeromedical Research Laboratory, where Mr. Joseph L. Haley, Jr., was the Technical Monitor. Funds were also provided by the Naval Air Development Center. The dummies and load cells were provided by the Protection and Survival Laboratory of the FAA Civil Aeromedical Institute, where testing was conducted under the leadership of Mr. Richard F. Chandler. Testing at Wayne State University was performed under the direction of Dr. Albert I. King.

8.0 REFERENCES

1. Singley, G. T., III, and Desjardins, S. P., Crashworthy Helicopter Seats and Occupant Restraint Systems, in Operational Helicopter Aviation Medicine, AGARD Conference Proceedings No. 255, North Atlantic Treaty Organization, Advisory Group for Aerospace Research and Development, Neuilly sur Seine, France, May 1978.

2. Crash Survival Design Guide, Dynamic Science, A Division of Marshall Industries, USAAMRDL Technical Report 71-22, Fort Eustis, Virginia, Eustis Directorate, U.S. Army Air Mobility Research and Development Laboratory, 1971.

3. Military Standard, MIL-STD-1290(AV), Light Fixed - Rotary-Wing Aircraft Crashworthiness, Department of Defense, Washington, D.C., 25 January 1974.

4. Military Specification, MIL-S-58095(AV), Seat System: Crashworthy, Non-Ejection, Aircrew, General Specification For, Department of Defense, Washington, D.C., 27 August 1971.

5. Desjardins, S. P., and Harrison, H., The Design, Fabrication, and Testing of an Integrally Armored Crashworthy Crewseat, Dynamic Science, Division of Marshall Industries; USAAMRDL Technical Report 71-54, Eustis Directorate, U.S. Army Air Mobility Research and Development Laboratory, Fort Eustis, Virginia, January 1972, AD 742733.

6. Desjardins, S. P., and Laananen, D. H., Aircraft Crash Survival Design Guide, Volume IV - Aircraft Seats, Restraints, Litters, and Padding, Simula Inc., USARTL-TR-79-22D, Applied Technology Laboratory, U.S. Army Research and Technology Laboratories (AVRADCOM), Fort Eustis, Virginia, June 1980.

7. Laananen, D. H., Aircraft Crash Survival Design Guide, Volume II - Aircraft Crash Environment and Human Tolerance, Simula Inc., USARTL-TR-79-22B, Applied Technology Laboratory, U.S. Army Research and Technology Laboratories (AVRADCOM), Fort Eustis, Virginia, January 1980.

8. King, A. I., and Levine, R. S., Human Cadaveric Response to Simulated Helicopter Crashes, in Impact Injury: Mechanisms, Prevention and Cost, AGARD, North Atlantic Treaty Organization, Advisory Group for Aerospace Research and Development, Neuilly sur Seine, France, April 1982.

9. Chandler, R. F., and Young, J., Uniform Mass Distribution Properties and Body Size Appropriate for the 50 Percentile Male Aircrewmember During 1980-1990, Civil Aeromedical Institute, Protection and Survival Laboratory, Memorandum Report No. AAC-119-81-4 (Draft), Federal Aviation Administration, Mike Monroney Aeronautical Center, Oklahoma City, March 1981.

10. Code of Federal Regulations, "Anthropomorphic Test Dummy," Title 49, Chapter 5, Part 572, Federal Register, Vol. 38, No. 62, April 2, 1973, pp. 8455-8458.

11. Stech, E. L., and Payne, P. R., Dynamic Models of the Human Body, Frost Engineering Development Corp. AMRL Technical Report 66-157, Aerospace Medical Research Laboratory, Wright-Patterson Air Force Base, Ohio, November 1969, AD 701383.

12. Brinkley, J. W., and Shaffer, J. T., Dynamic Simulation Techniques for the Design of Escape Systems: Current Applications and Future Air Force Requirements, Aerospace Medical Research Laboratory; AMRL Technical Report 71-29-2, Wright-Patterson Air Force Base, Ohio, December 1971, AD 740439.

13. Mertz, H. J., and Patrick, L. M., "Strength and Response of the Human Neck," SAE Paper 710855, Proceedings of the Fifteenth Stapp Car Crash Conference, Society of Automotive Engineers, Inc., 1971.

APPENDIX A

CAMI RIGID SEAT TESTS

A81-121	Part 572 (50th-percentile) Dummy
A81-122	VIP-95 Dummy

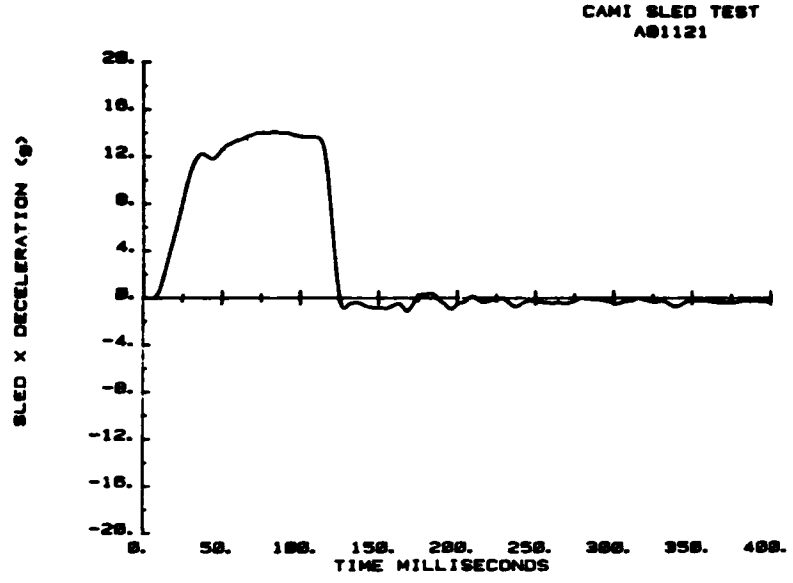

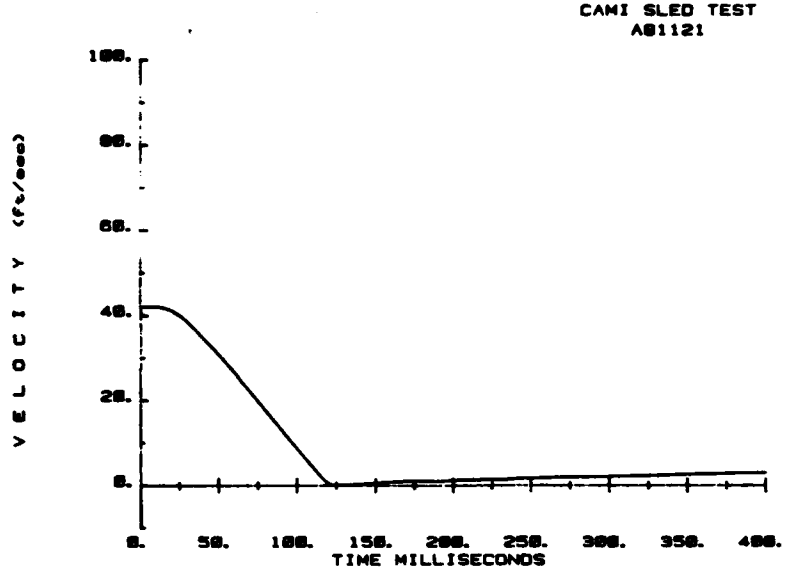

Sled deceleration and velocity.

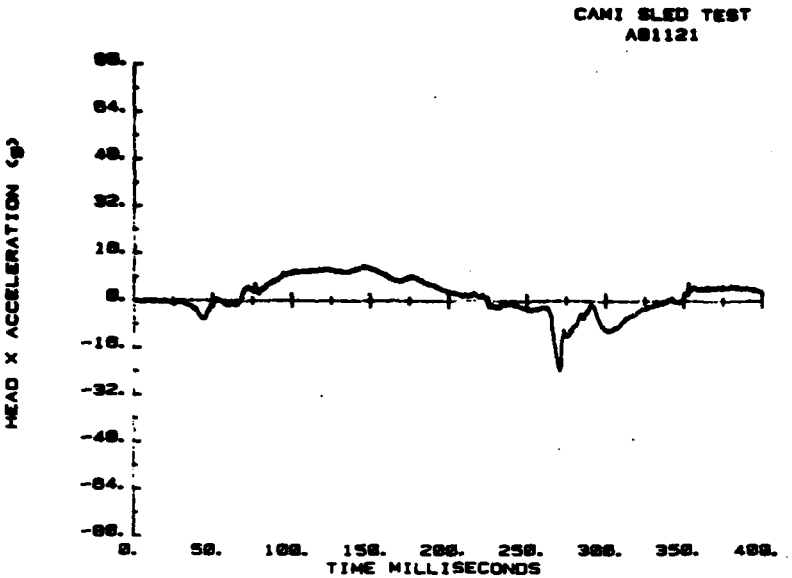

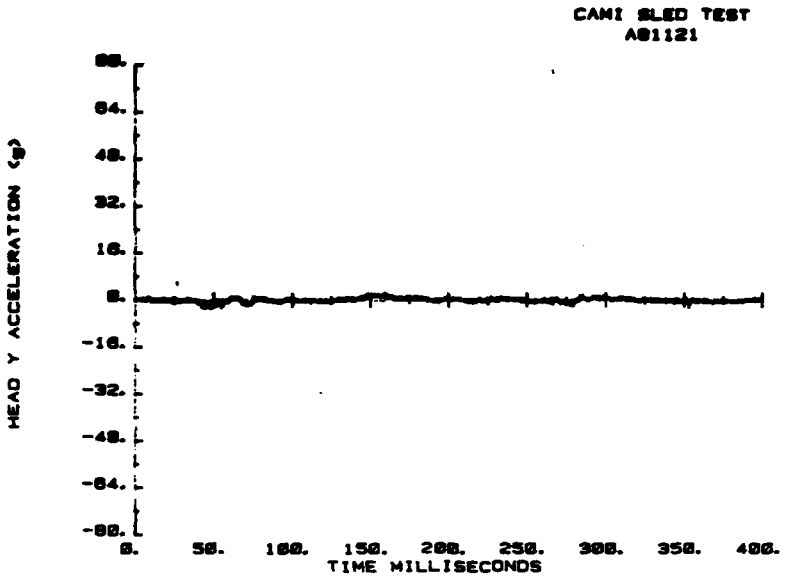

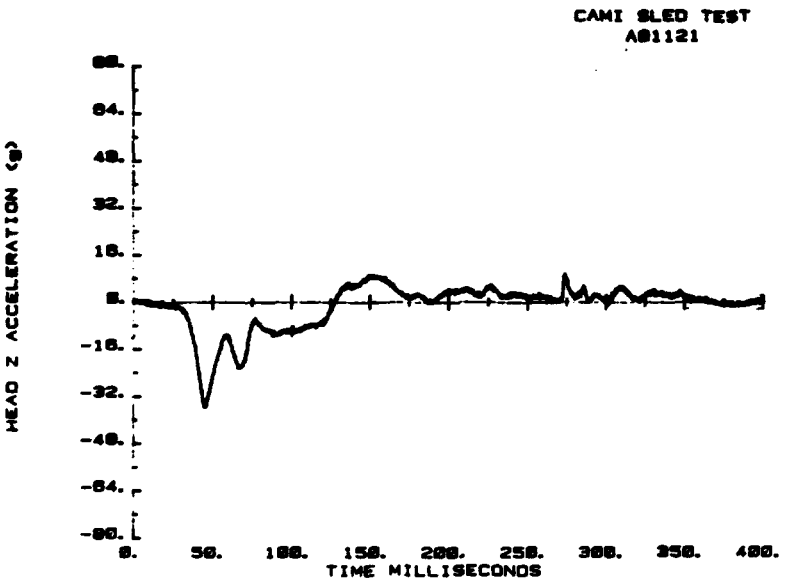

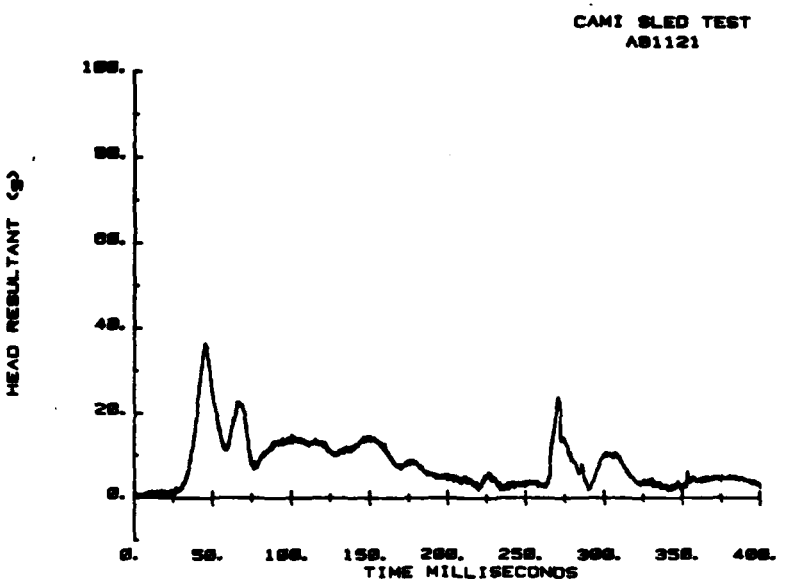

Head acceleration.

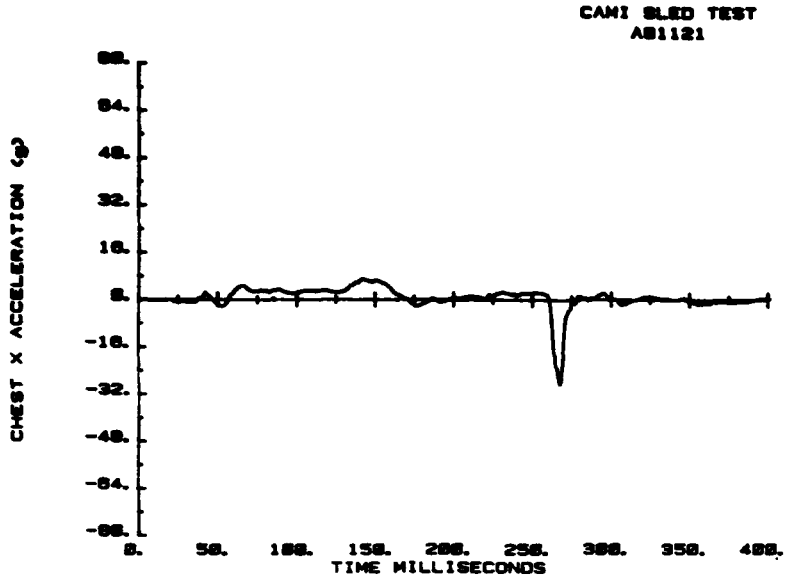

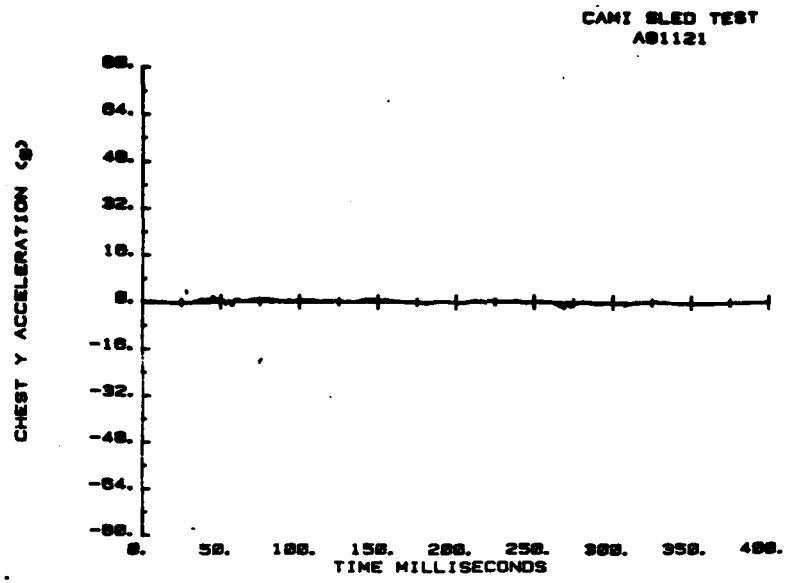

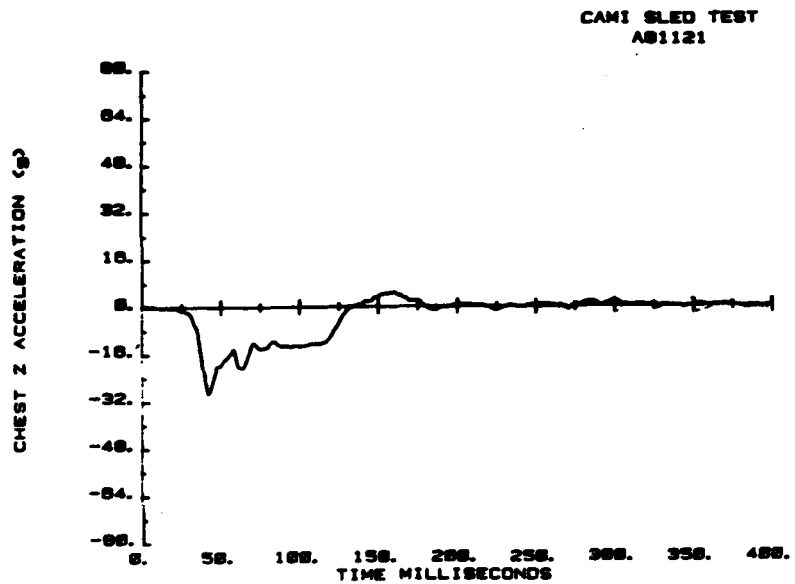

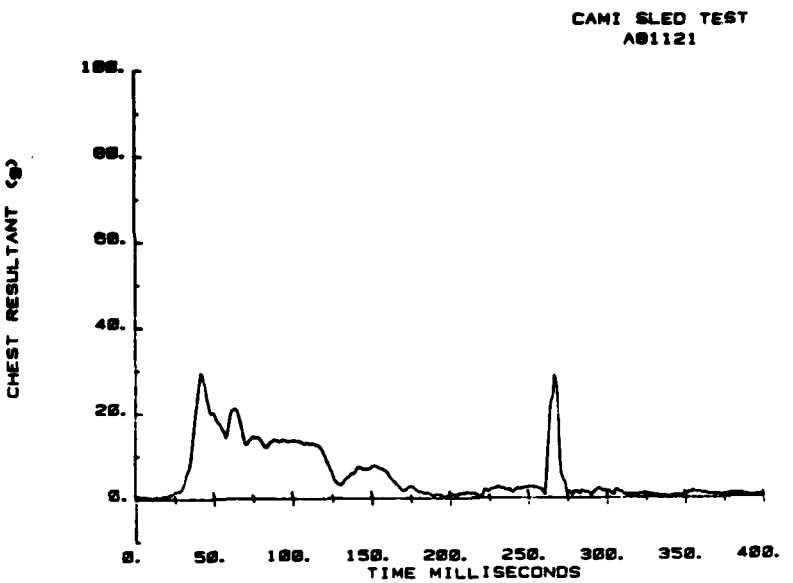

Chest acceleration.

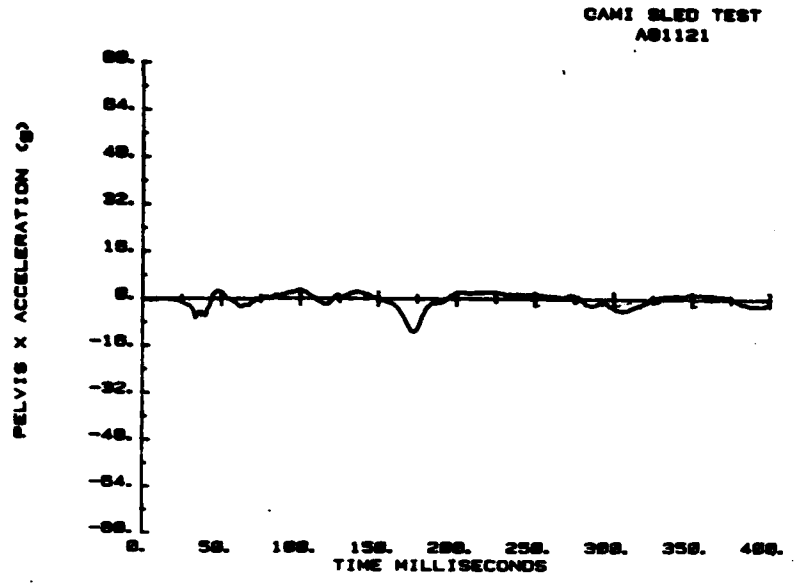

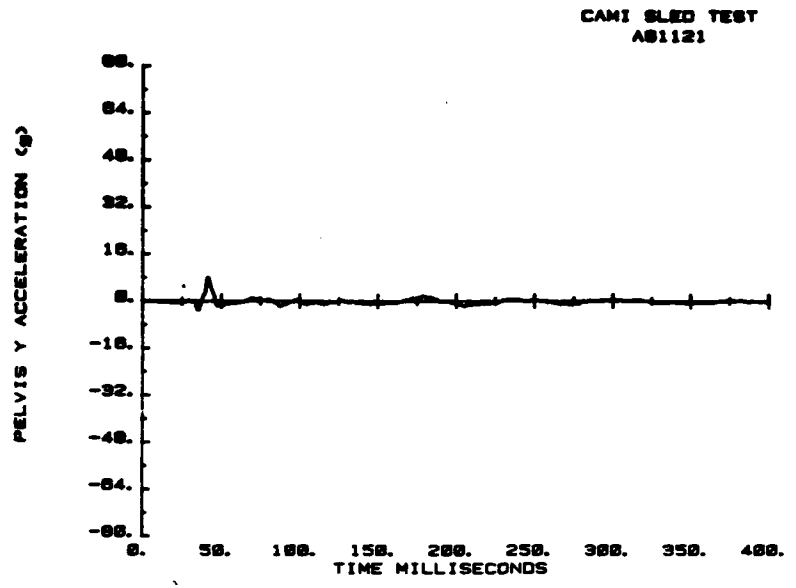

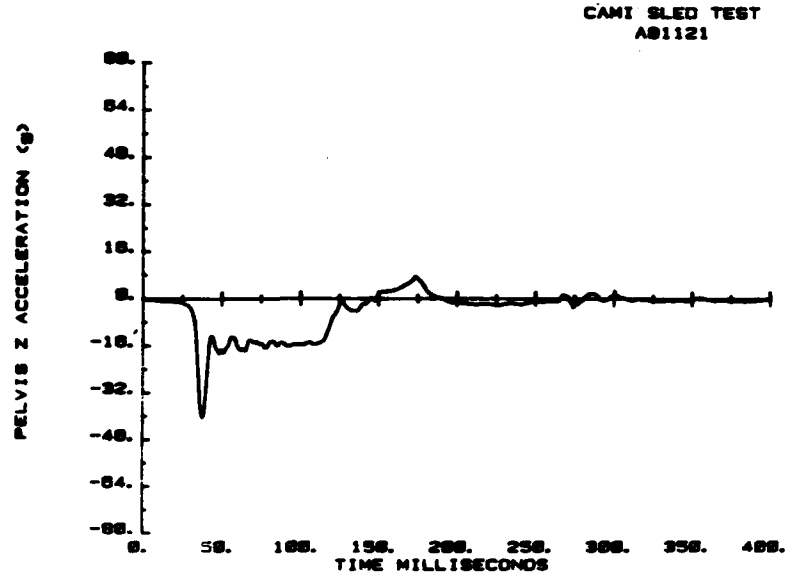

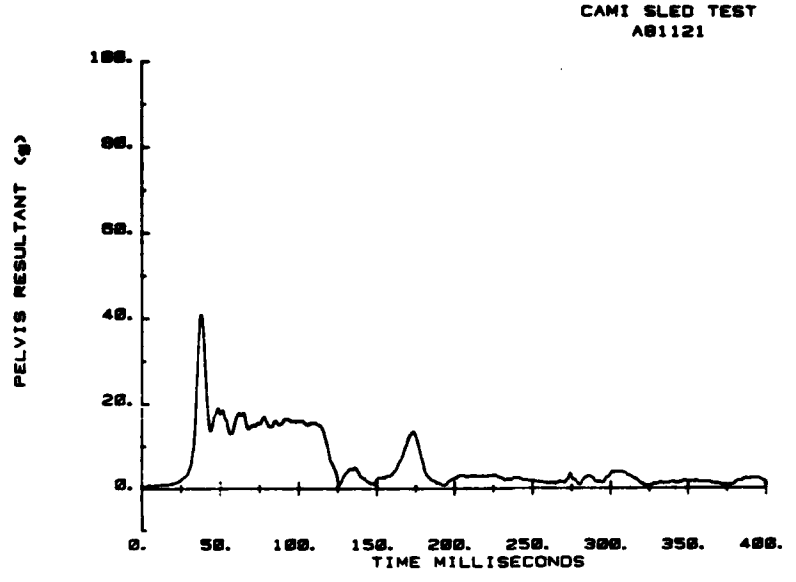

Pelvis acceleration.

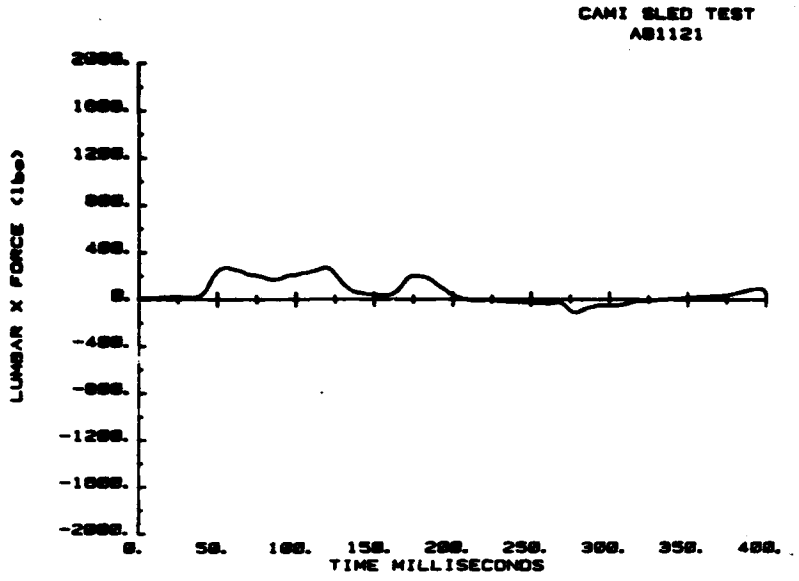

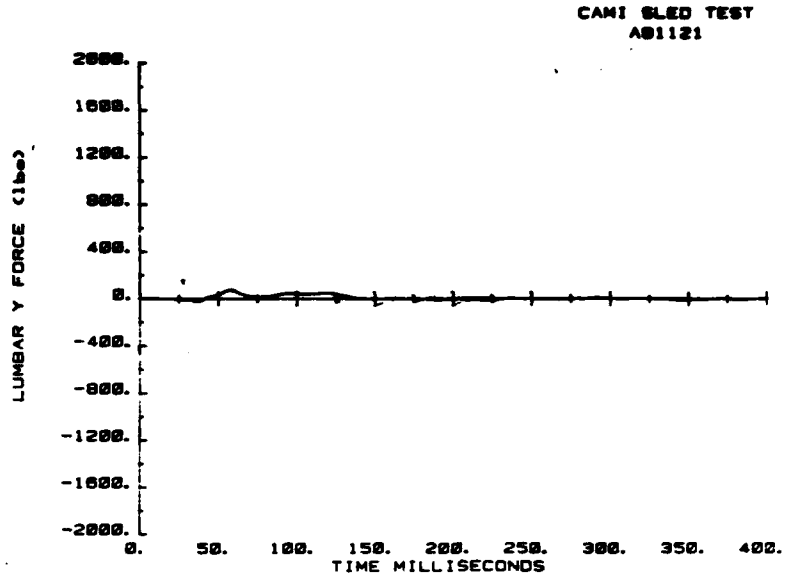

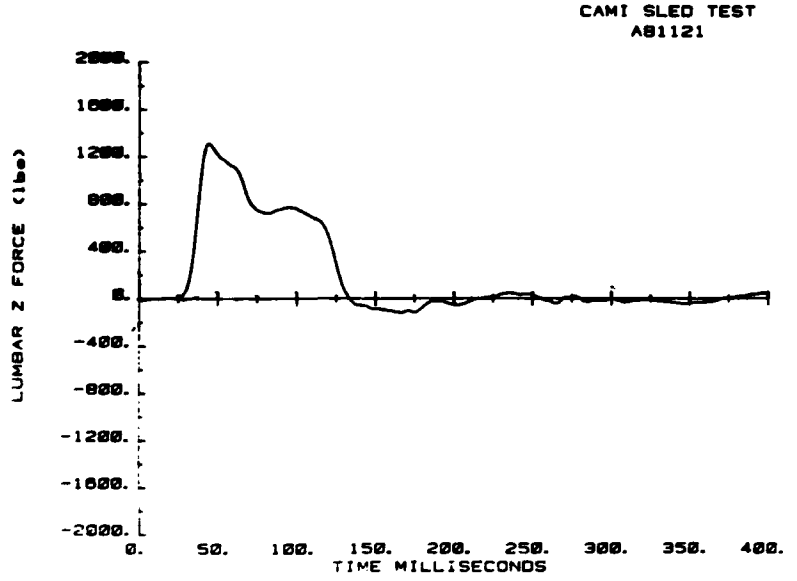

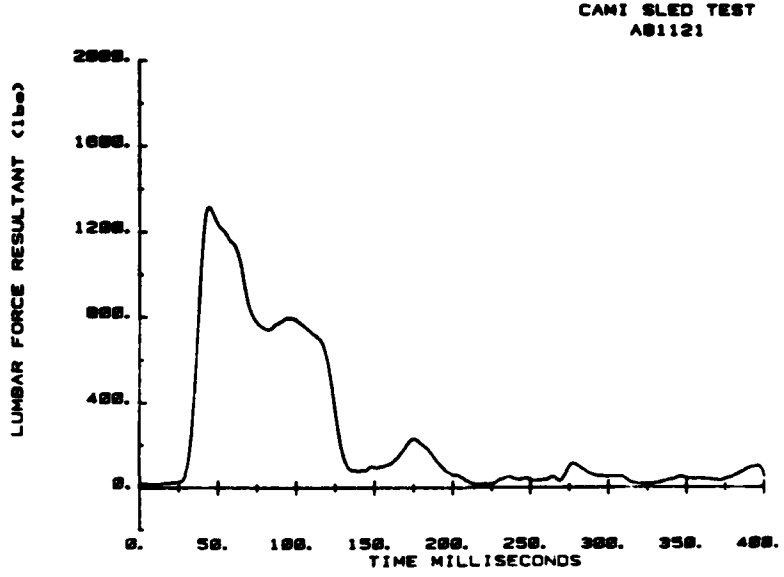

Lumbar force.

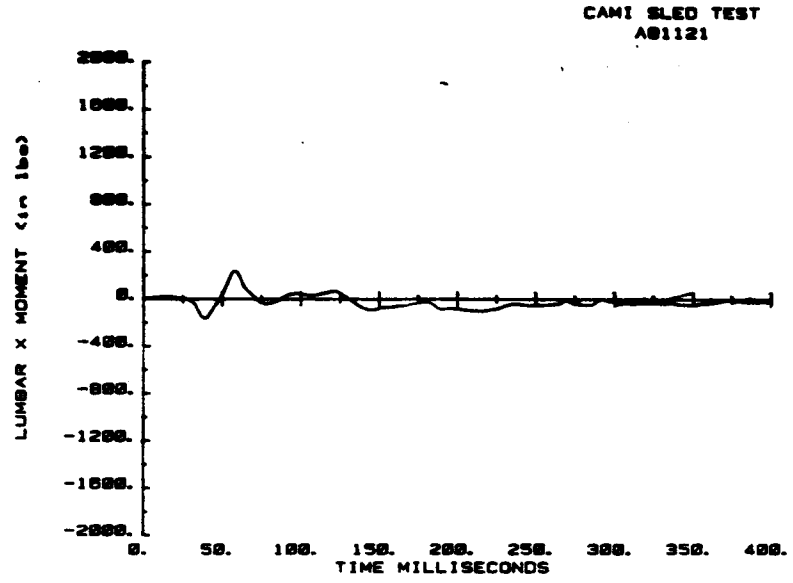

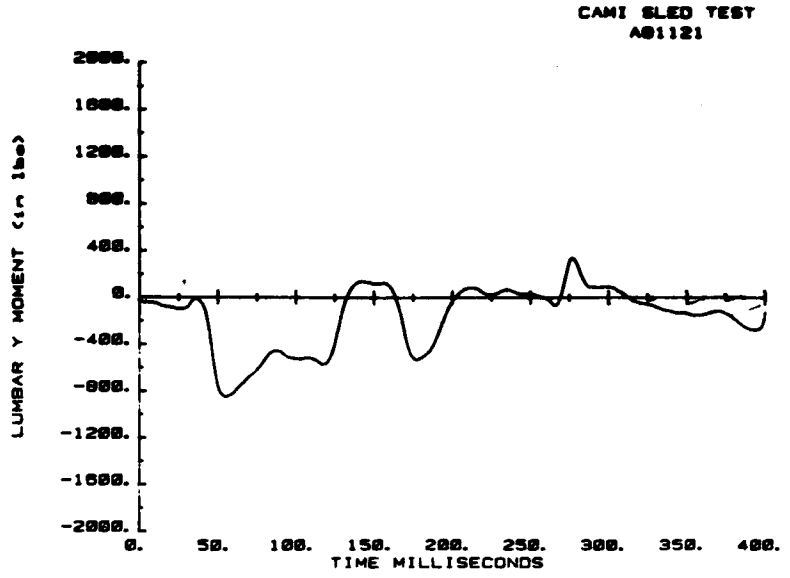

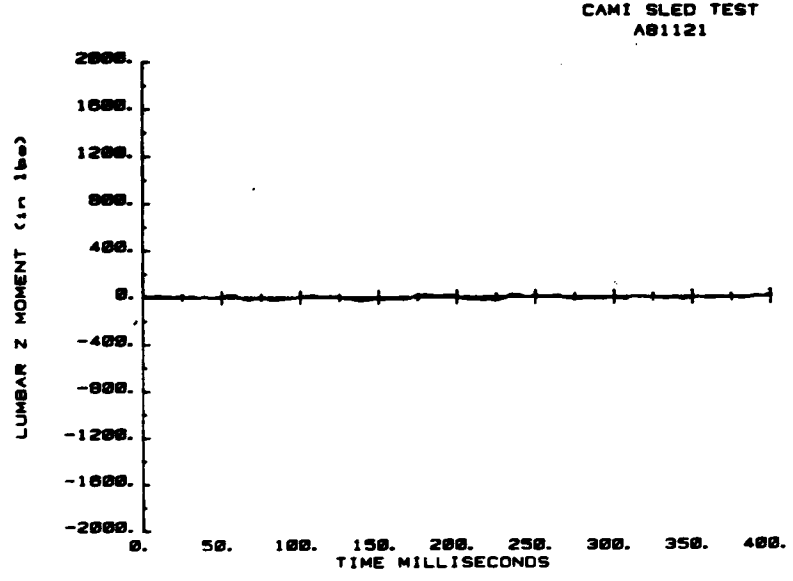

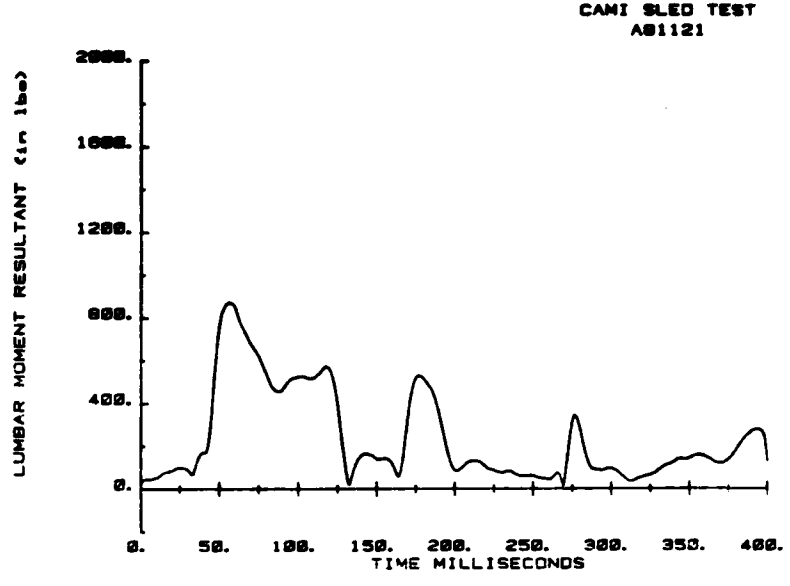

Lumbar moment.

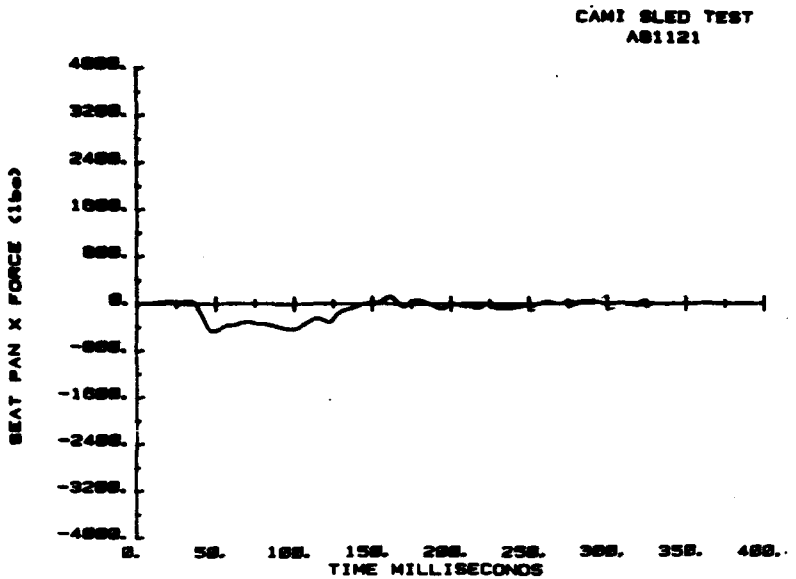

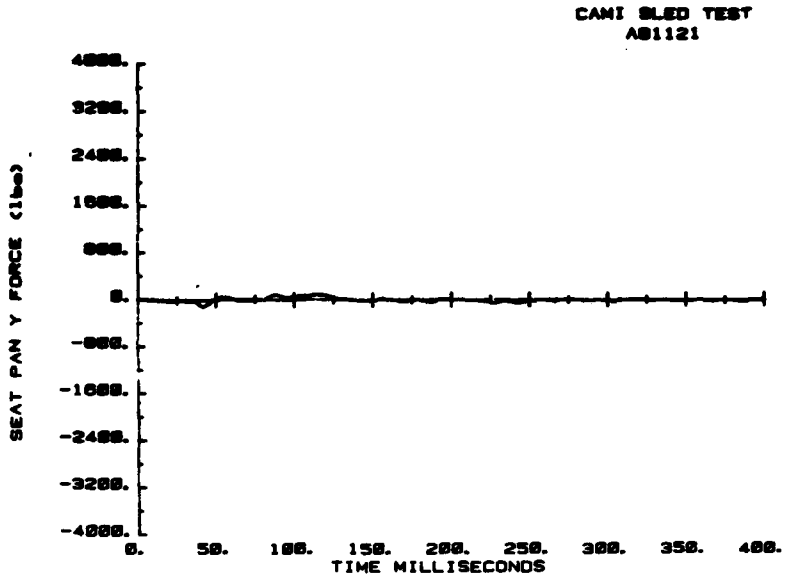

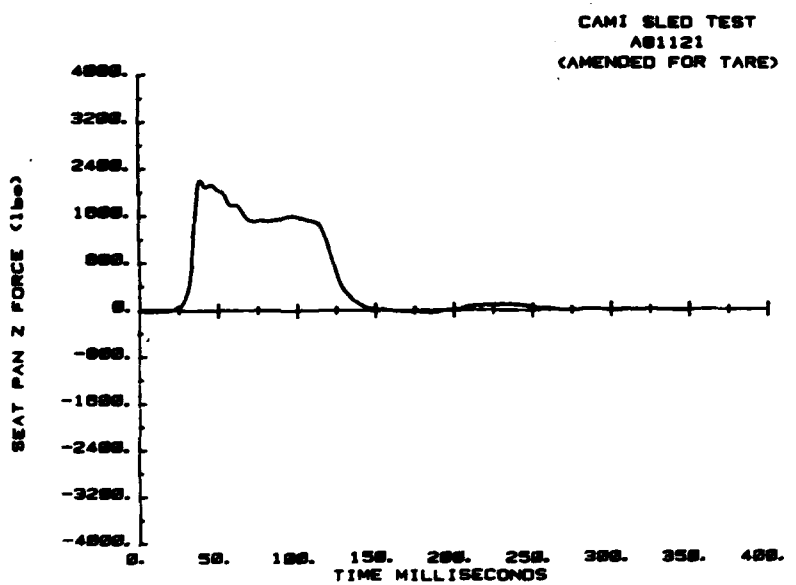

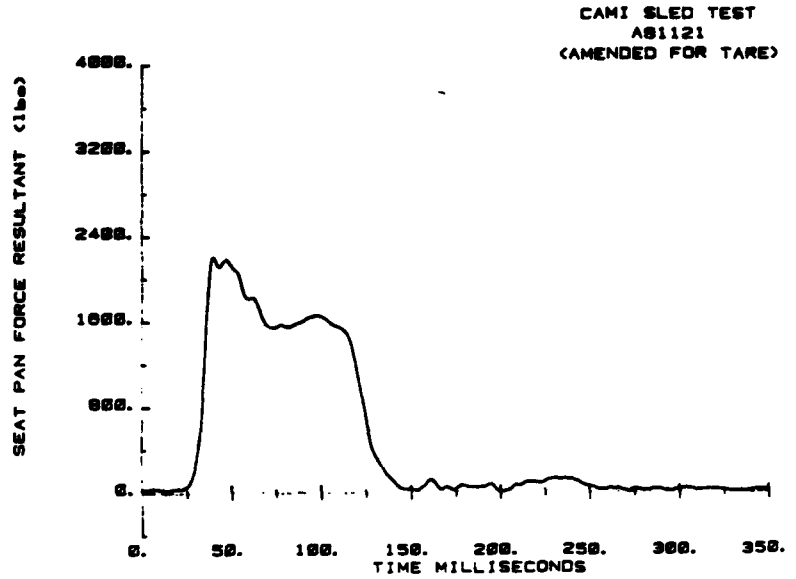

Seat pan force.

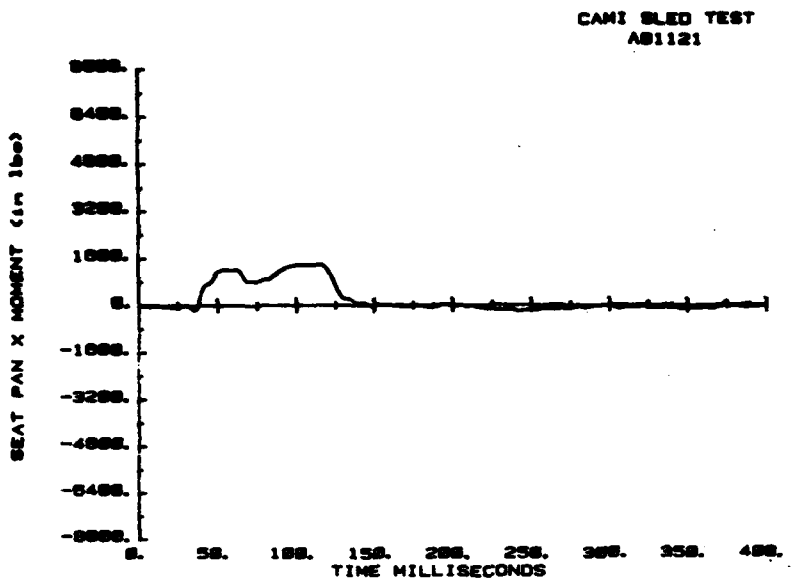

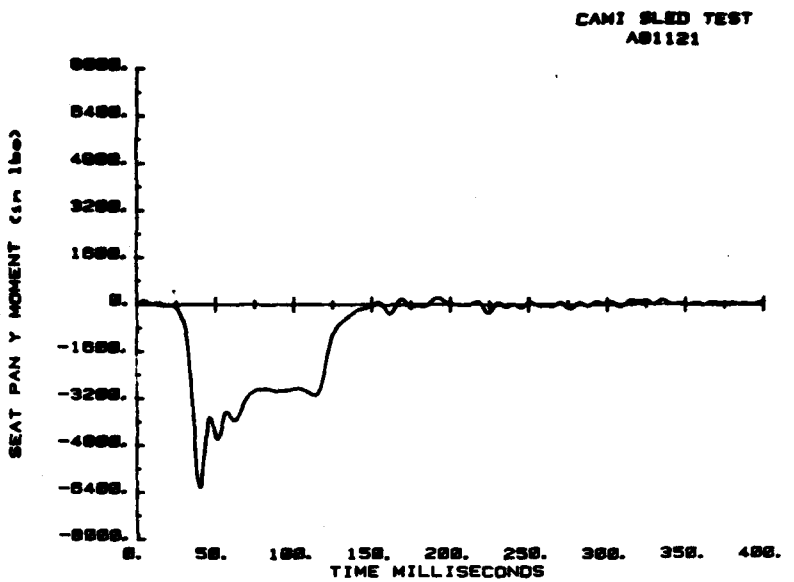

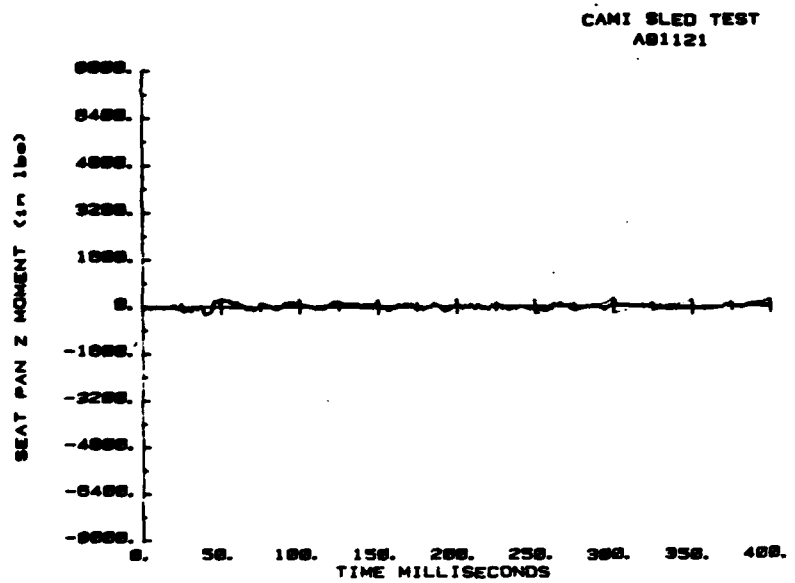

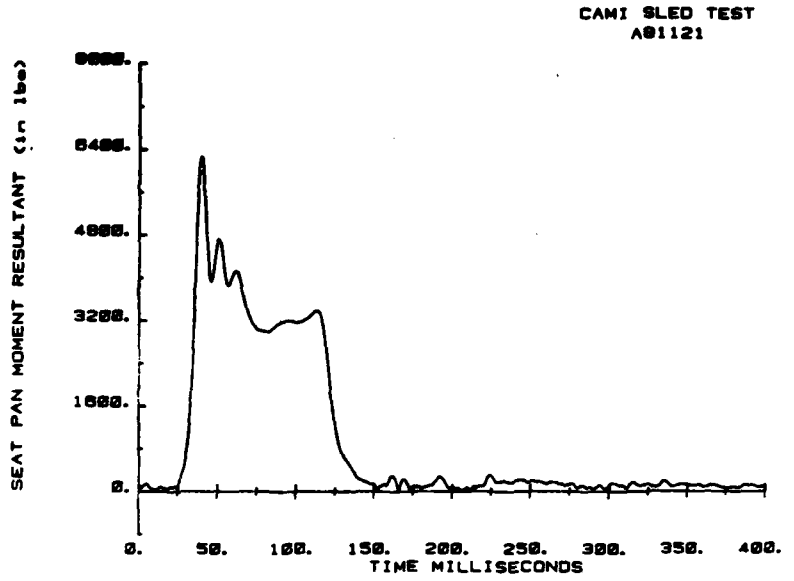

Seat pan moment.

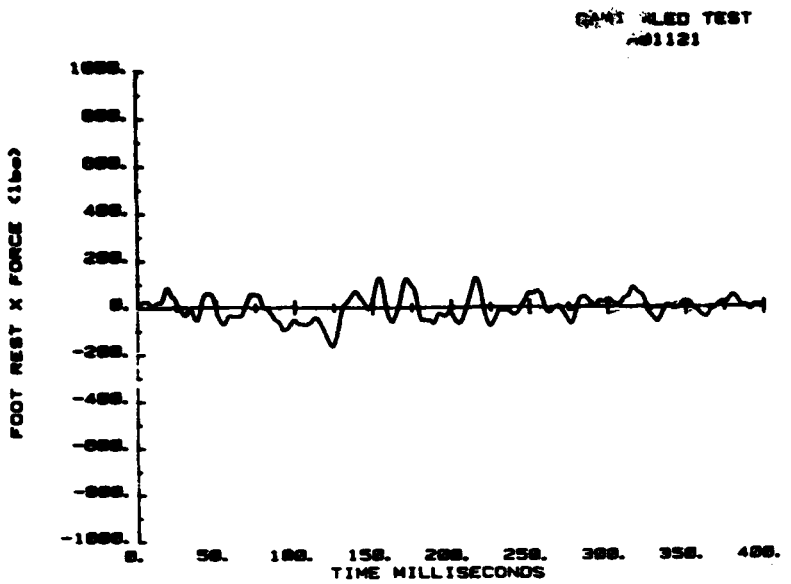

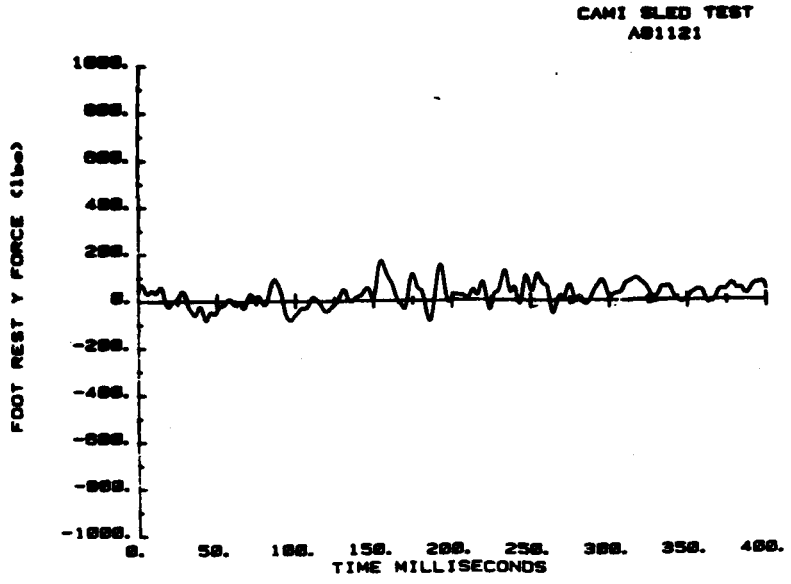

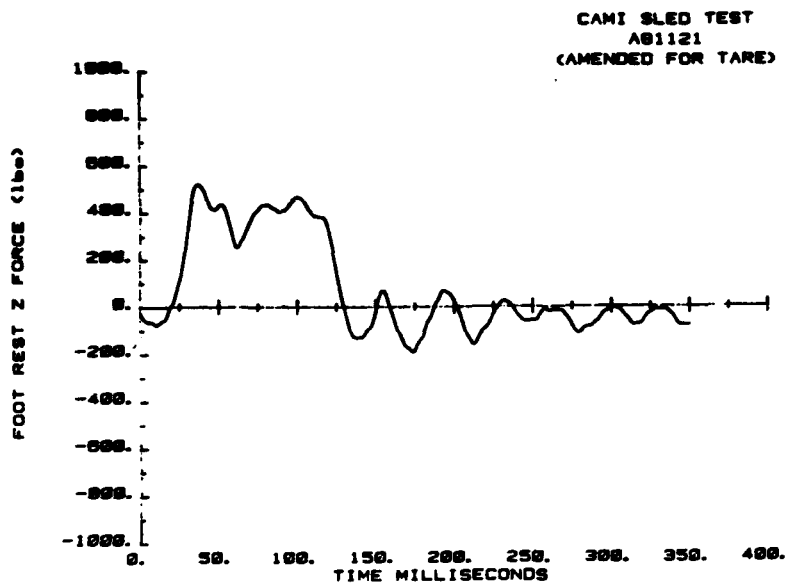

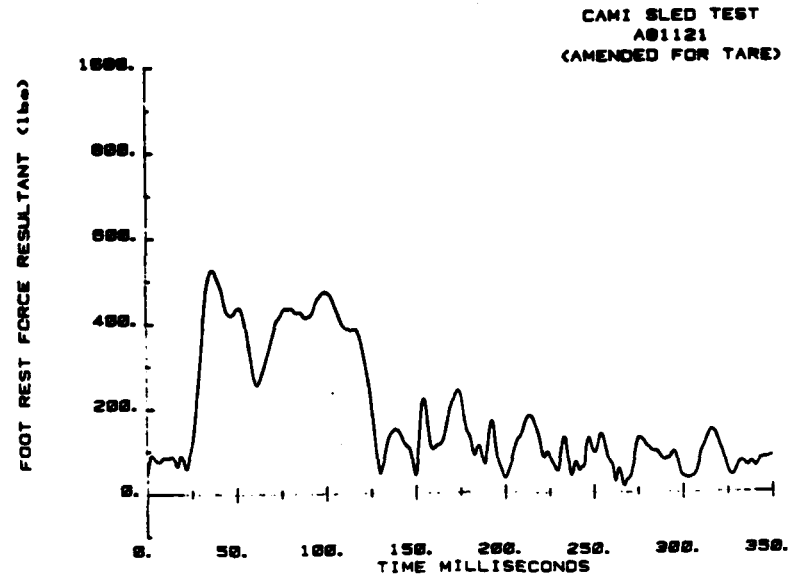

Footrest force.

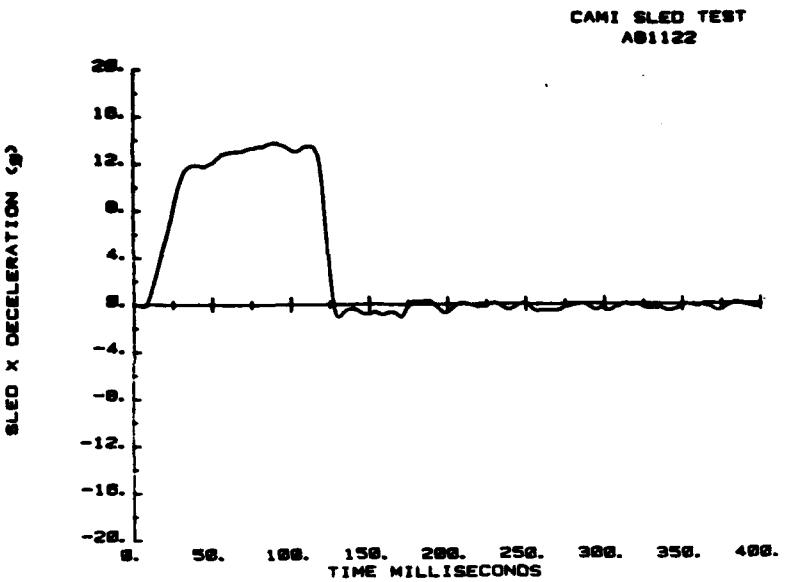

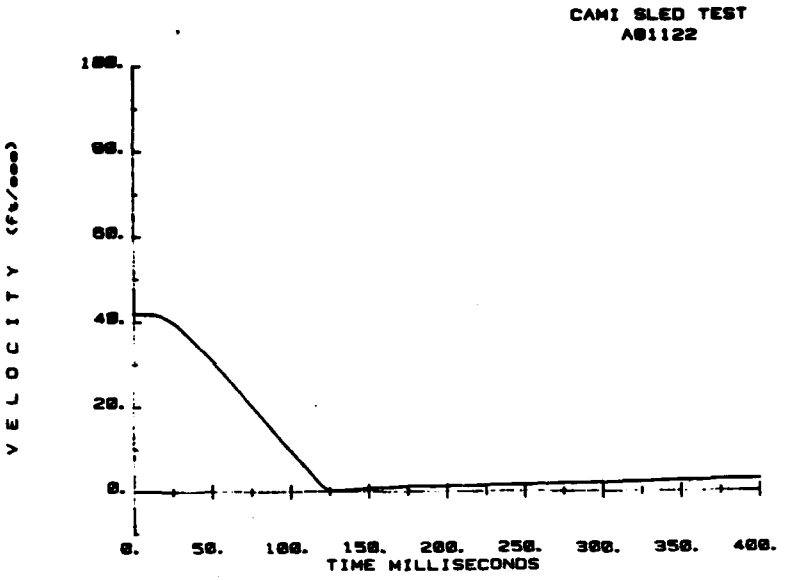

Sled deceleration and velocity.

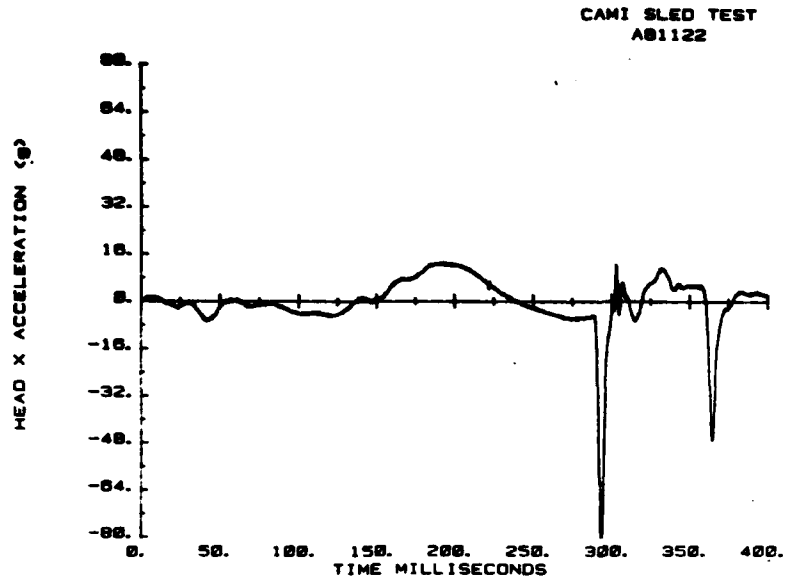

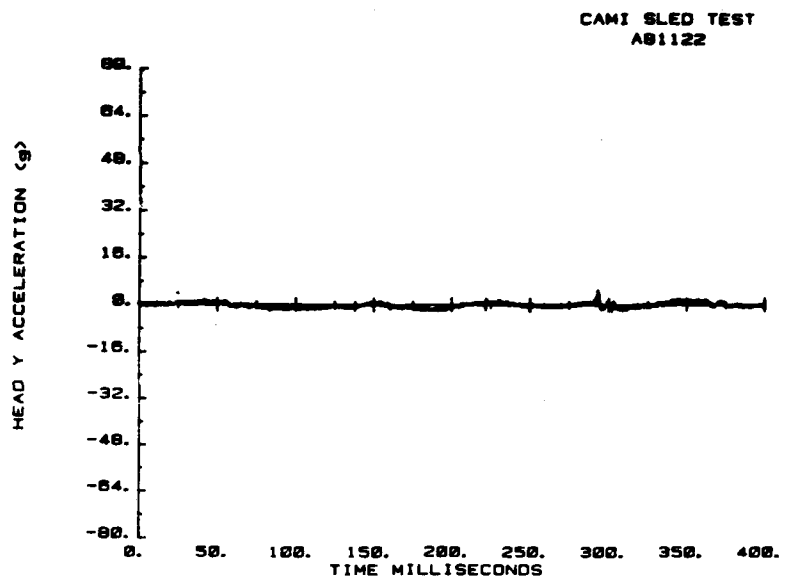

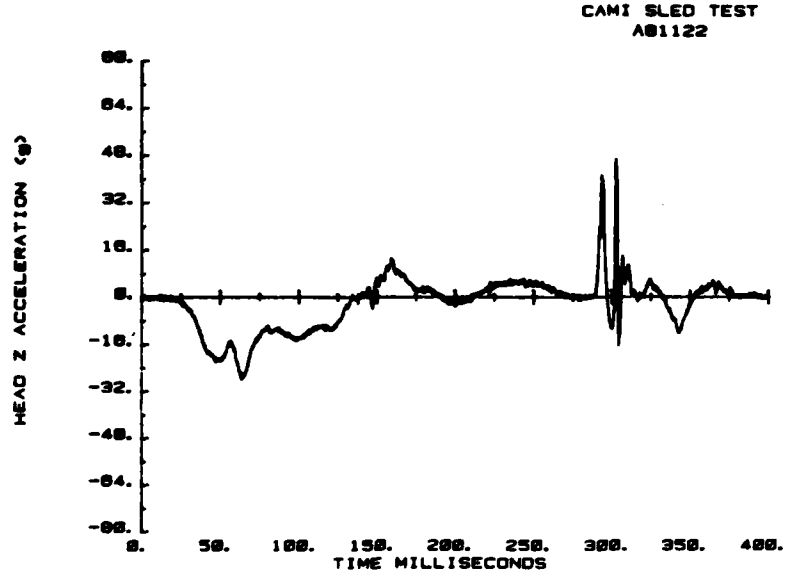

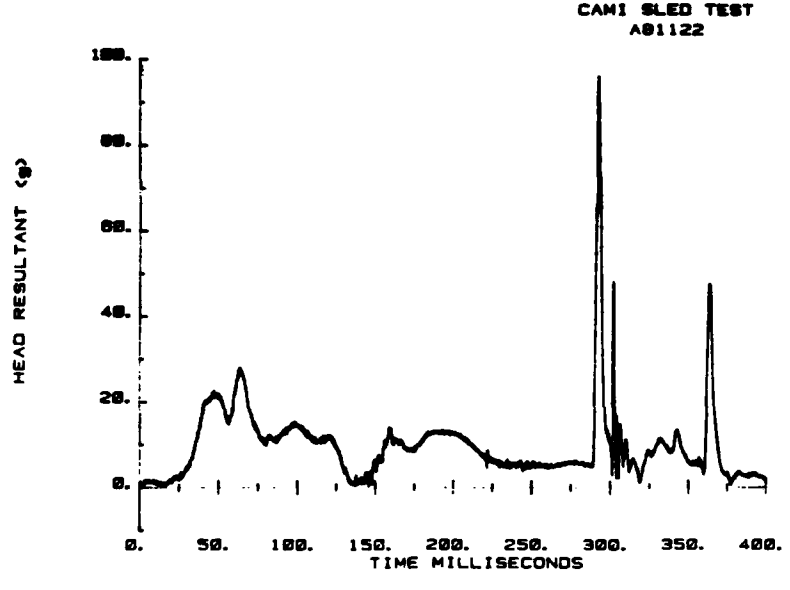

Head acceleration.

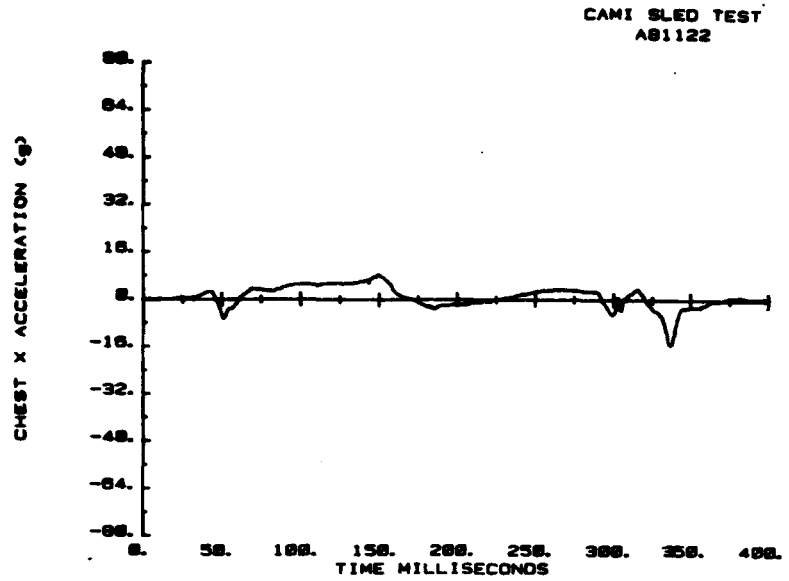

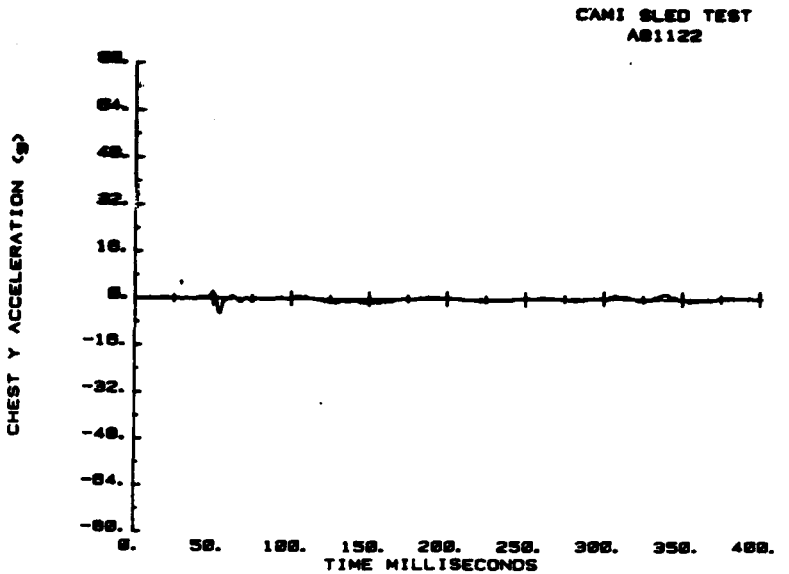

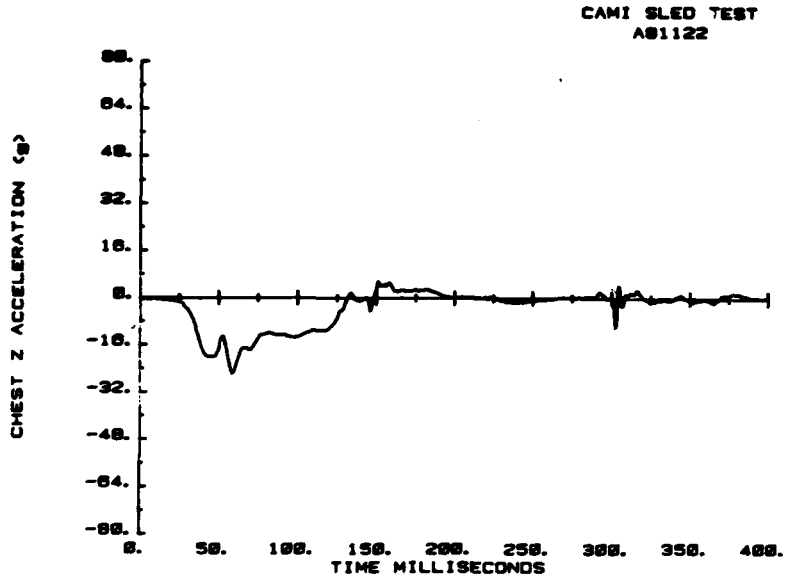

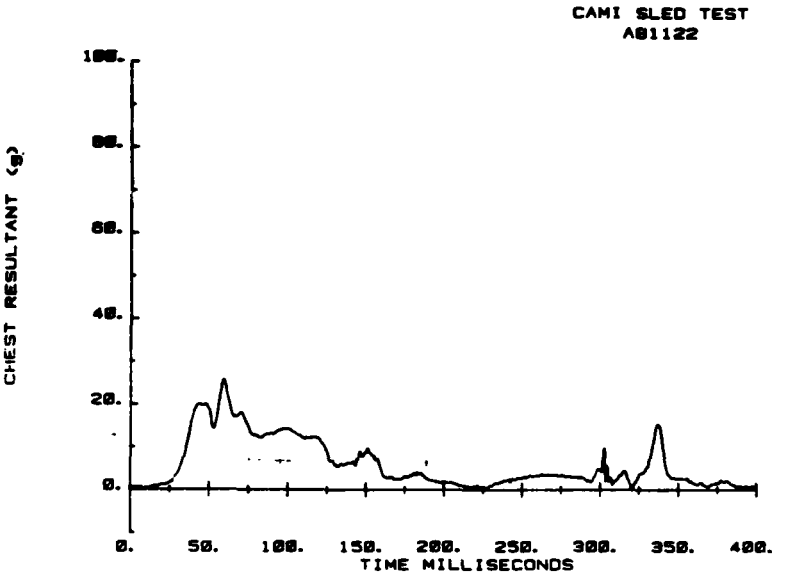

Chest acceleration.

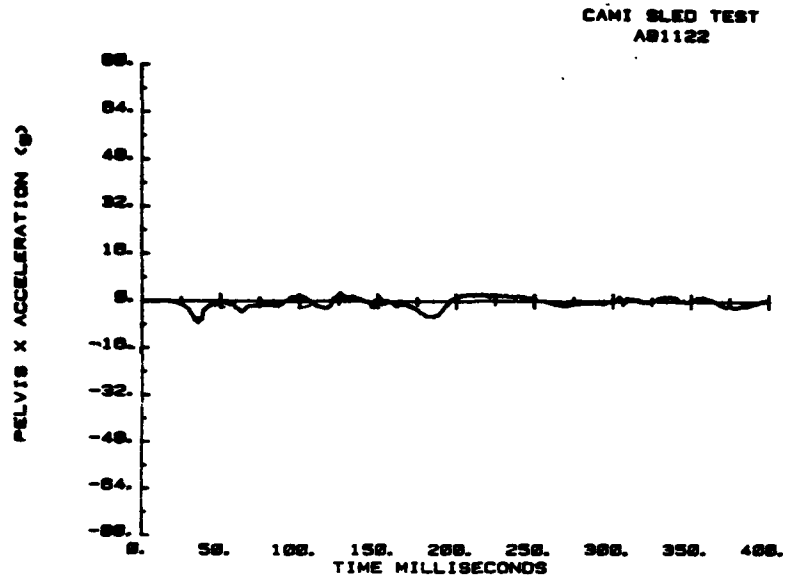

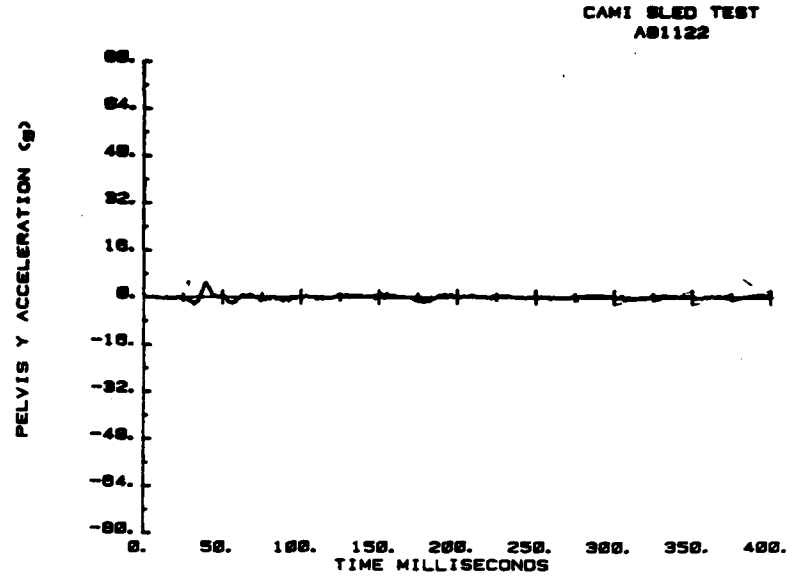

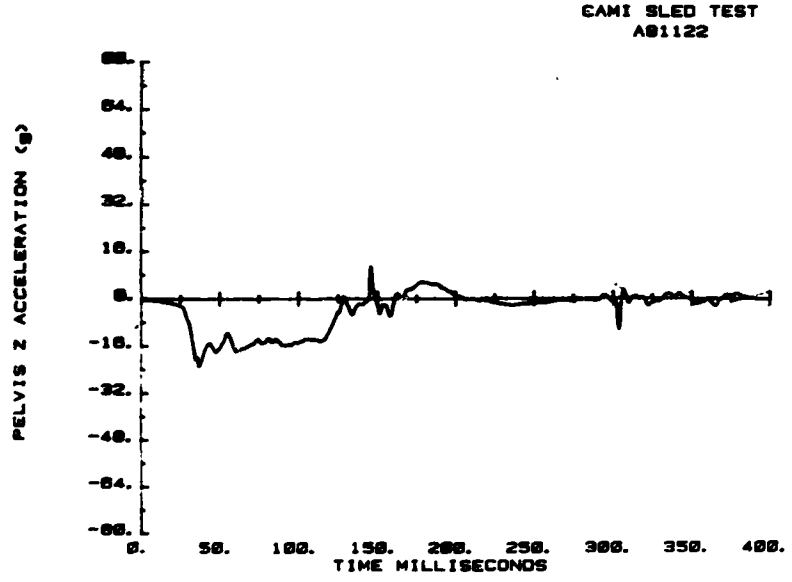

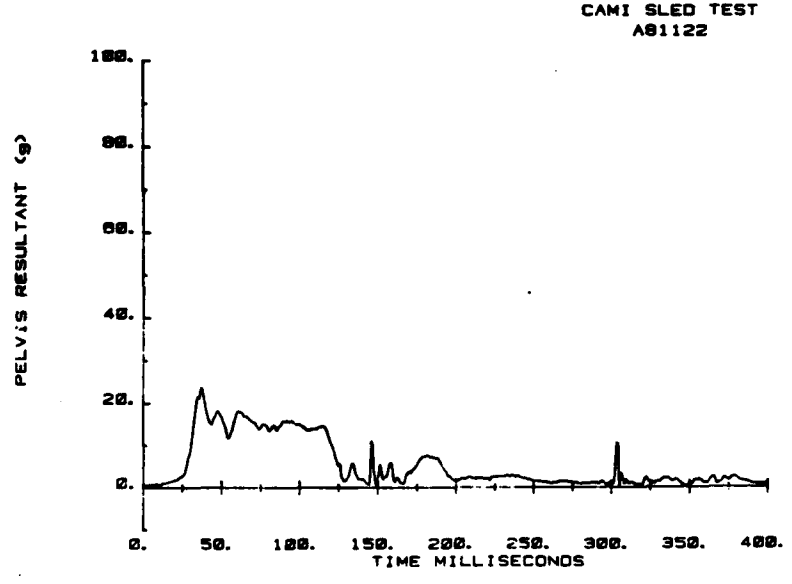

Pelvis acceleration.

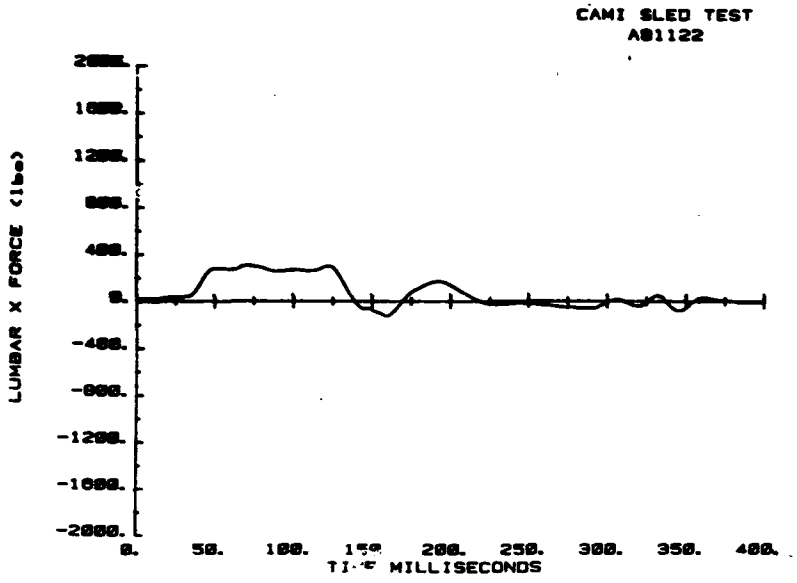

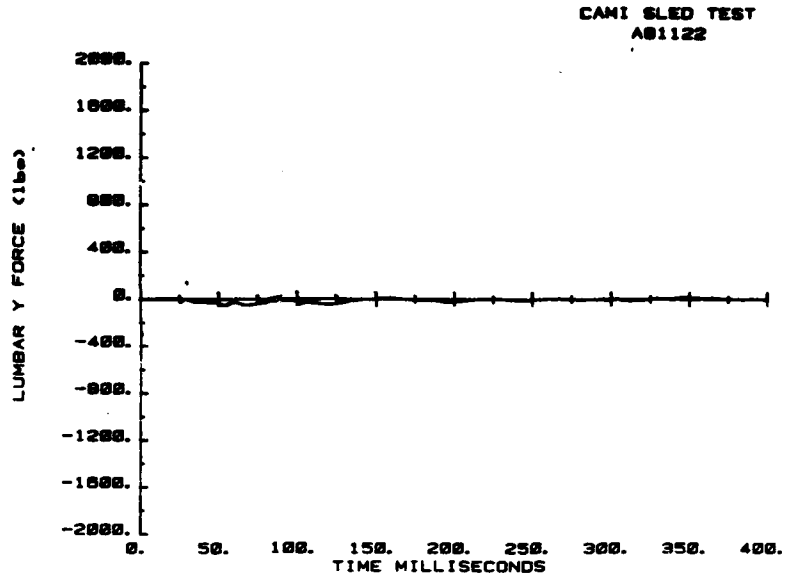

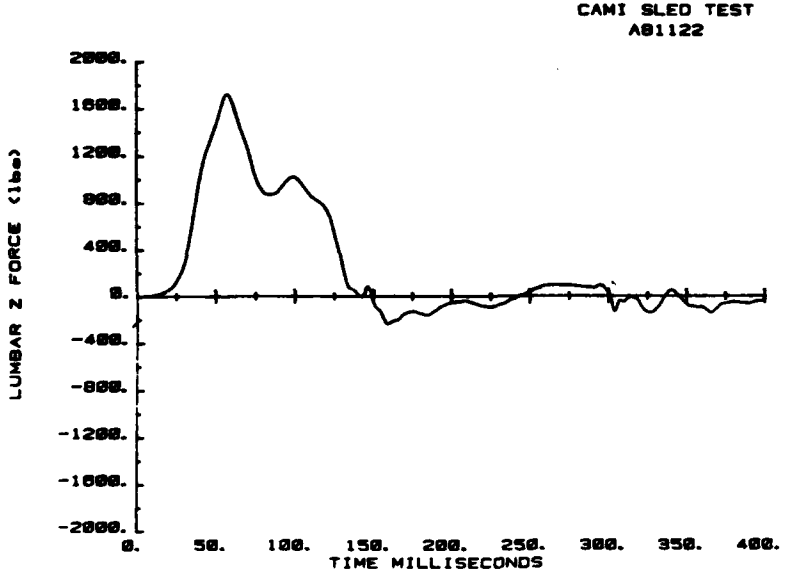

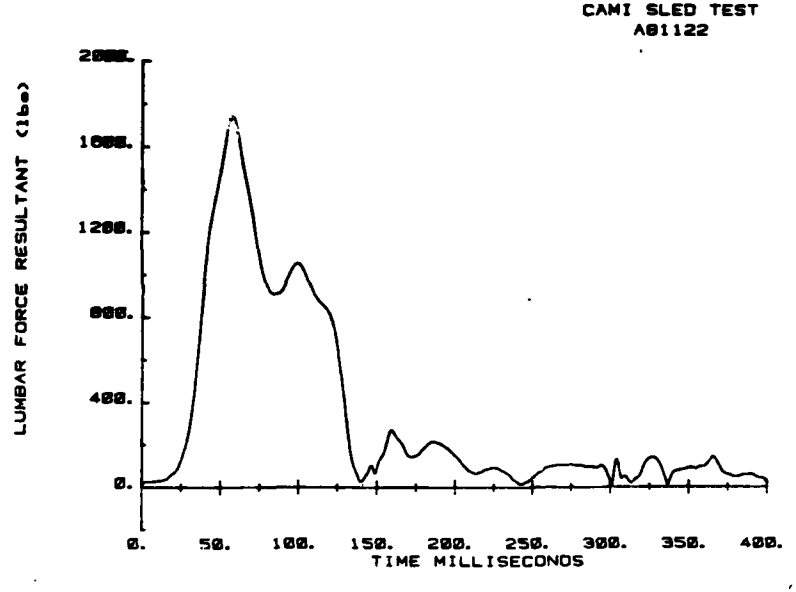

Lumbar force.

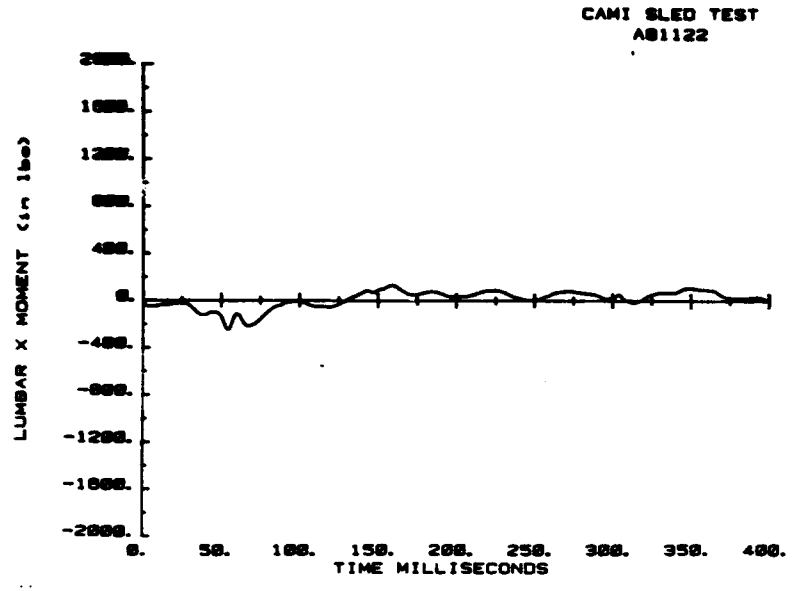

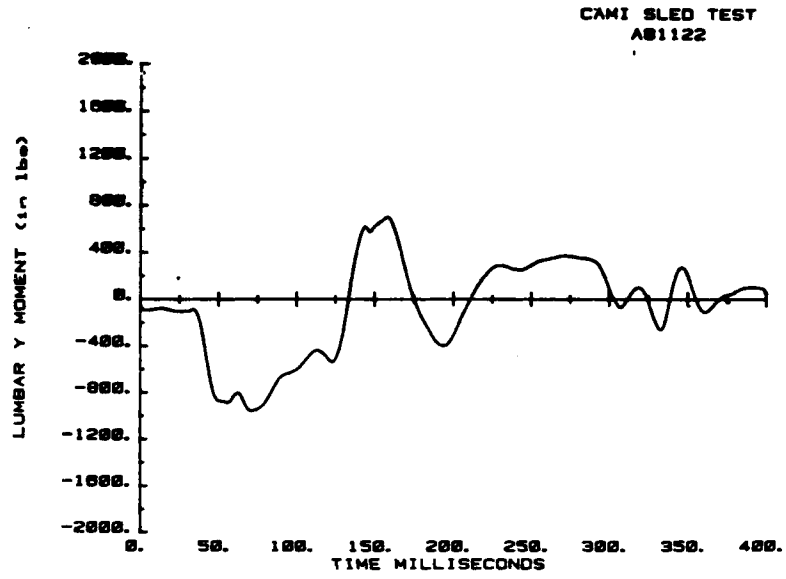

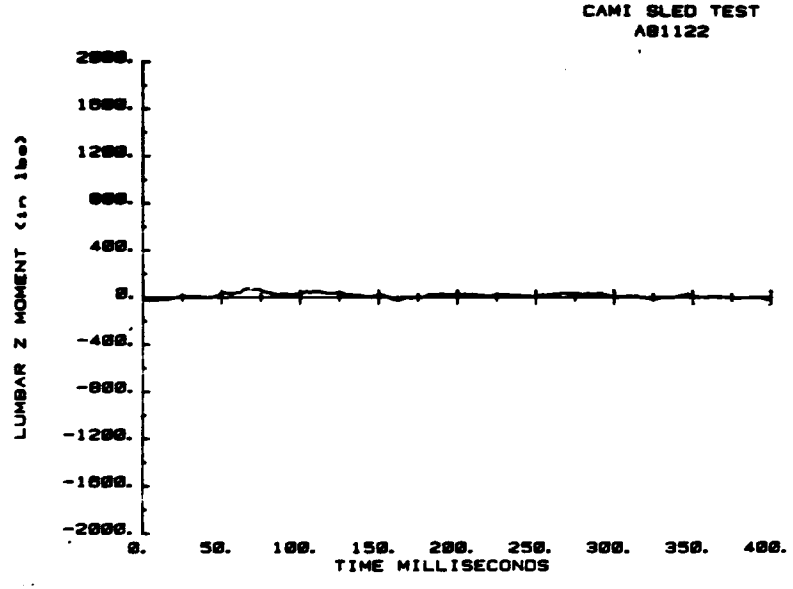

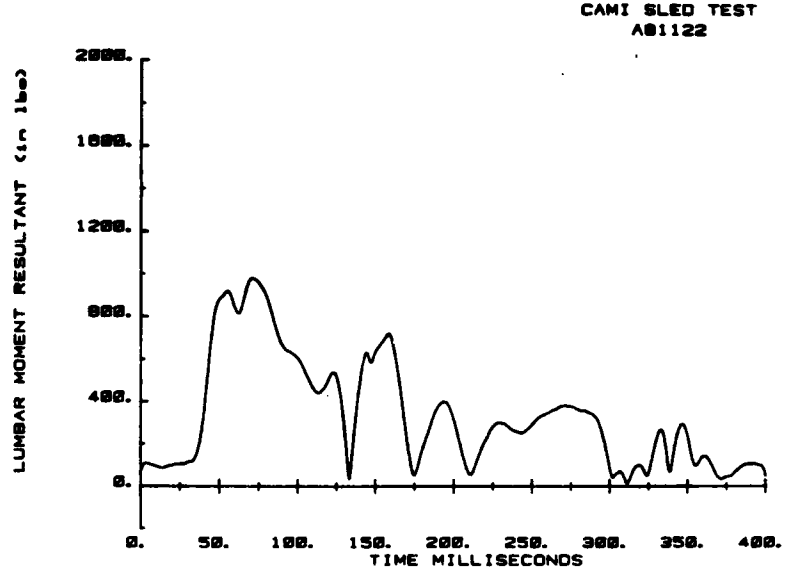

Lumbar moment.

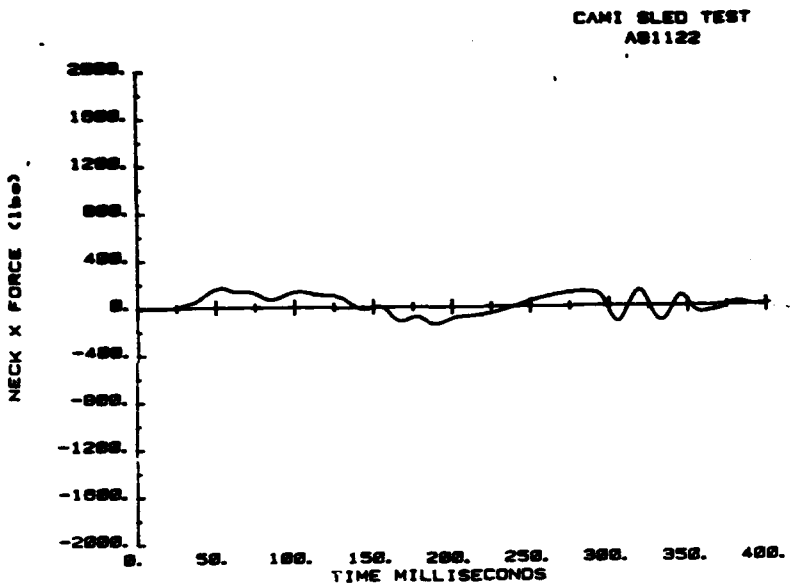
CAMI SLED TEST
AB1122
NECK X FORCE (lbs)
2000.
1600.
1200.
800.
400.
0.
-400.
-800.
-1200.
-1600.
-2000.
0.
50.
100.
150.
200.
250.
300.
350.
400.
TIME MILLISECONDS

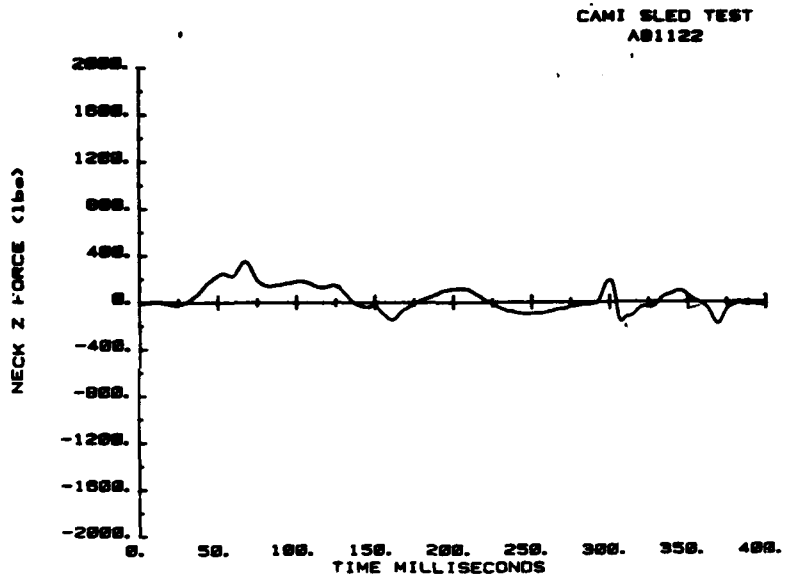
CAMI SLED TEST
AB1122
NECK Z FORCE (lbs)
2000.
1600.
1200.
800.
400.
0.
-400.
-800.
-1200.
-1600.
-2000.
0.
50.
100.
150.
200.
250.
300.
350.
400.
TIME MILLISECONDS

Neck force.

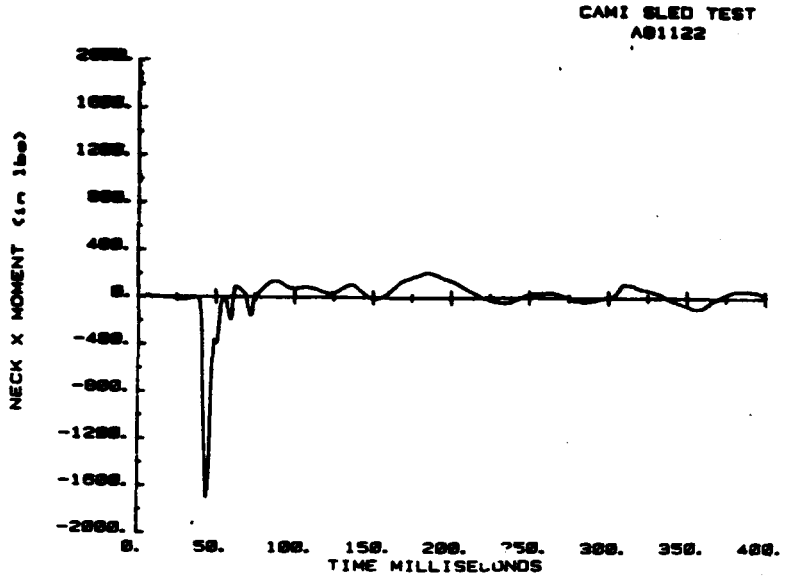
CAMI SLED TEST
A01122
NECK X MOMENT (in lbs)
2000.
1600.
1200.
800.
400.
0.
-400.
-800.
-1200.
-1600.
-2000.
0. 50. 100. 150. 200. 250. 300. 350. 400.
TIME MILLISECONDS

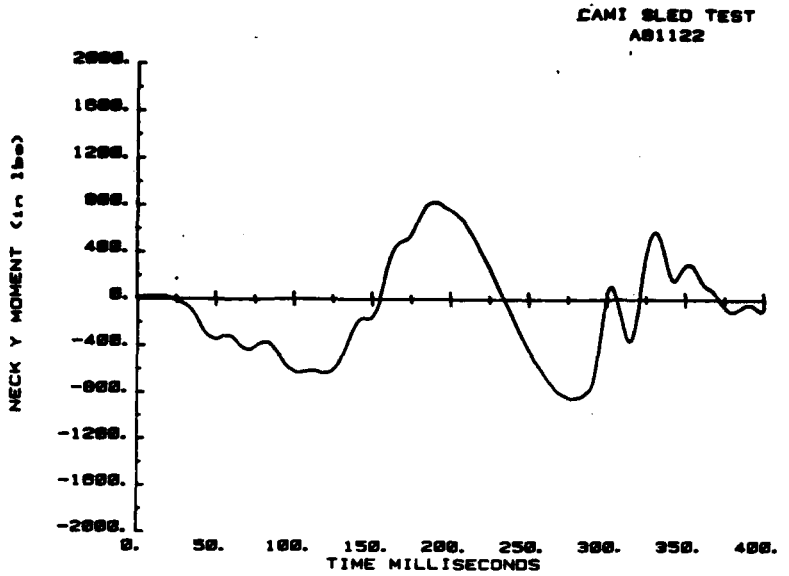
CAMI SLED TEST
A01122
NECK Y MOMENT (in lbs)
2000.
1600.
1200.
800.
400.
0.
-400.
-800.
-1200.
-1600.
-2000.
0. 50. 100. 150. 200. 250. 300. 350. 400.
TIME MILLISECONDS

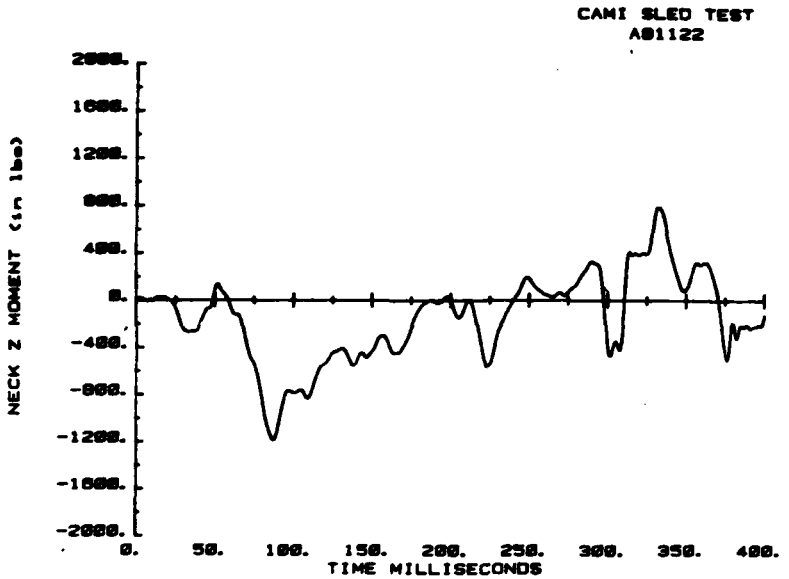
CAMI SLED TEST
A01122
NECK Z MOMENT (in lbs)
2000.
1600.
1200.
800.
400.
0.
-400.
-800.
-1200.
-1600.
-2000.
0. 50. 100. 150. 200. 250. 300. 350. 400.
TIME MILLISECONDS

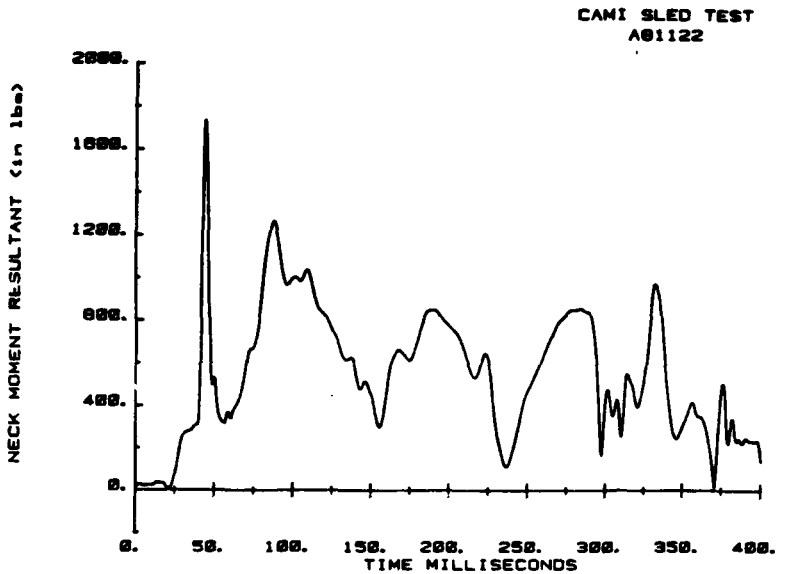
CAMI SLED TEST
A01122
NECK MOMENT RESULTANT (in lbs)
2000.
1600.
1200.
800.
400.
0.
0. 50. 100. 150. 200. 250. 300. 350. 400.
TIME MILLISECONDS

Neck moment.

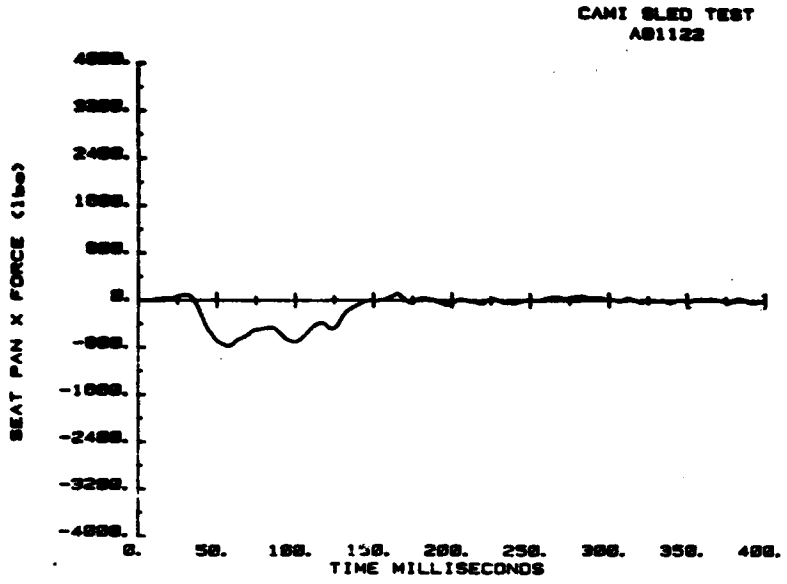

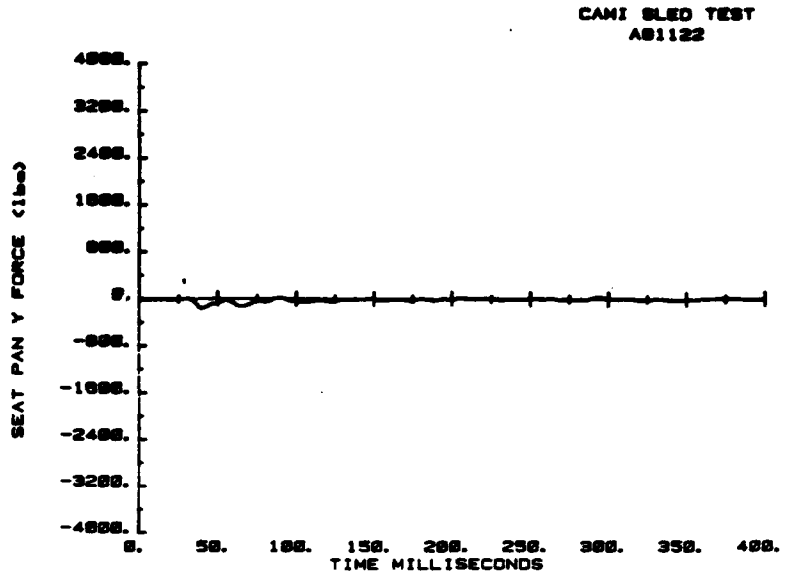

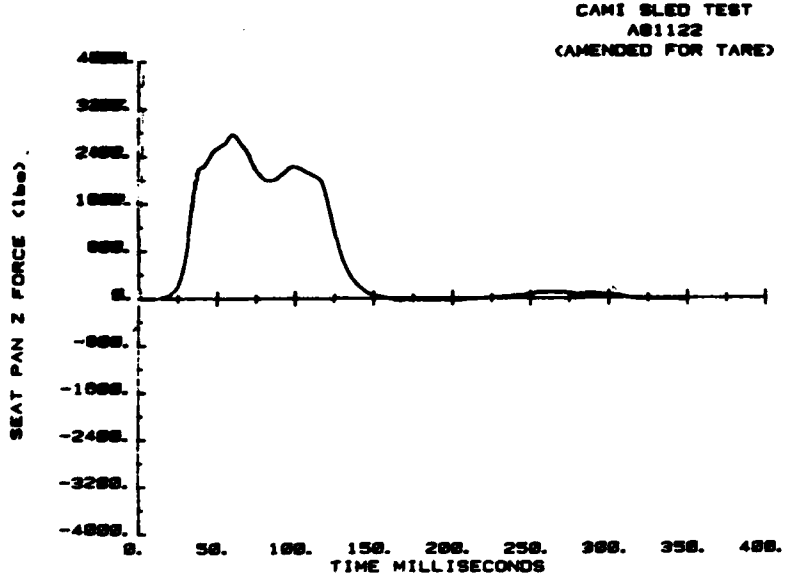

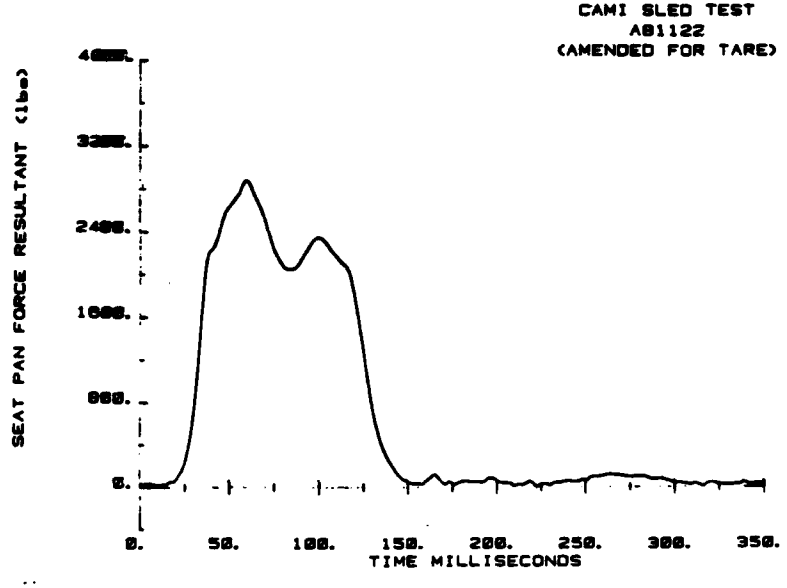

Seat pan force.

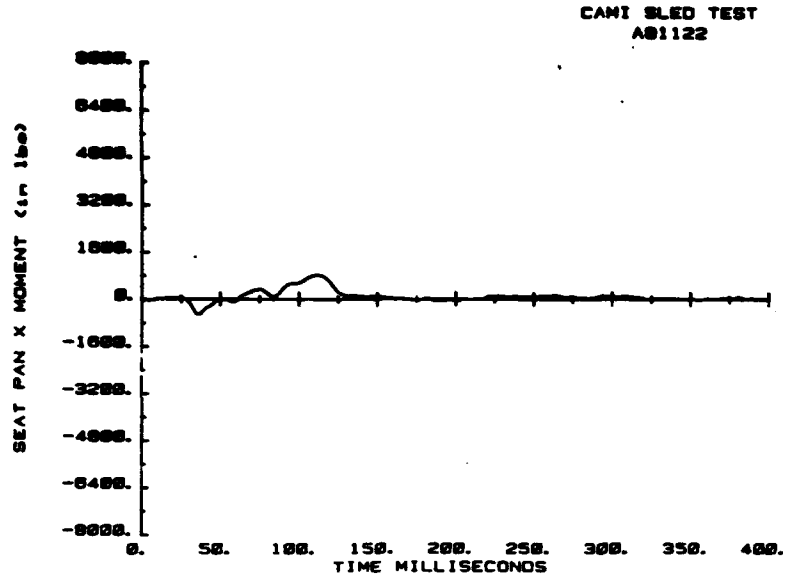

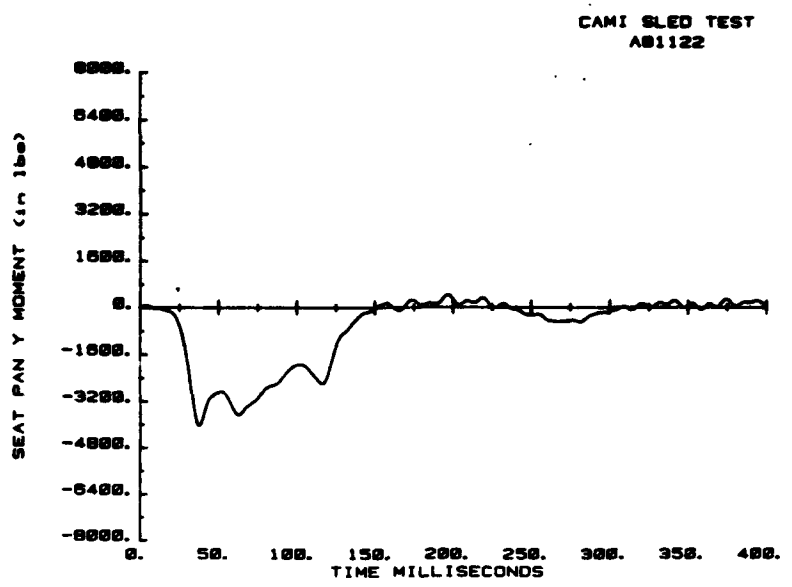

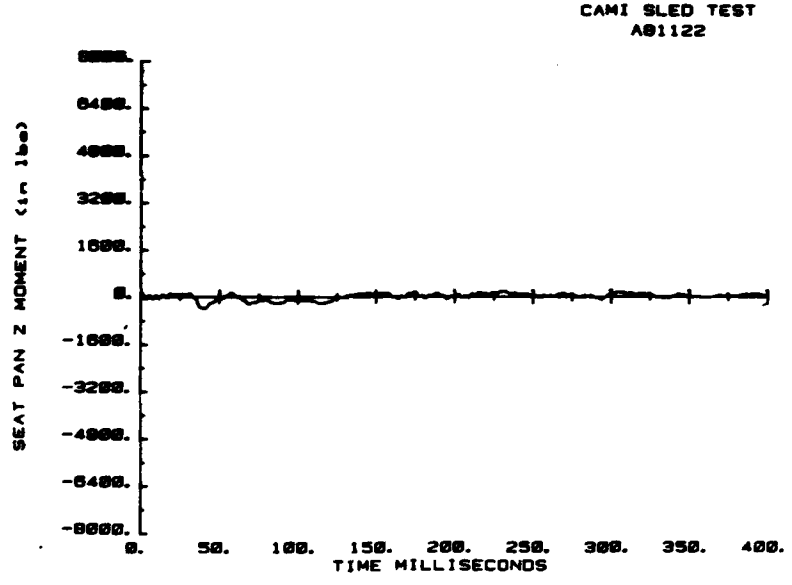

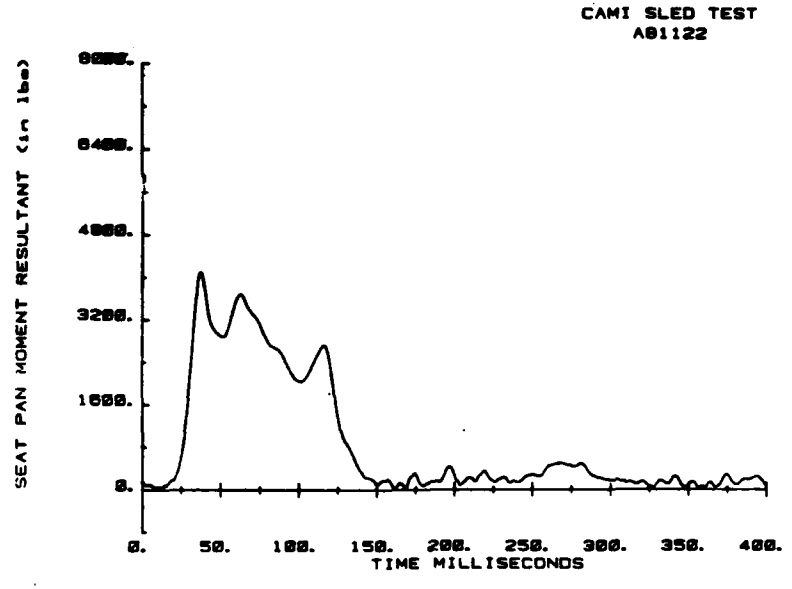

Seat pan moment.

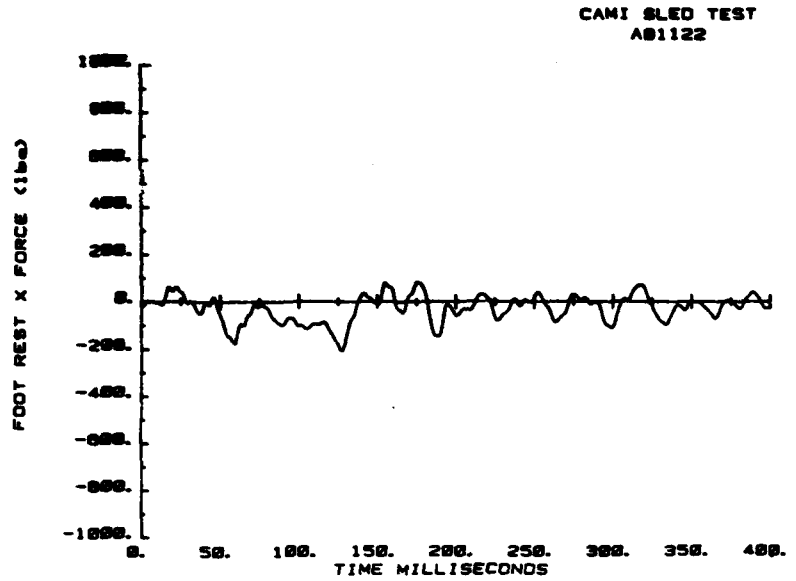

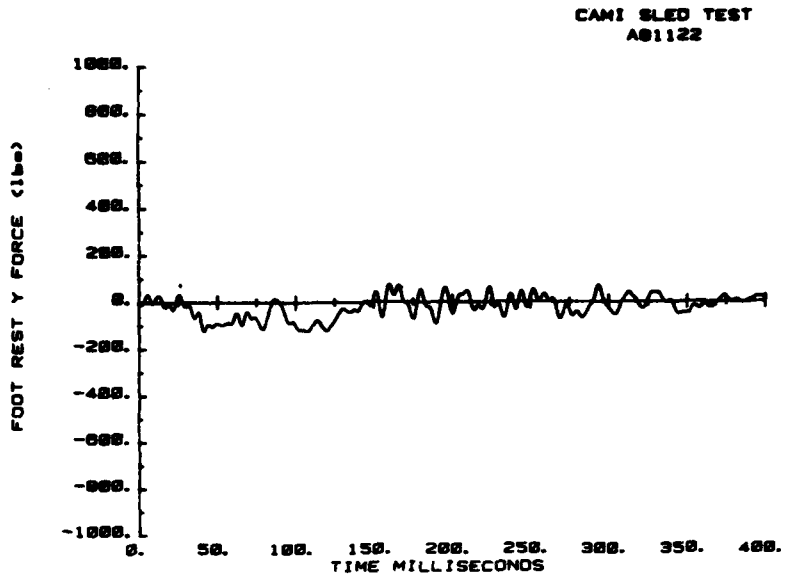

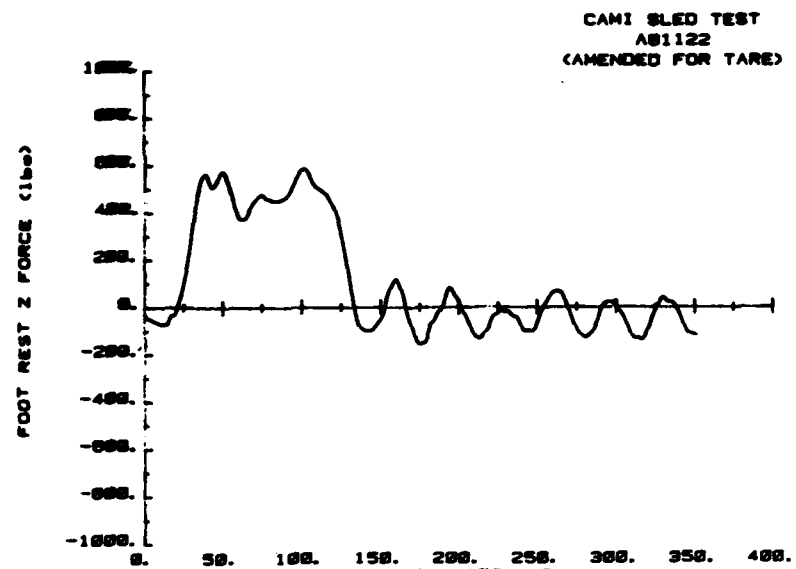

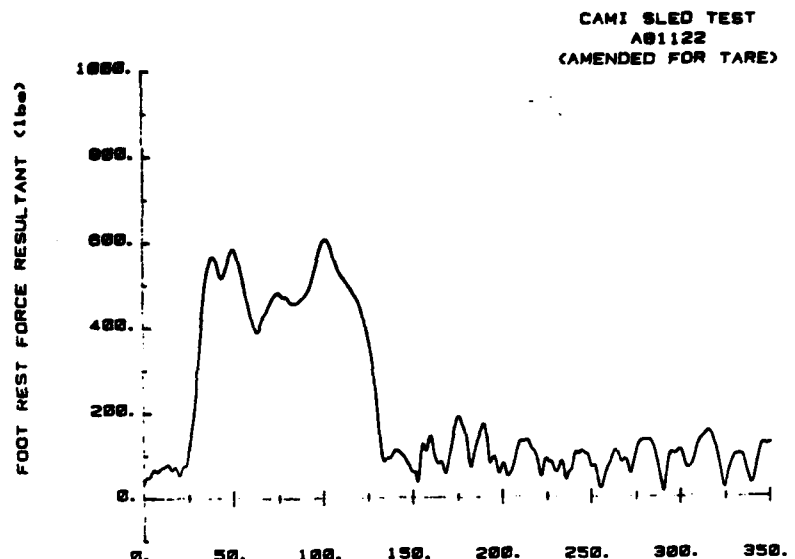

Footrest force.

APPENDIX B

CAMI ENERGY-ABSORBING SEAT TESTS

Vertical Tests

A81-123	VIP-95 Dummy
A81-124	Part 572 Dummy

Combined Test

A81-127	Part 572 Dummy

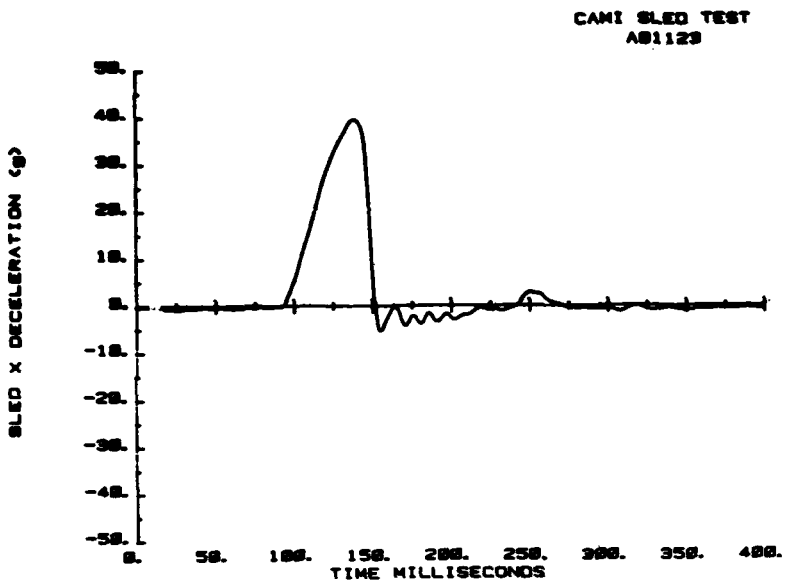

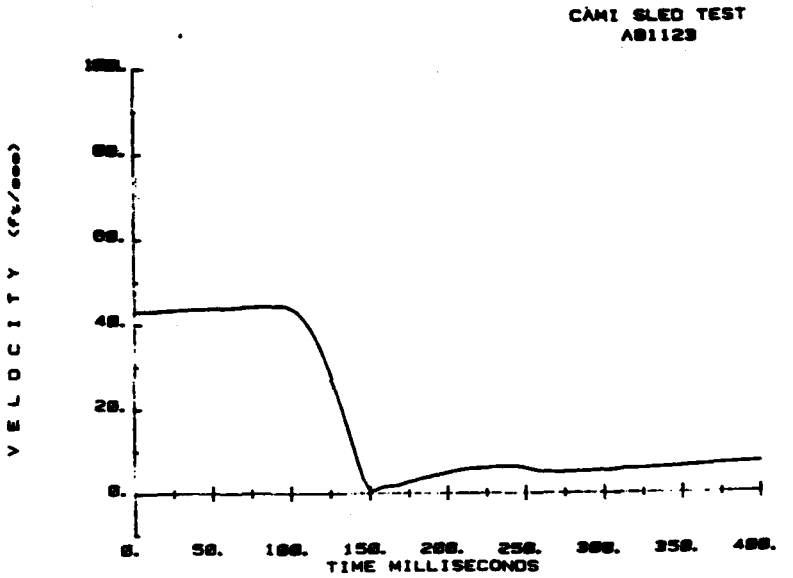

Sled deceleration and velocity.

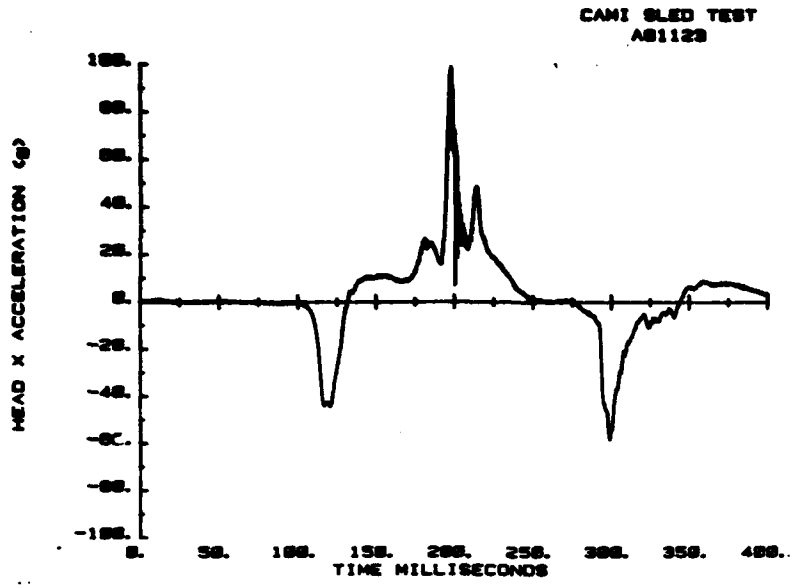

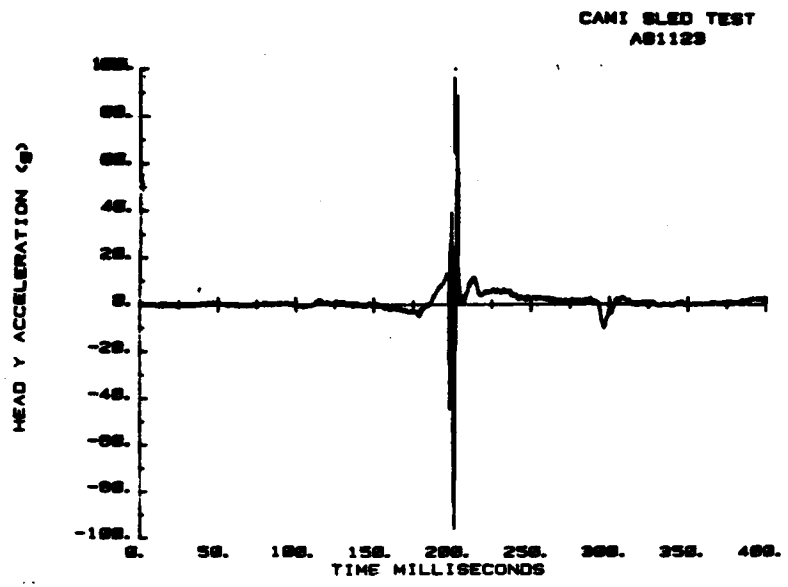

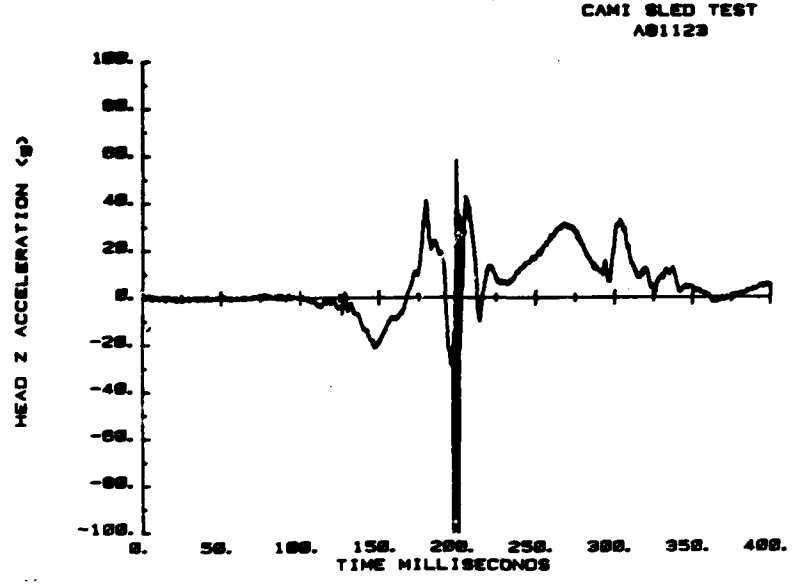

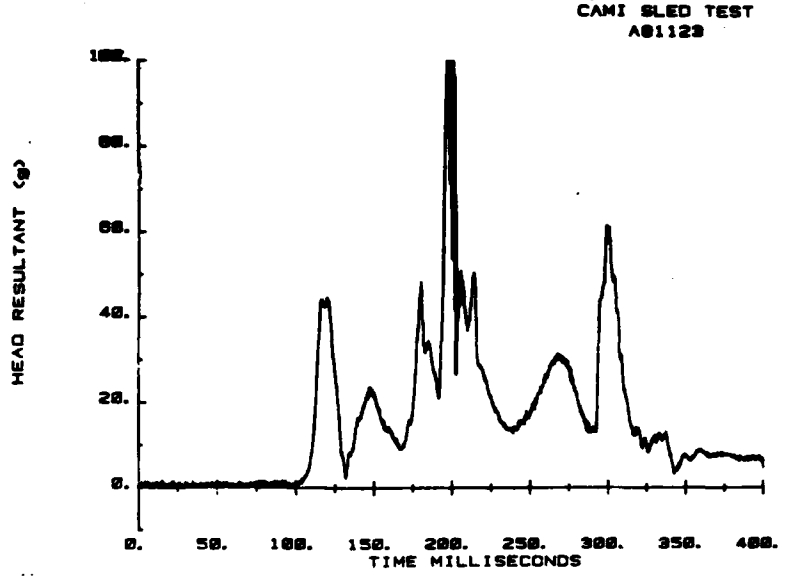

Head acceleration.

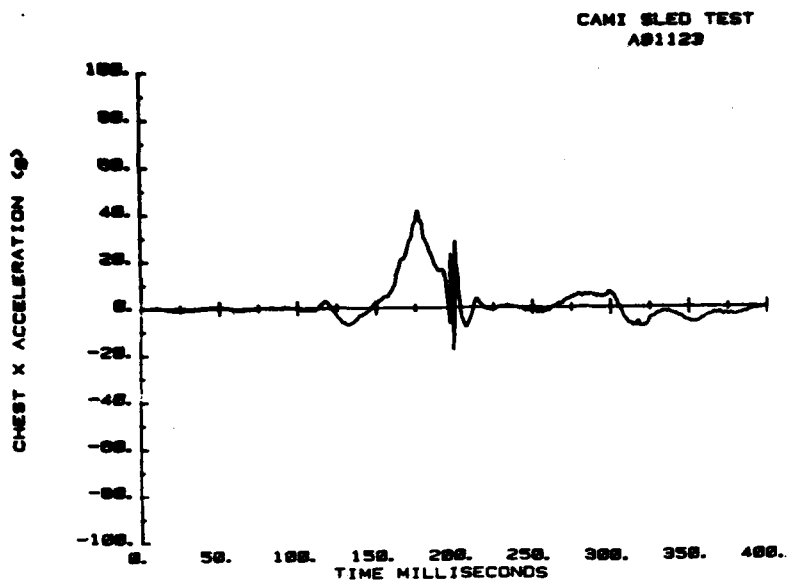

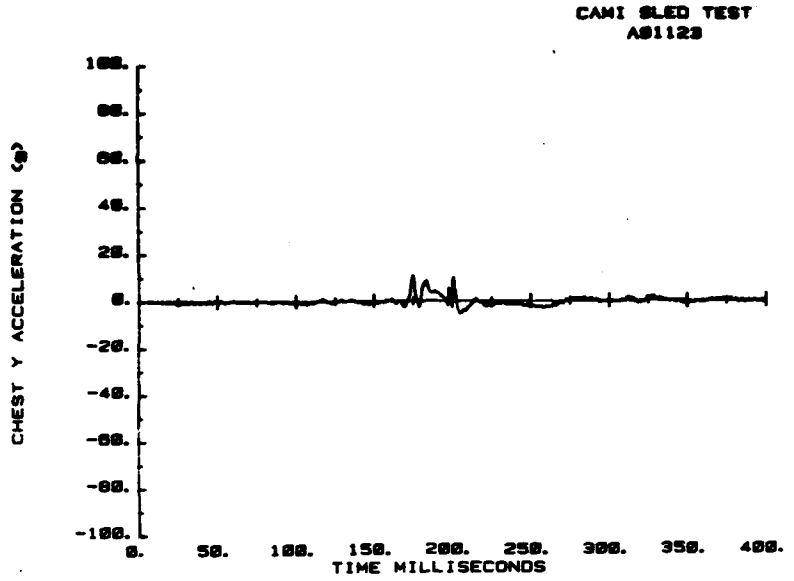

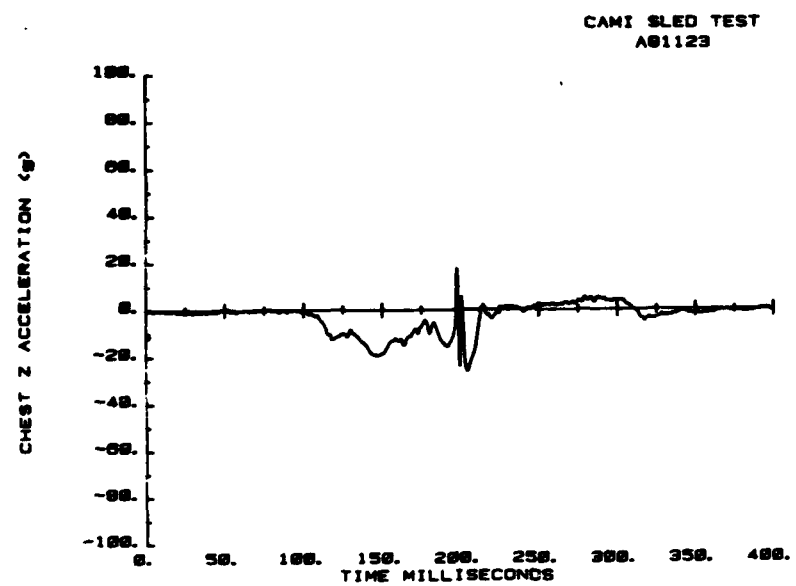

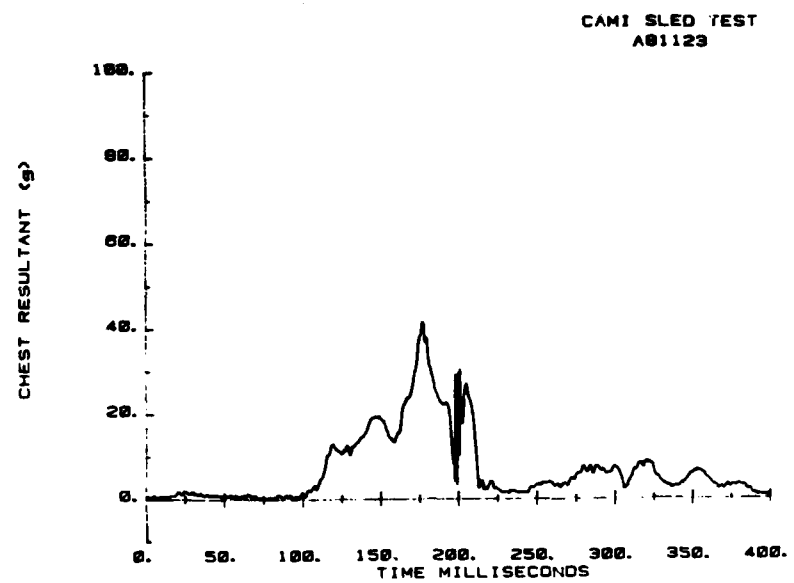

Chest acceleration.

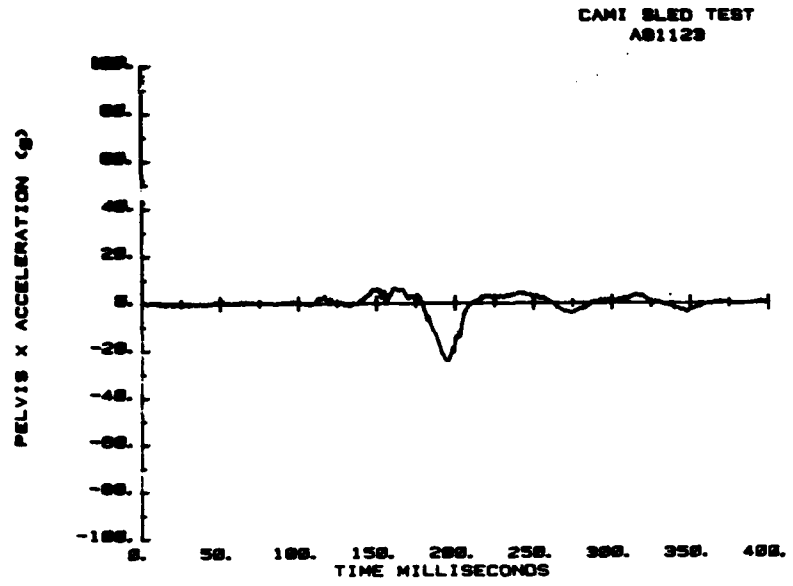

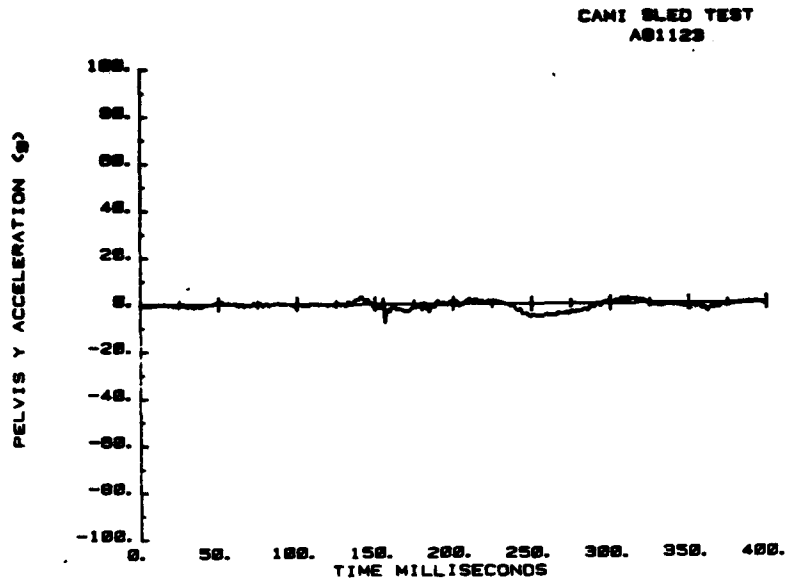

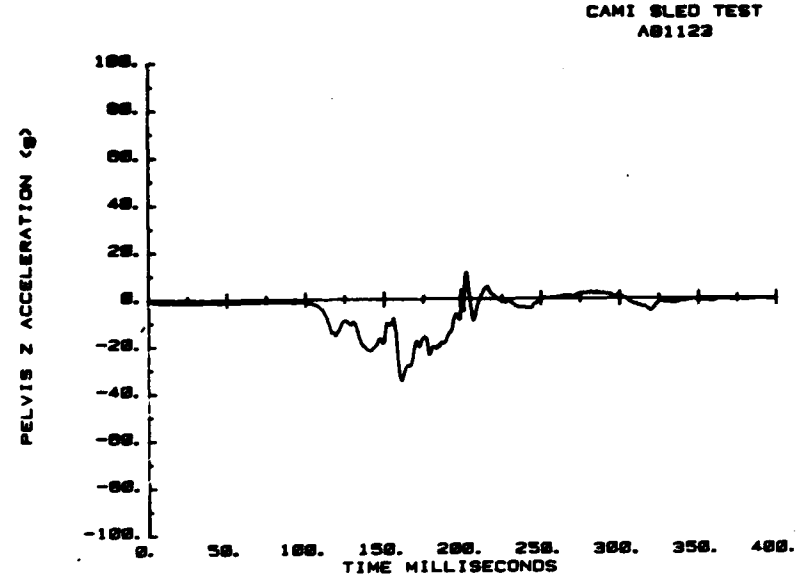

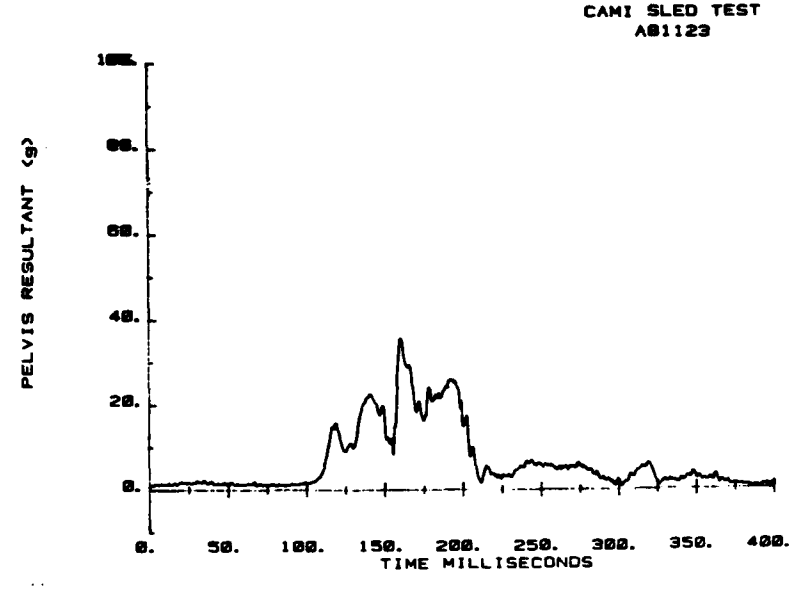

Pelvis acceleration.

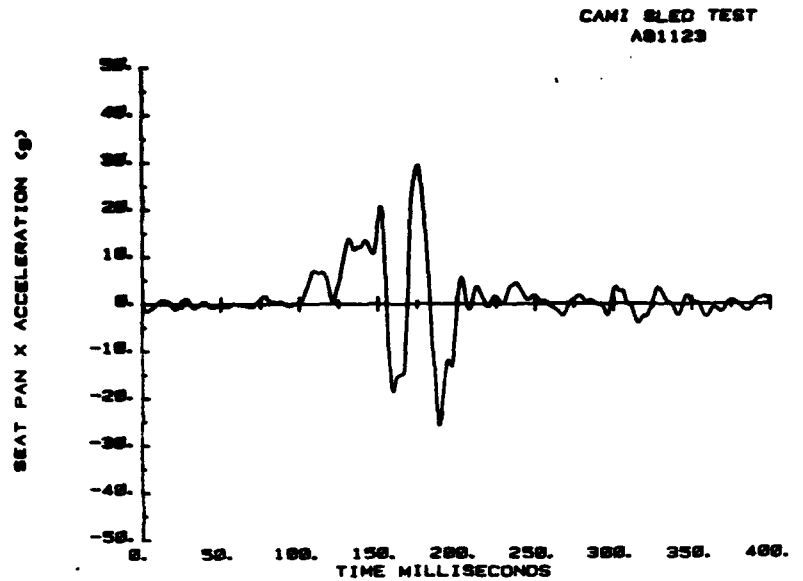

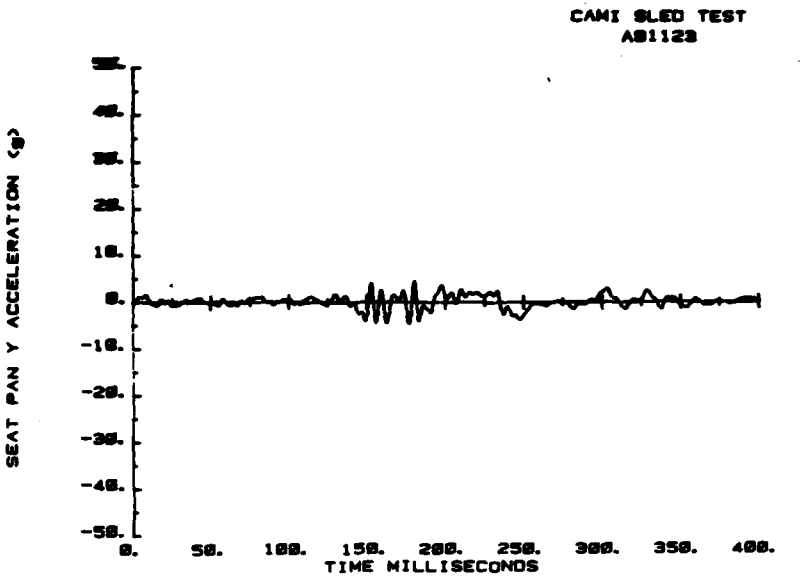

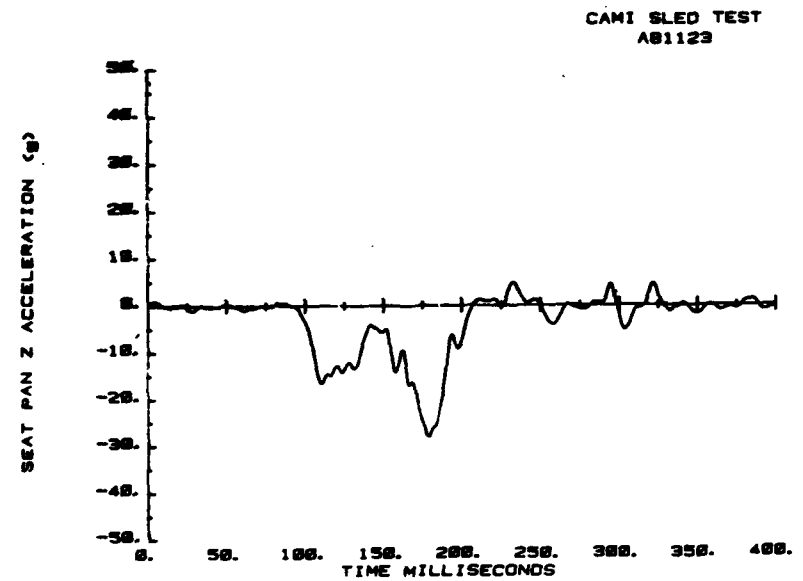

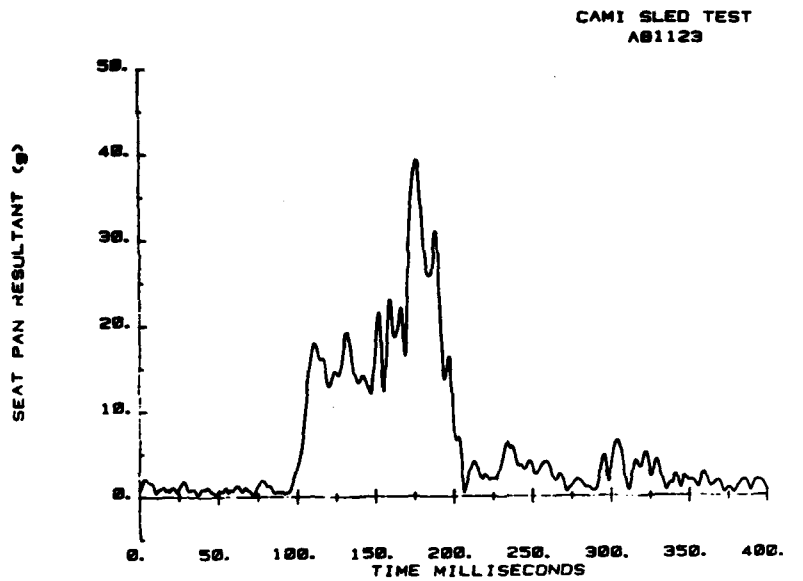

Seat pan acceleration.

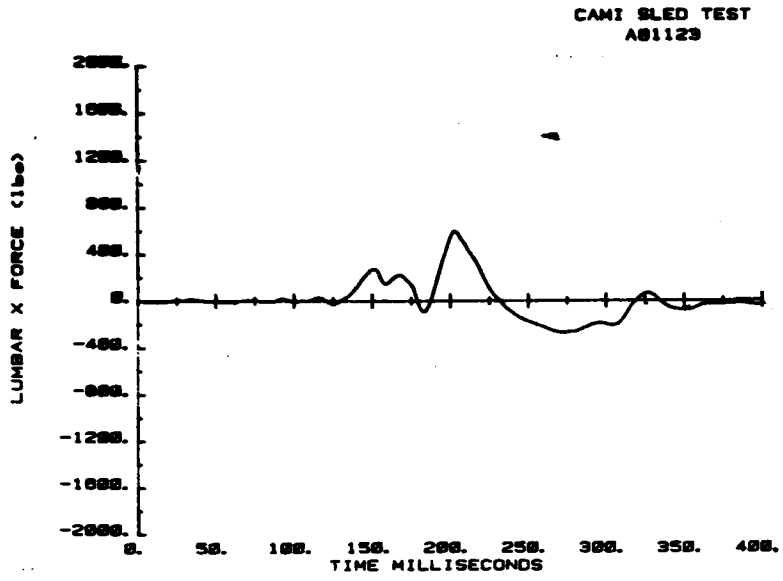

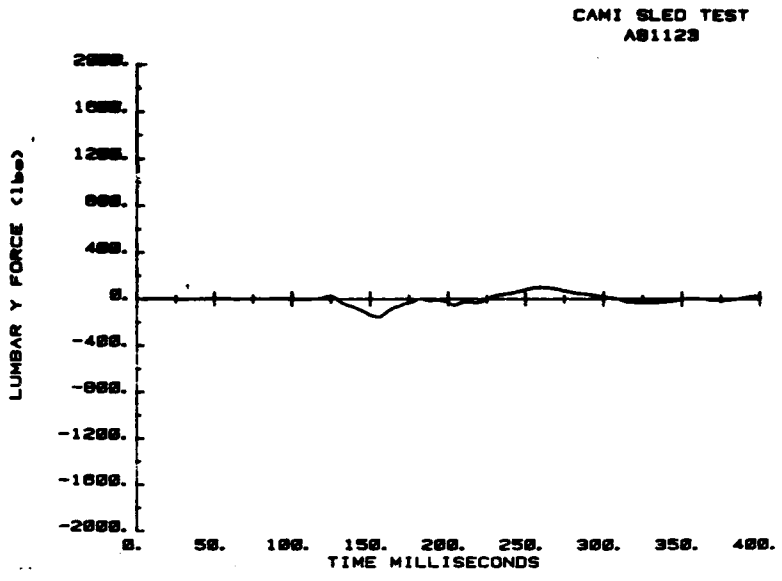

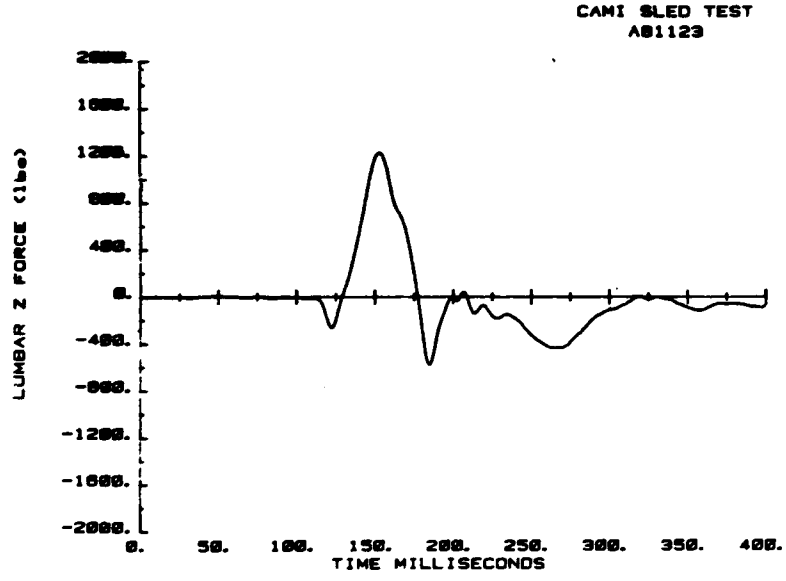

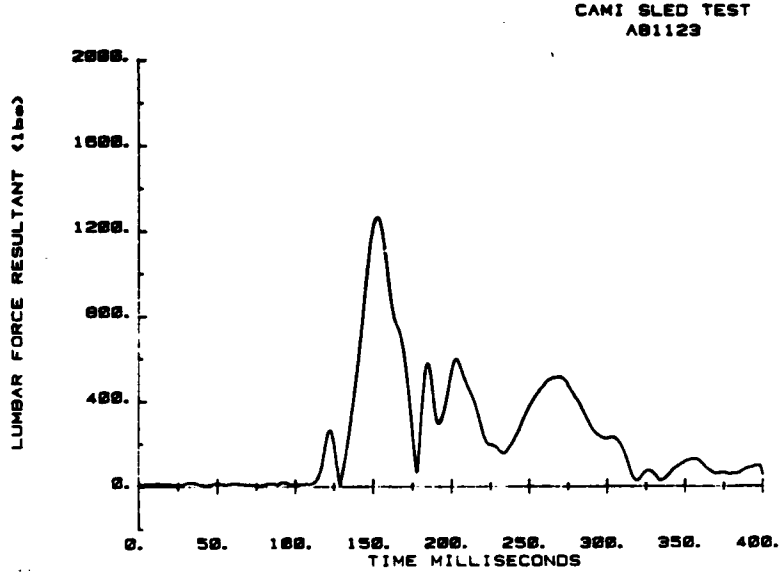

Lumbar force.

AD-A135 244 MEASUREMENT OF SPINAL LOADS IN TWO MODIFIED ANTHROPOMORPHIC DUMMIES(U) SIMULA INC TEMPE AZ D H LAANANEN ET AL. 05 MAY 82 TR-82405 DAMD17-81-C-1175 2/2

UNCLASSIFIED F/G 5/5 NL

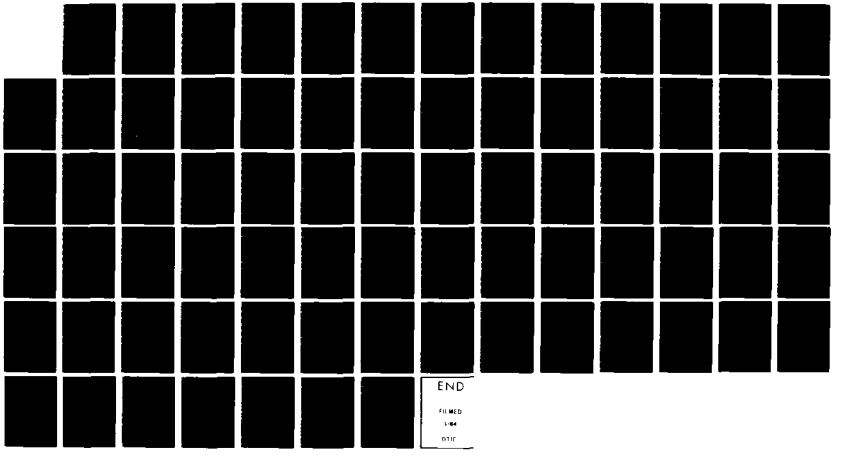

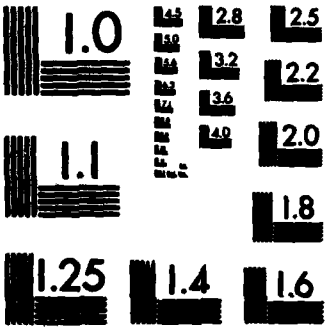

MICROCOPY RESOLUTION TEST CHART
NATIONAL BUREAU OF STANDARDS-1963-A

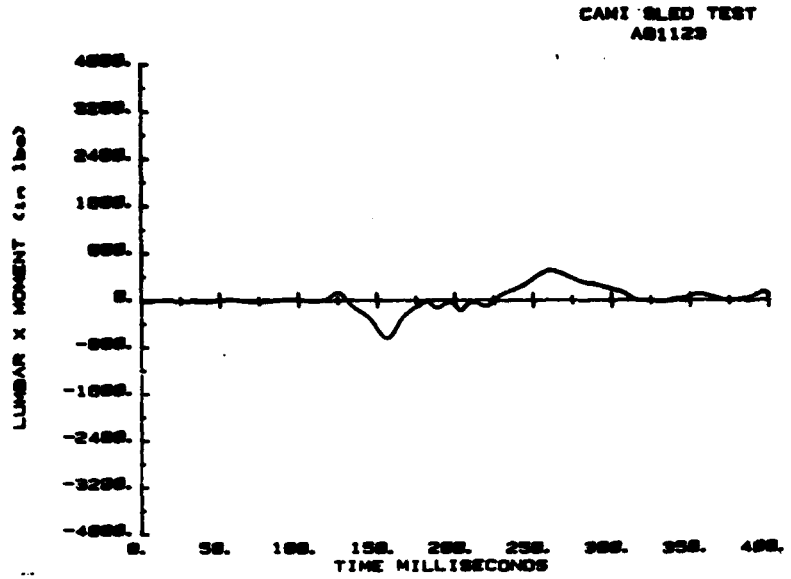

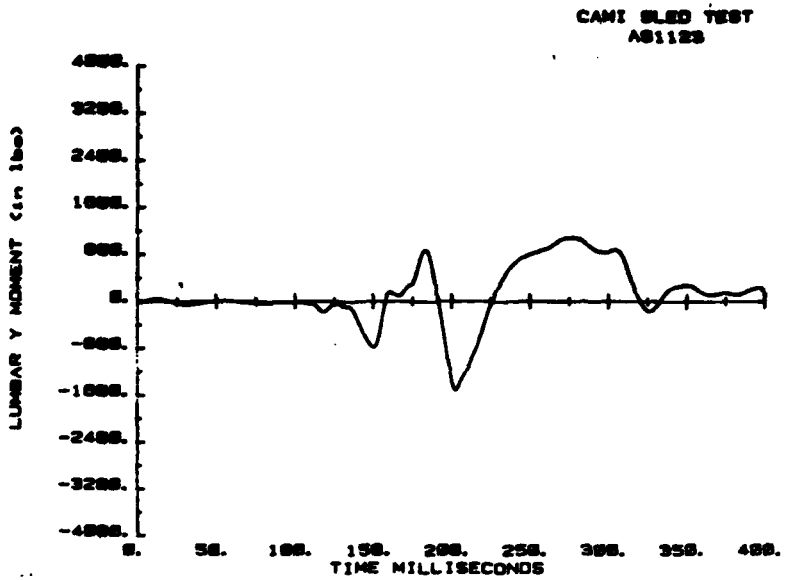

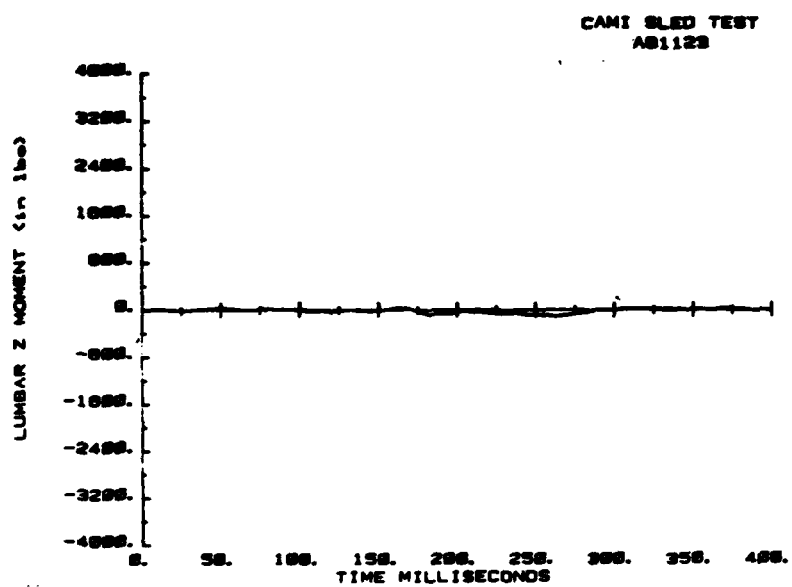

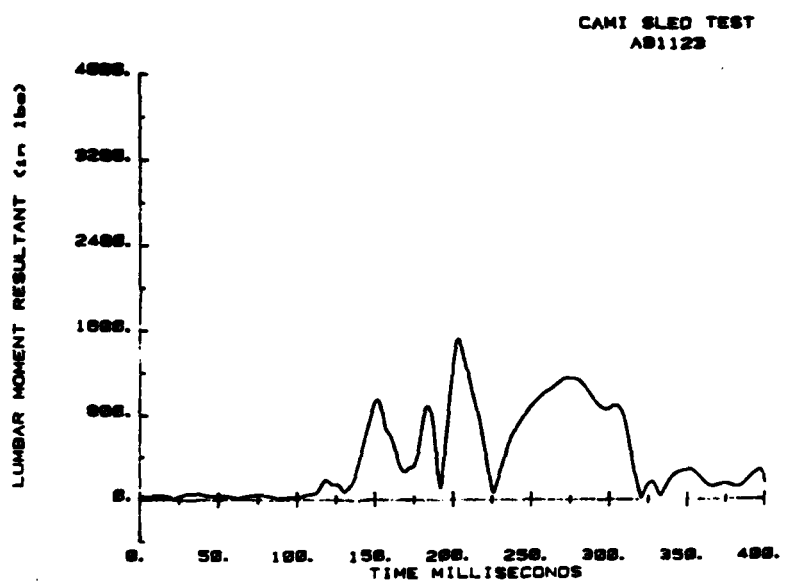

Lumbar moment.

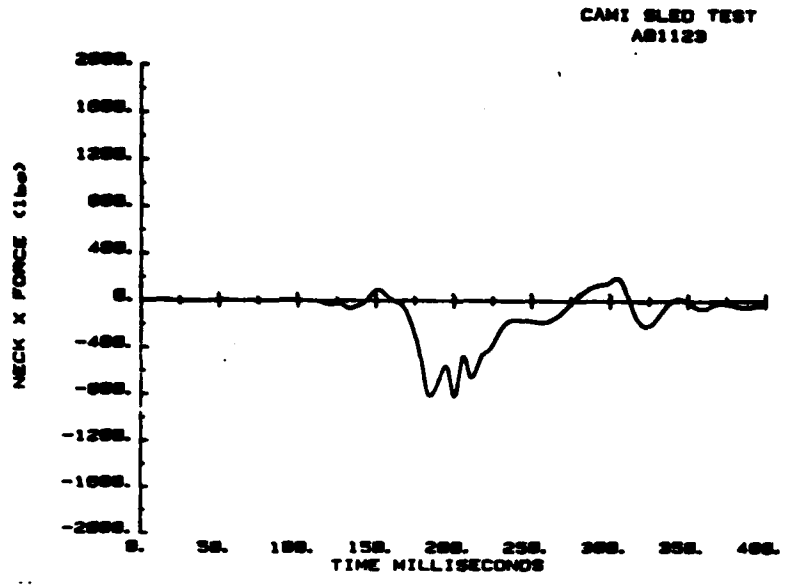

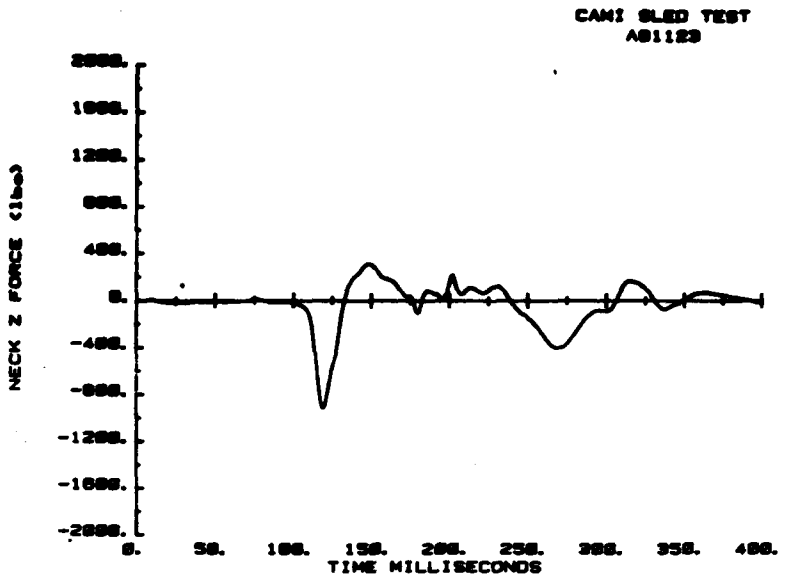

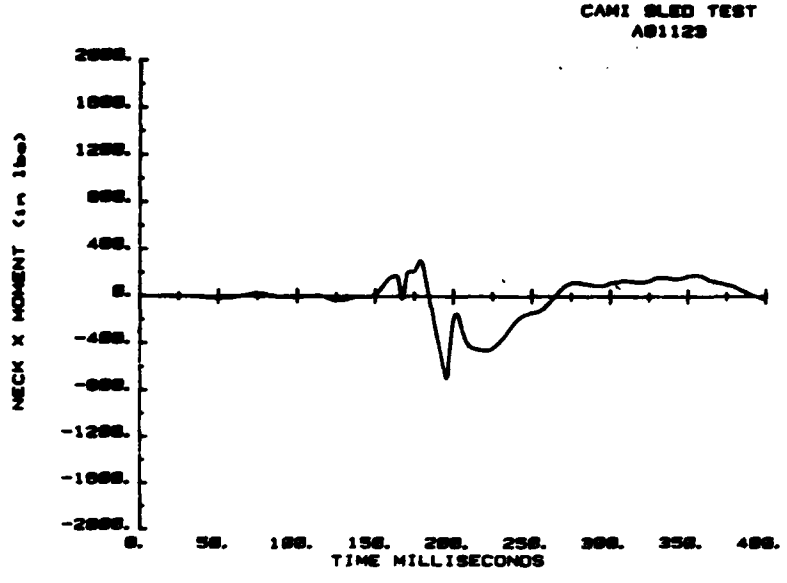

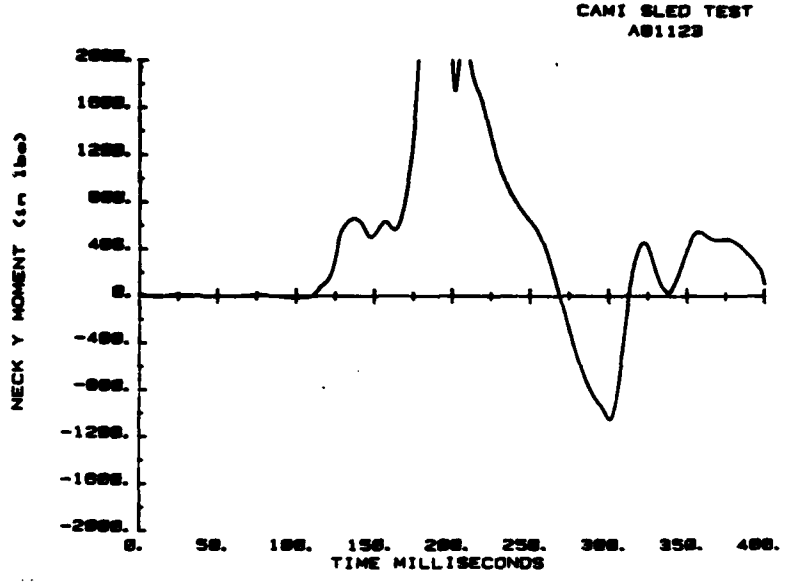

Neck force and moment.

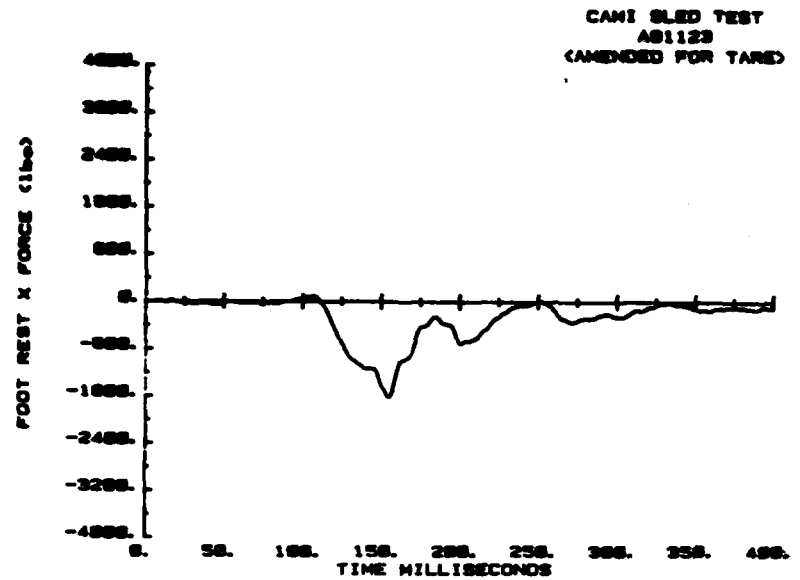

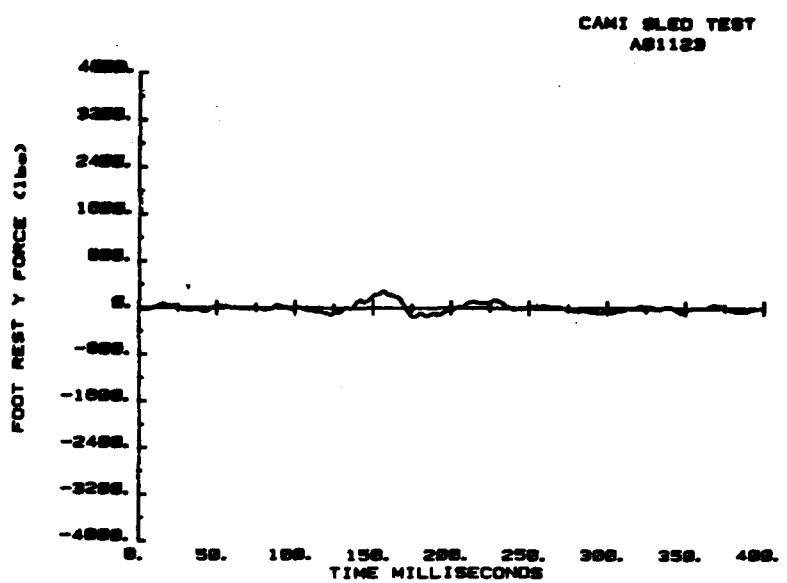

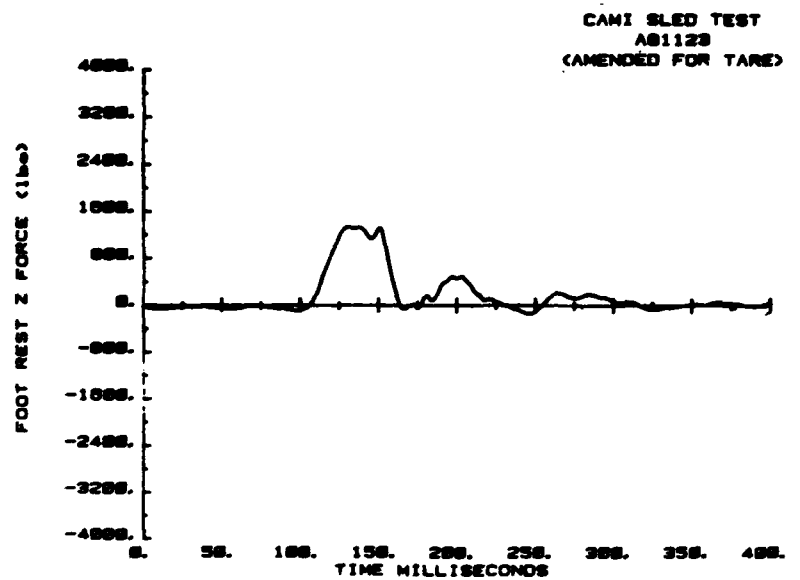

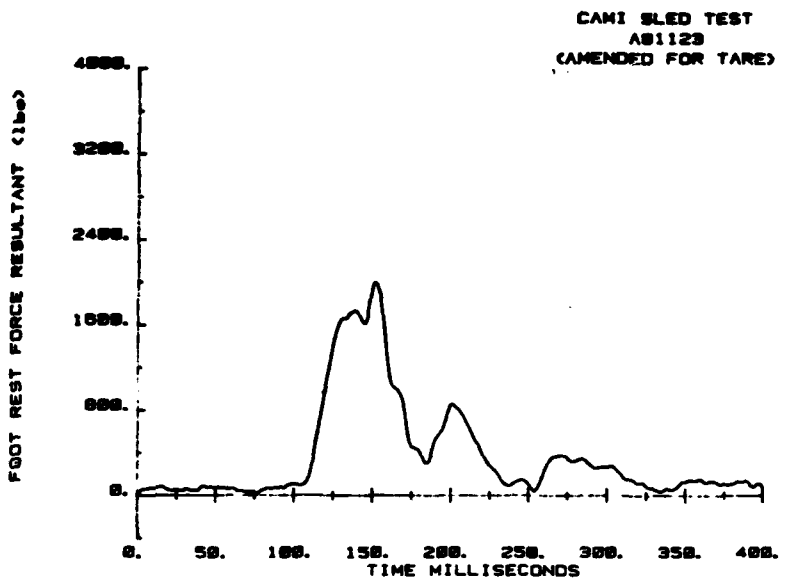

Footrest force.

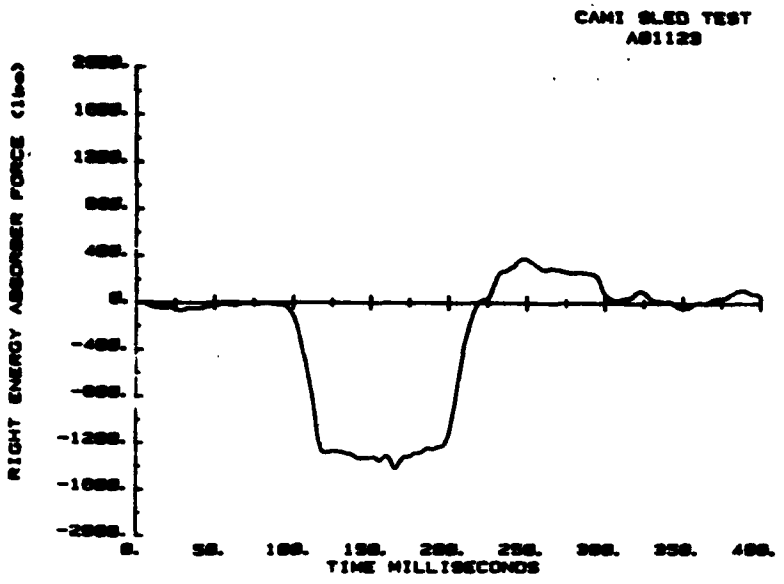

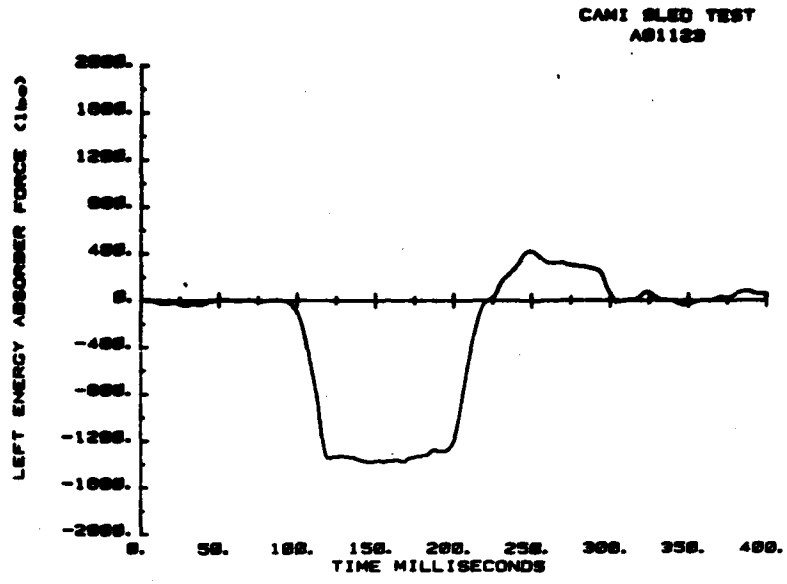

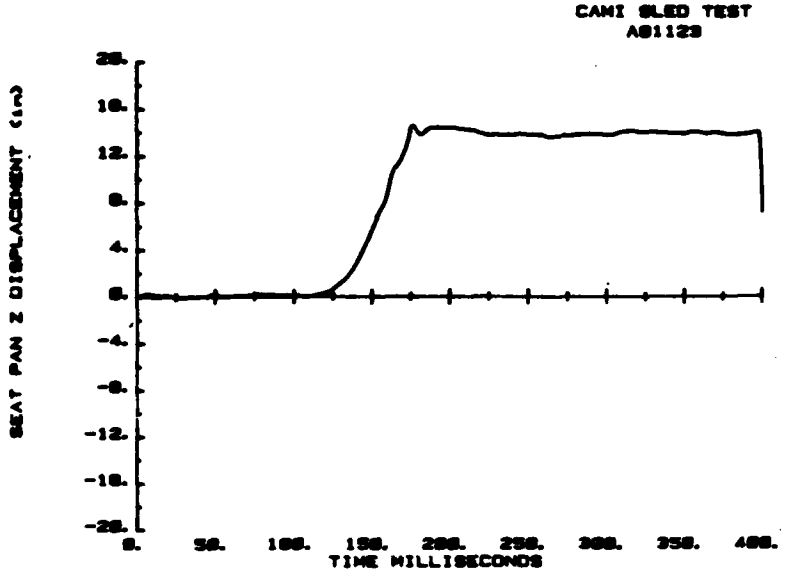

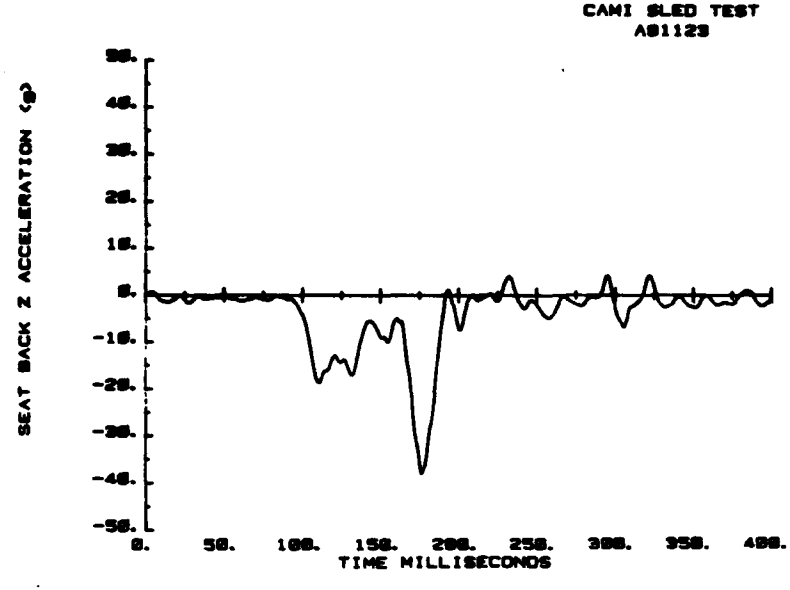

Energy absorber force and stroke.

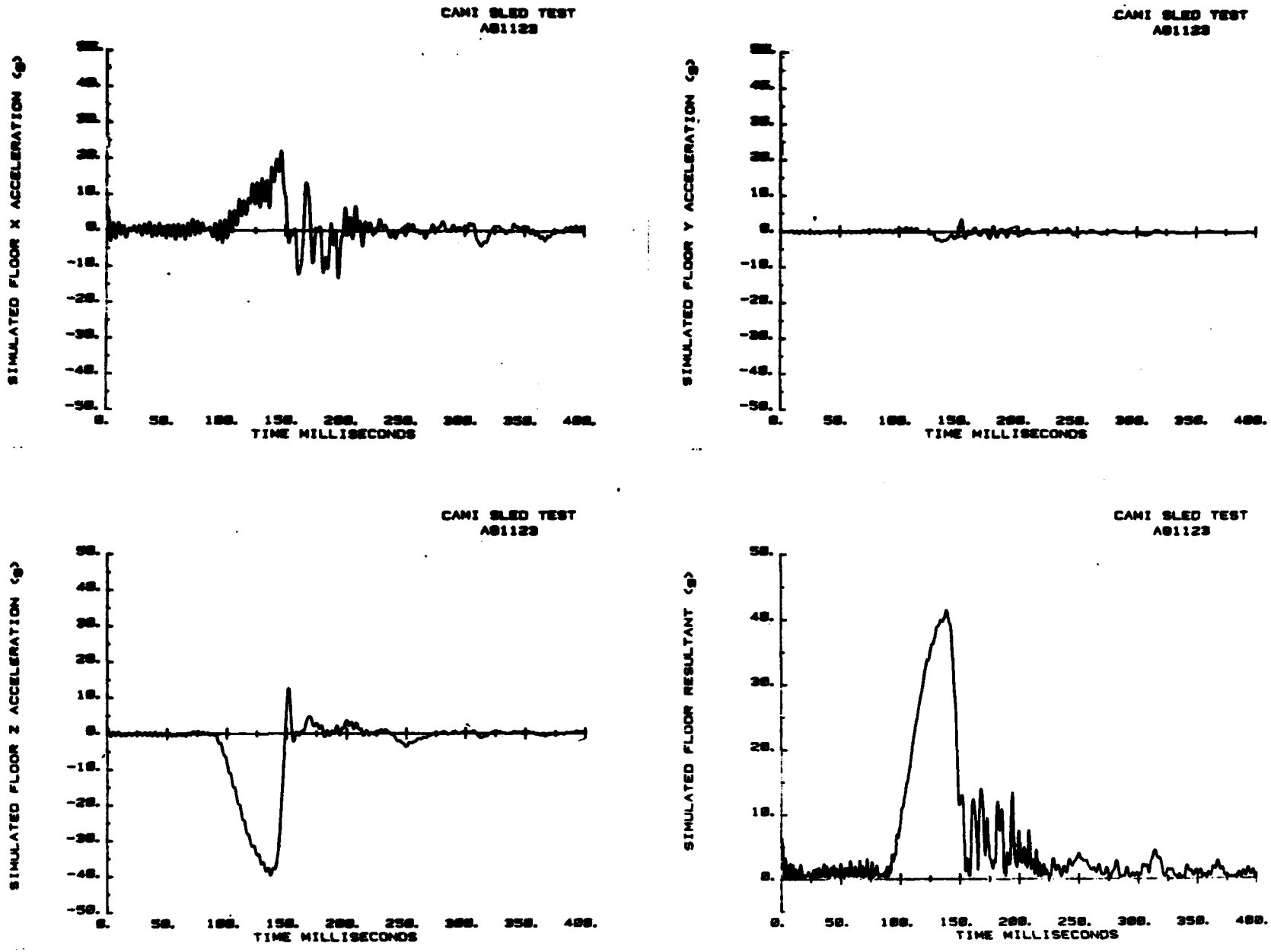

Floor acceleration.

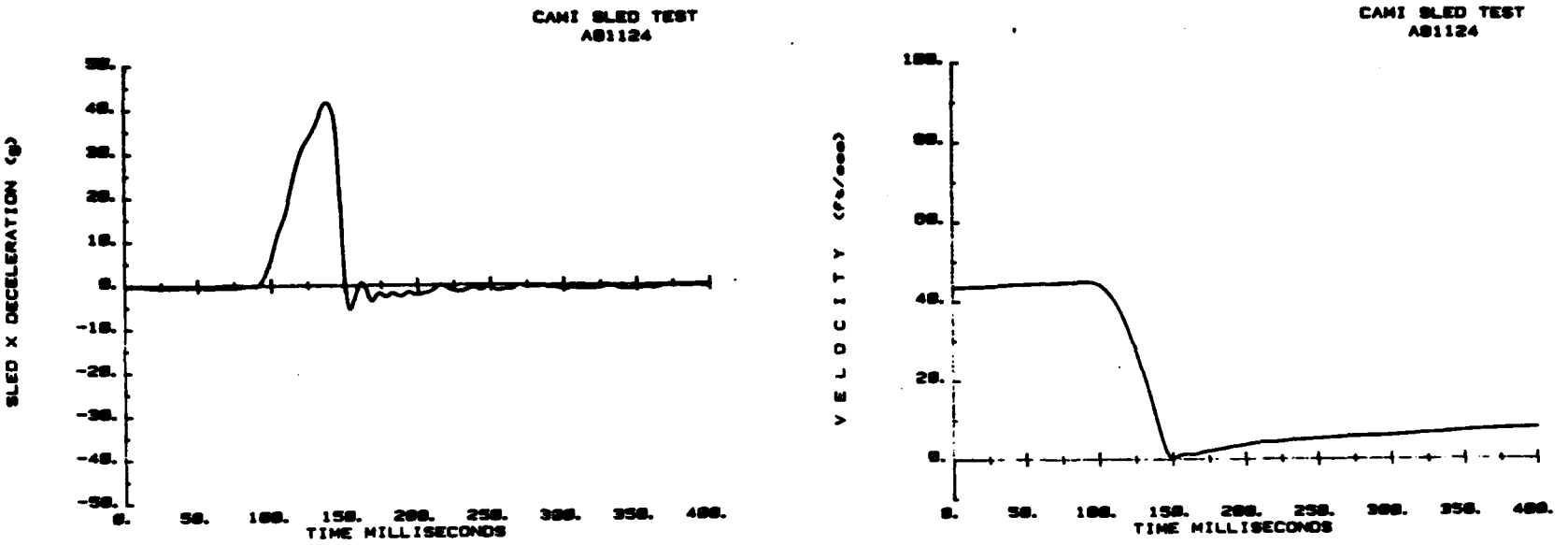

Sled deceleration and velocity.

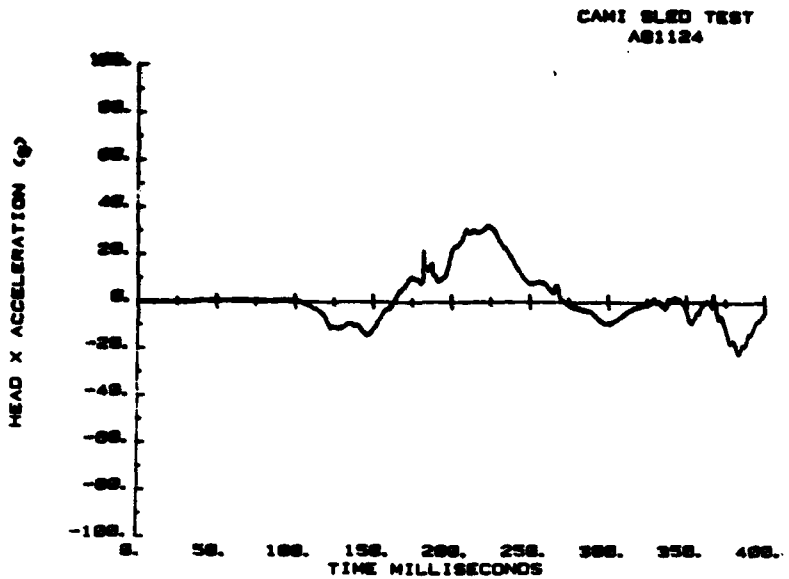

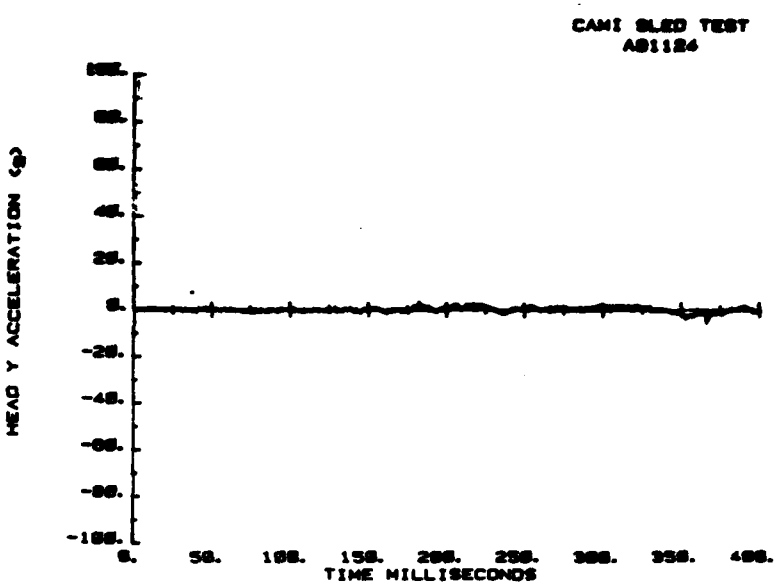

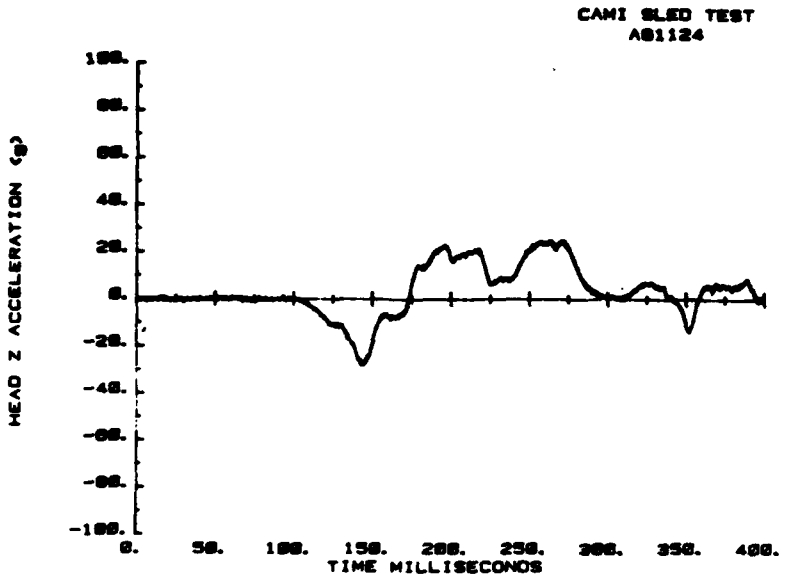

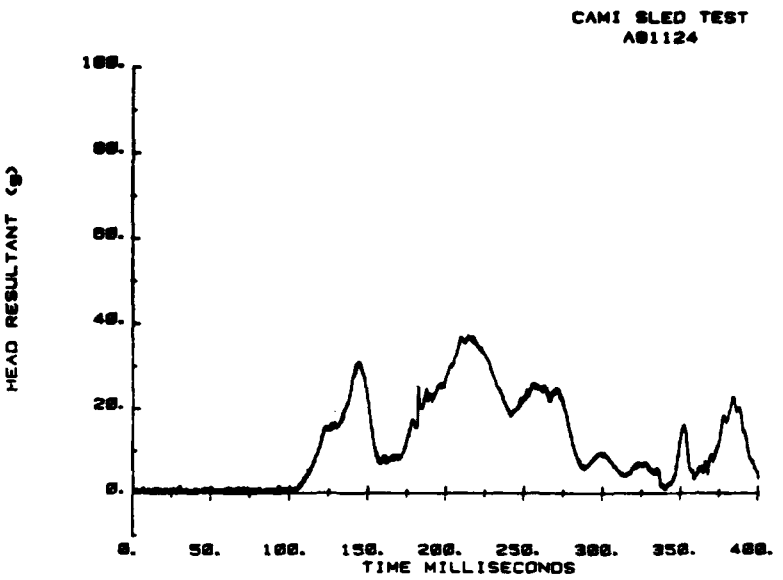

Head acceleration.

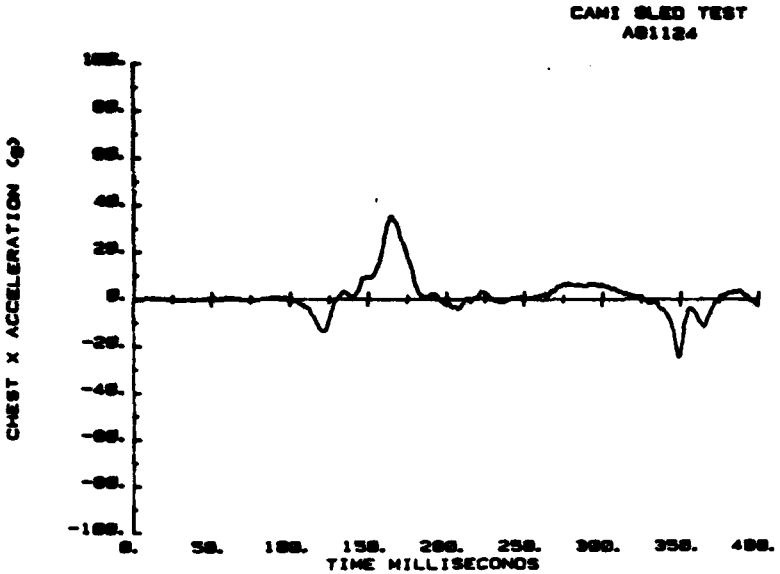

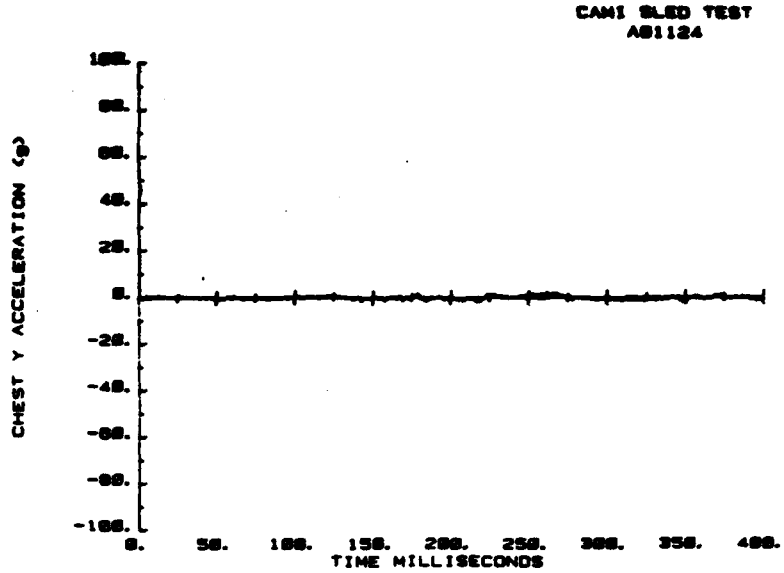

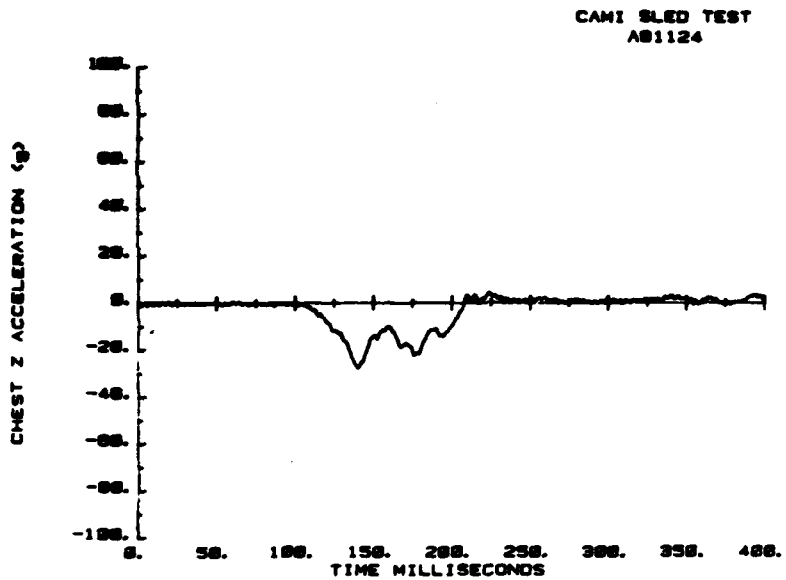

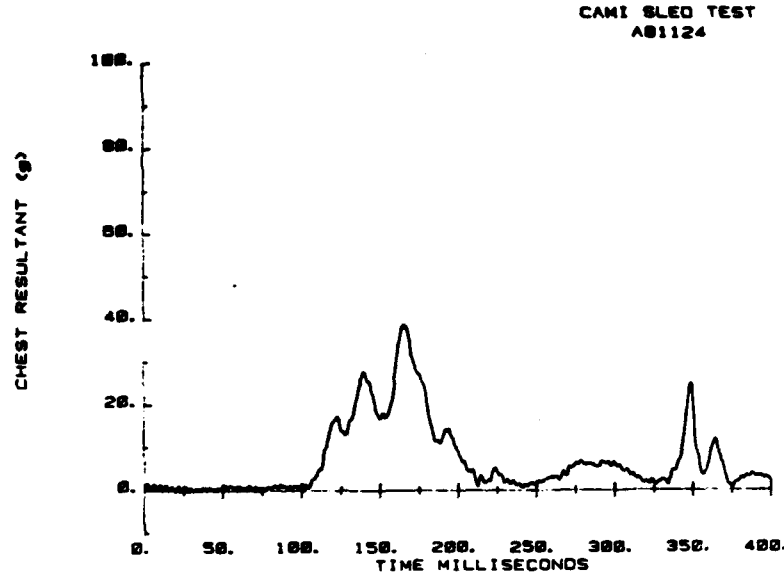

Chest acceleration.

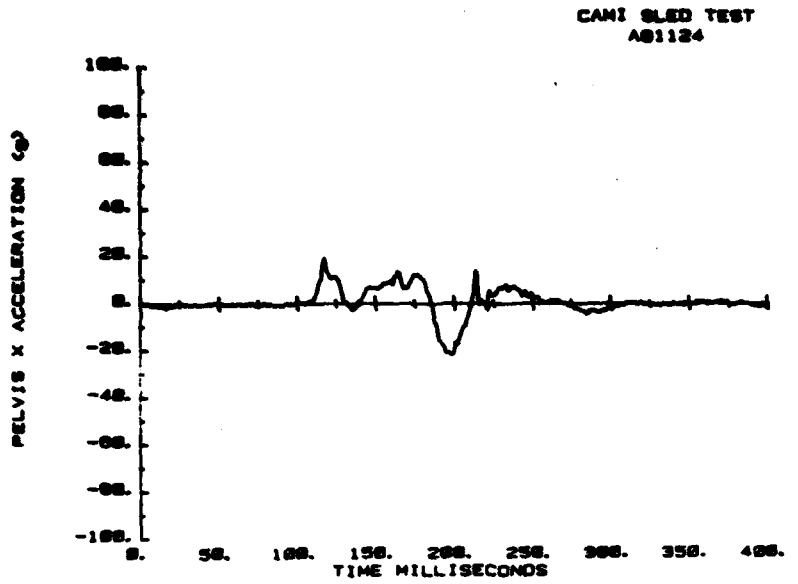

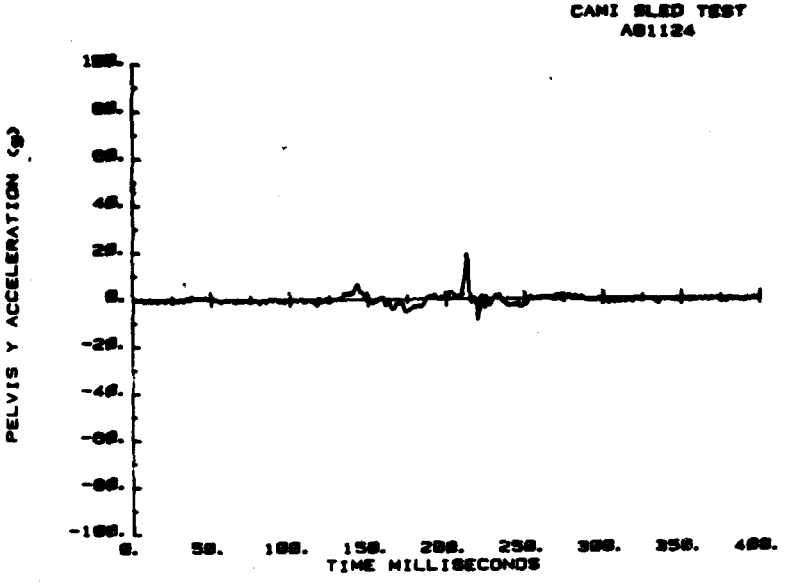

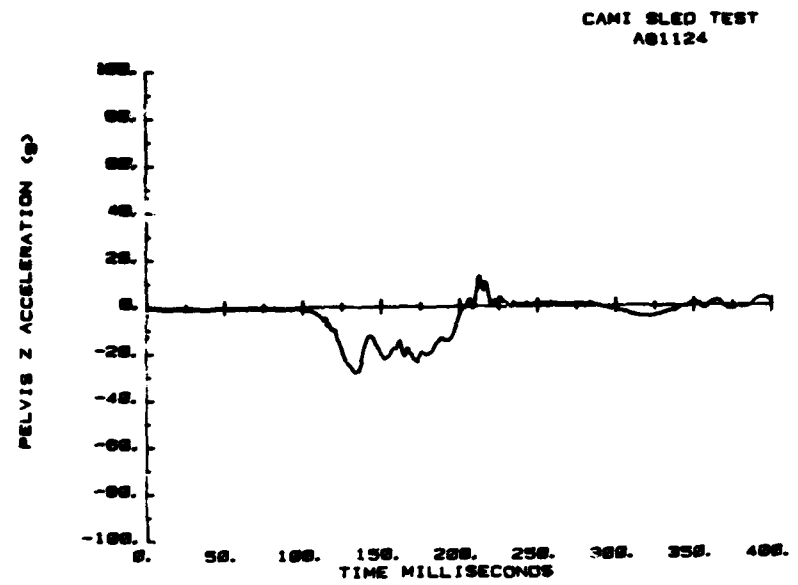

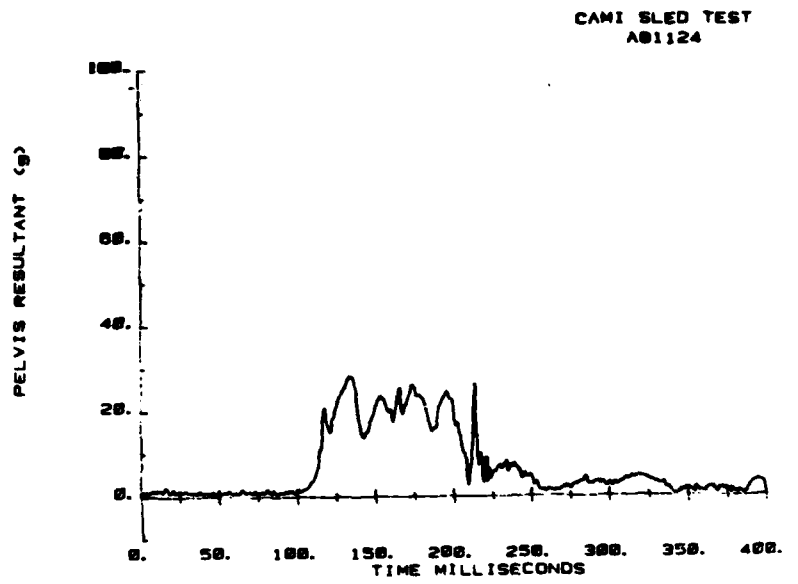

Pelvis acceleration.

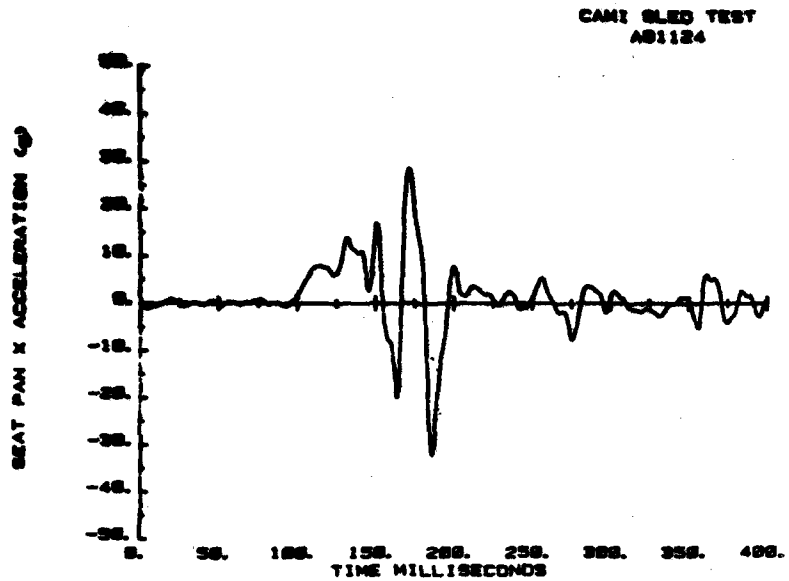

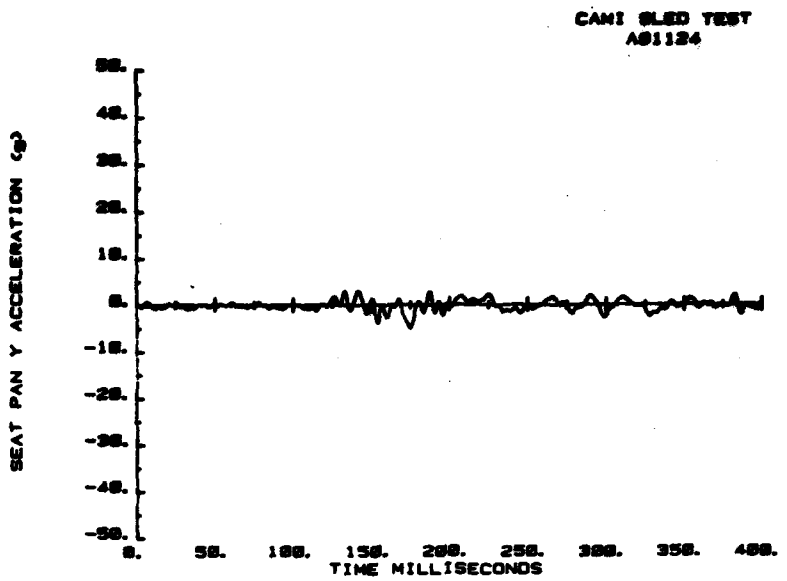

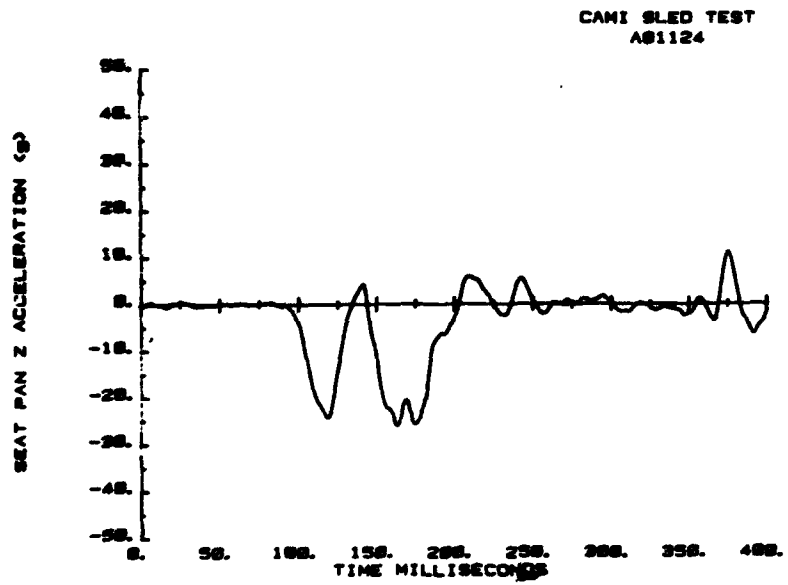

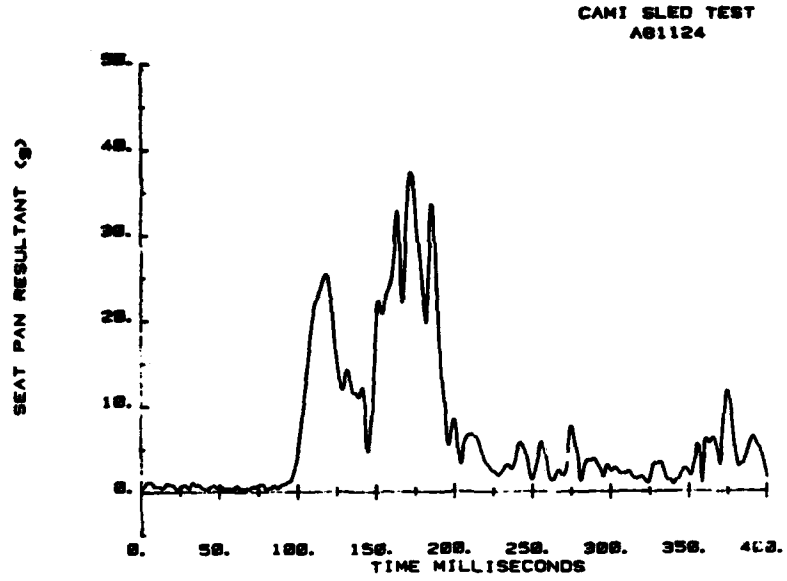

Seat pan acceleration.

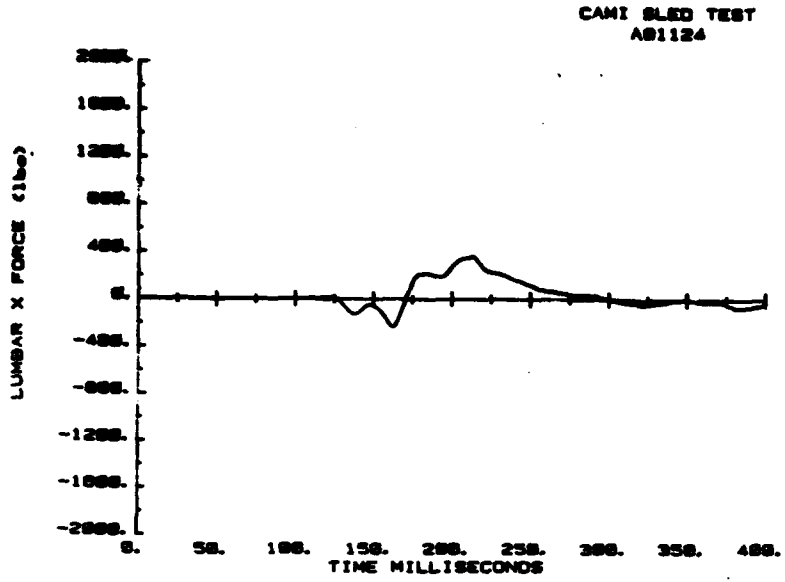

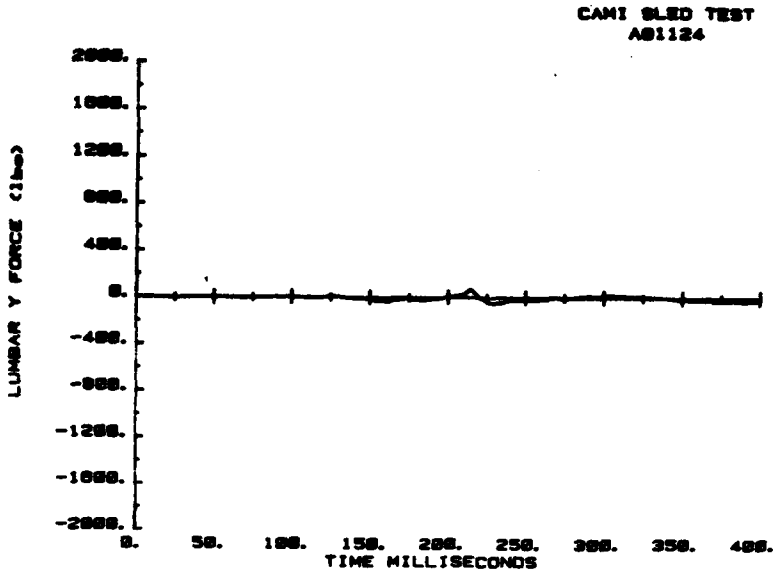

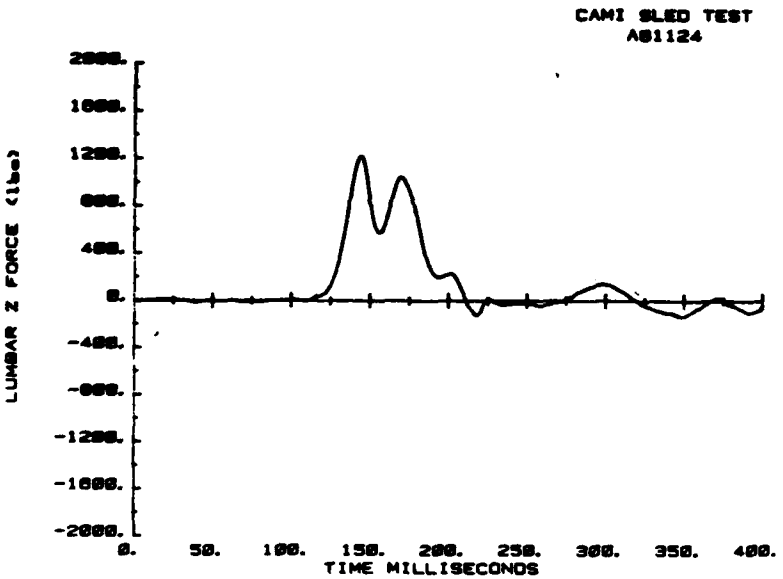

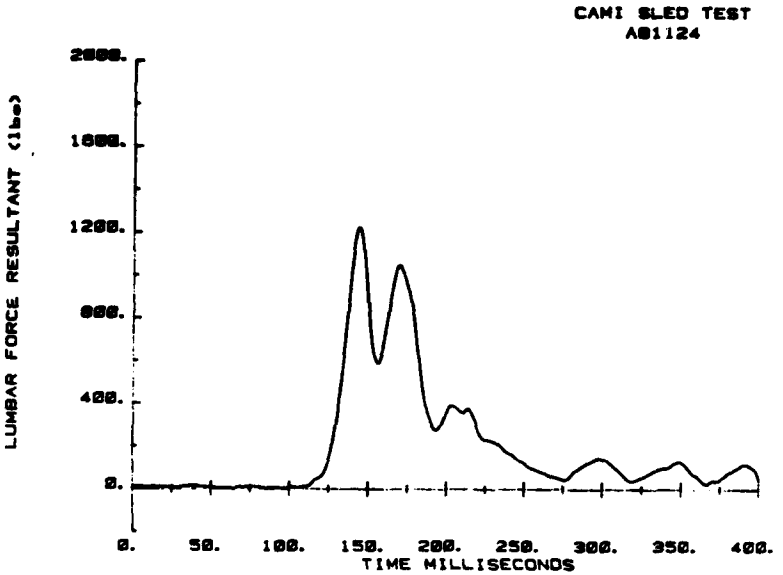

Lumbar force.

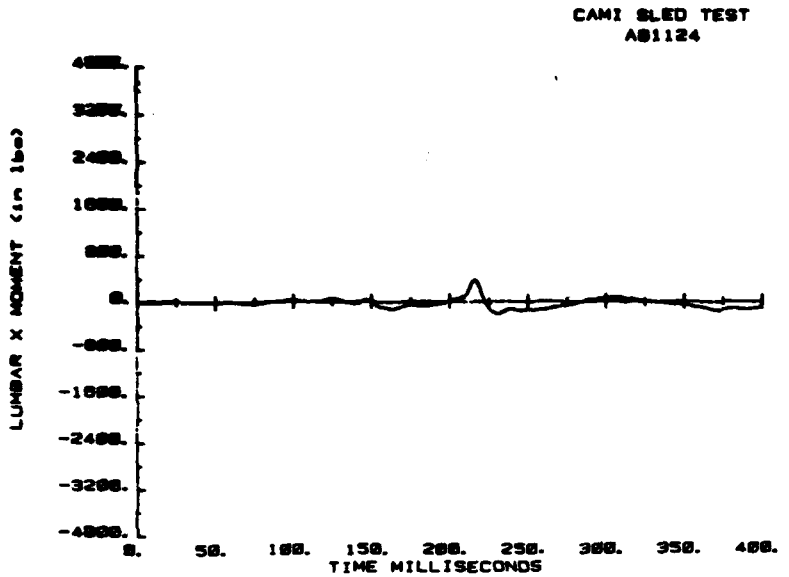

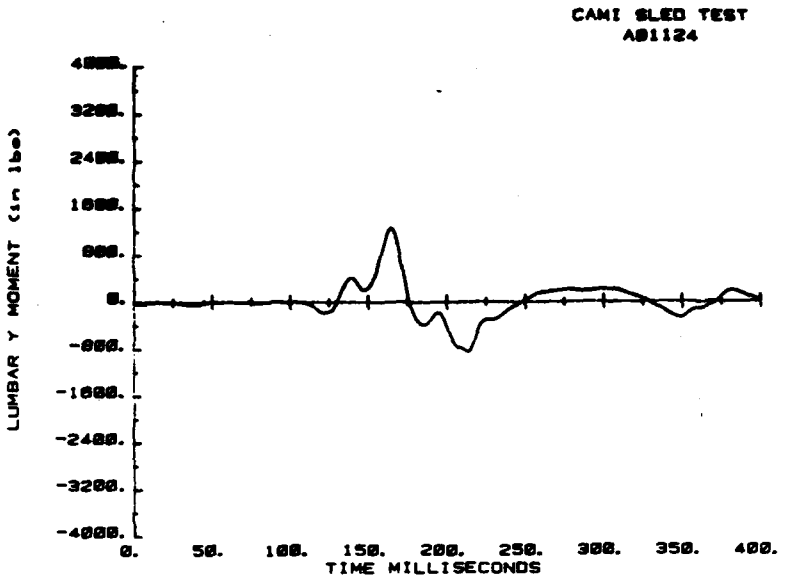

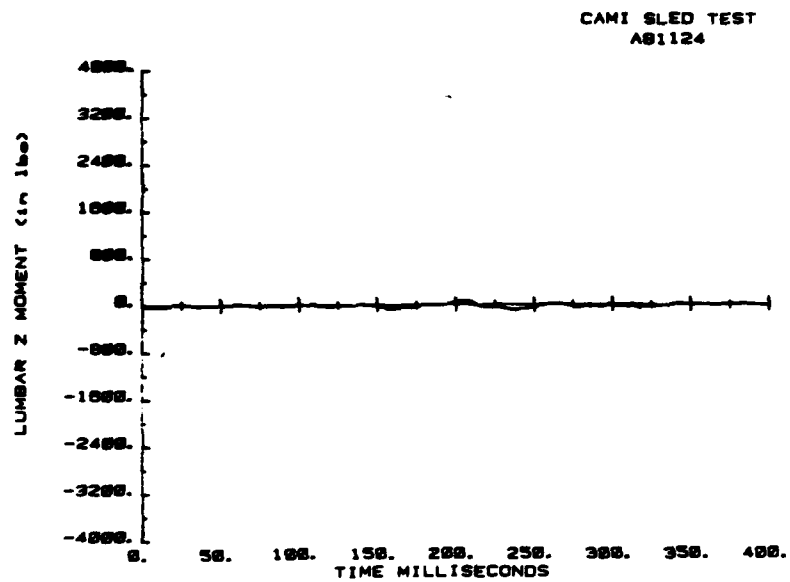

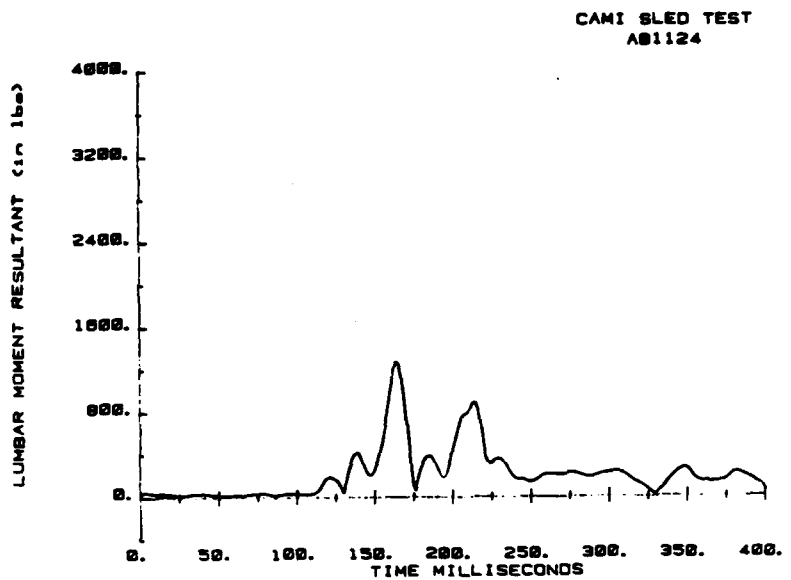

Lumbar moment.

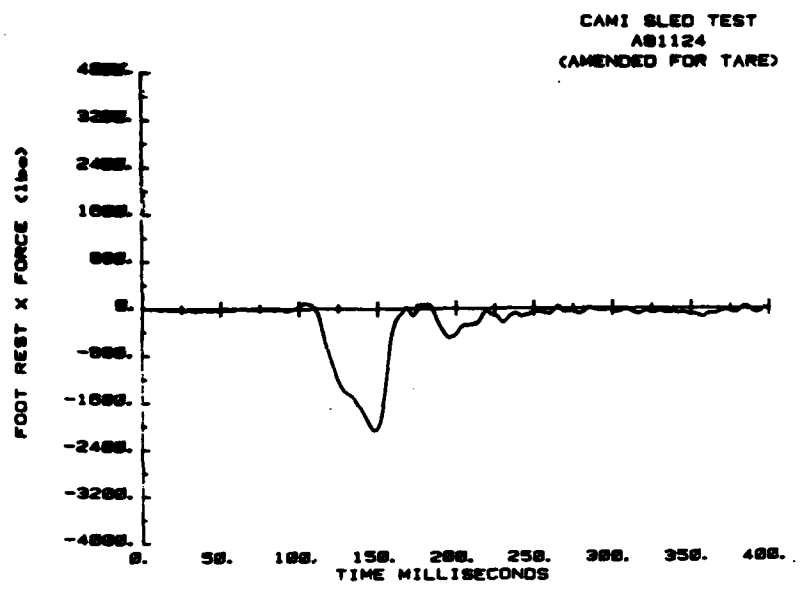

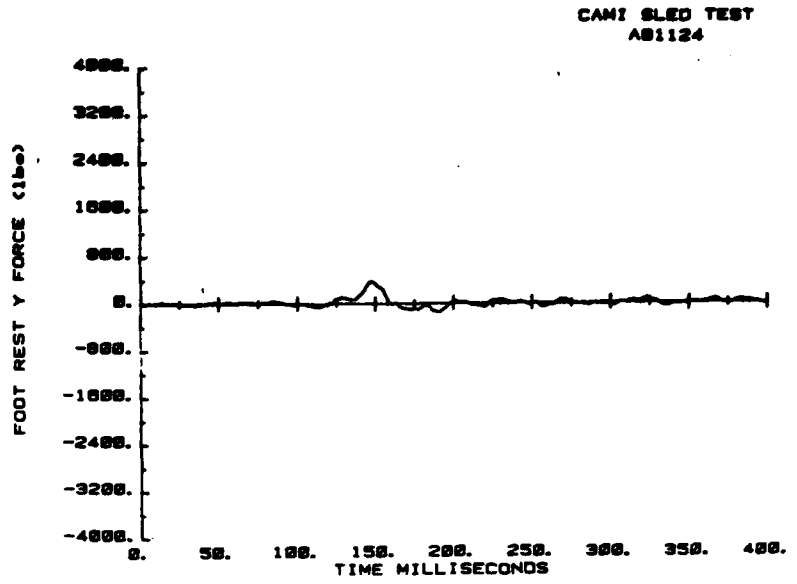

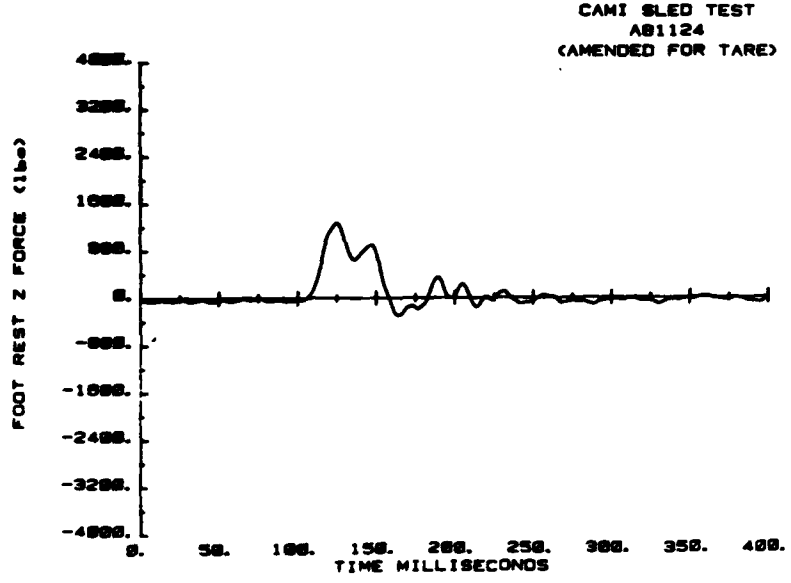

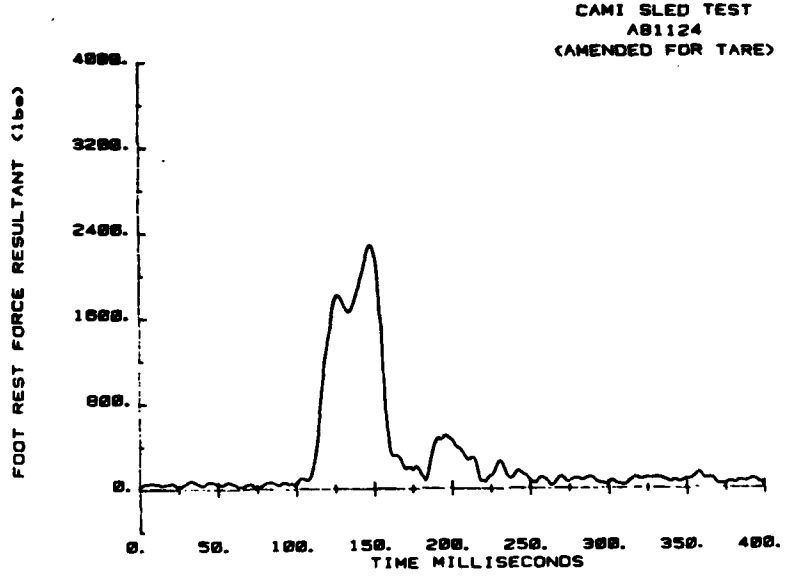

Footrest force.

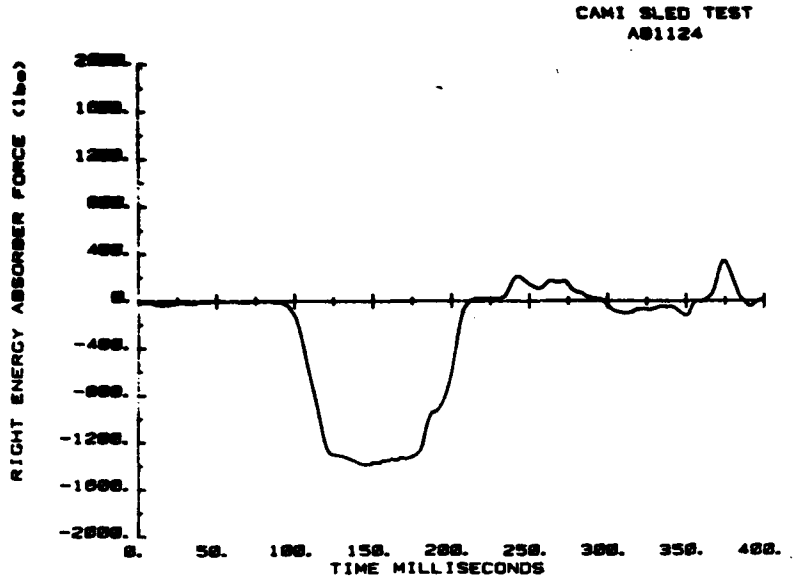

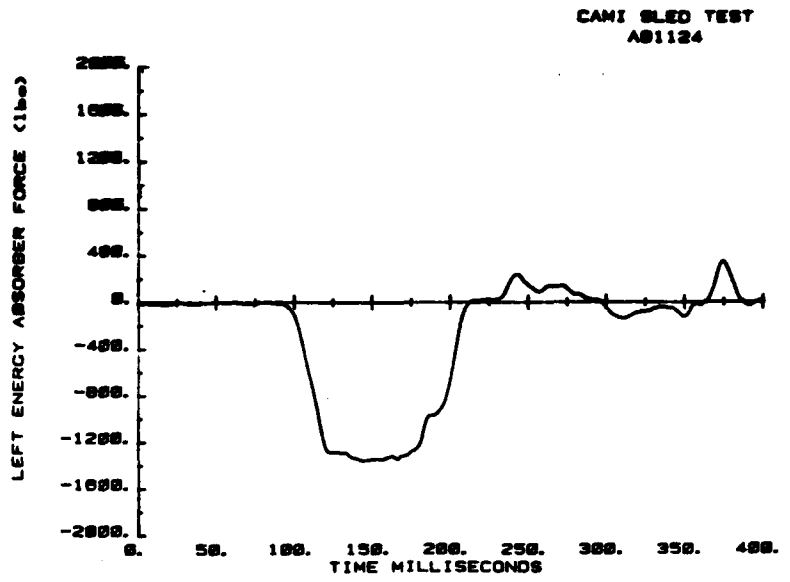

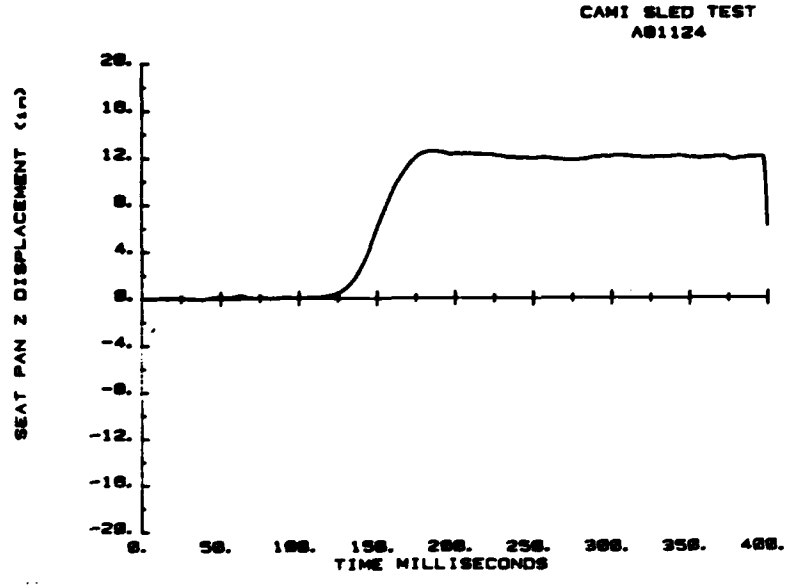

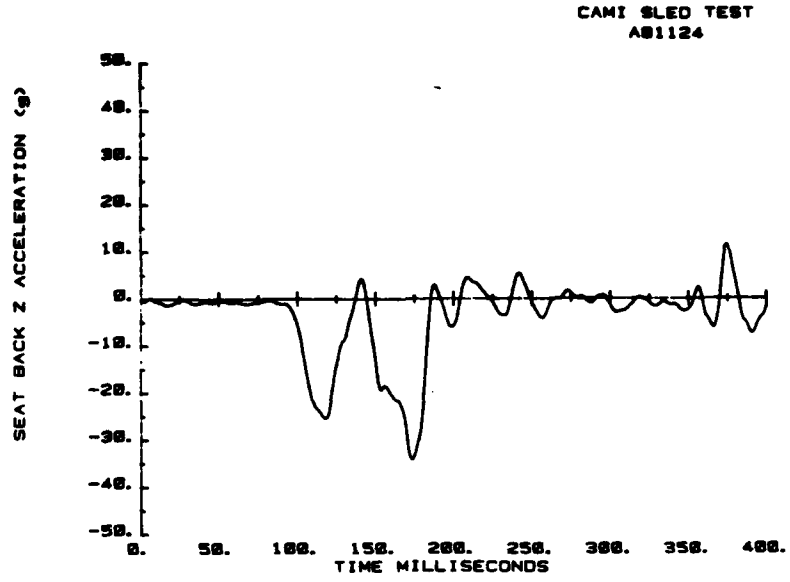

Energy absorber force and stroke.

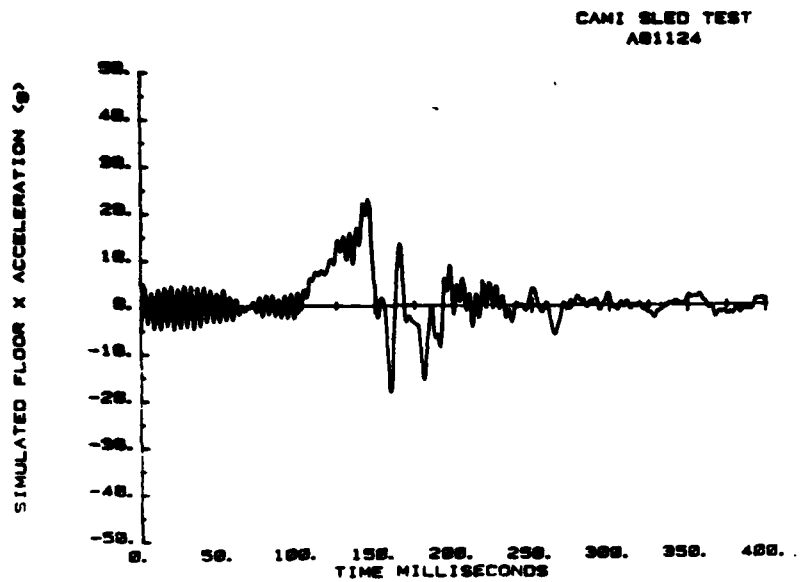

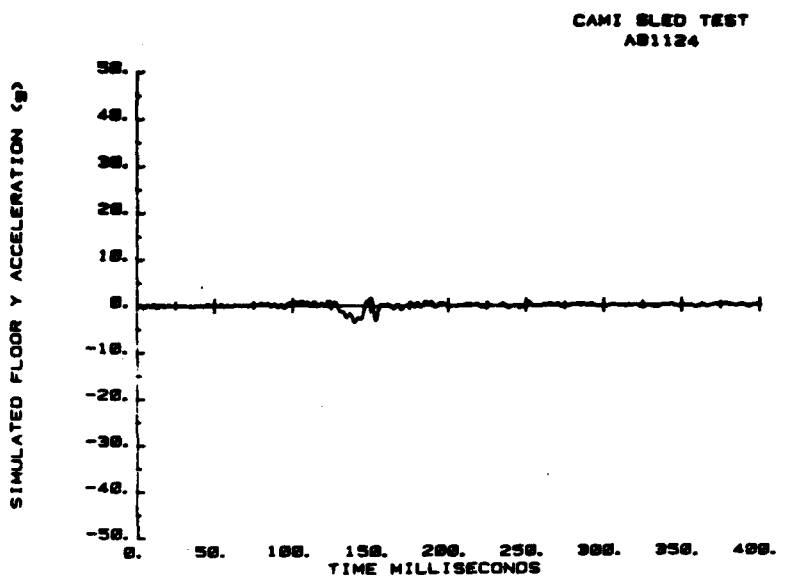

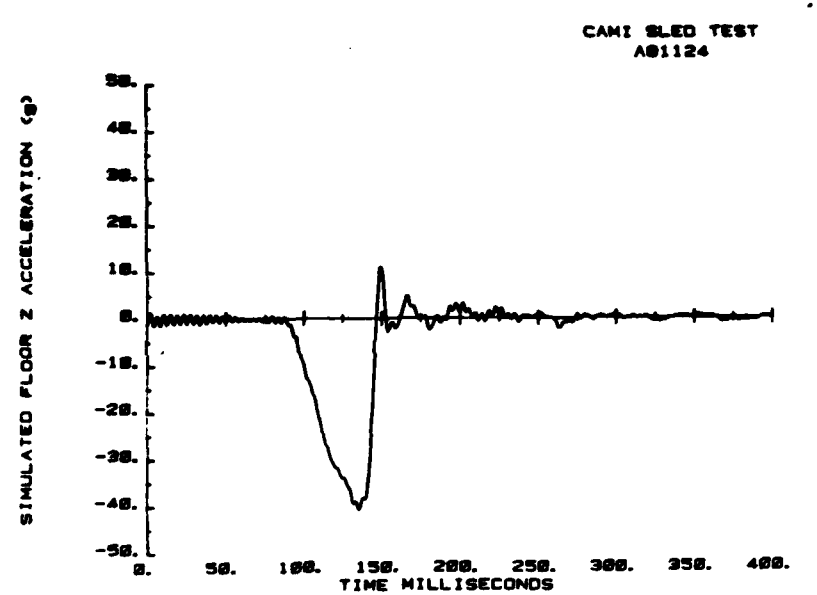

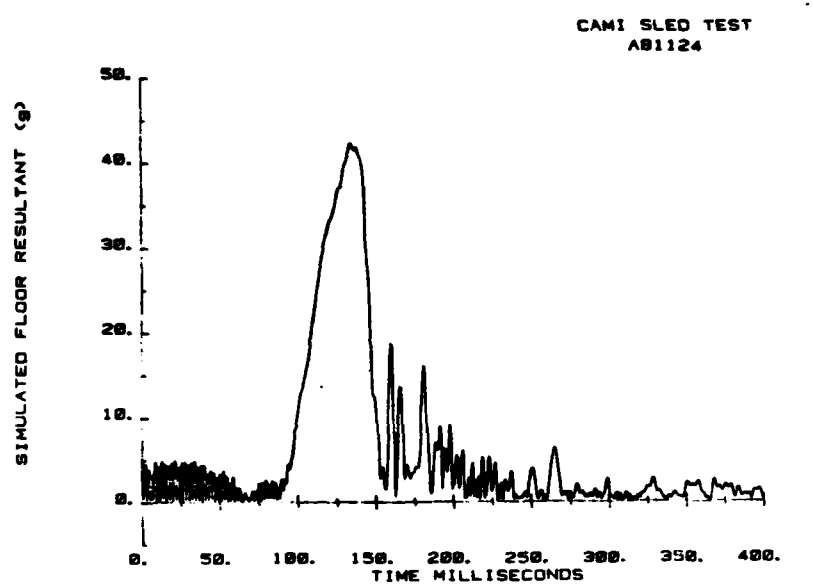

Floor acceleration.

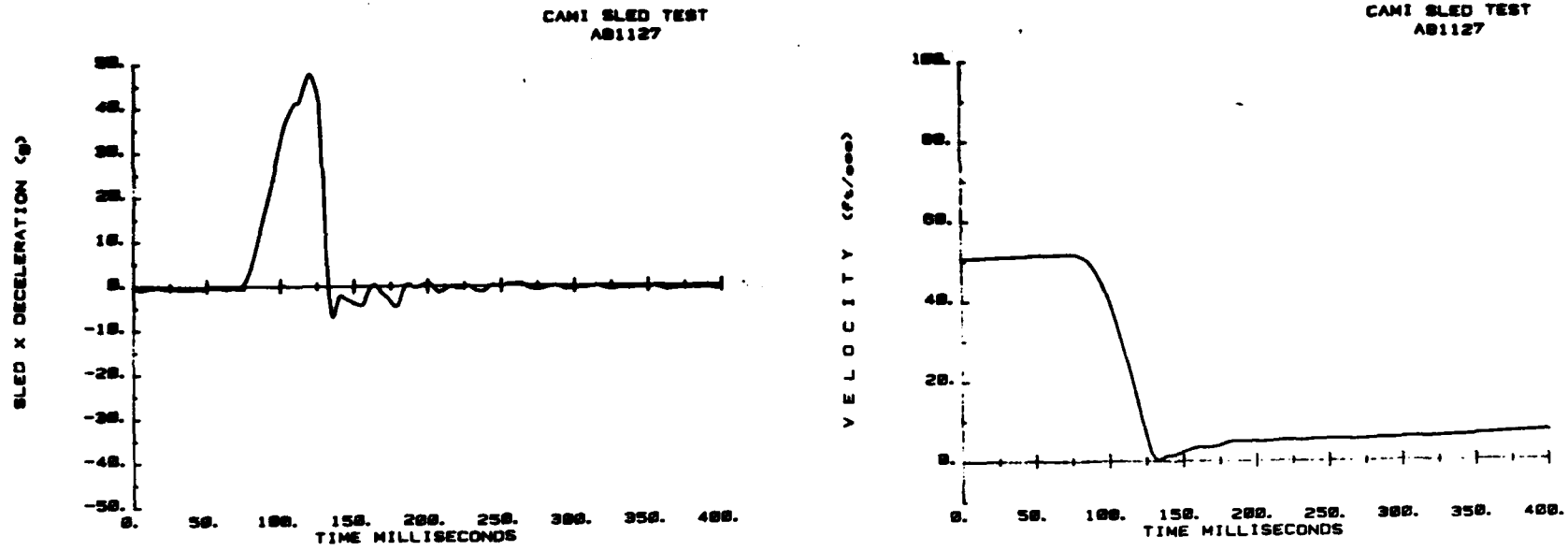

Sled deceleration and velocity.

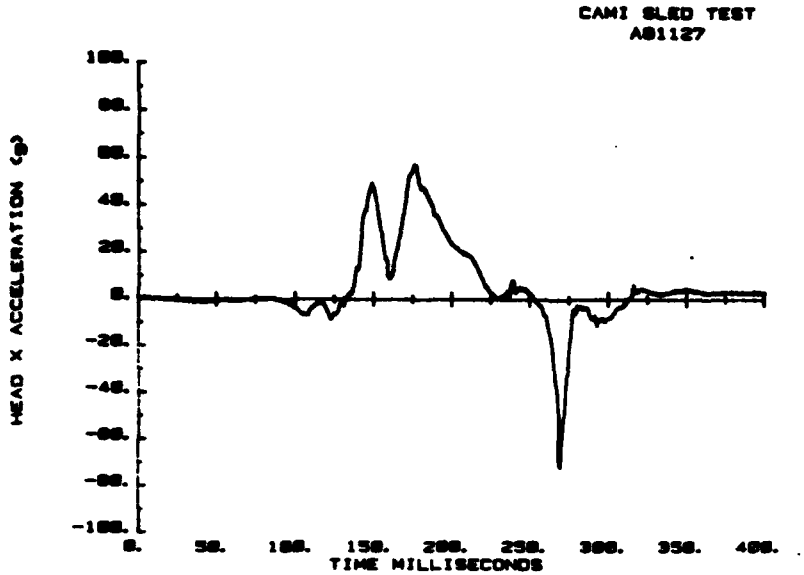

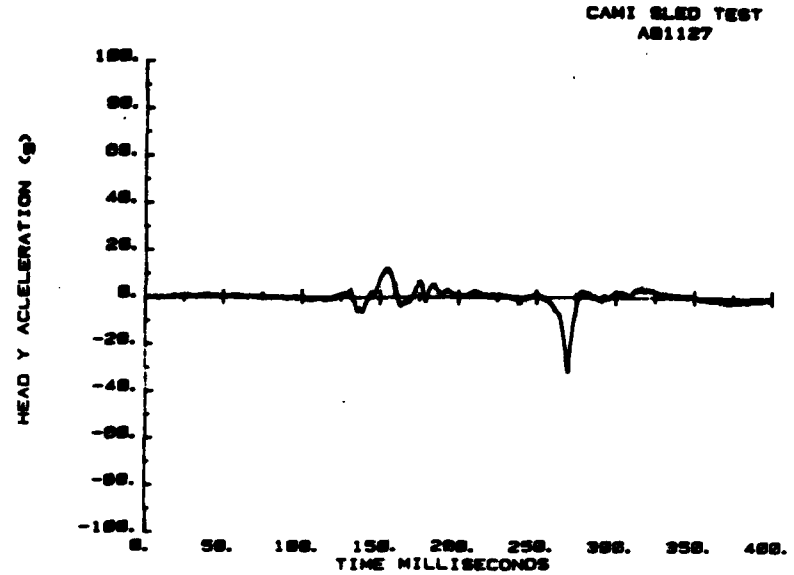

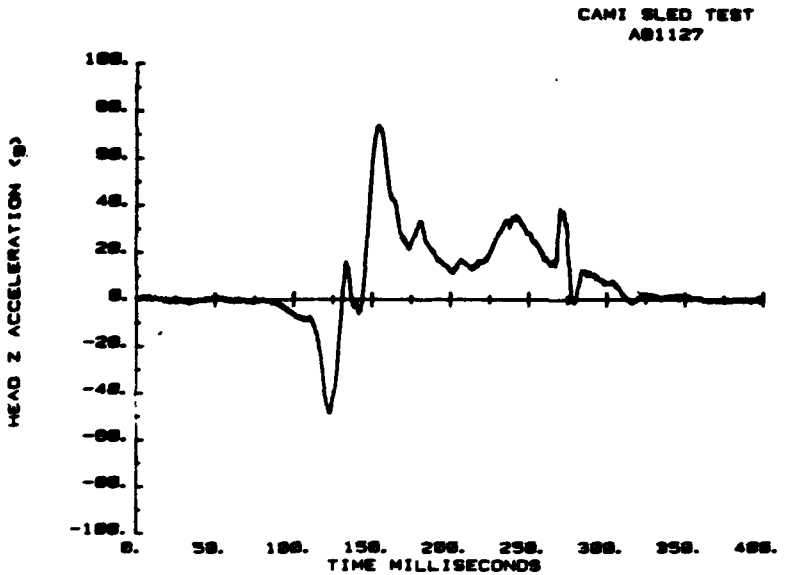

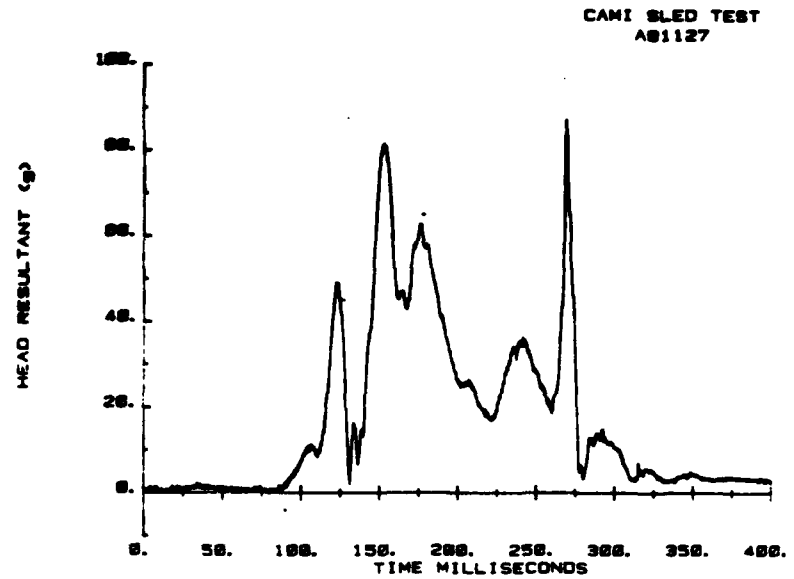

Head acceleration.

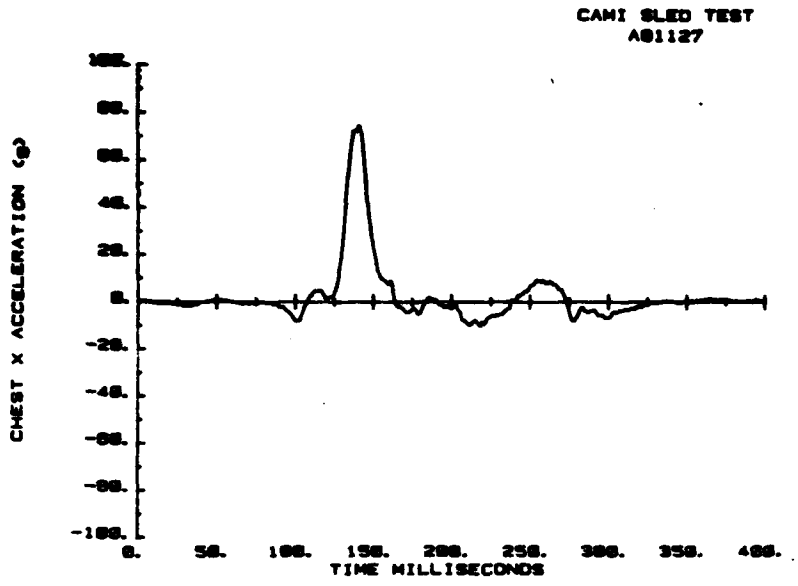

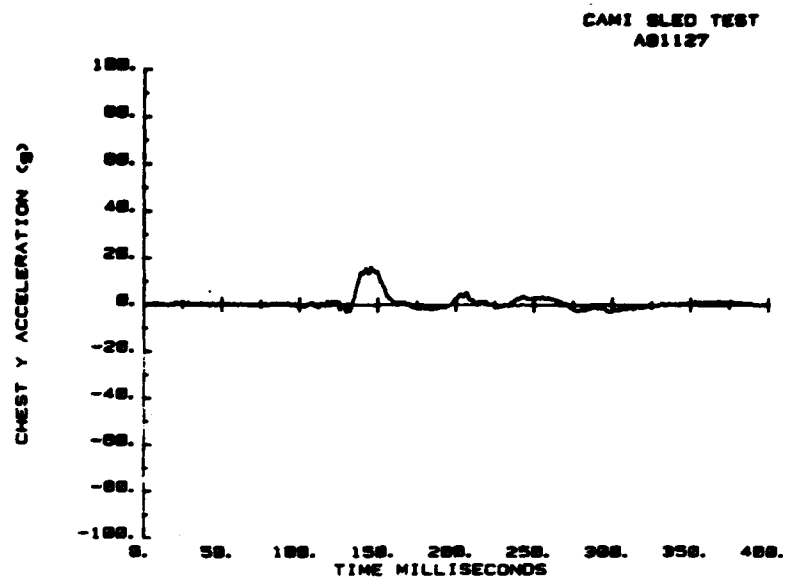

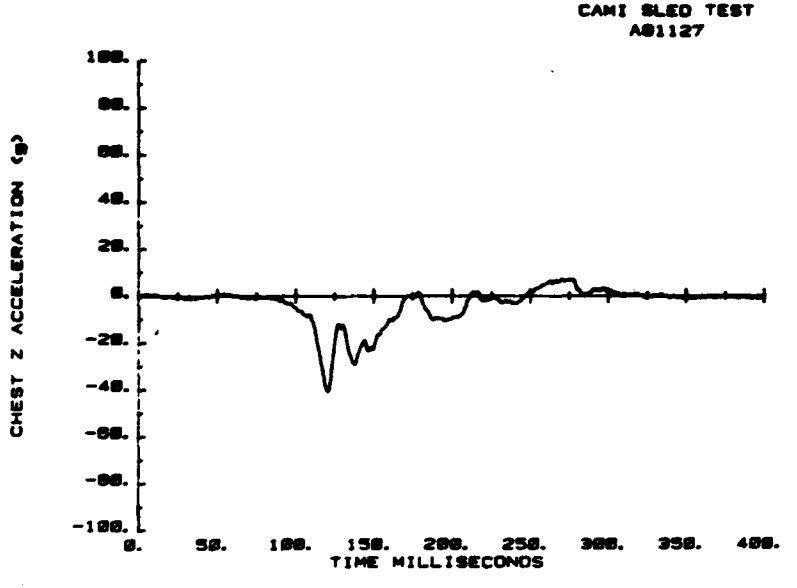

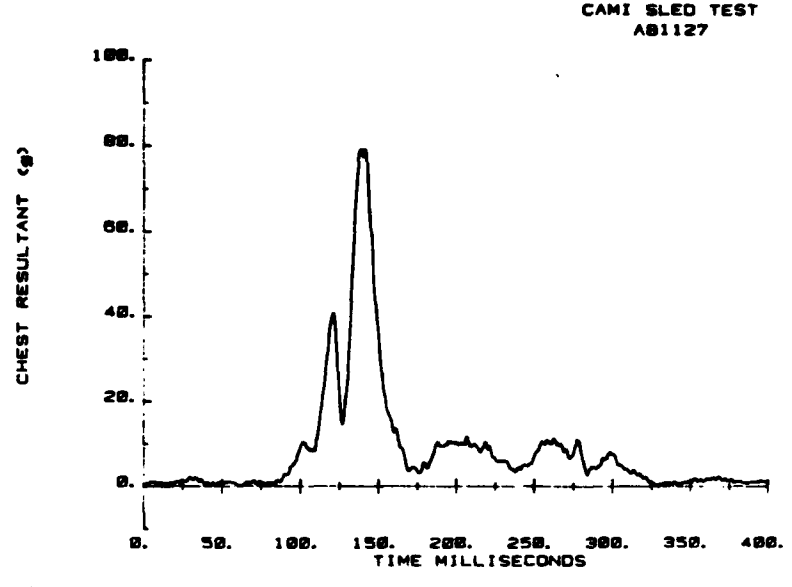

Chest acceleration.

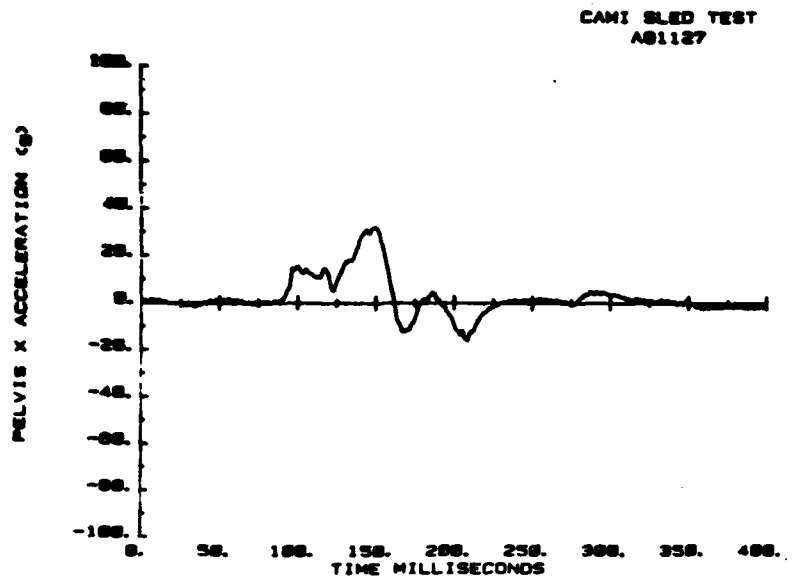

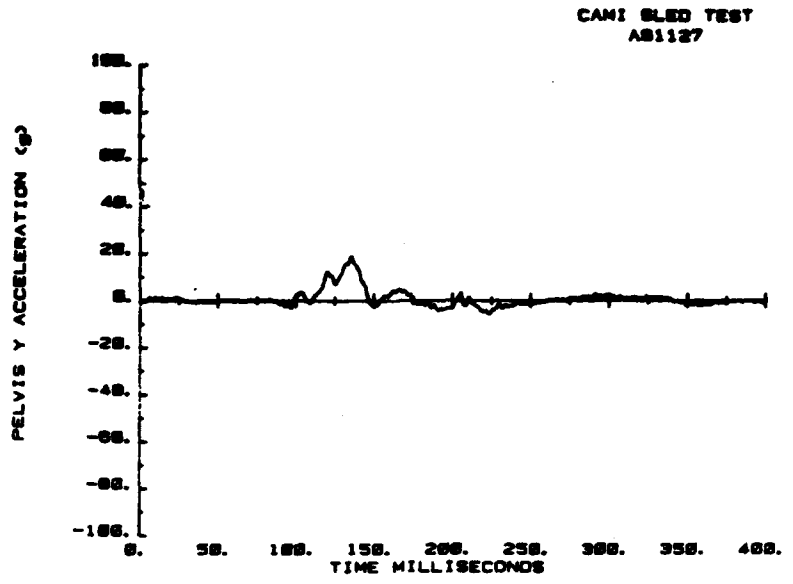

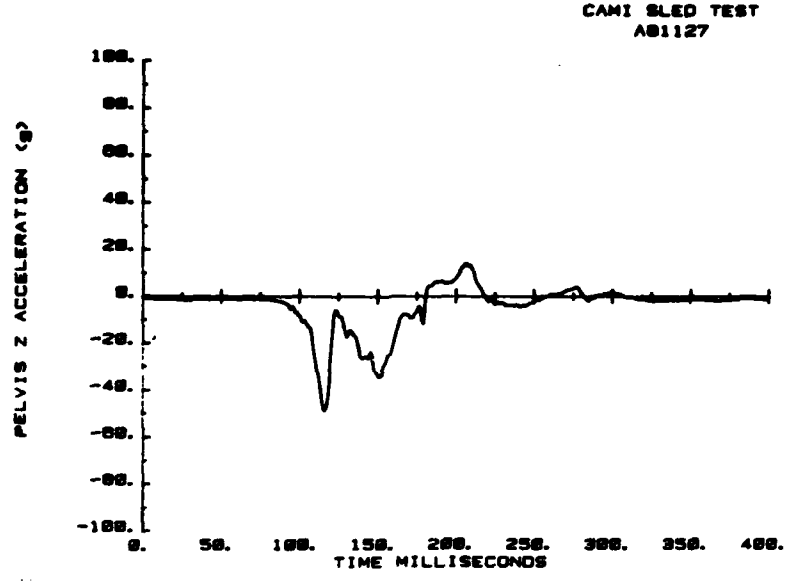

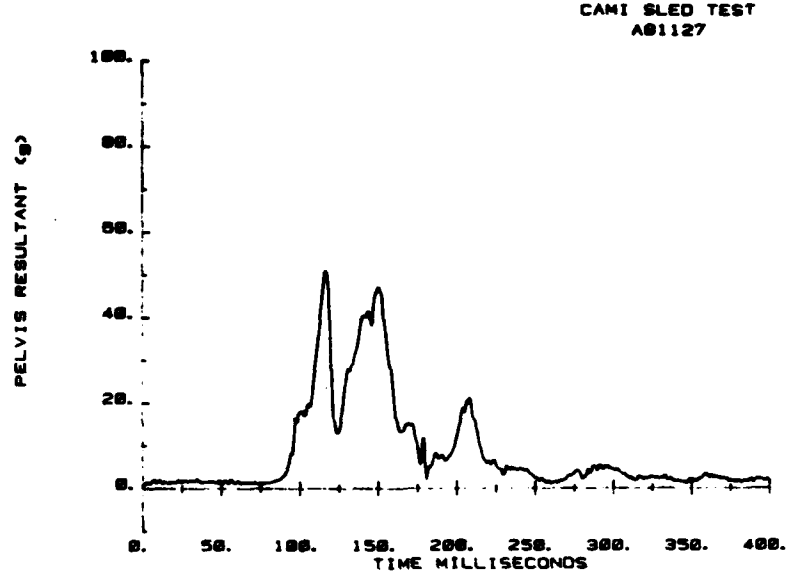

Pelvis acceleration.

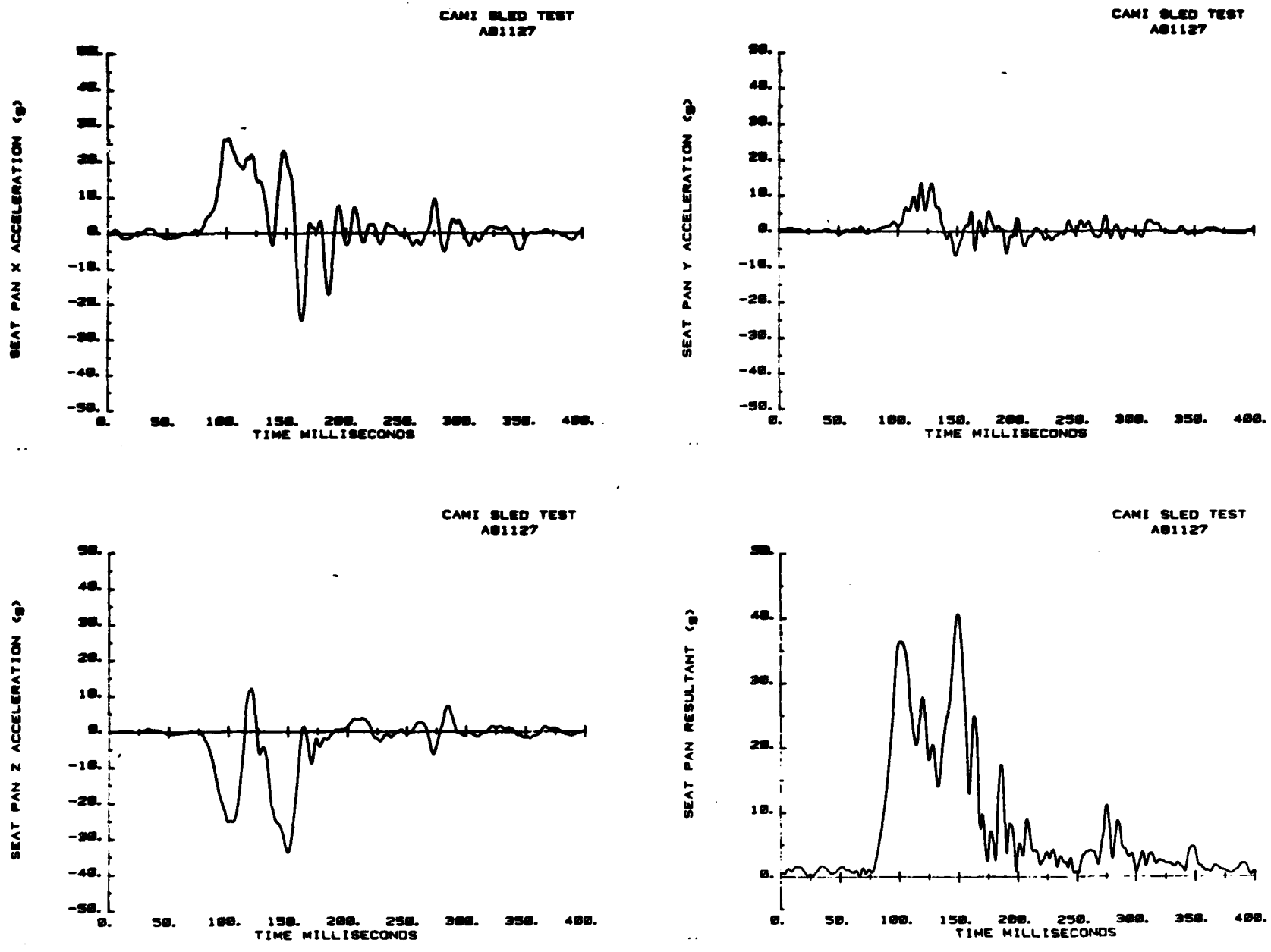

Seat pan acceleration.

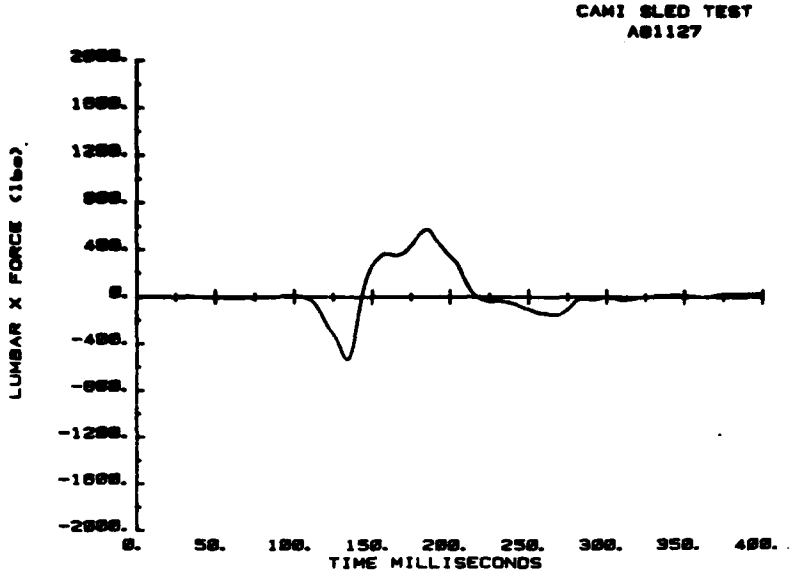

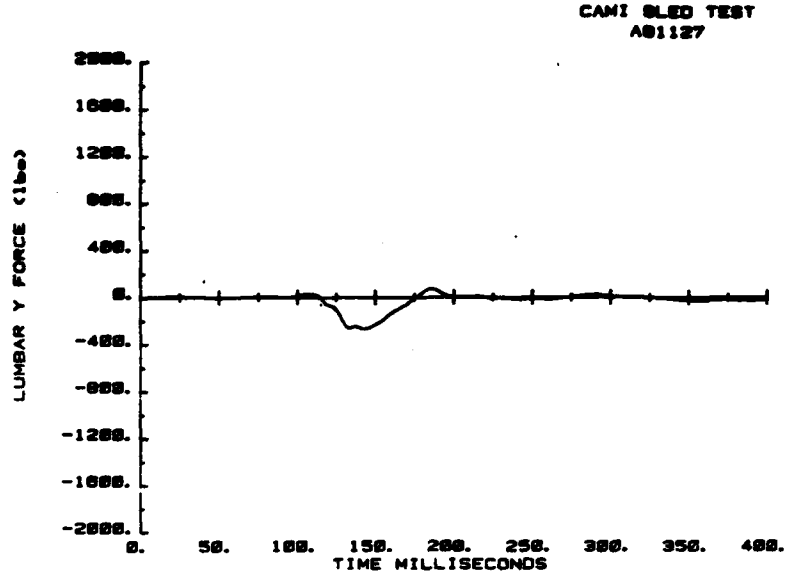

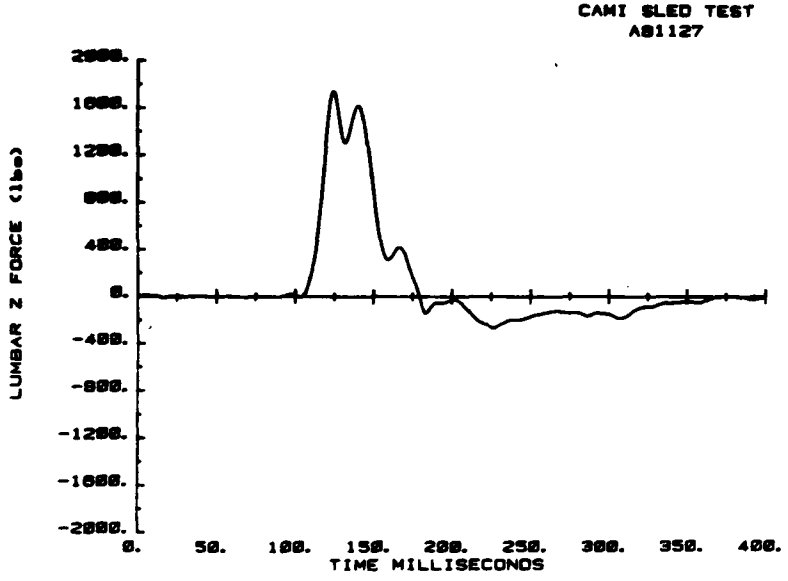

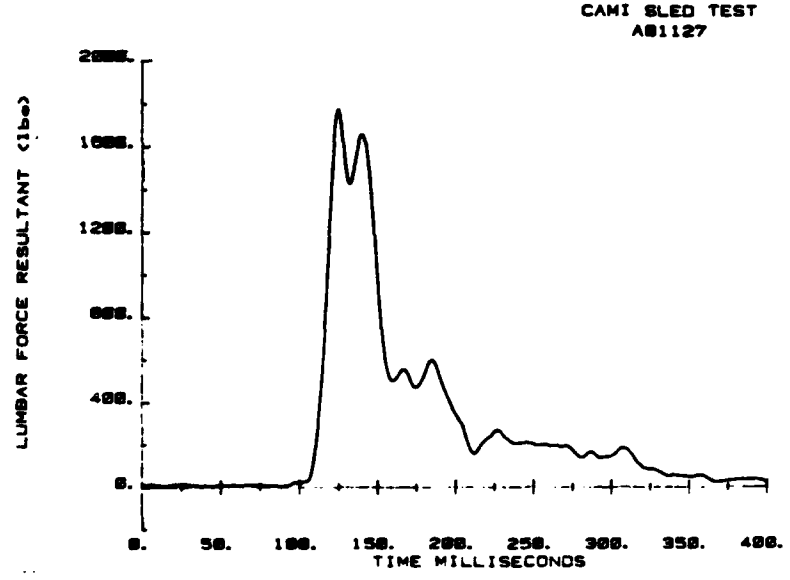

Lumbar force.

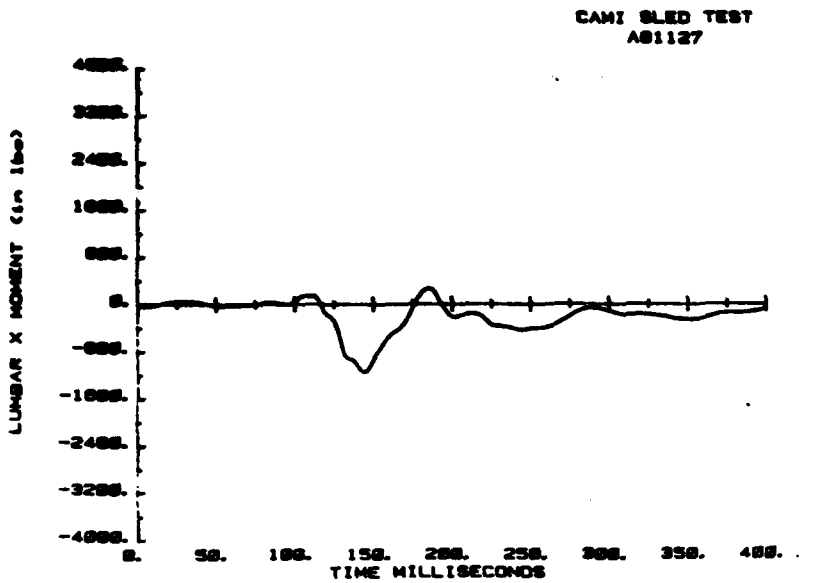

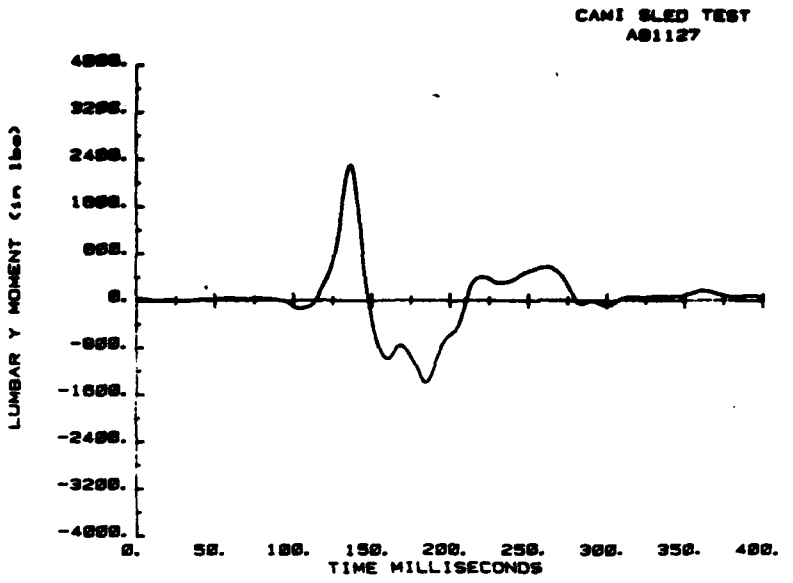

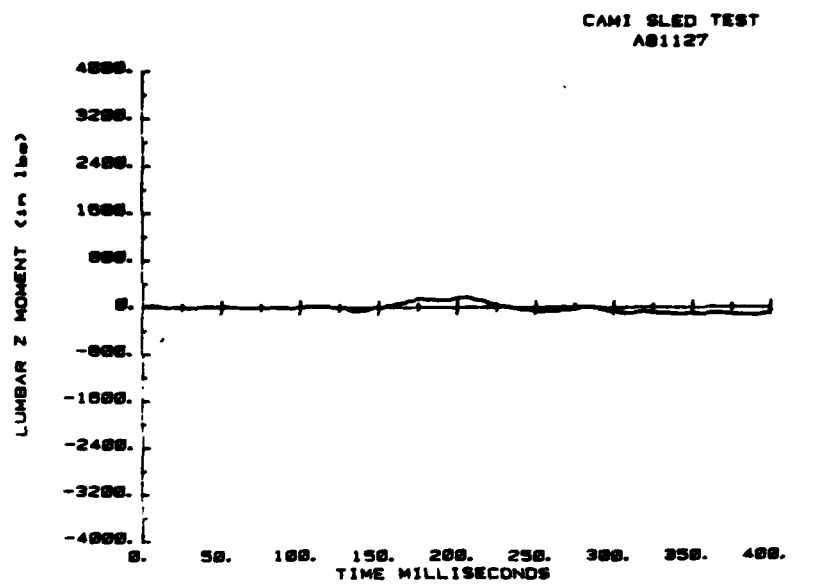

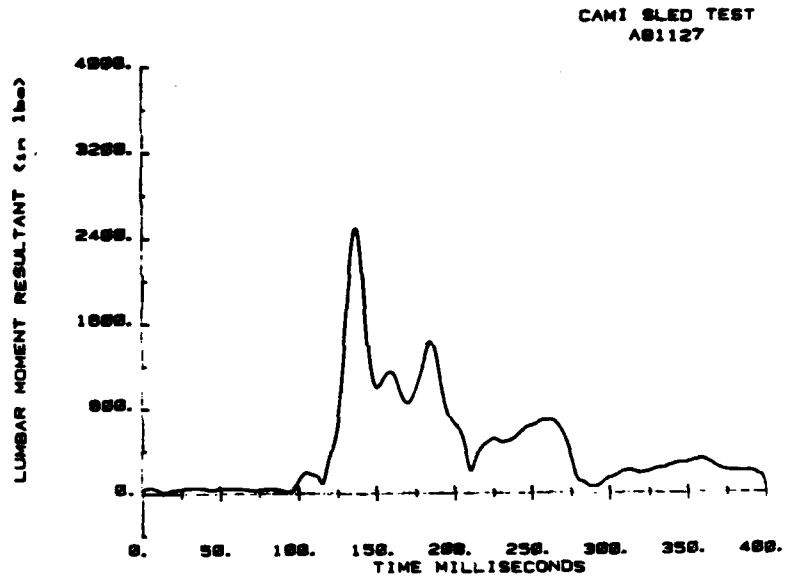

Lumbar moment.

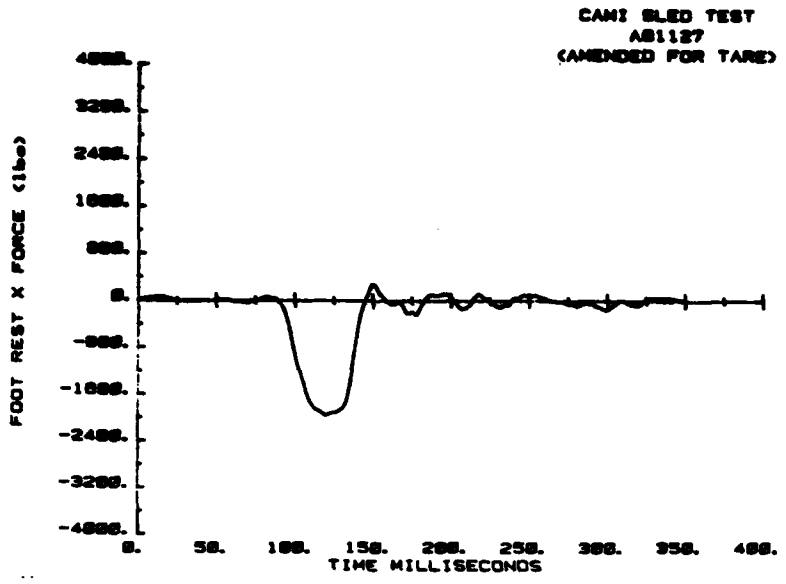

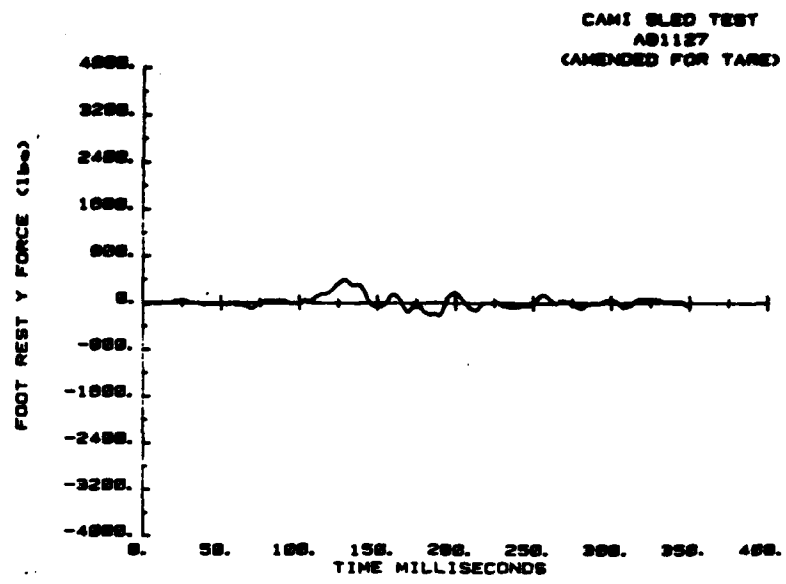

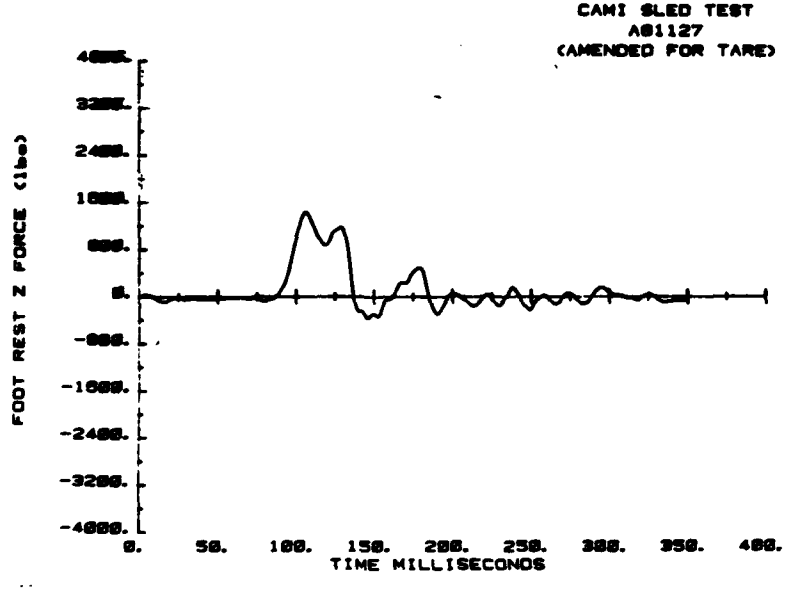

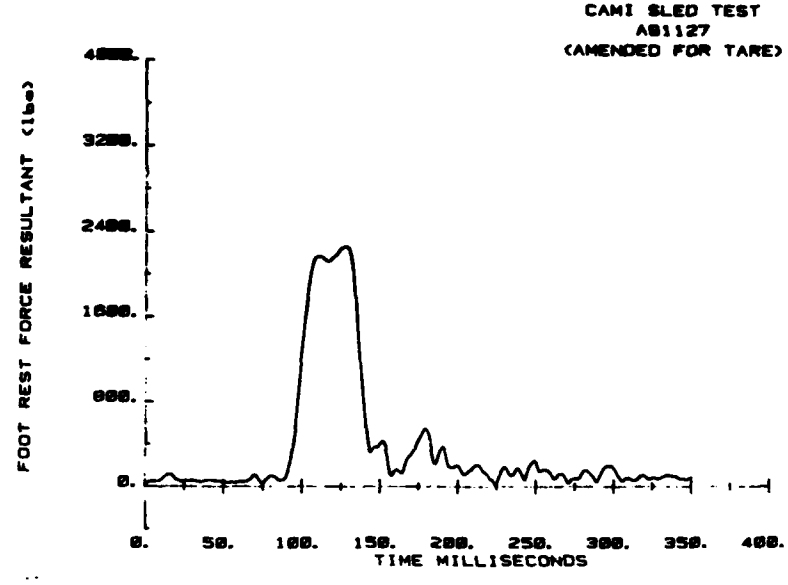

Footrest force.

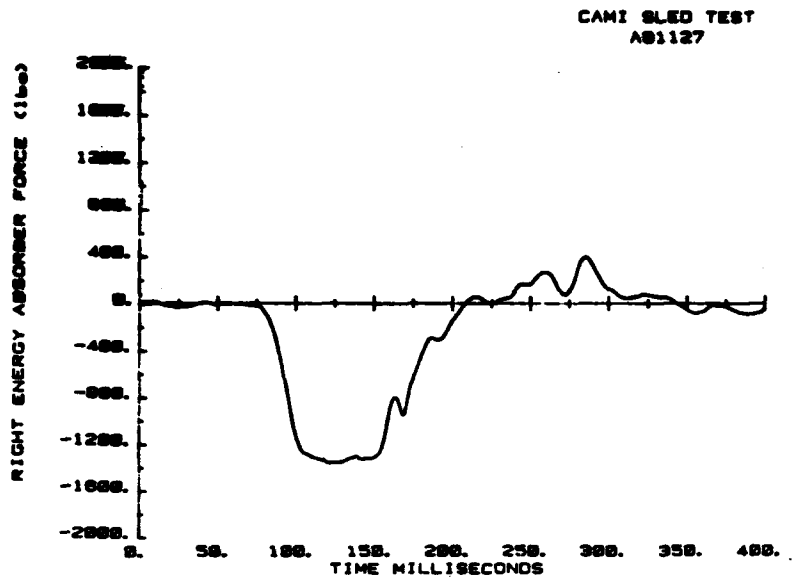

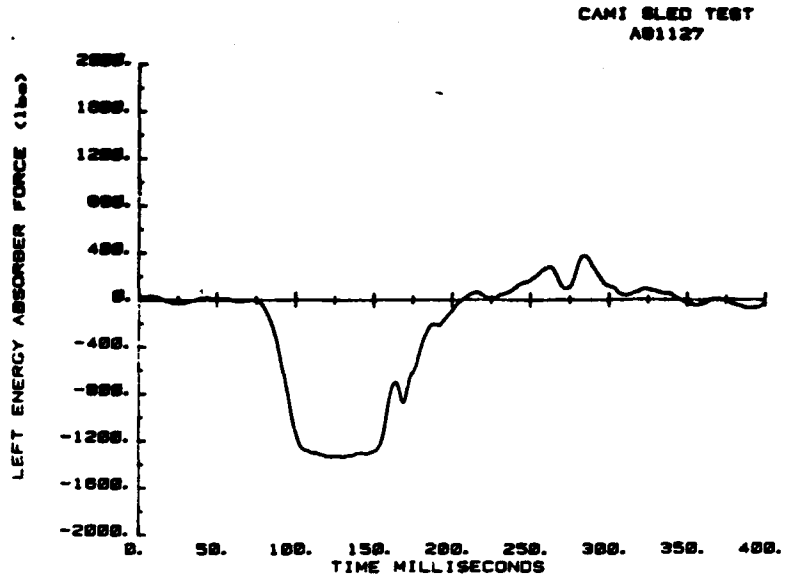

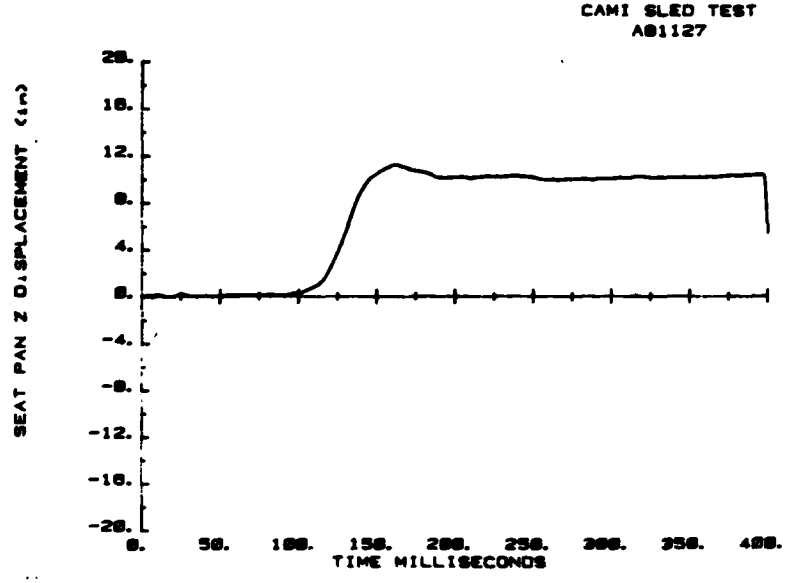

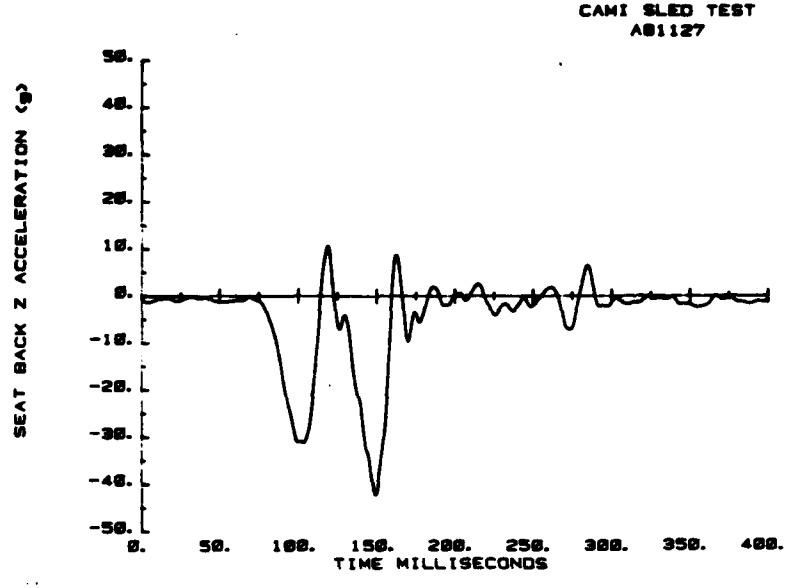

Energy absorber force and stroke.

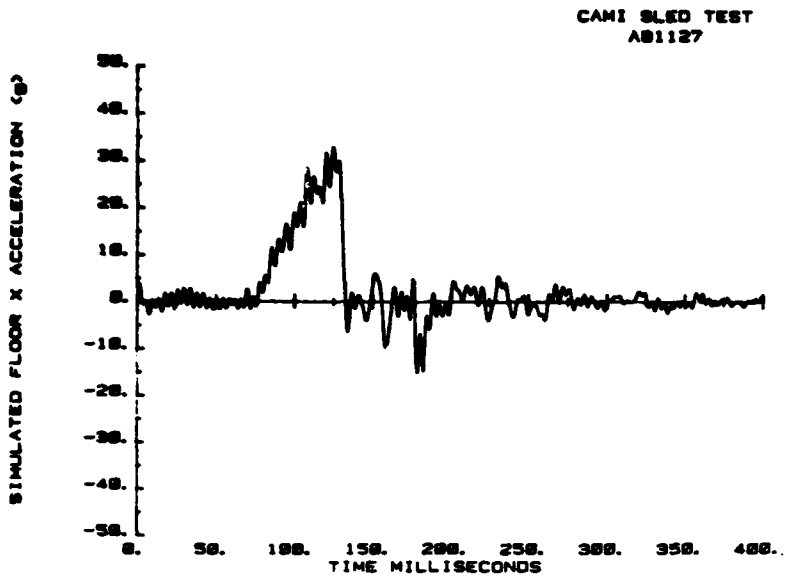

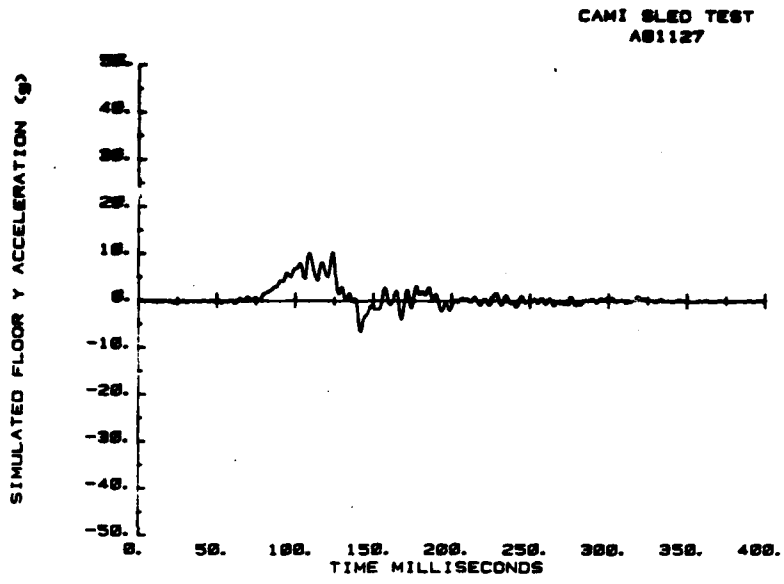

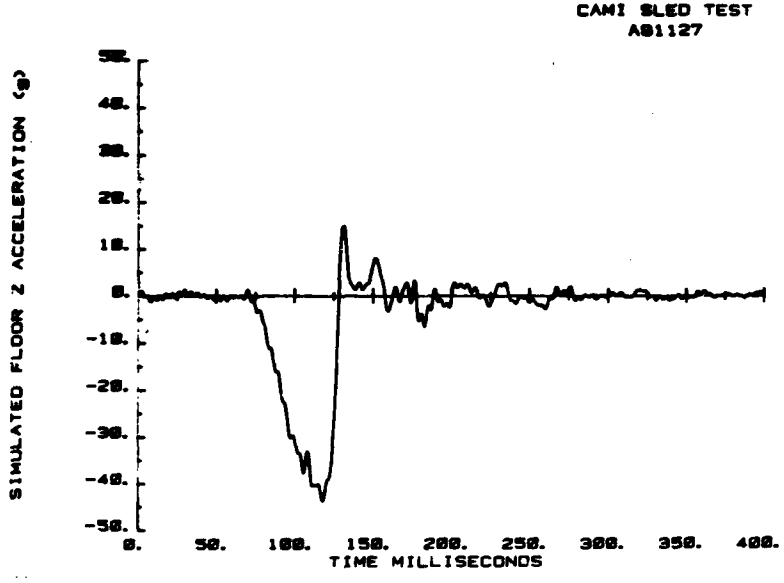

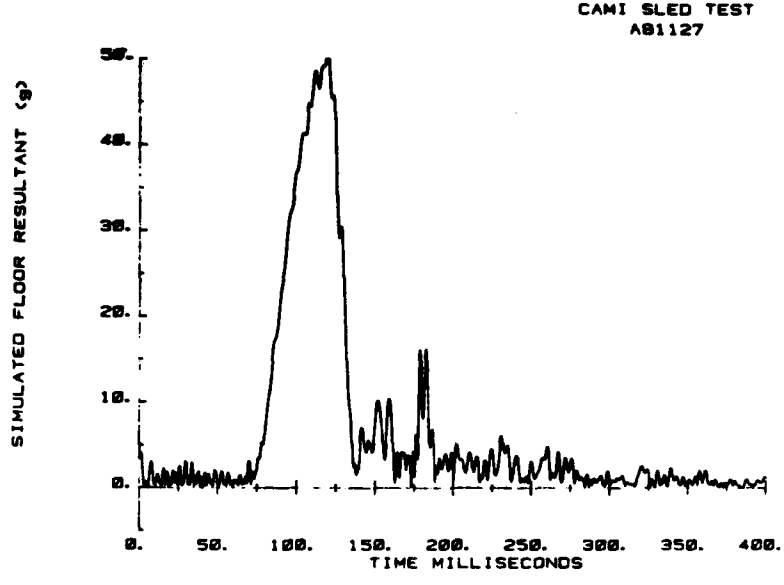

Floor acceleration.

APPENDIX C

WSU ENERGY-ABSORBING SEAT TESTS WITH MODIFIED PART 572 DUMMY

Combined Tests

Simula 01	WSU 156	14.5-G E/A
Simula 02	WSU 157	11.5-G E/A

Vertical Tests

Simula 03	WSU 158	14.5-G E/A

(Inadvertent buckle release by hand of dummy at approximately 0.075 sec after impact)

Simula 04	WSU 159	14.5-G E/A
Simula 05	WSU 160	11.5-G E/A

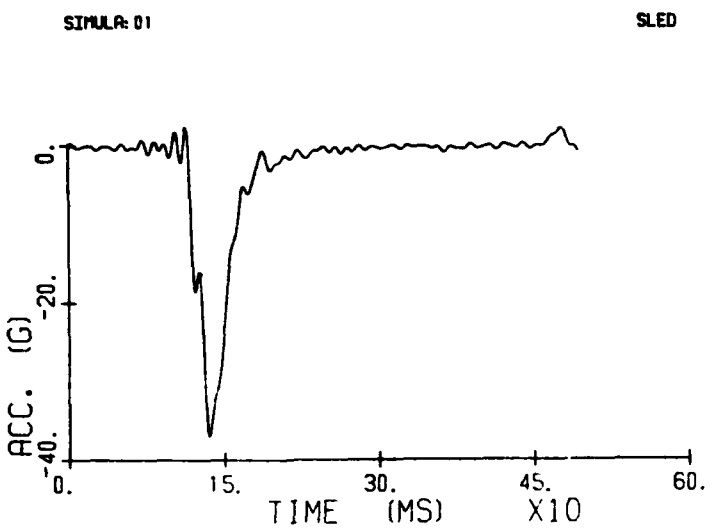

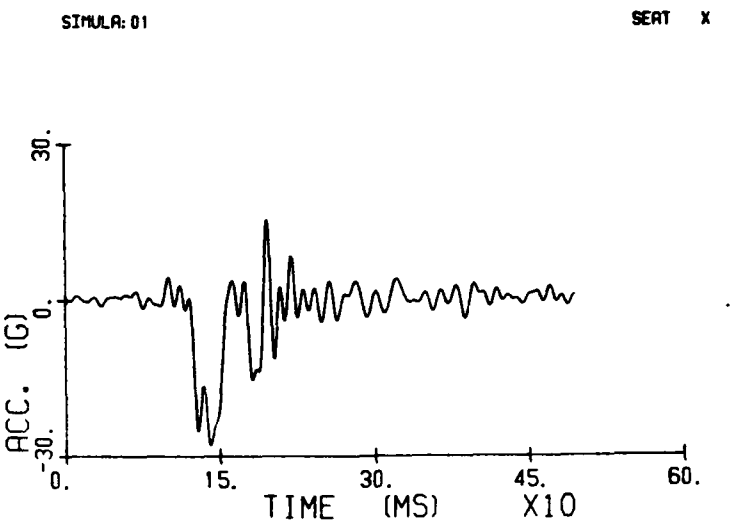

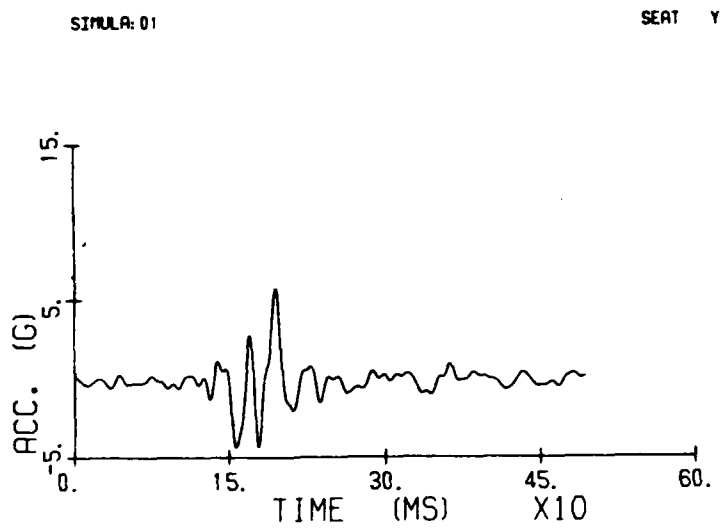

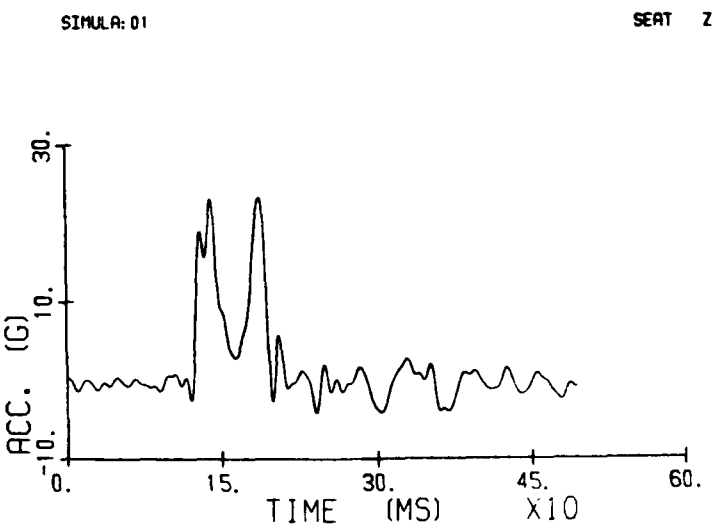

Sled and seat pan accelerations.

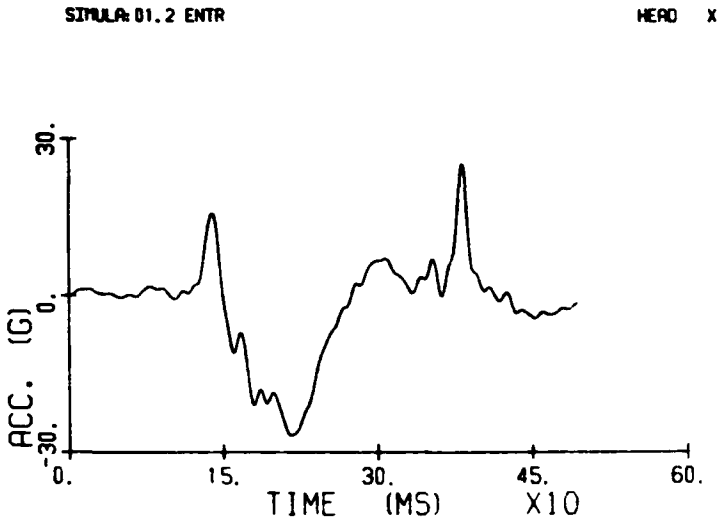

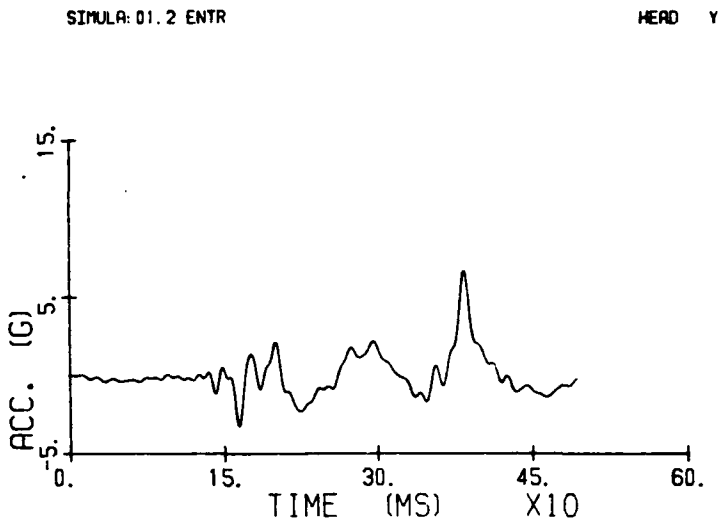

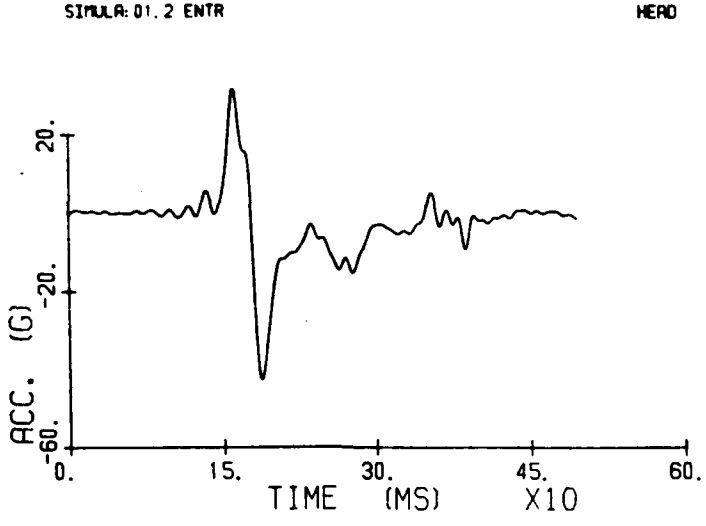

Head acceleration.

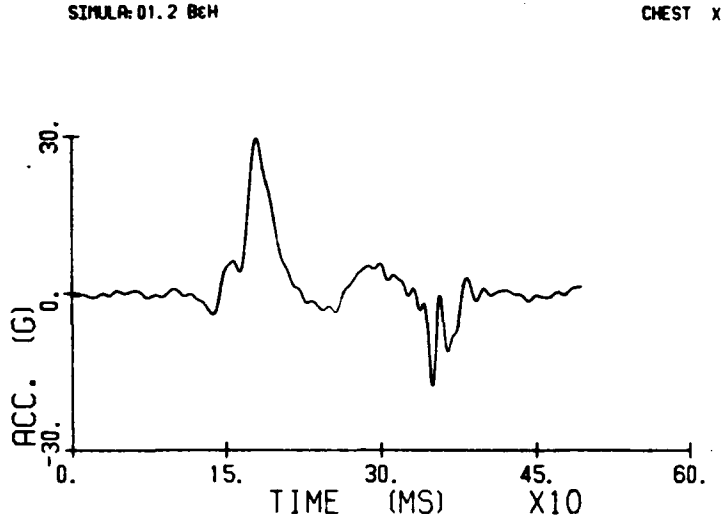

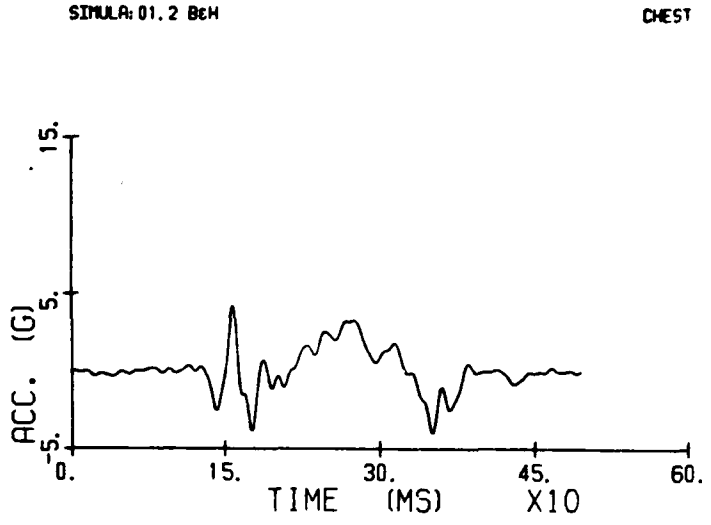

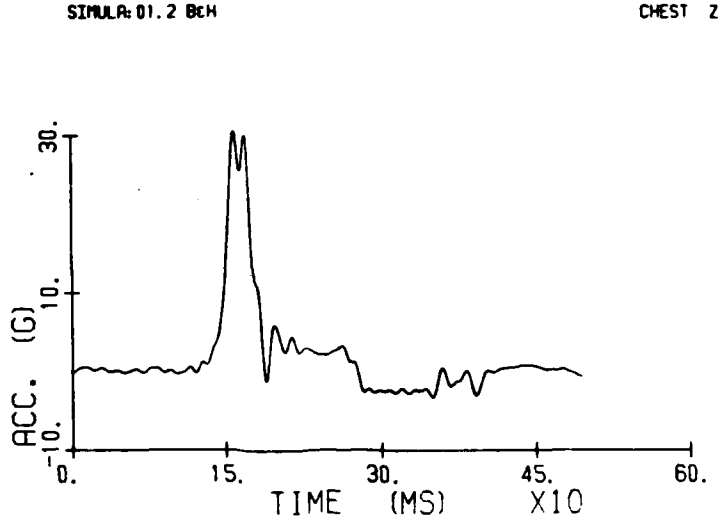

Chest acceleration.

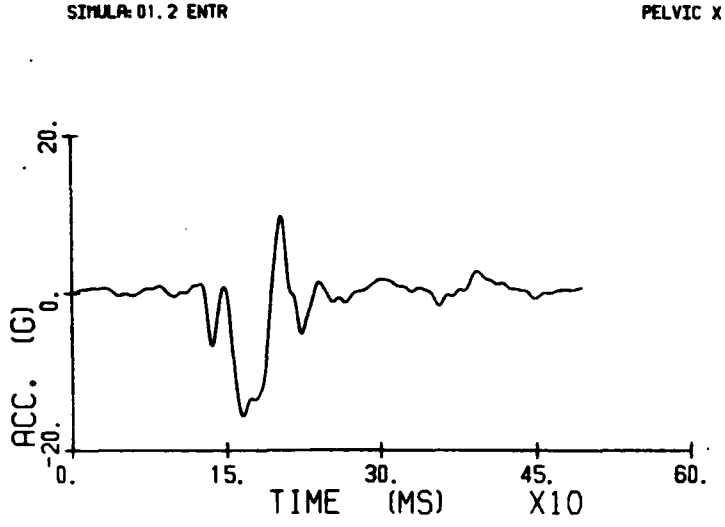

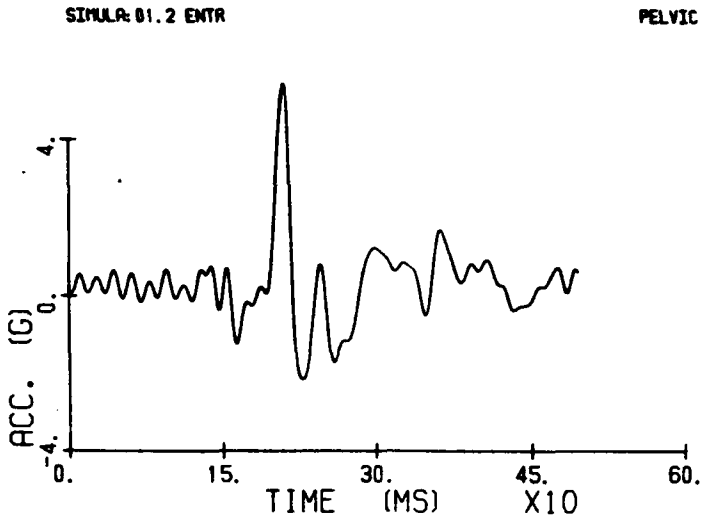

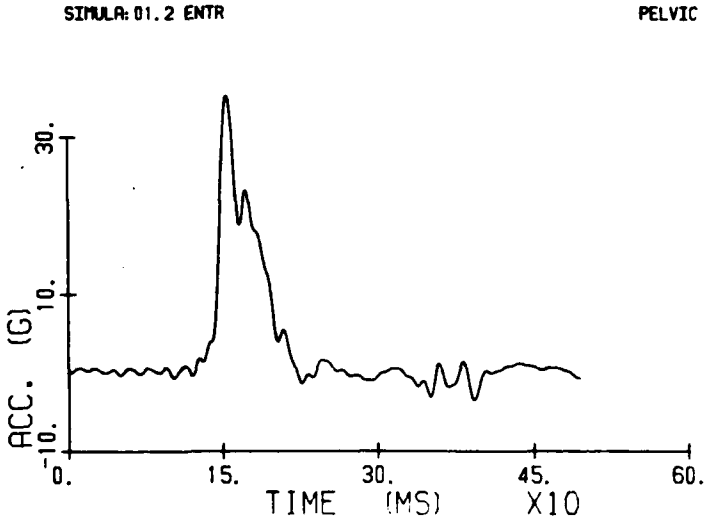

Pelvis acceleration.

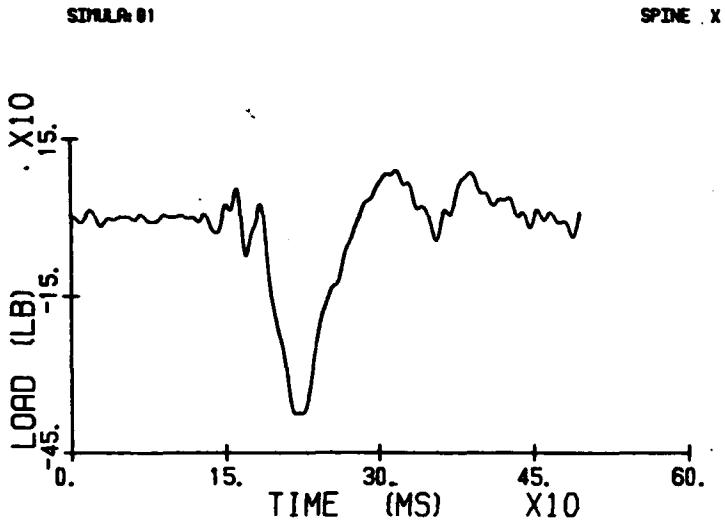

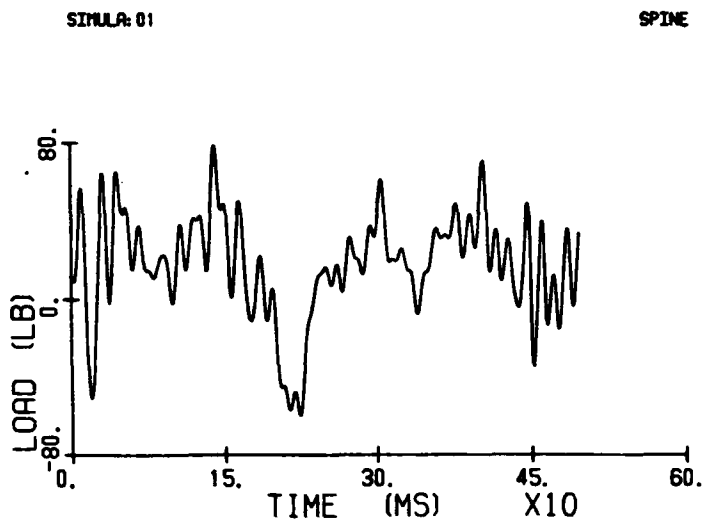

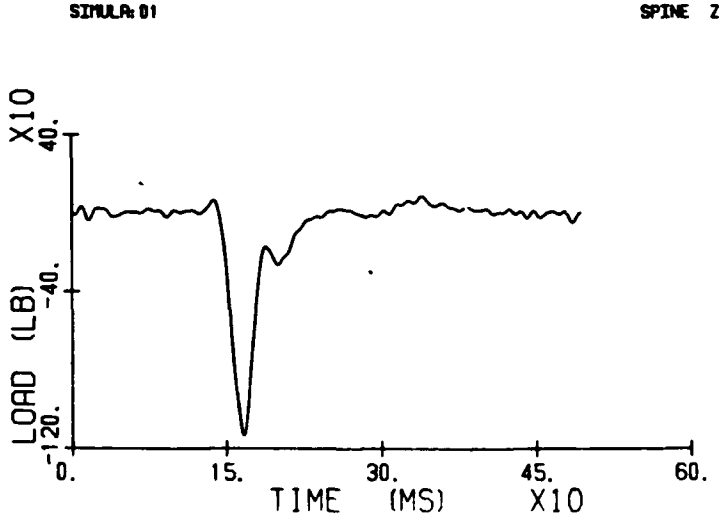

Lumbar force.

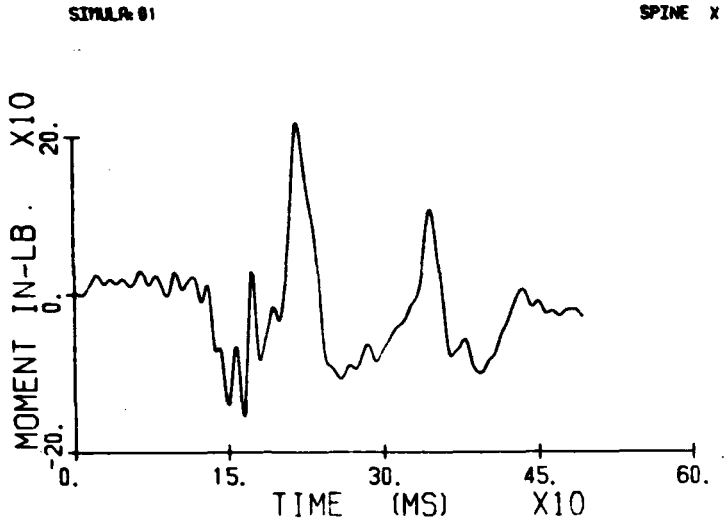

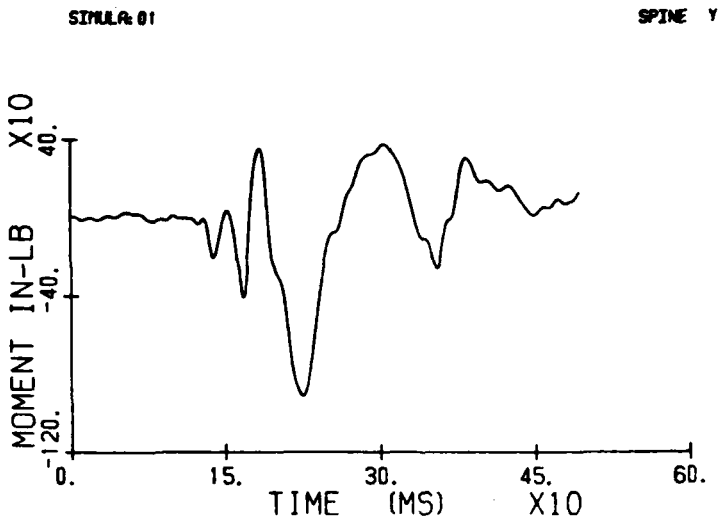

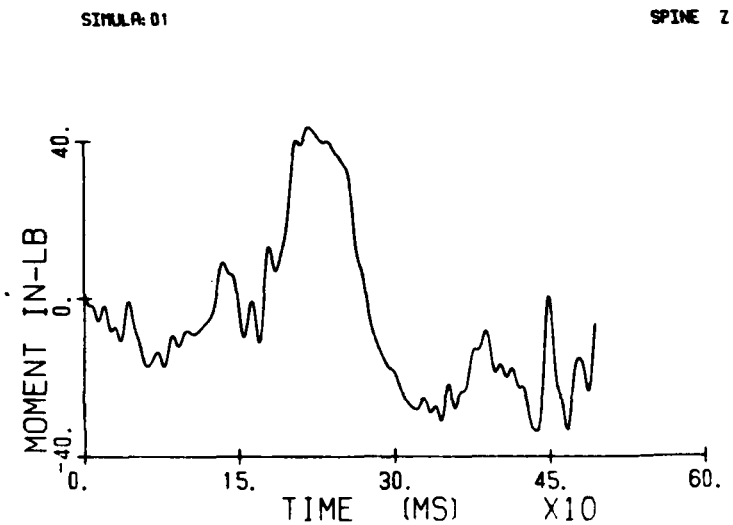

Lumbar moment.

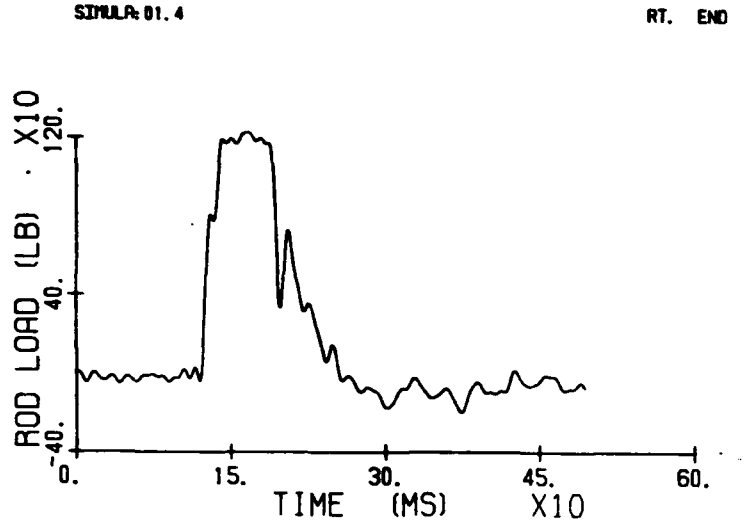

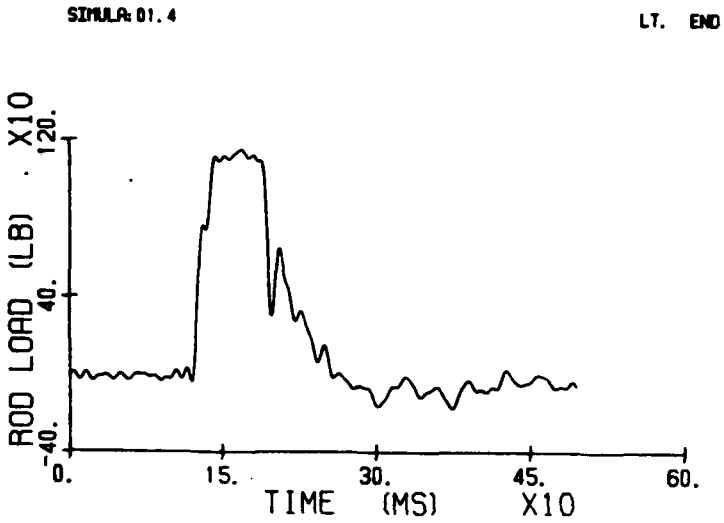

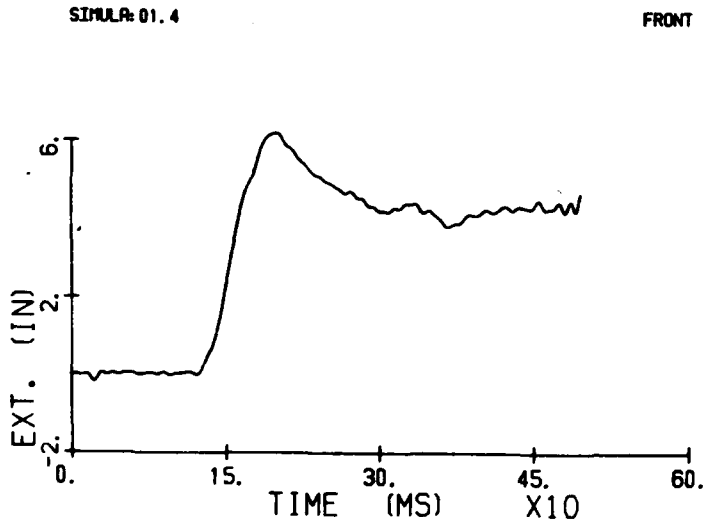

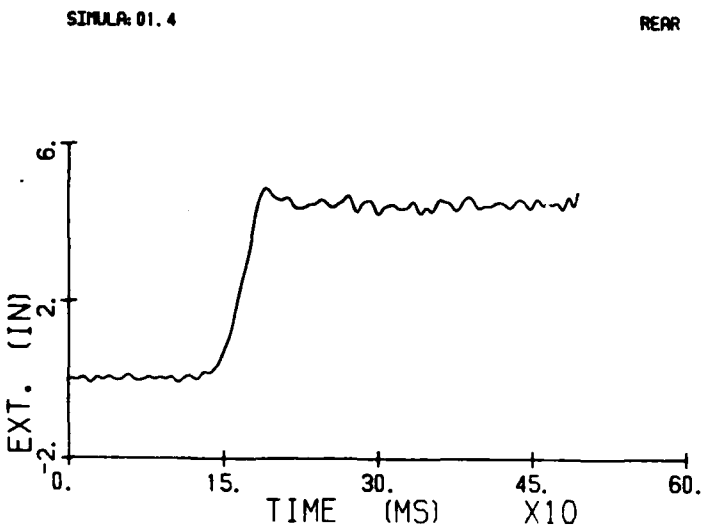

Energy absorber force and stroke.

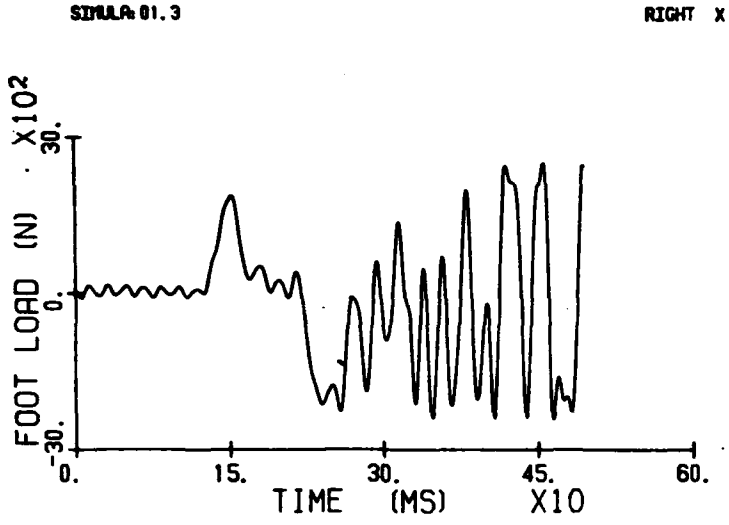

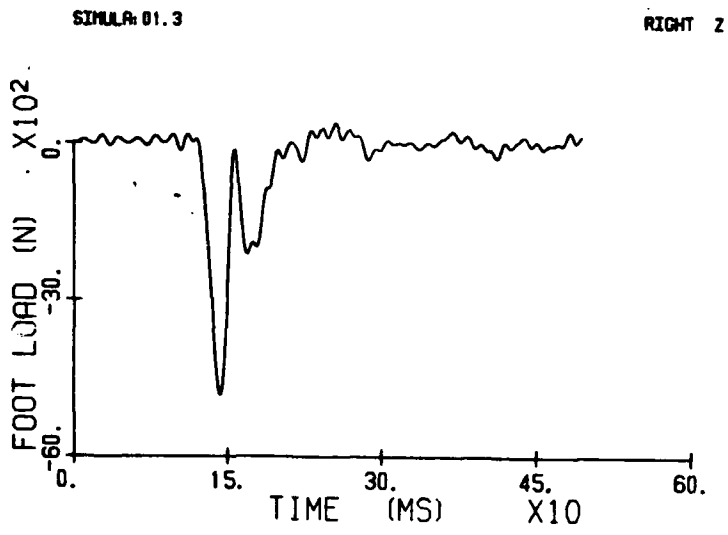

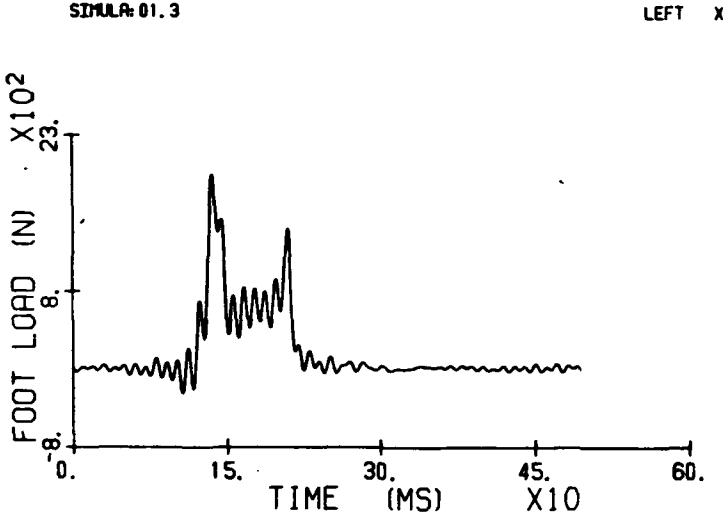

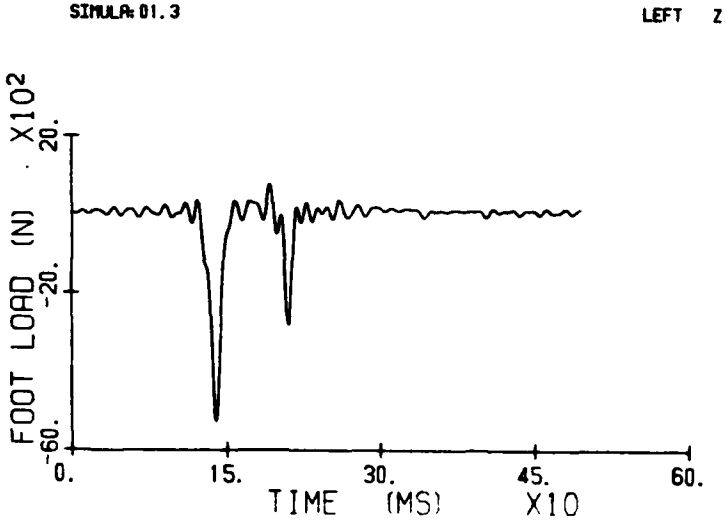

Footrest force.

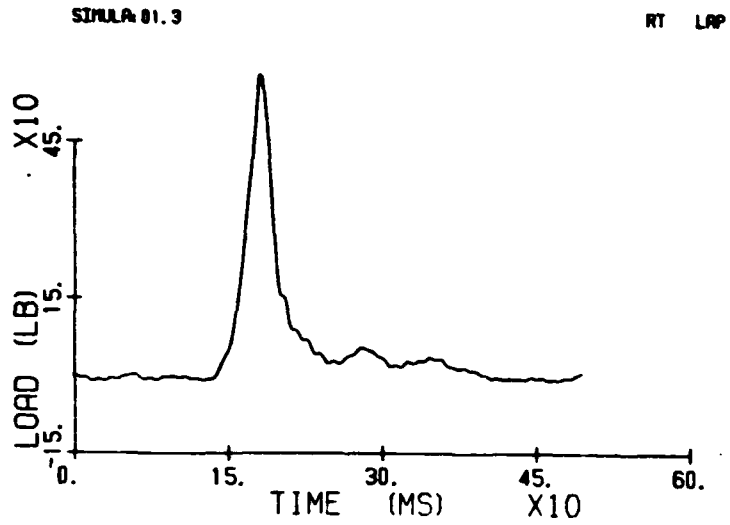

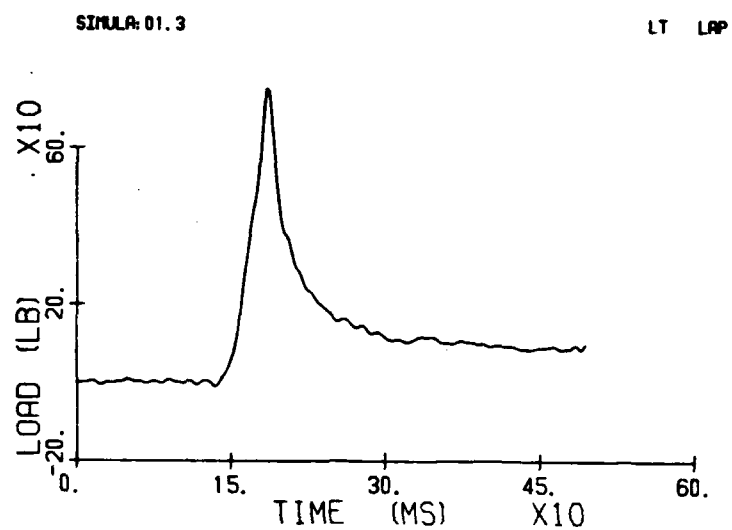

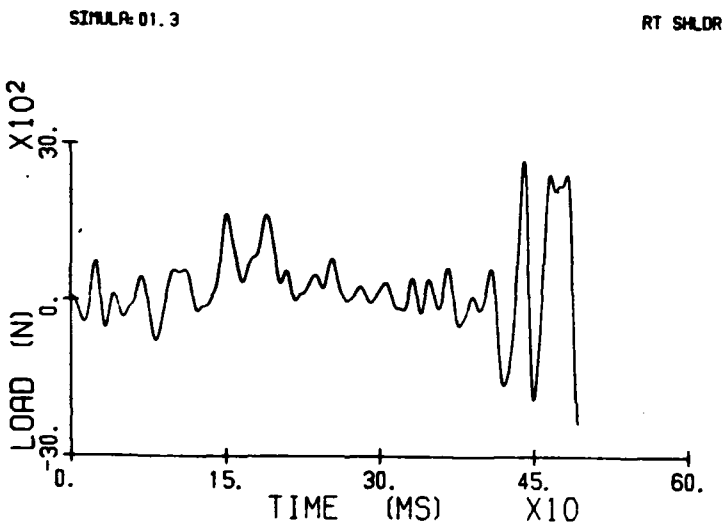

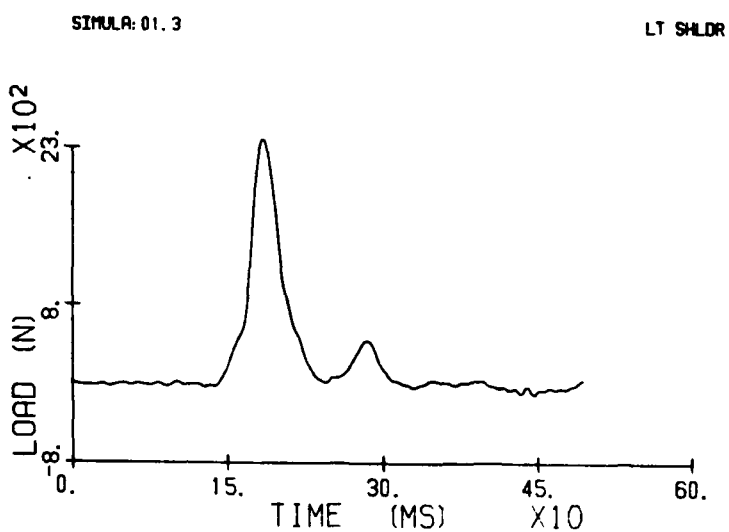

Lap and shoulder belt forces.

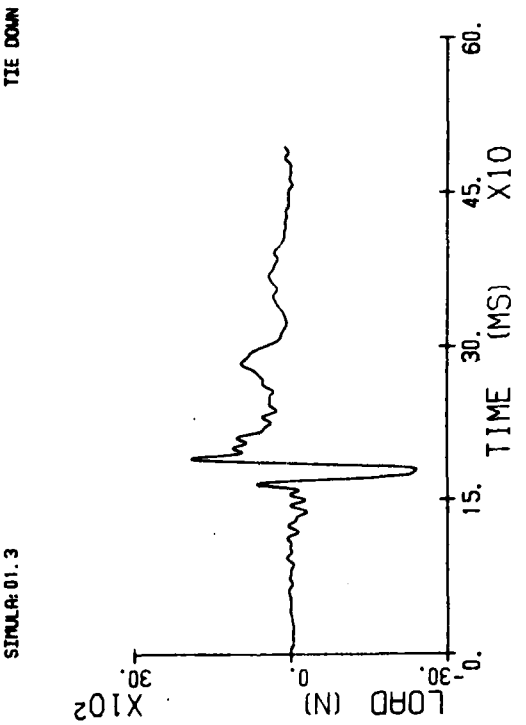

Tiedown strap.

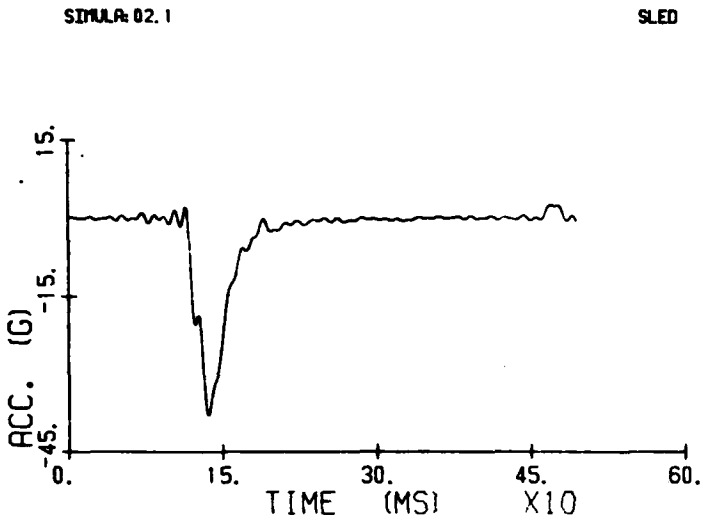

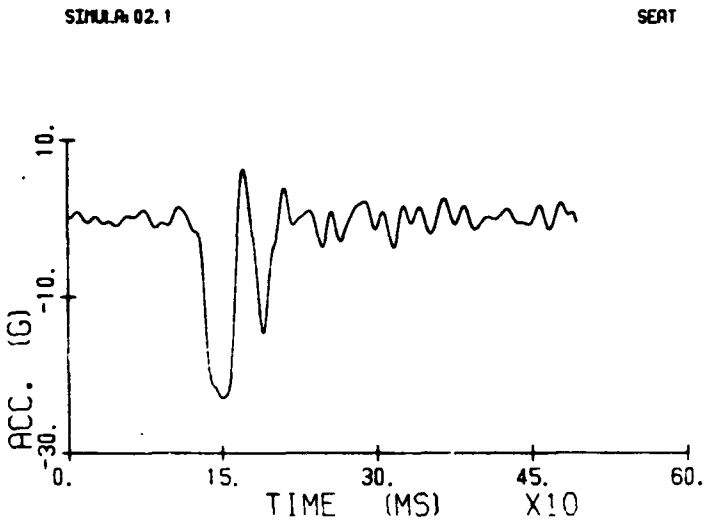

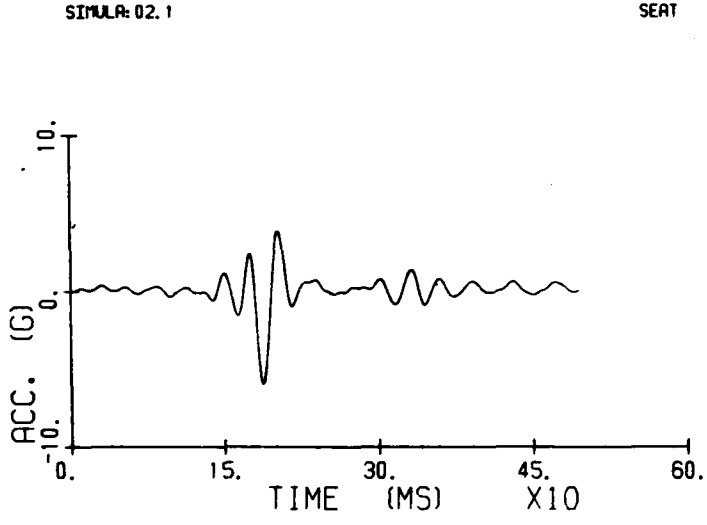

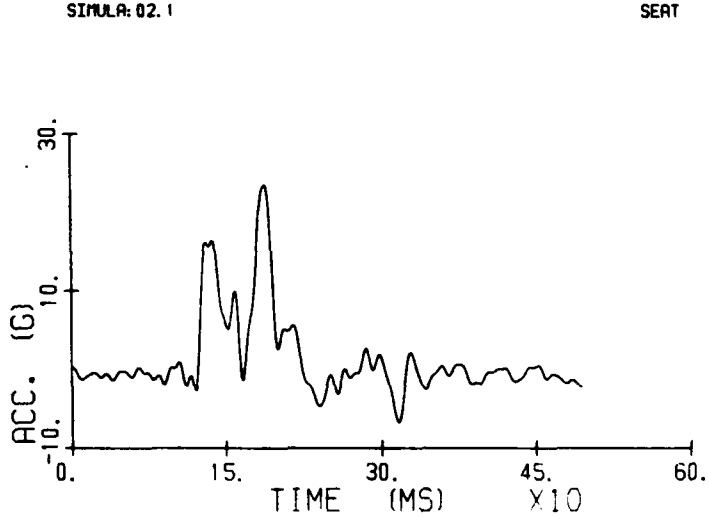

Sled and seat pan accelerations.

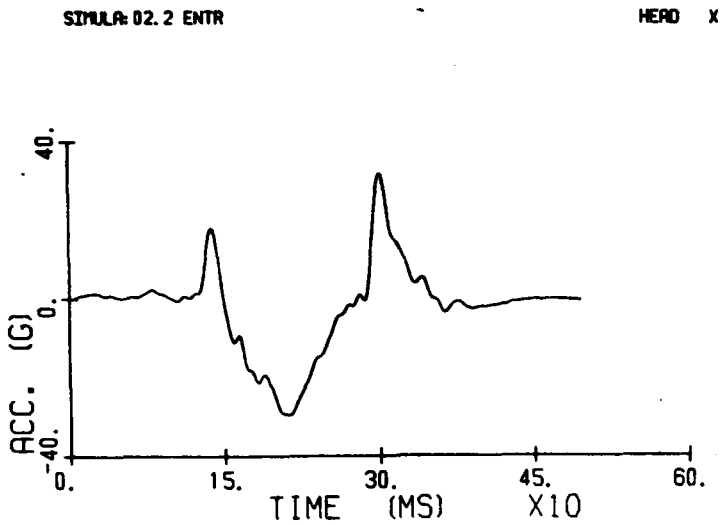

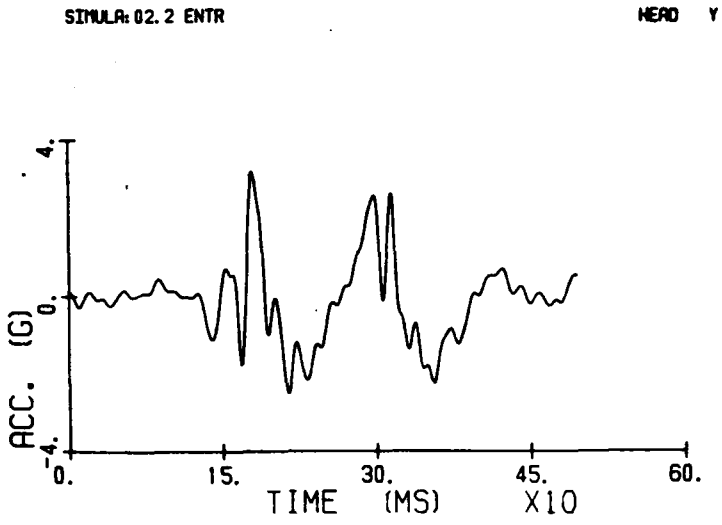

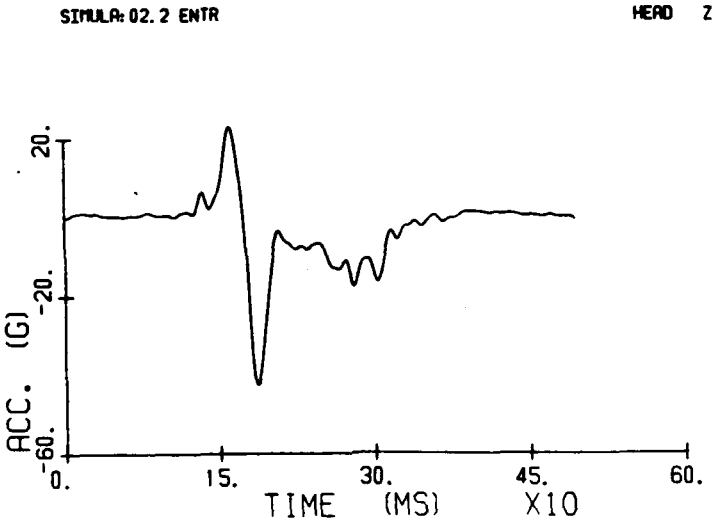

Head acceleration.

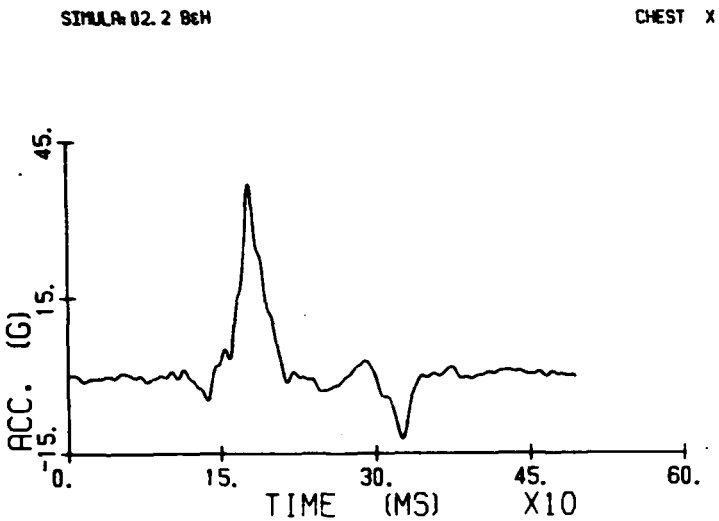

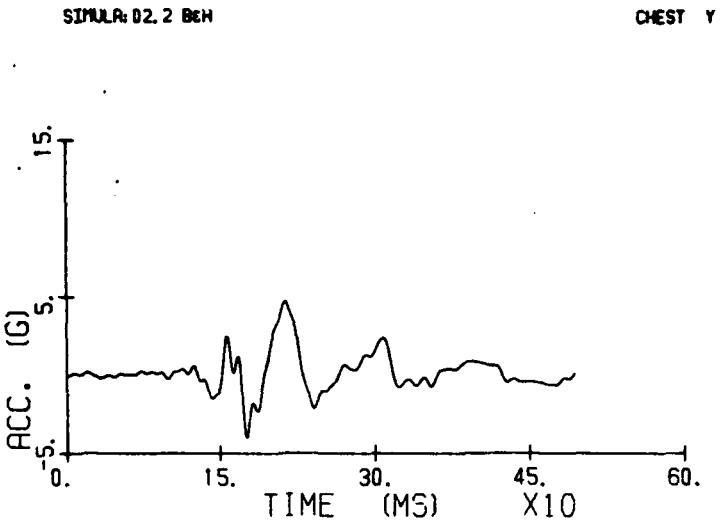

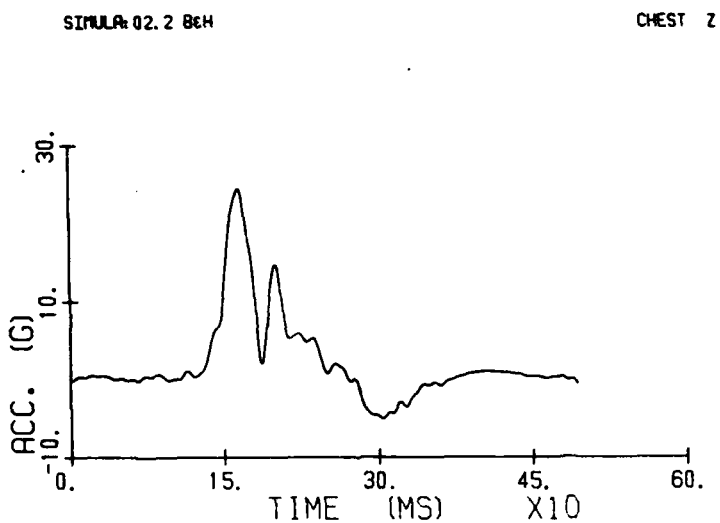

Chest acceleration.

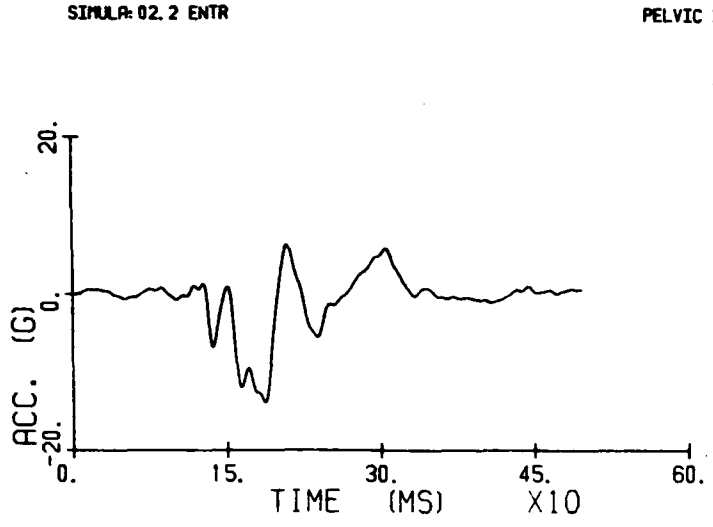

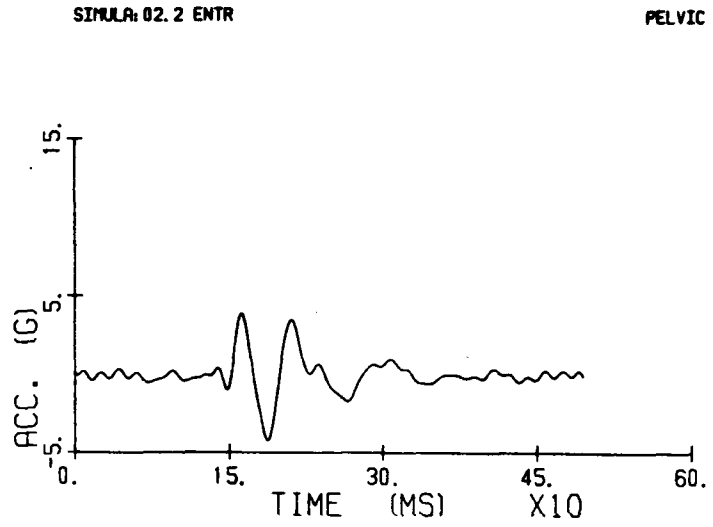

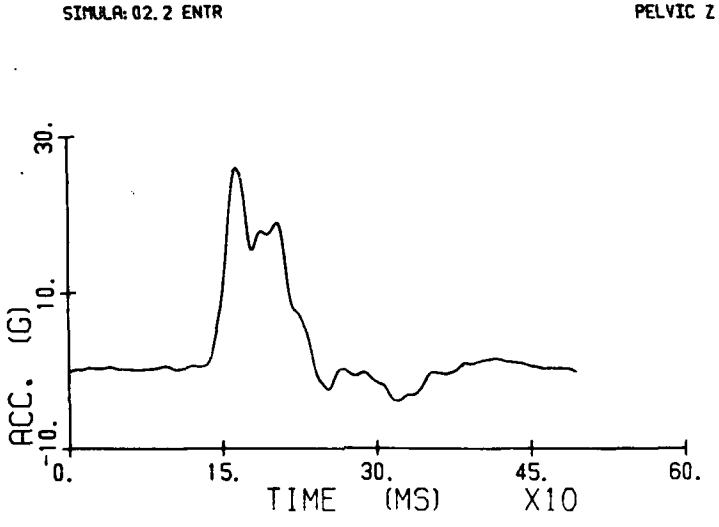

Pelvis acceleration.

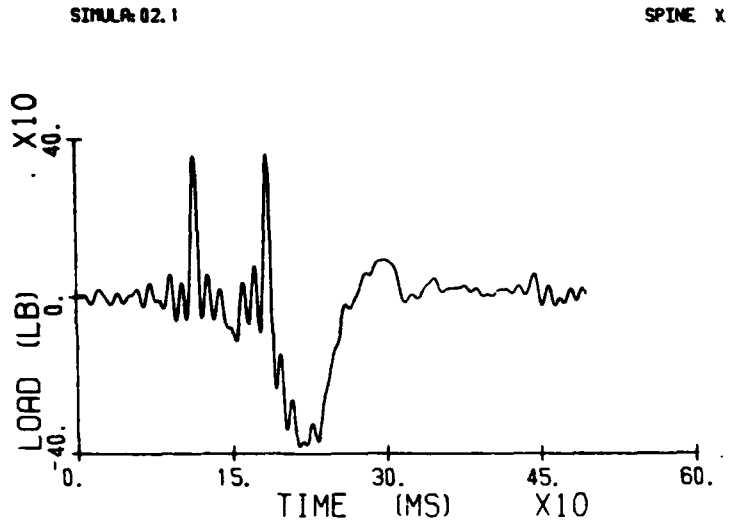

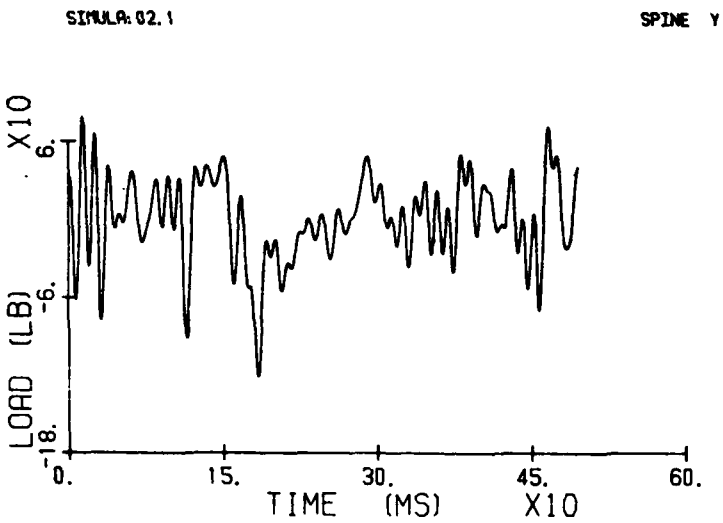

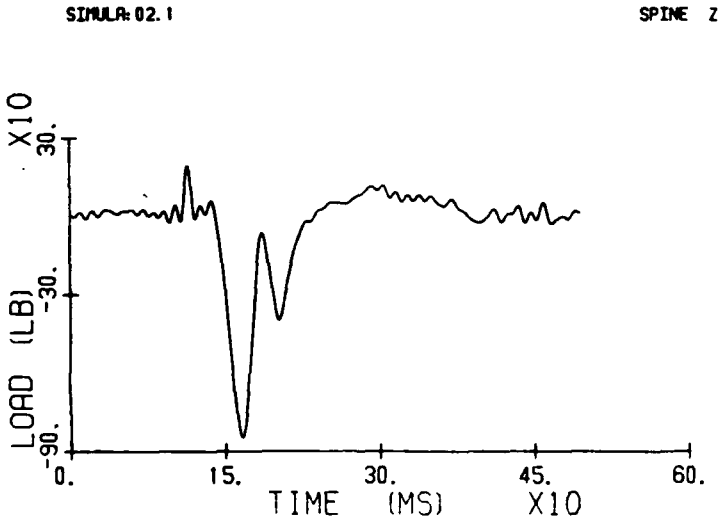

Lumbar force.

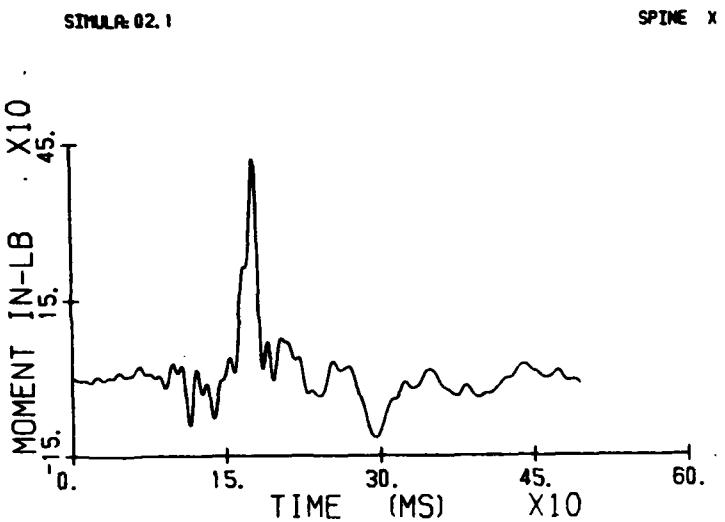

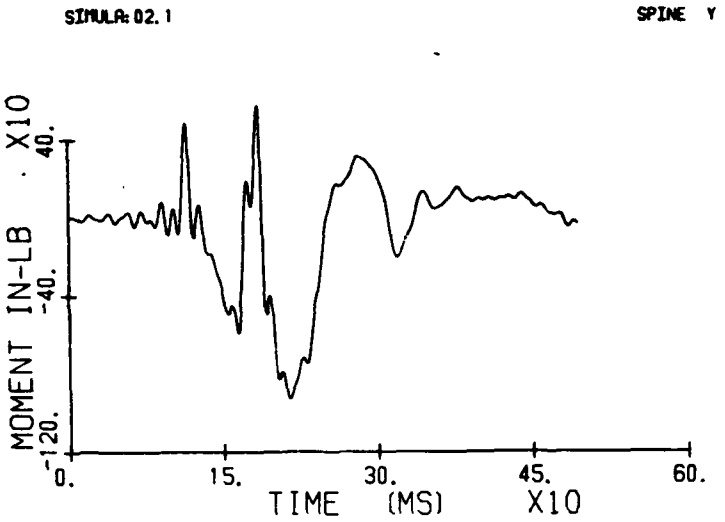

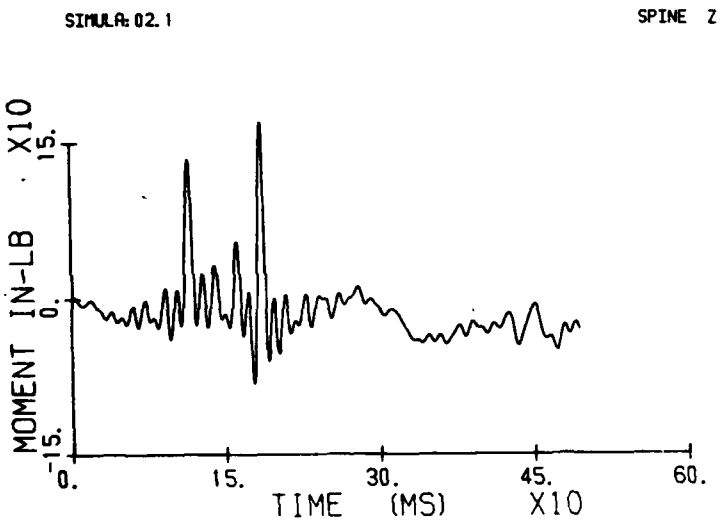

Lumbar moment.

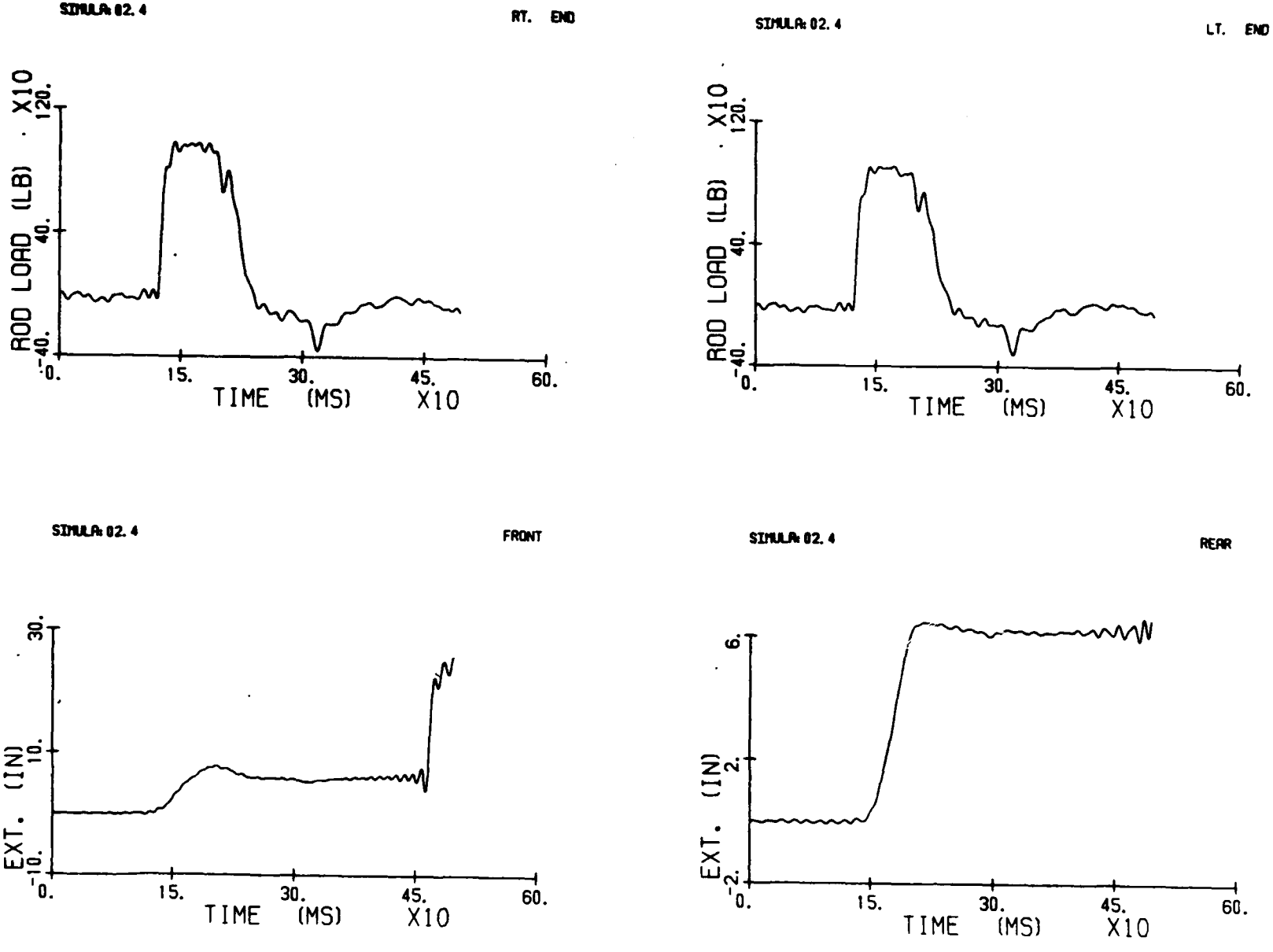

Energy absorber force and stroke.

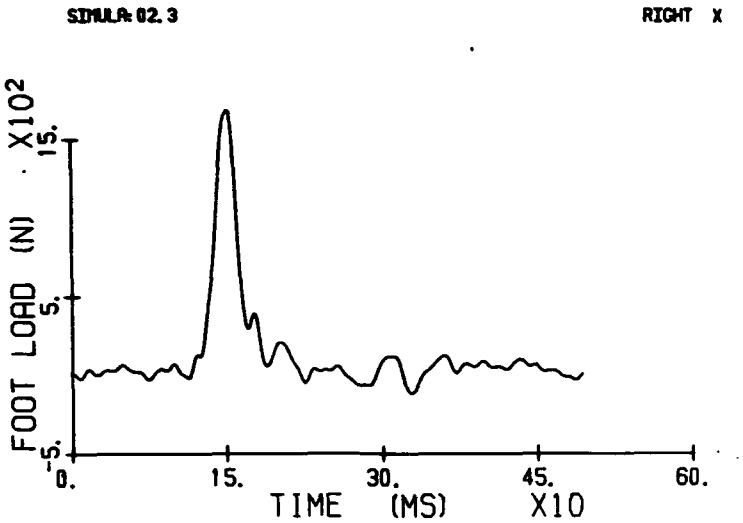

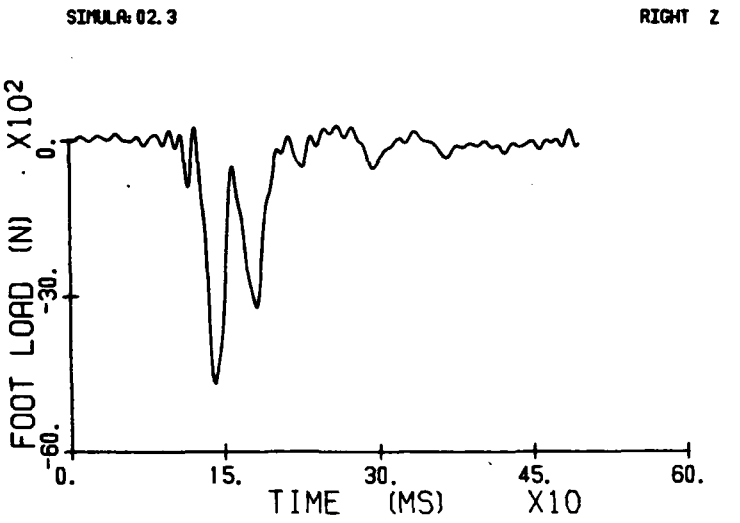

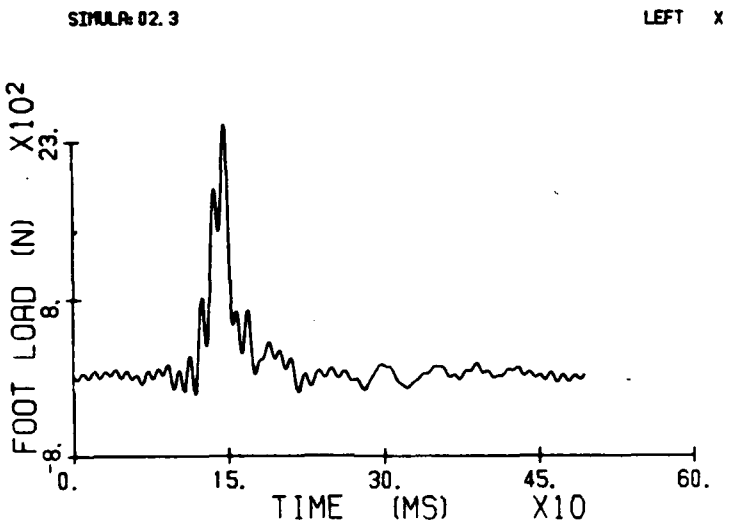

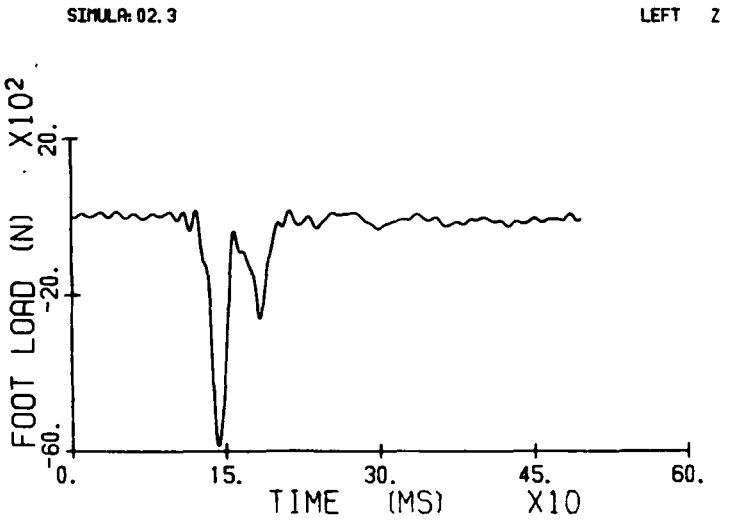

Footrest force.

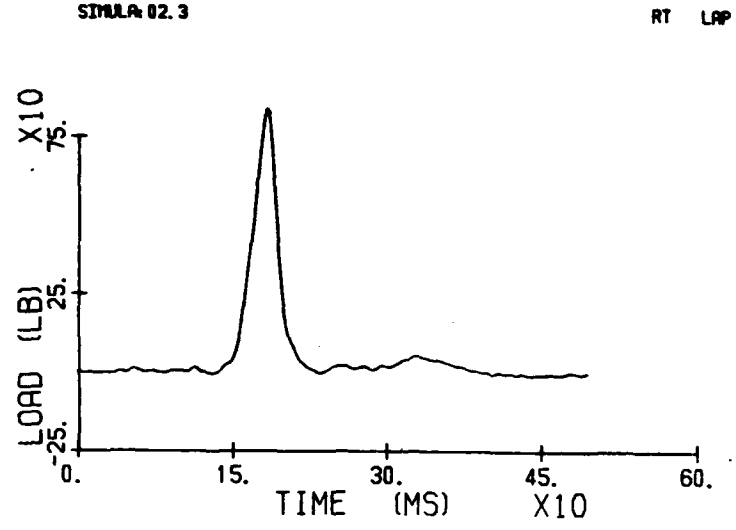

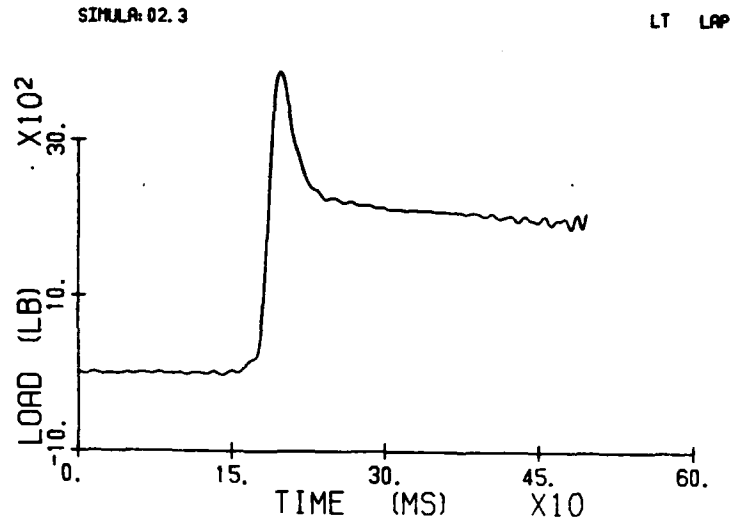

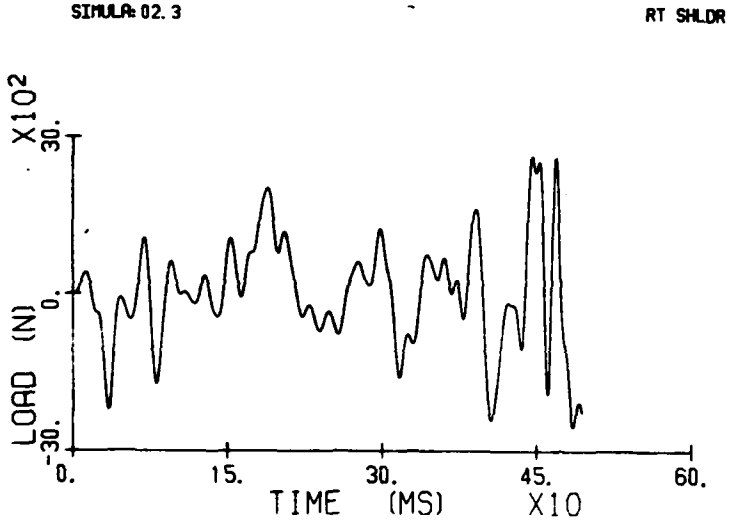

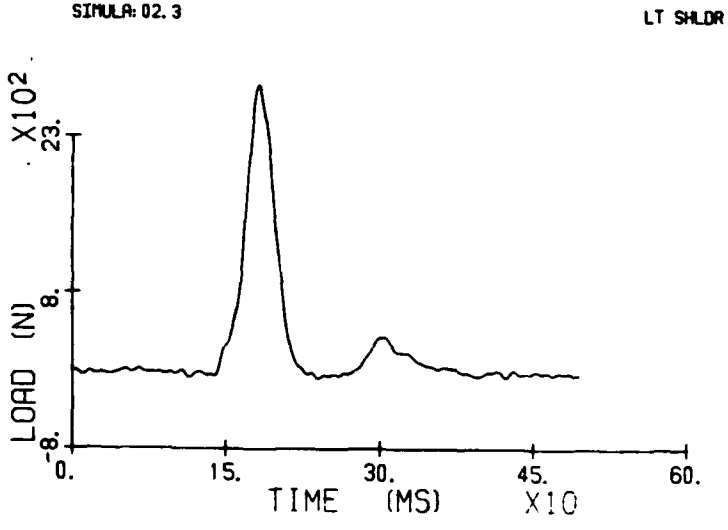

Lap and shoulder belt forces.

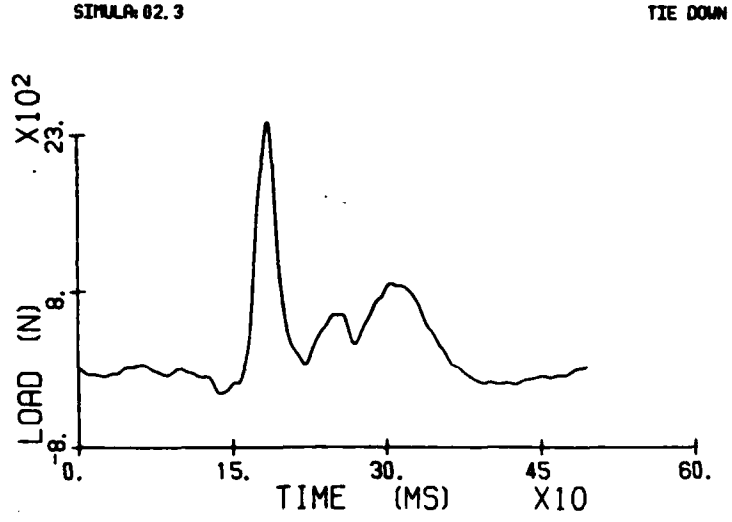

Tiedown strap.

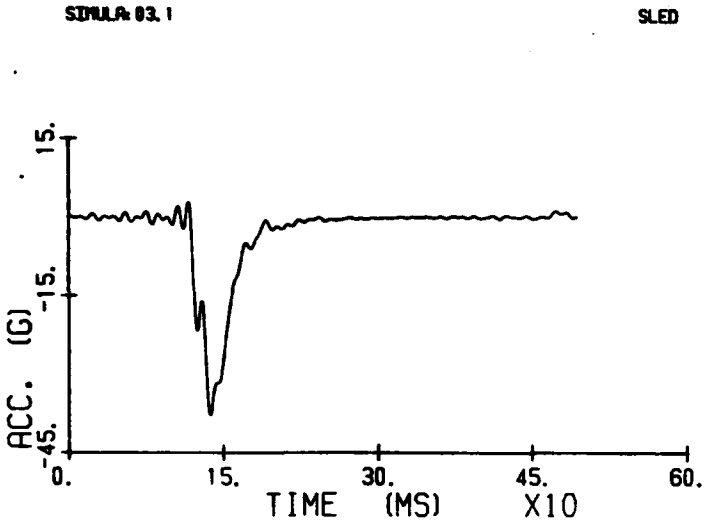

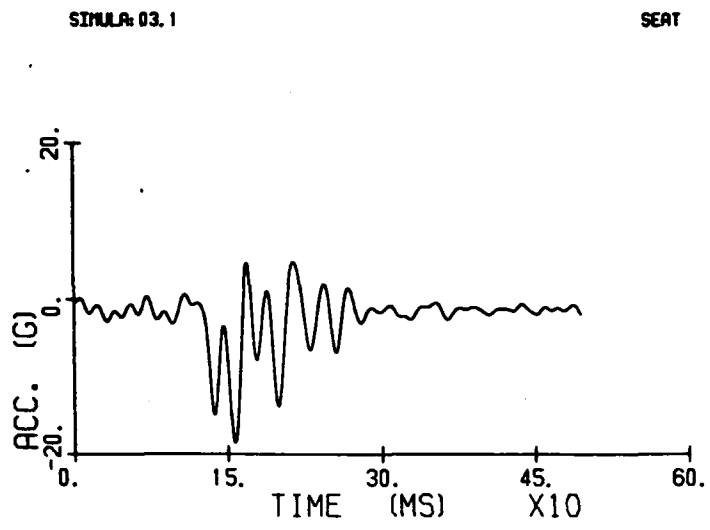

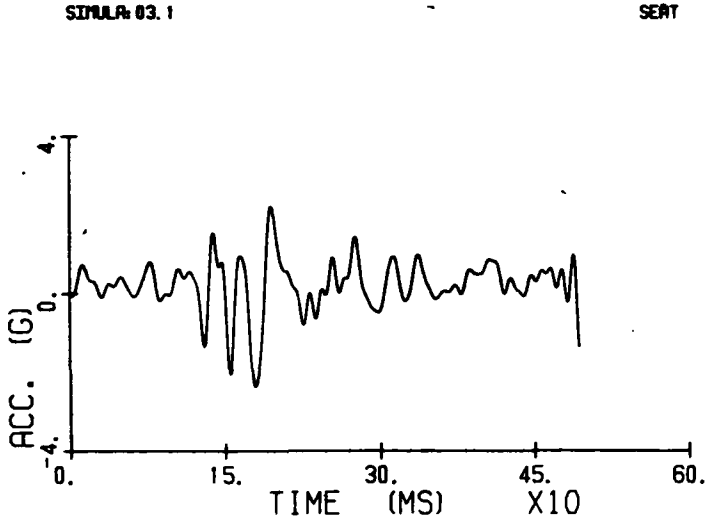

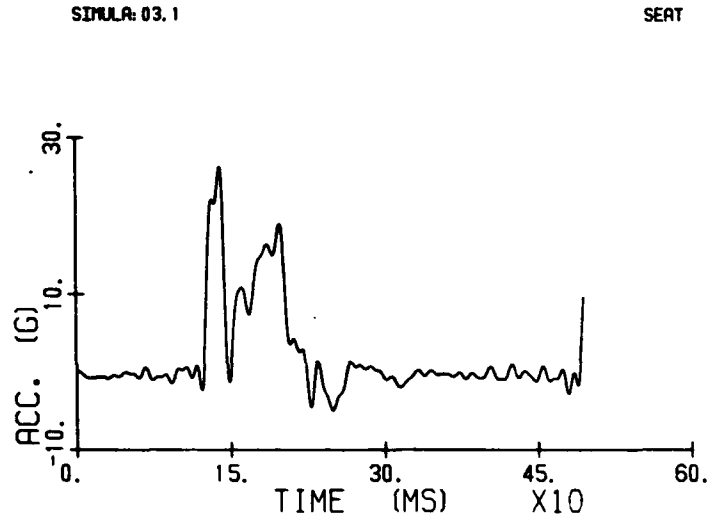

Sled and seat pan accelerations.

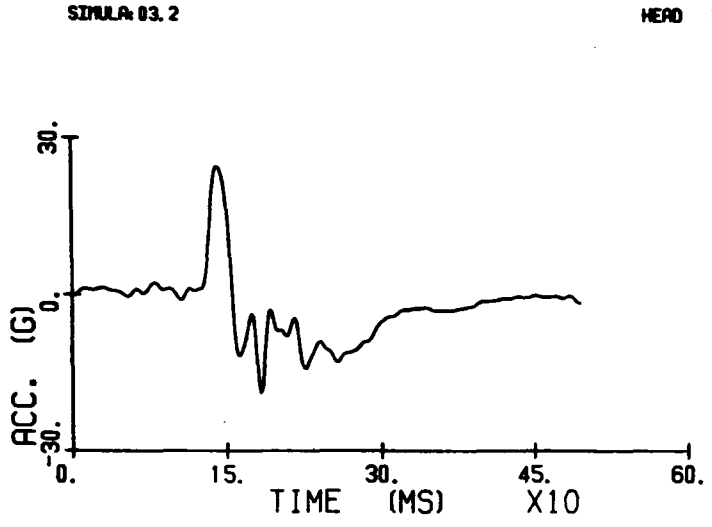

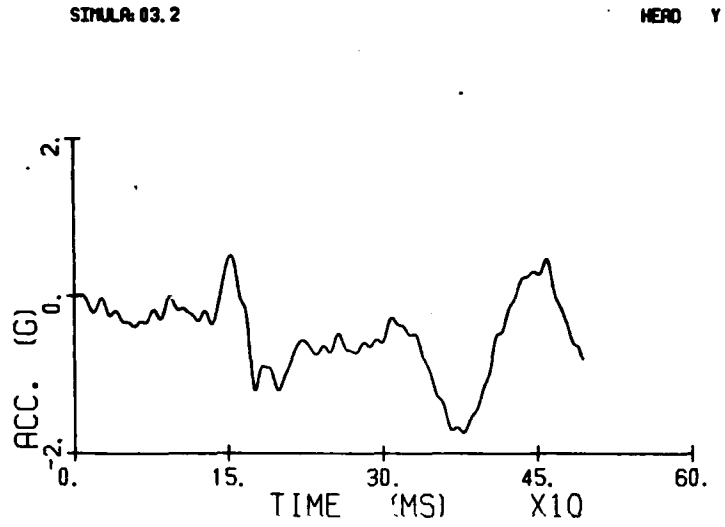

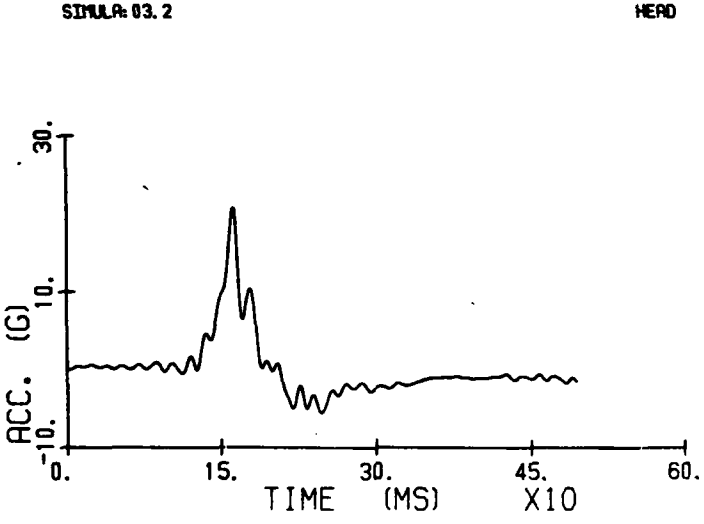

Head acceleration.

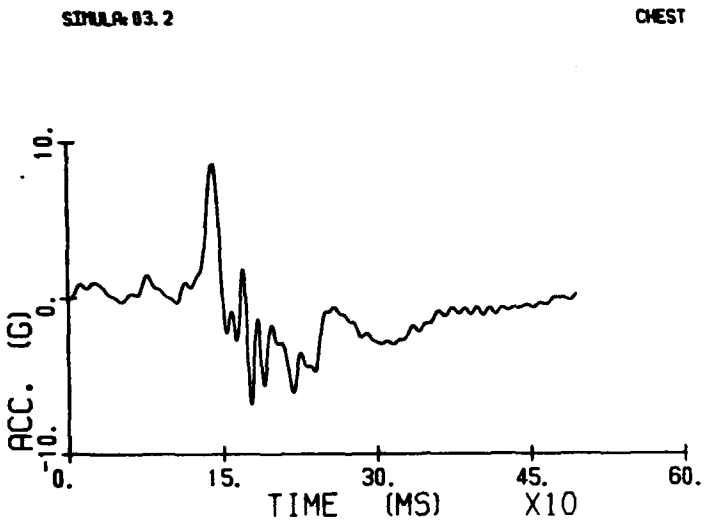

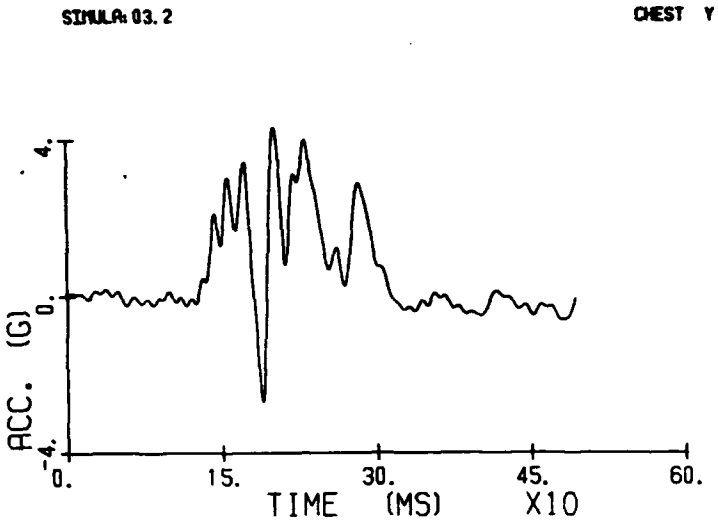

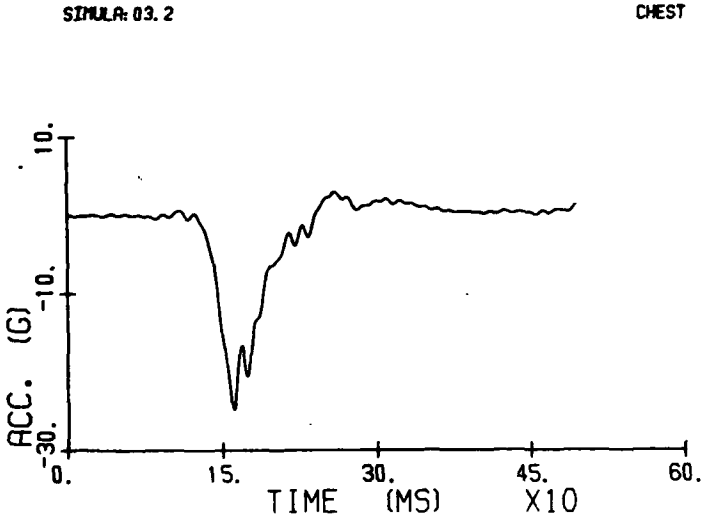

Chest acceleration.

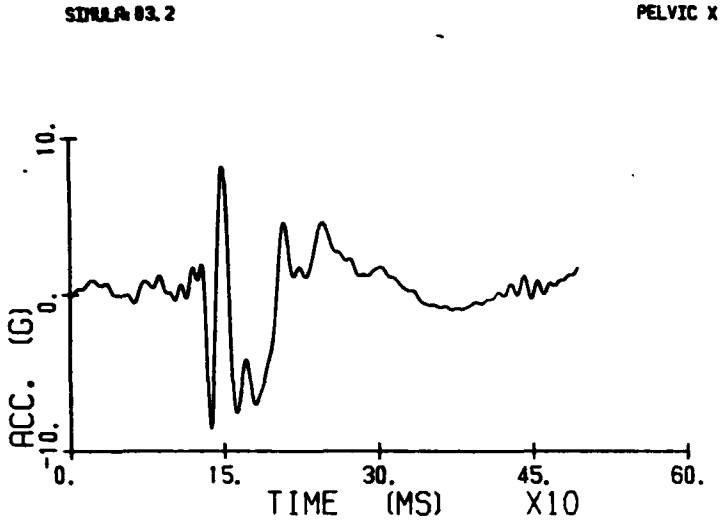

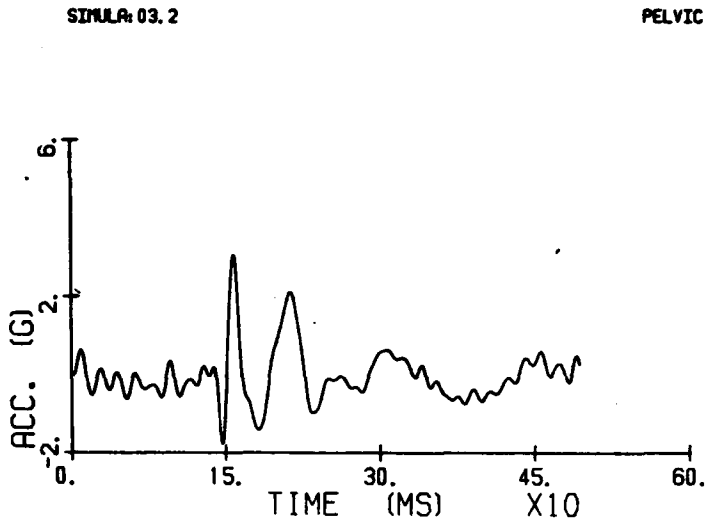

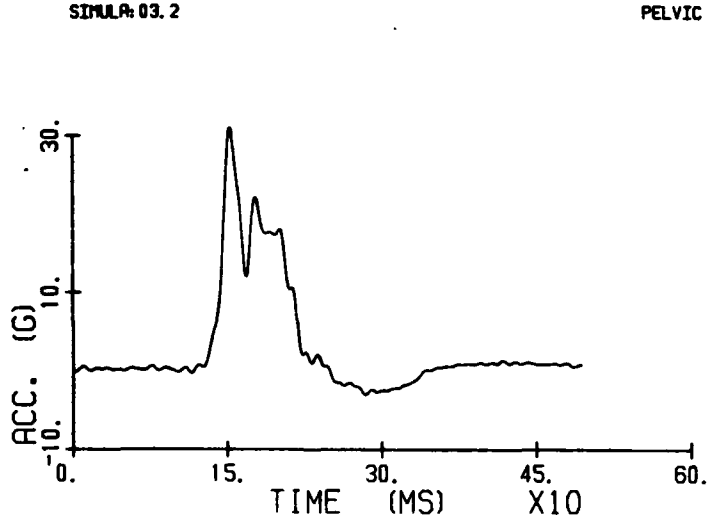

Pelvis acceleration.

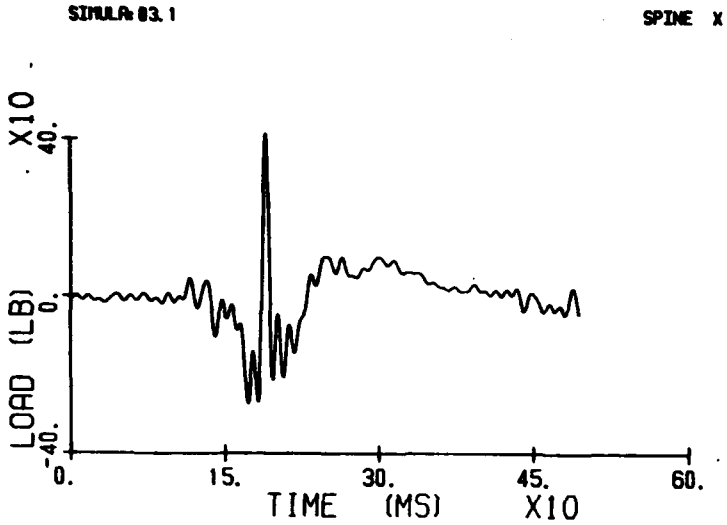

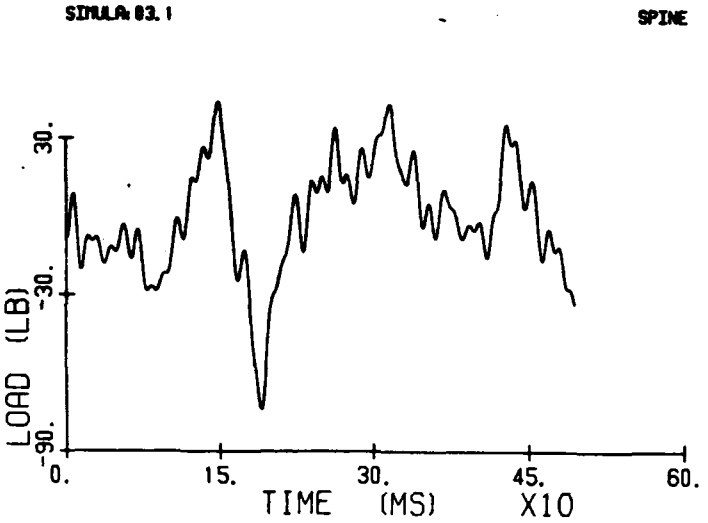

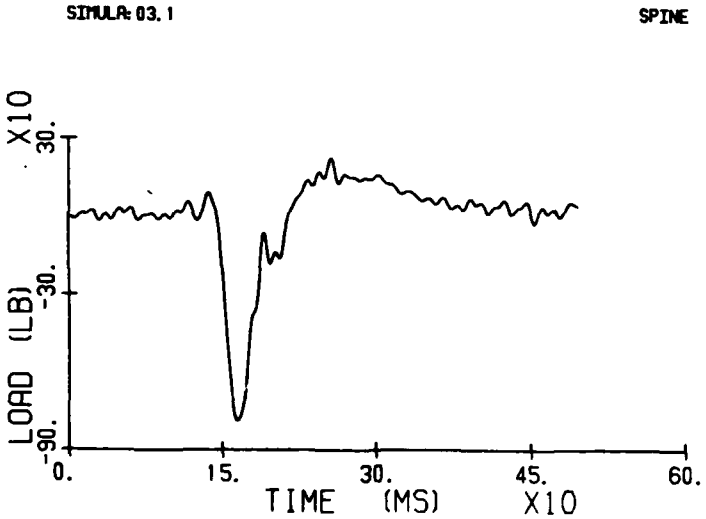

Lumbar force.

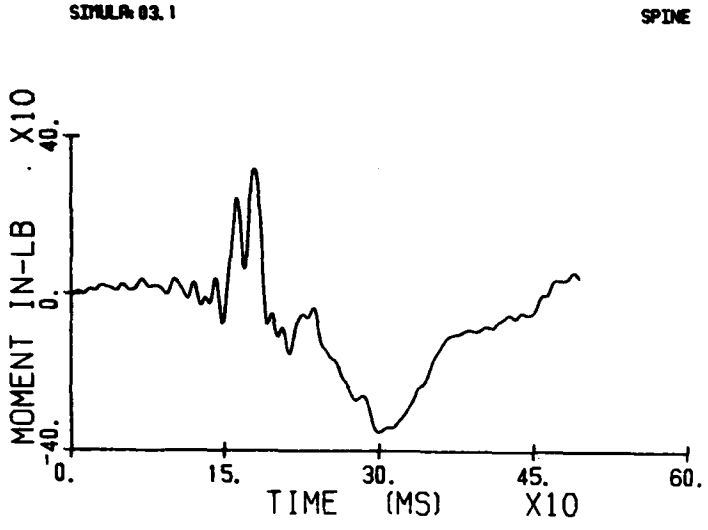

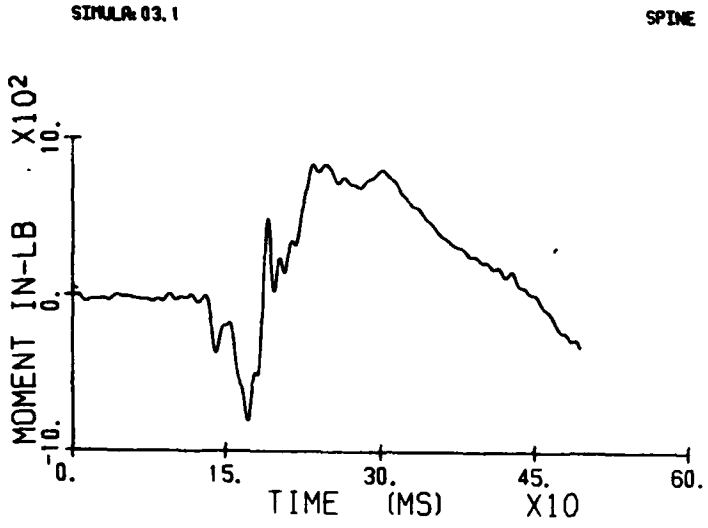

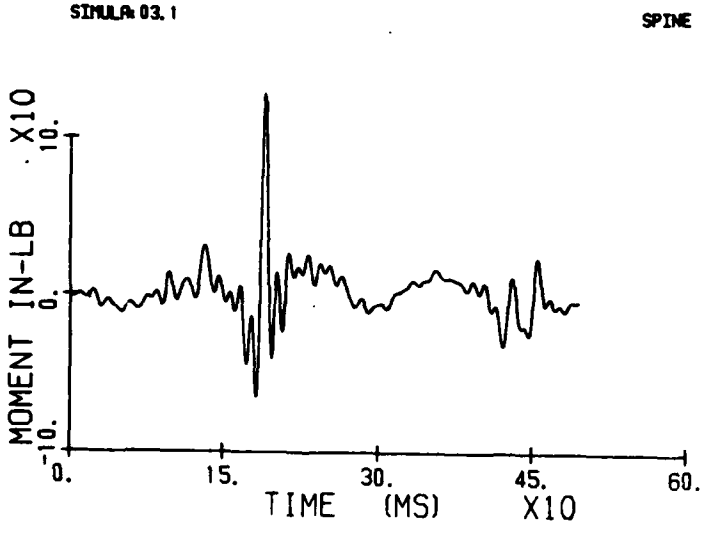

Lumbar moment.

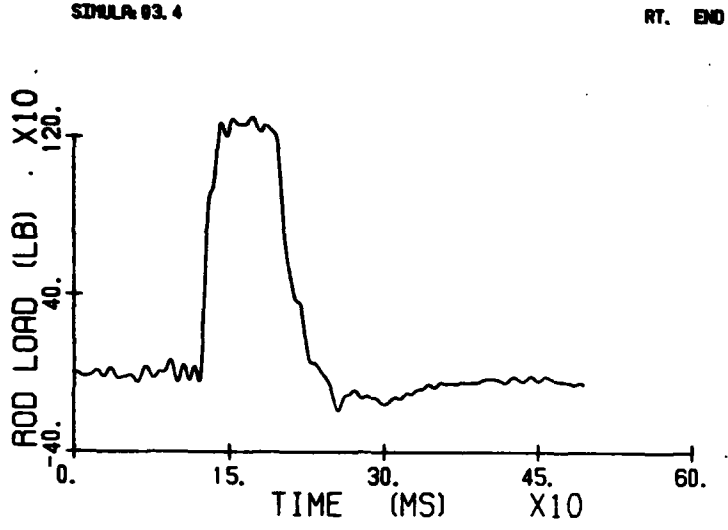

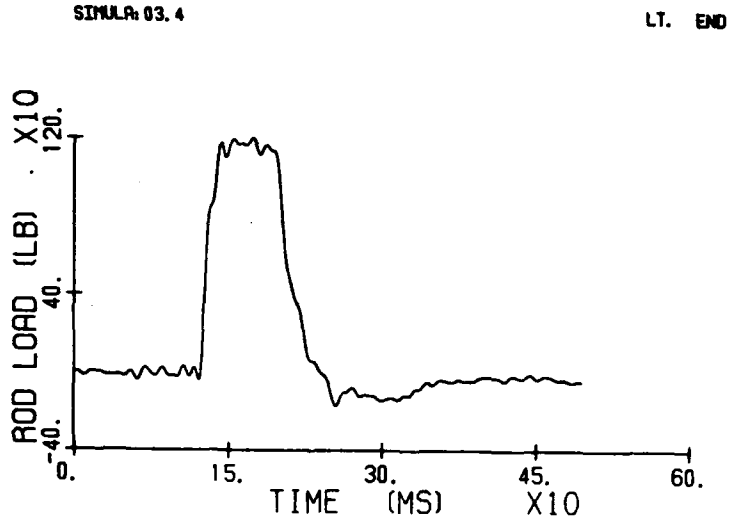

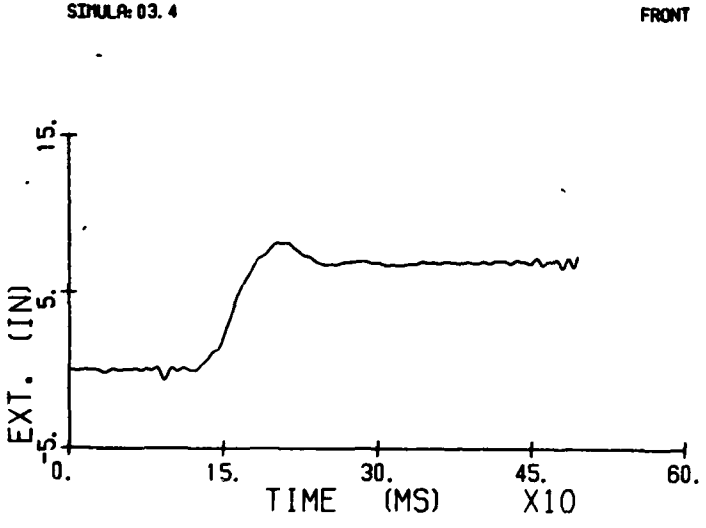

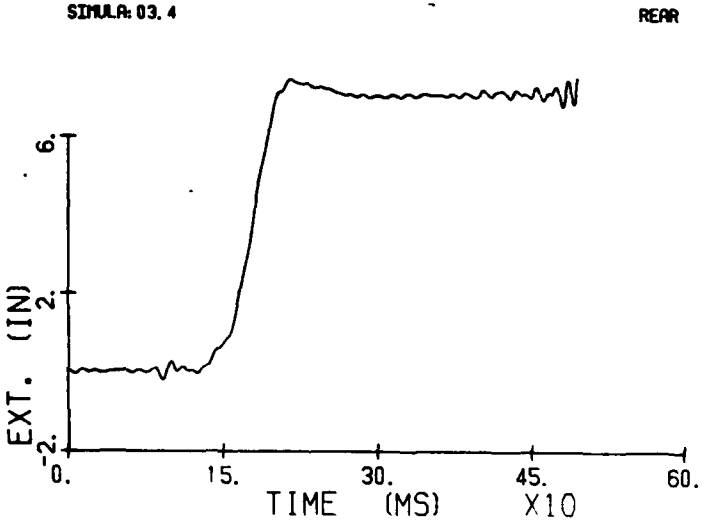

Energy absorber force and stroke.

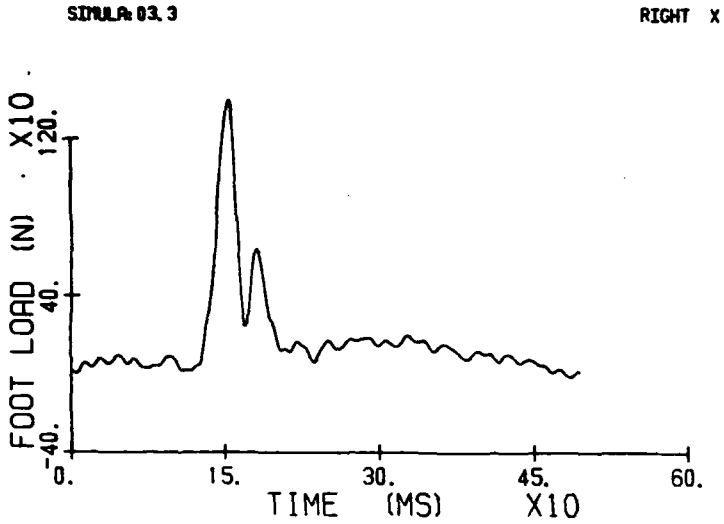

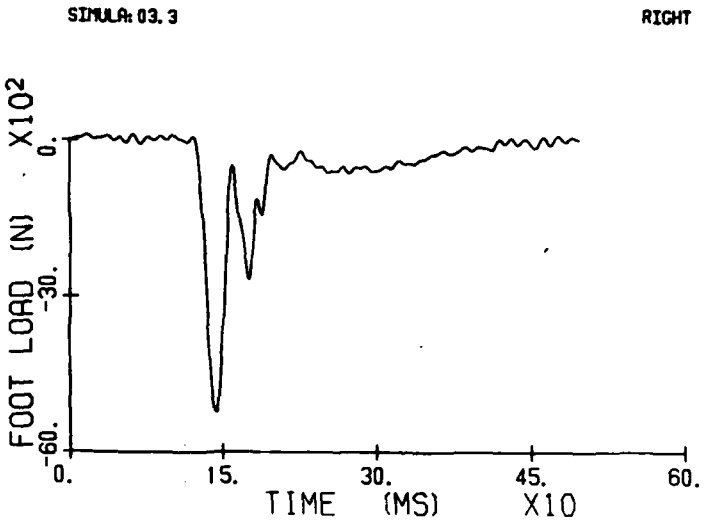

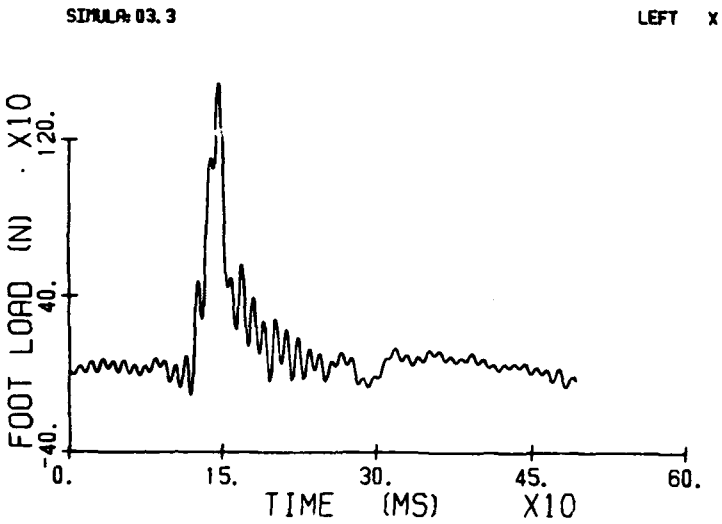

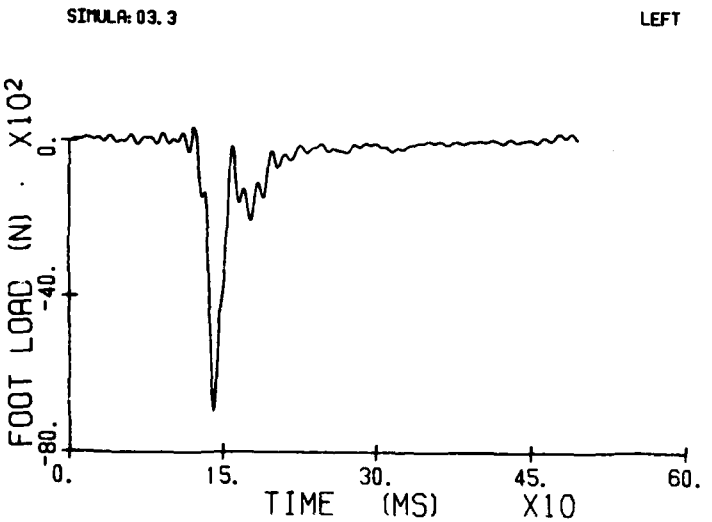

Footrest force.

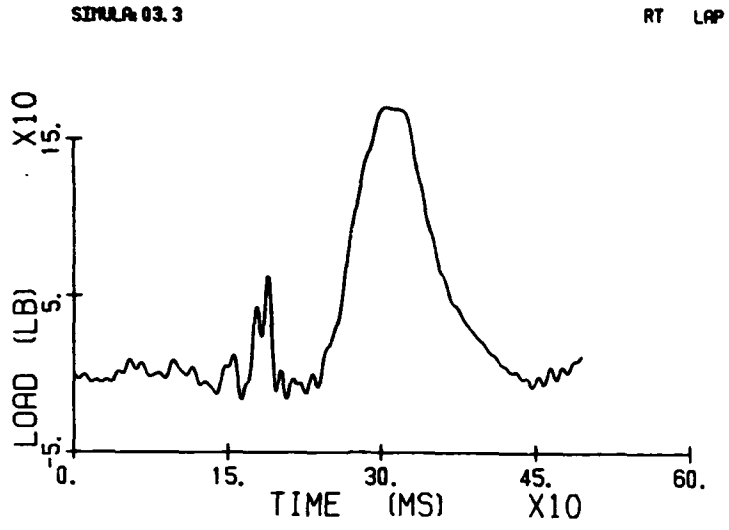

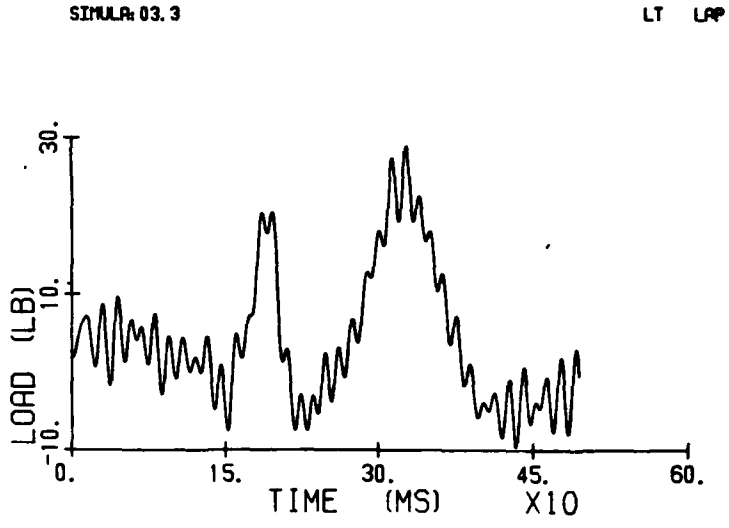

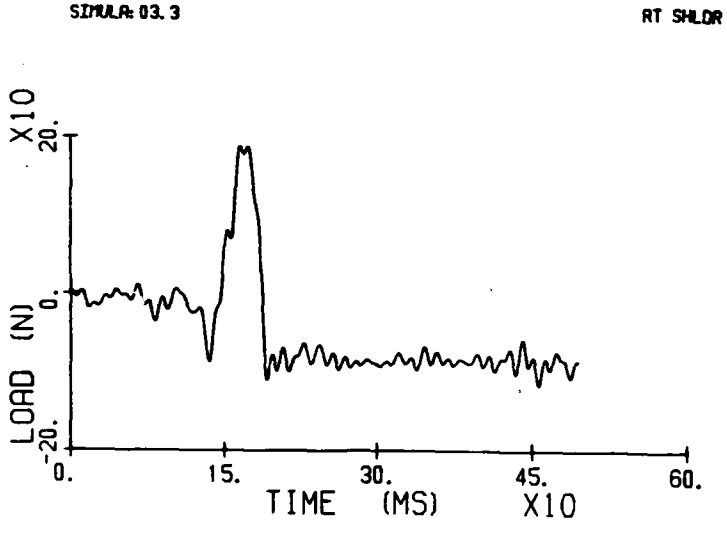

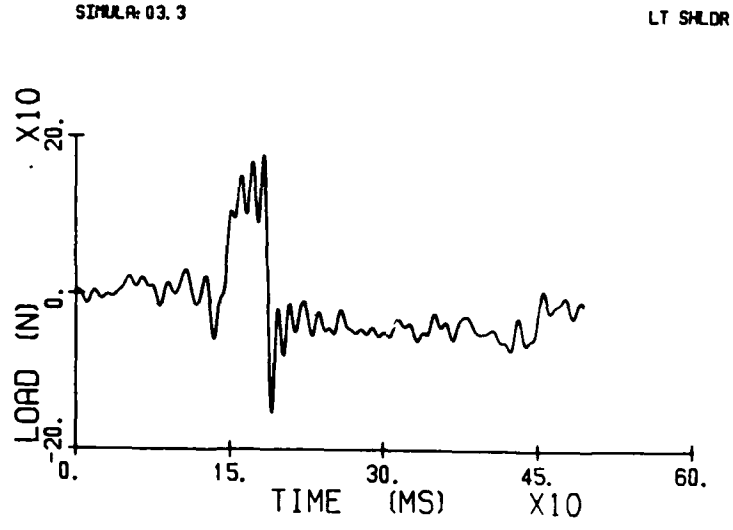

Lap and shoulder belt forces.

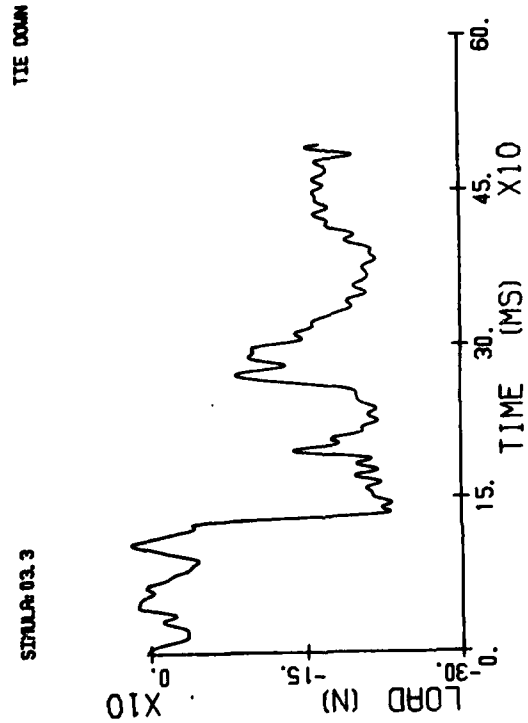

Tiedown strap.

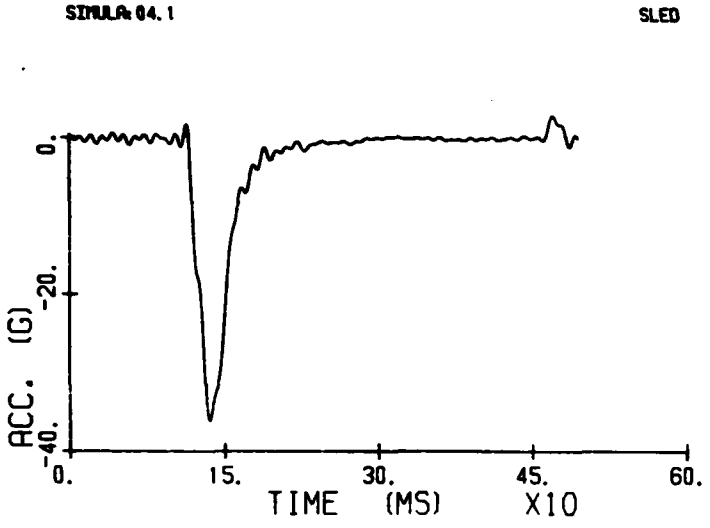

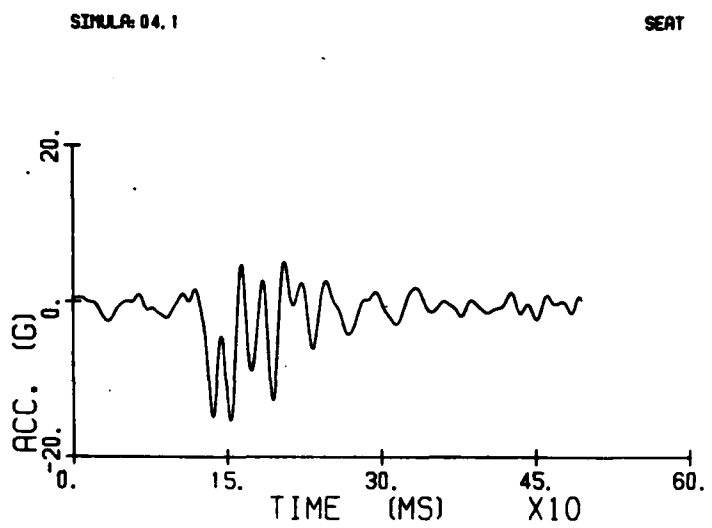

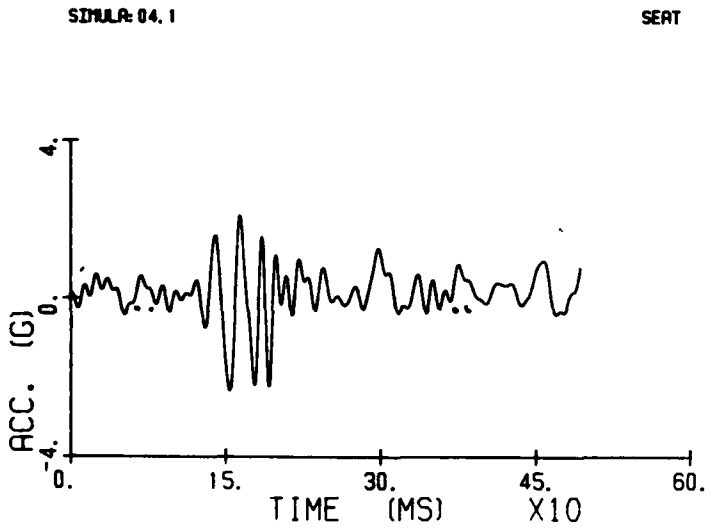

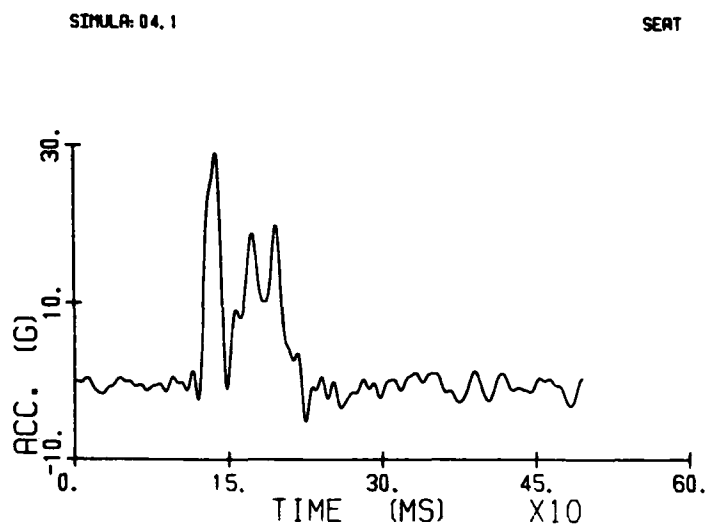

Sled and seat pan accelerations.

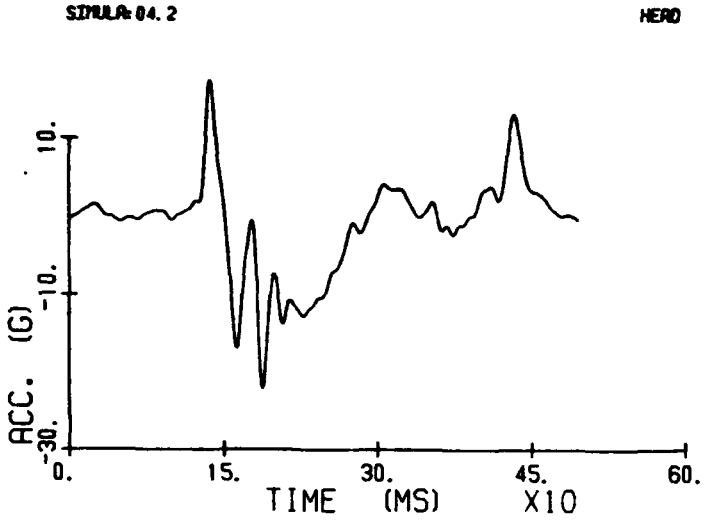

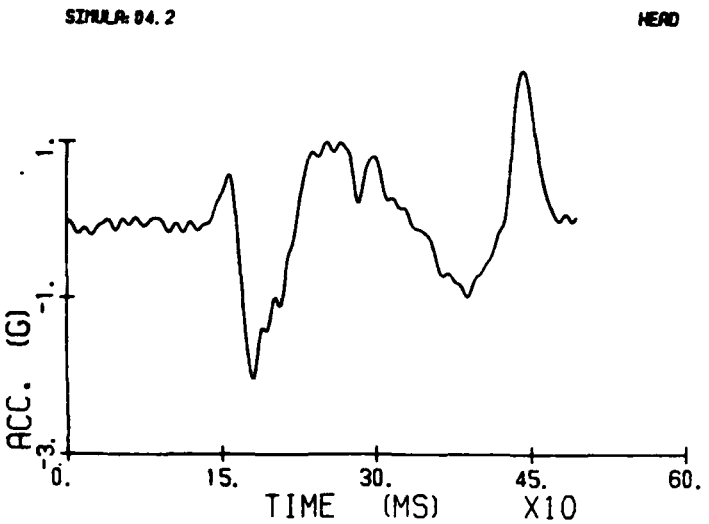

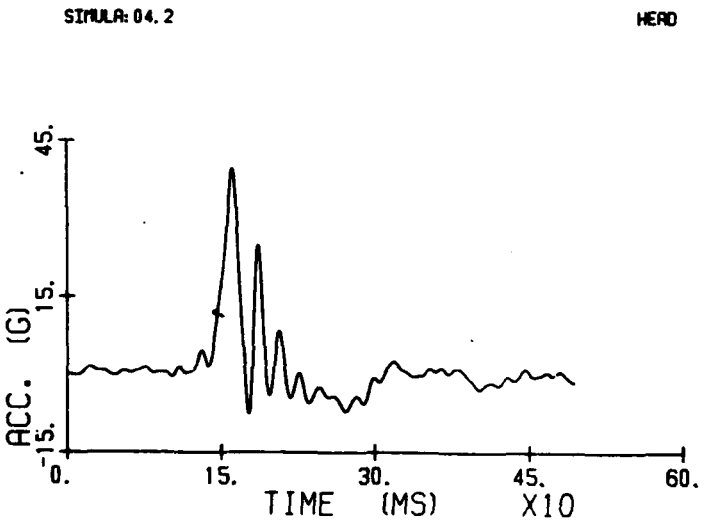

Head acceleration.

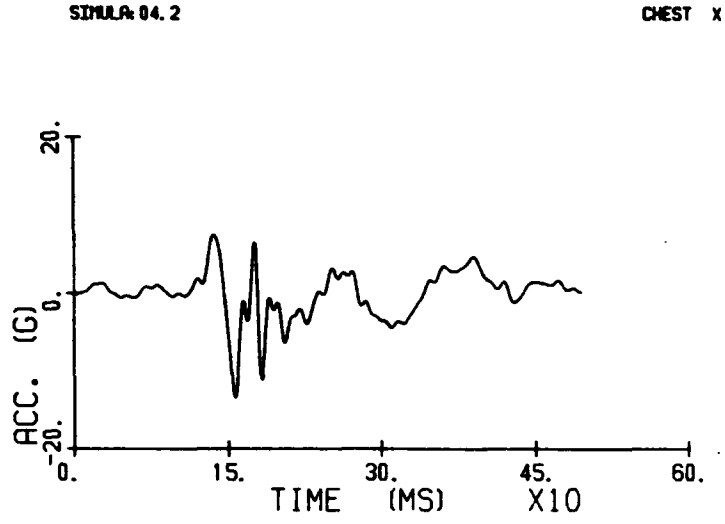

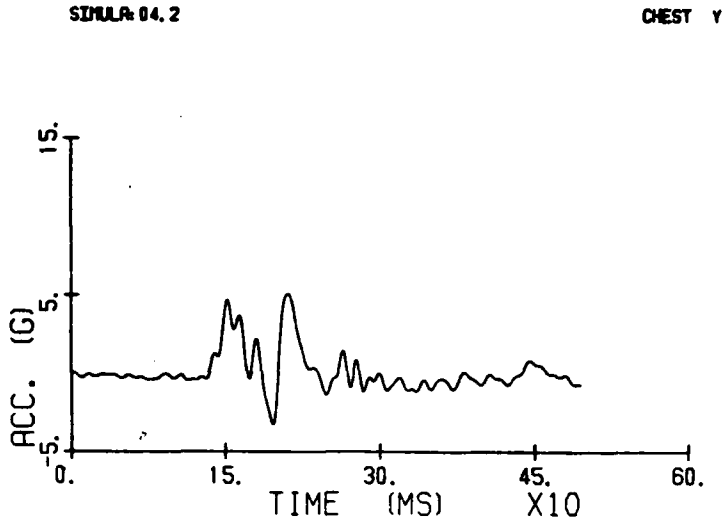

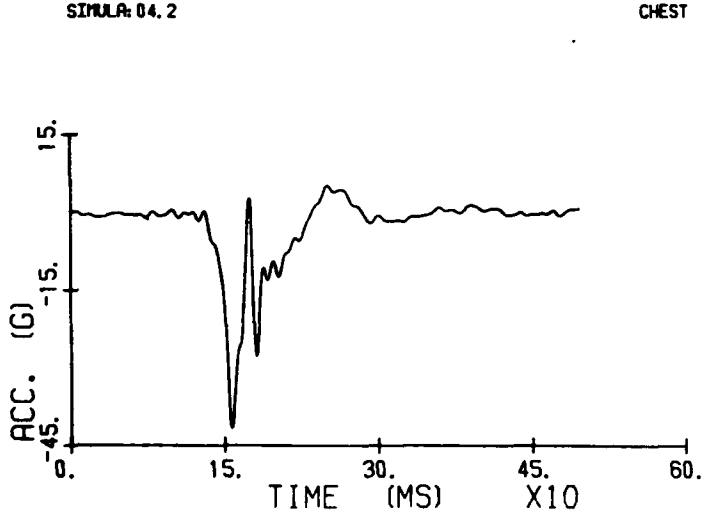

Chest acceleration.

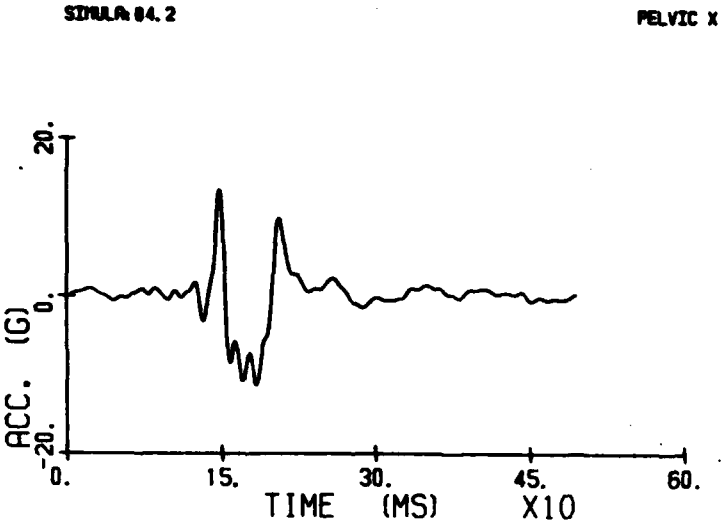

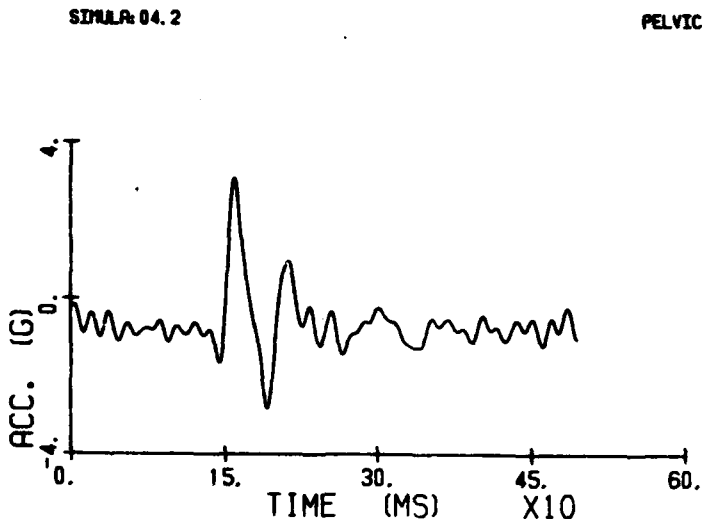

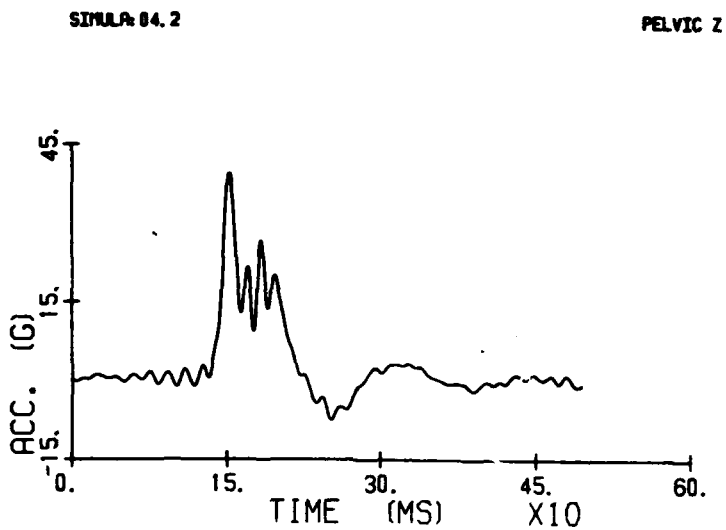

Pelvis acceleration.

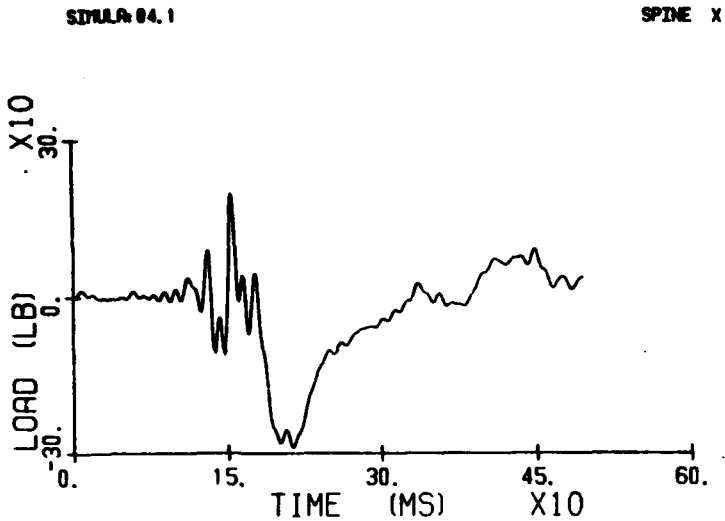

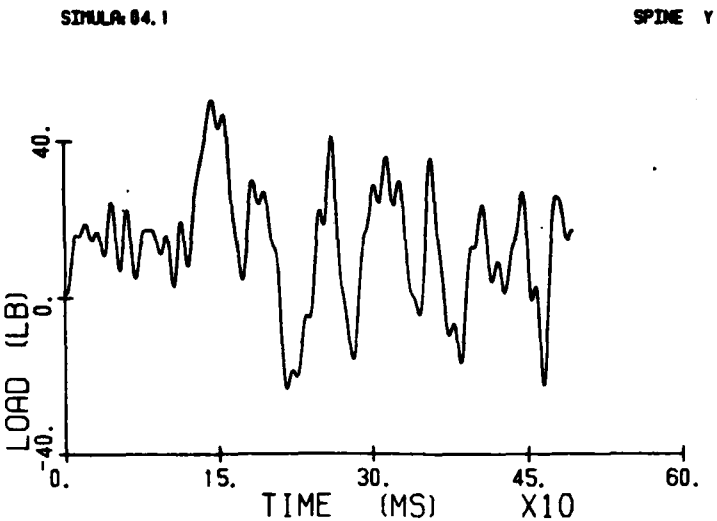

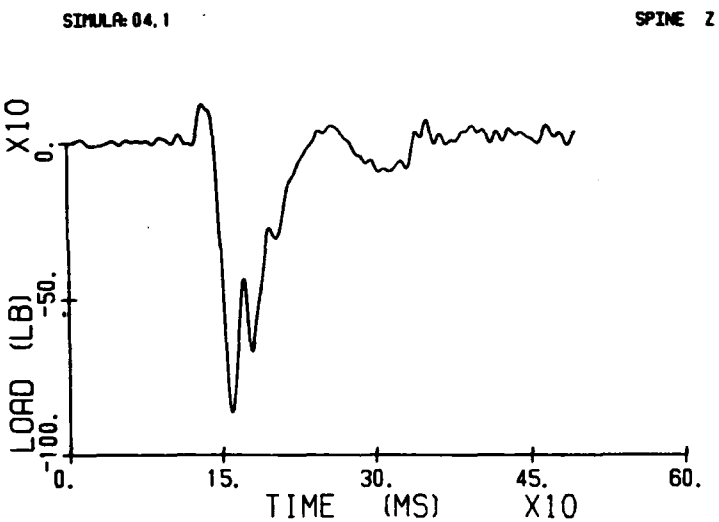

Lumbar force.

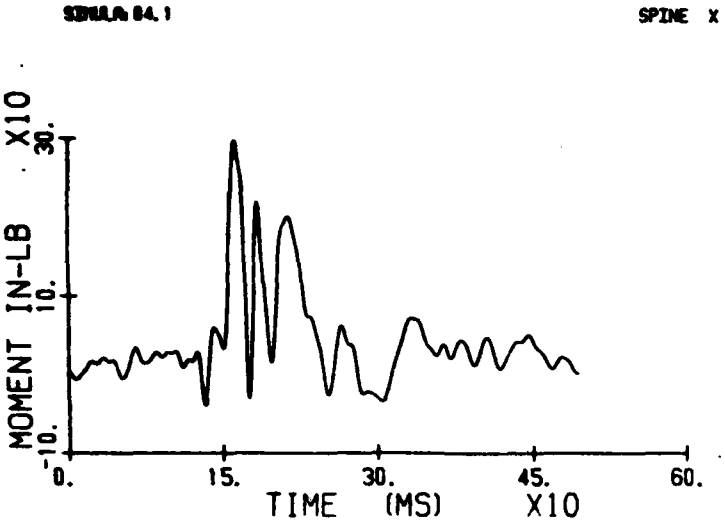

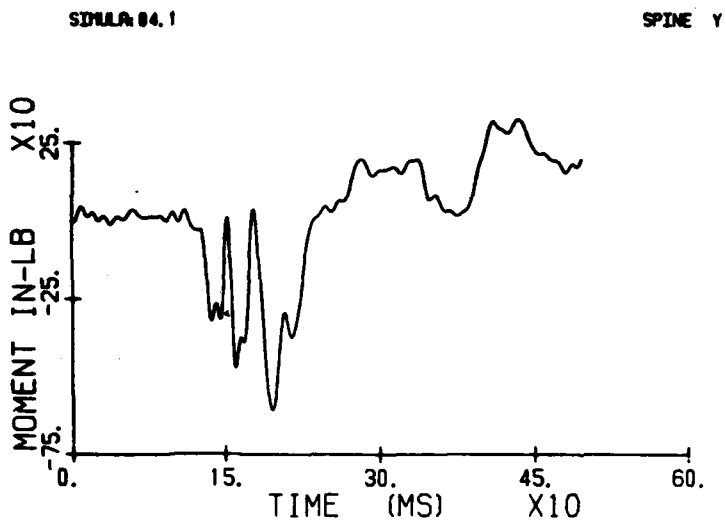

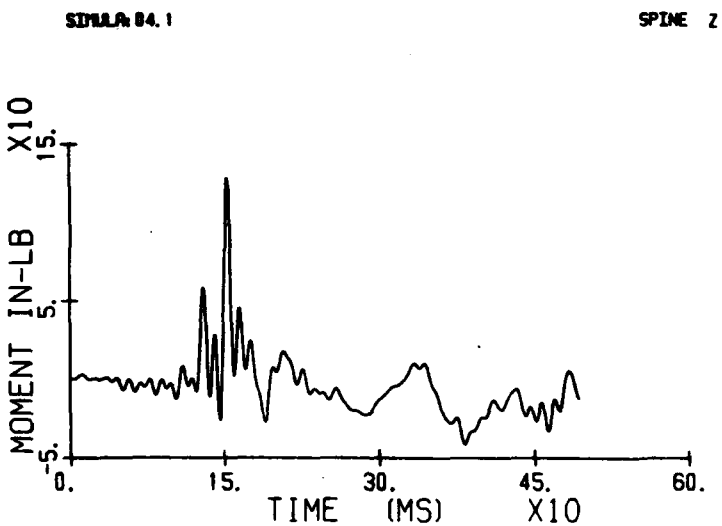

Lumbar moment.

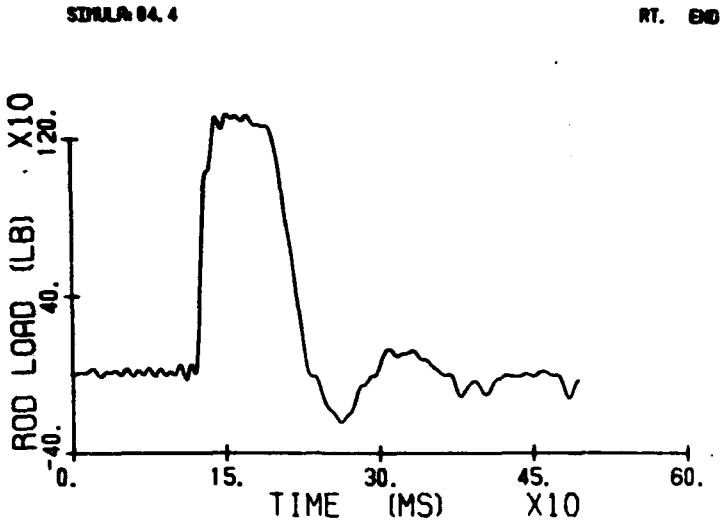

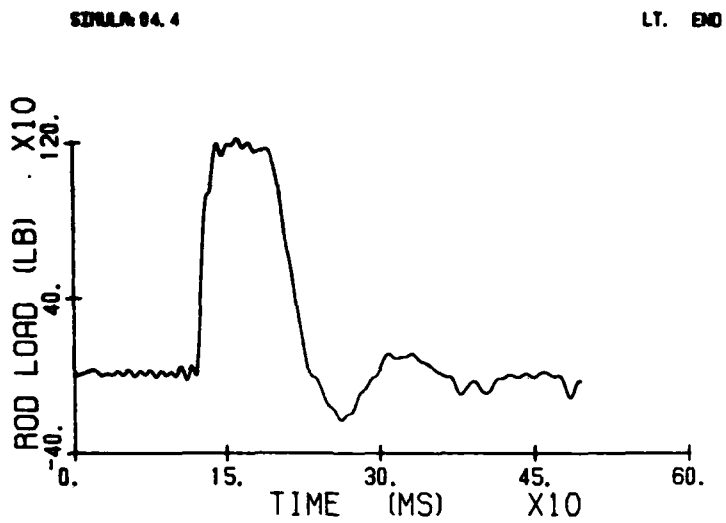

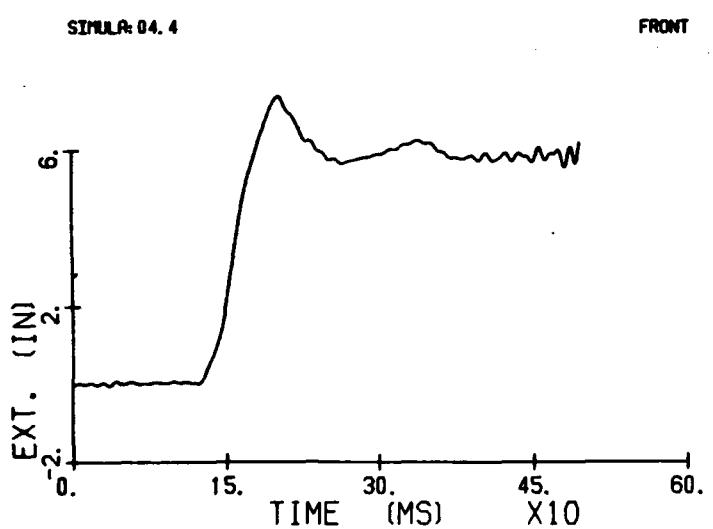

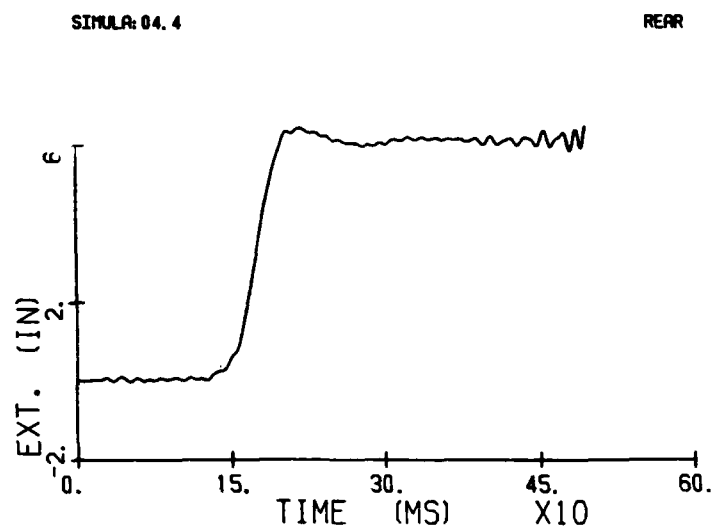

Energy absorber force and stroke.

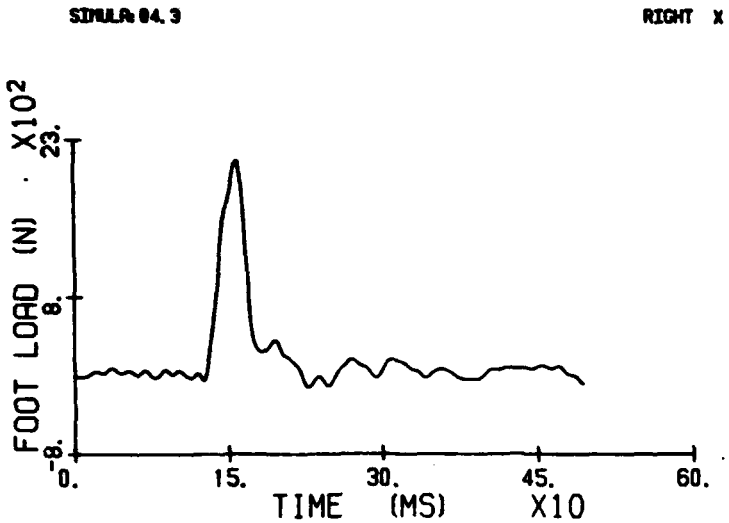

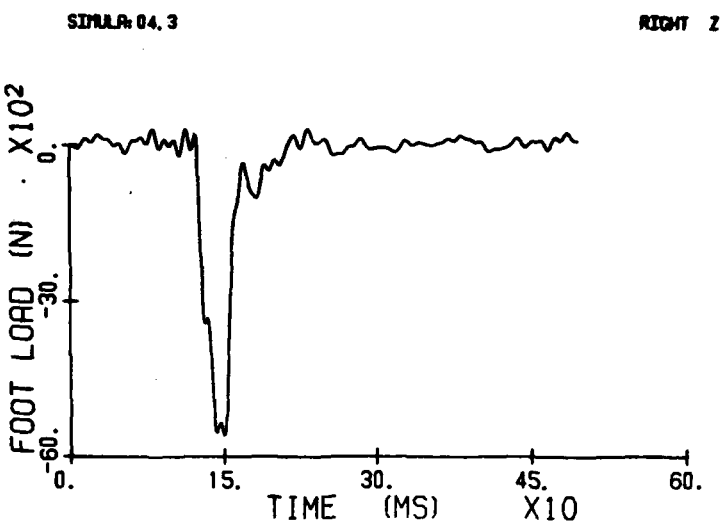

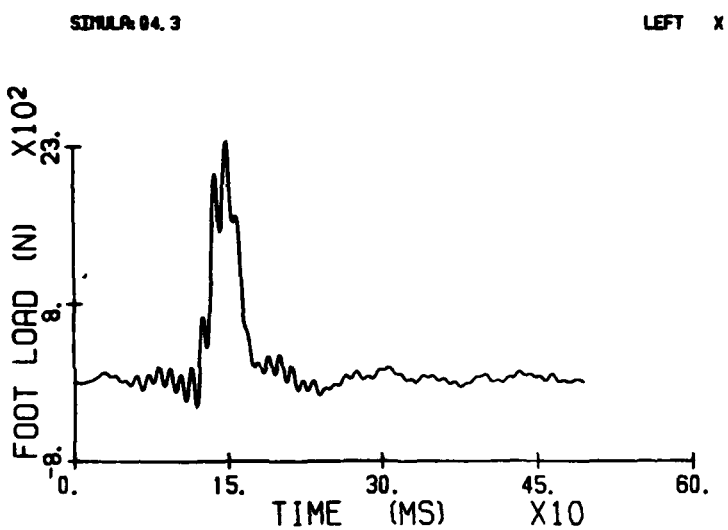

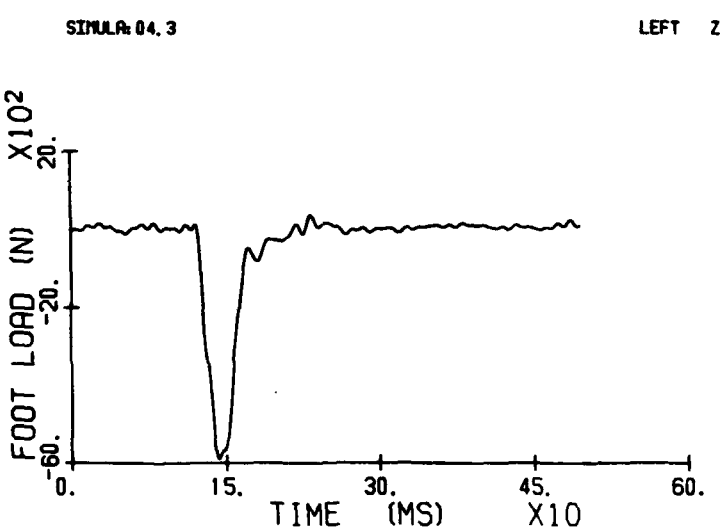

Footrest force.

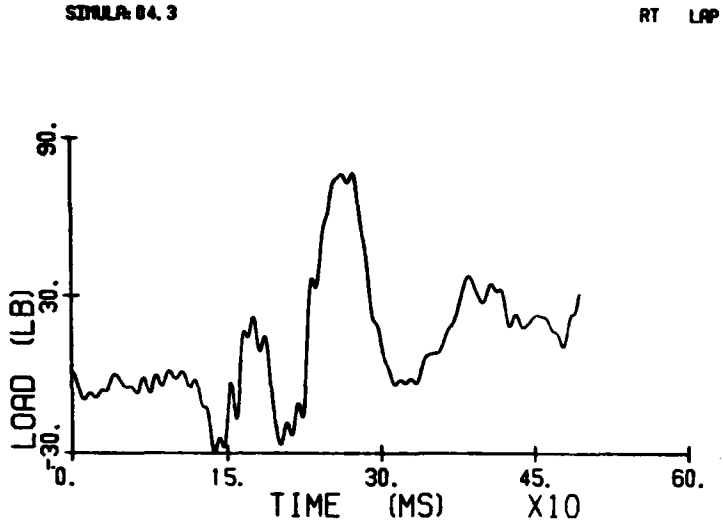

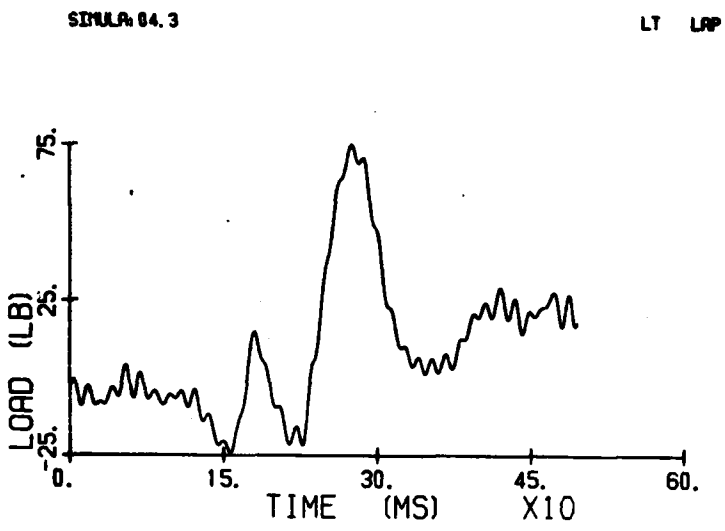

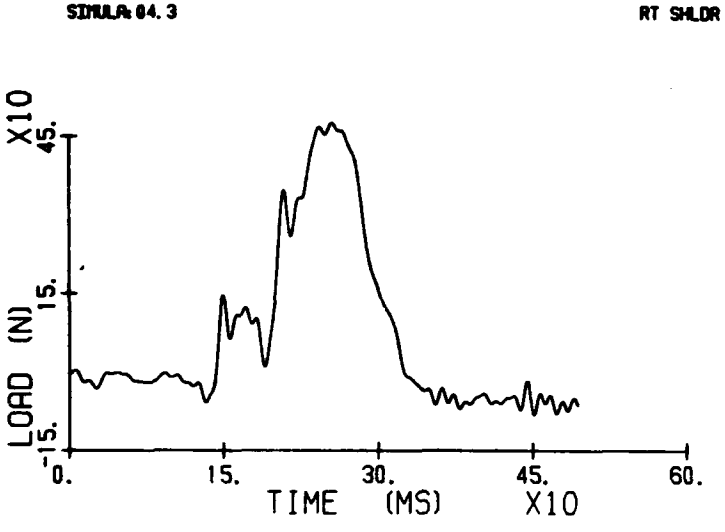

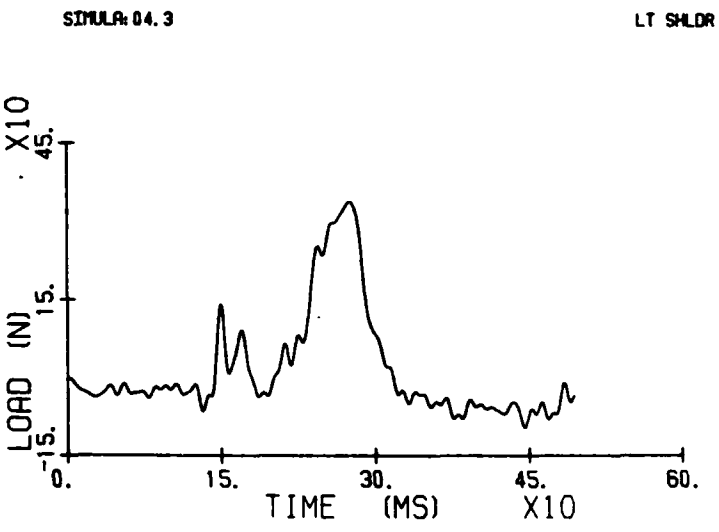

Lap and shoulder belt forces.

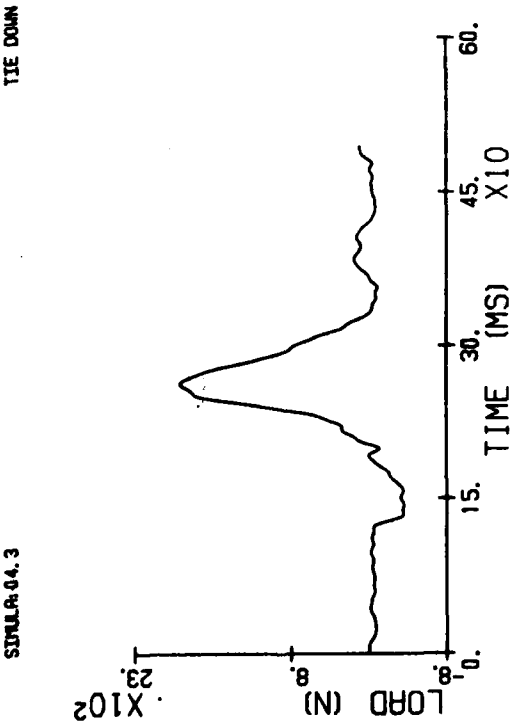

Tiedown strap.

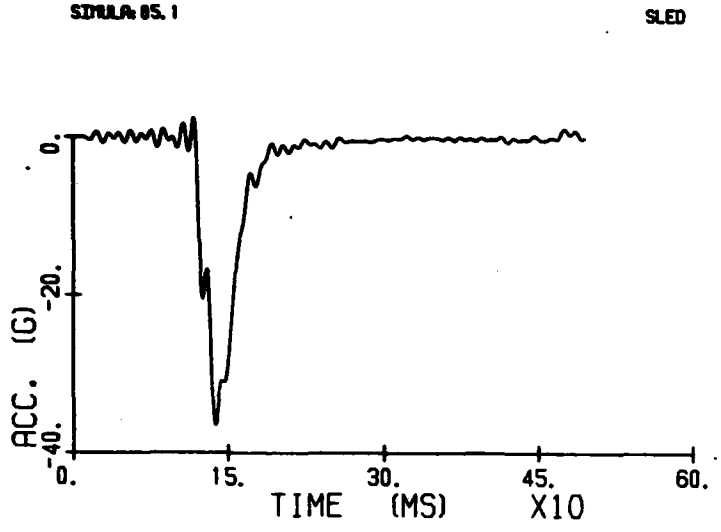

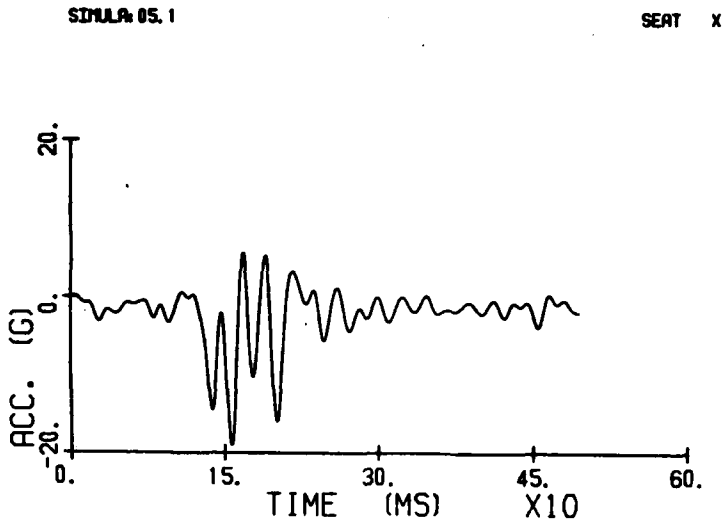

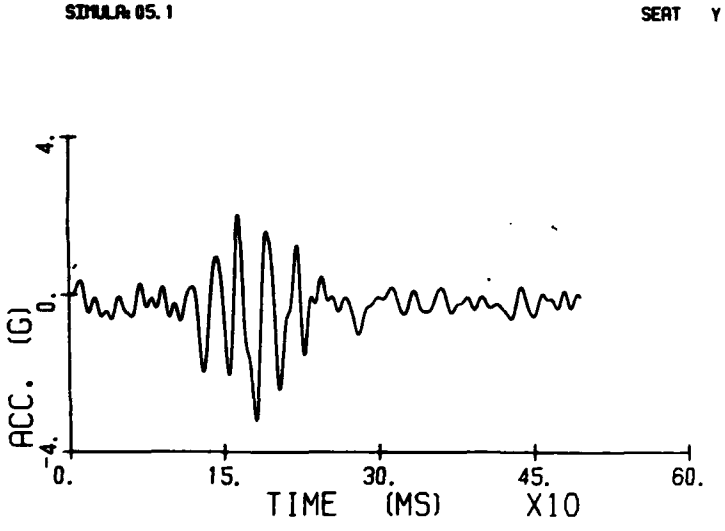

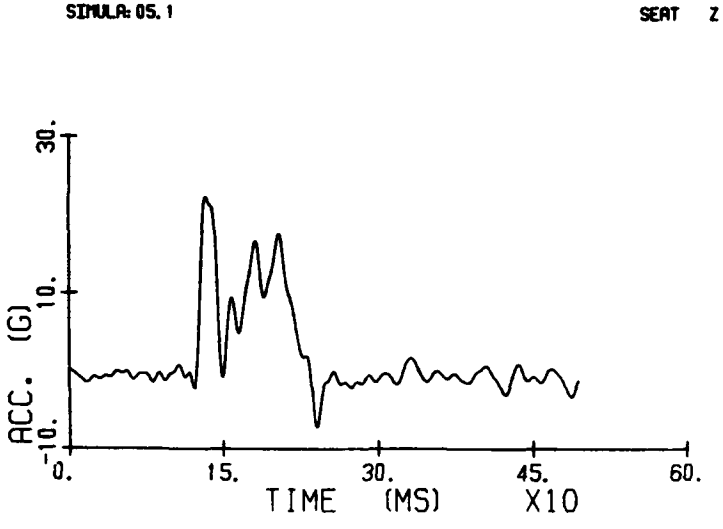

Sled and seat pan accelerations.

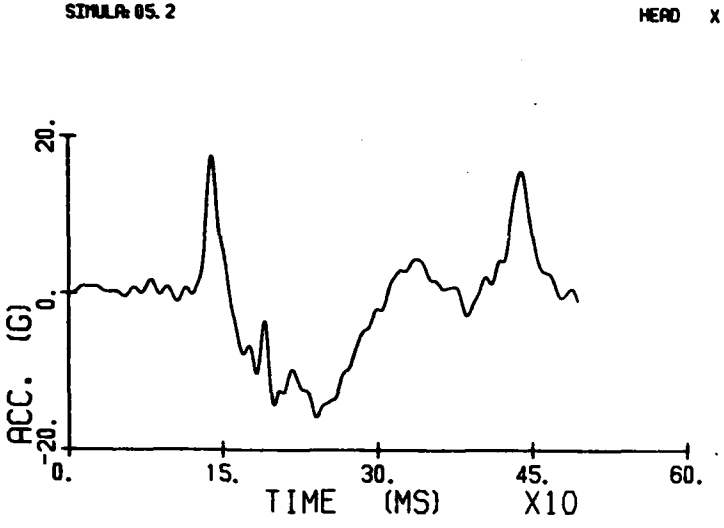

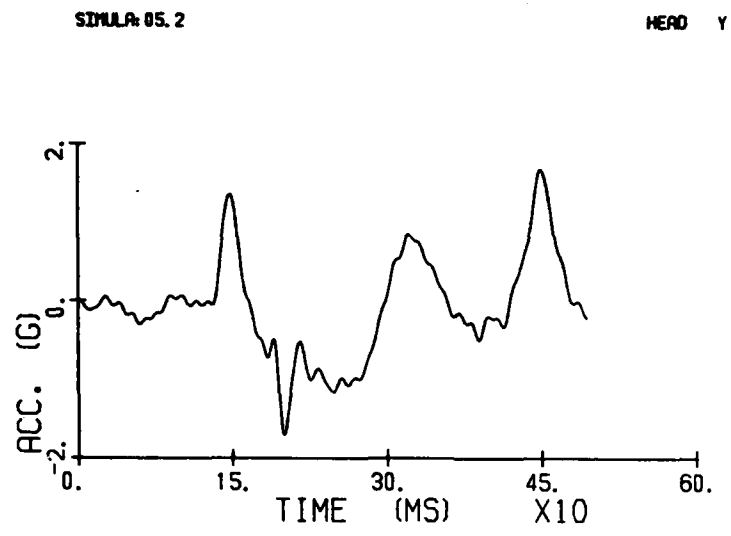

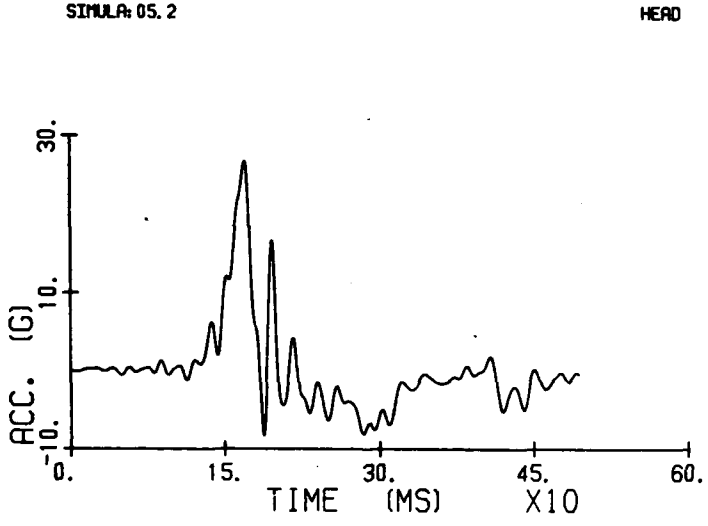

Head acceleration.

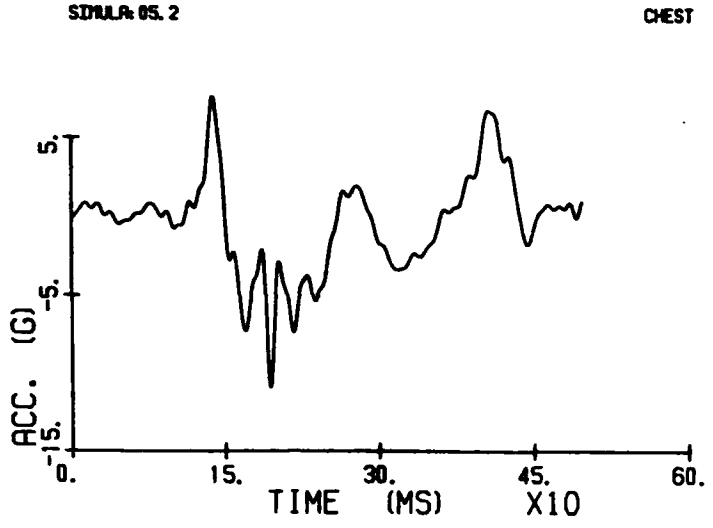

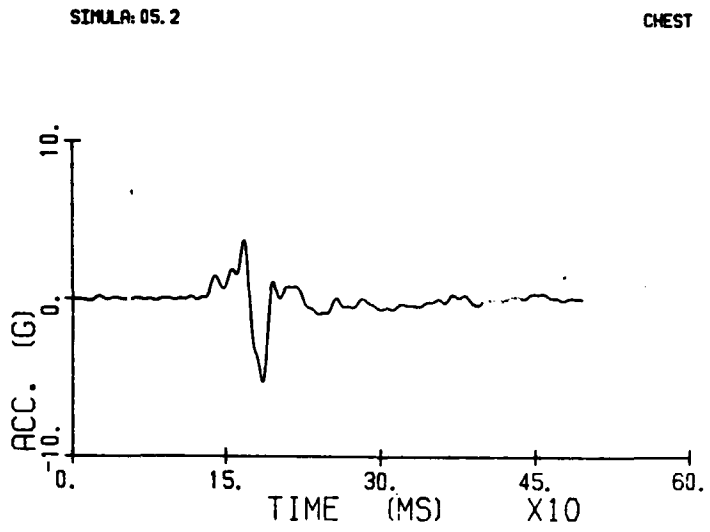

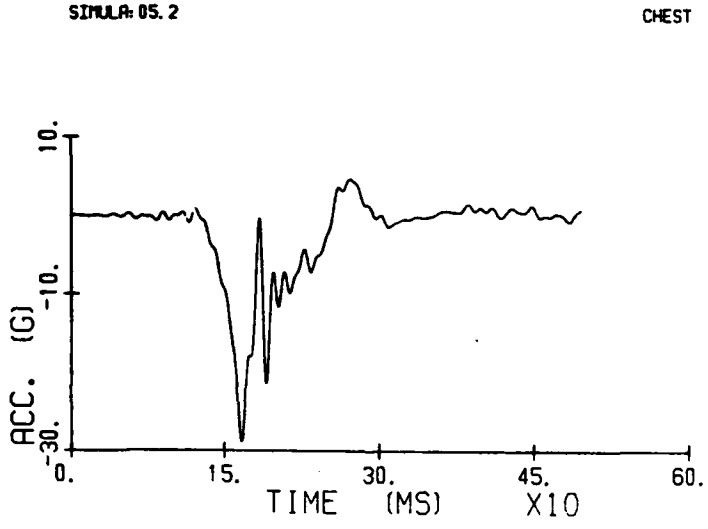

Chest acceleration.

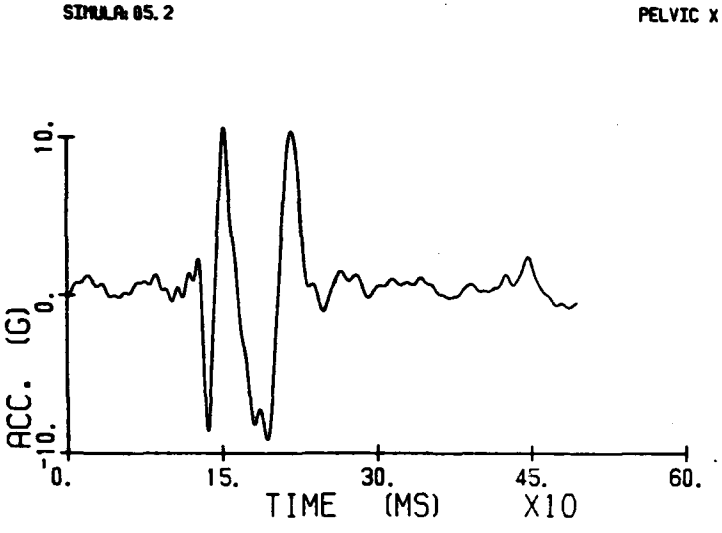

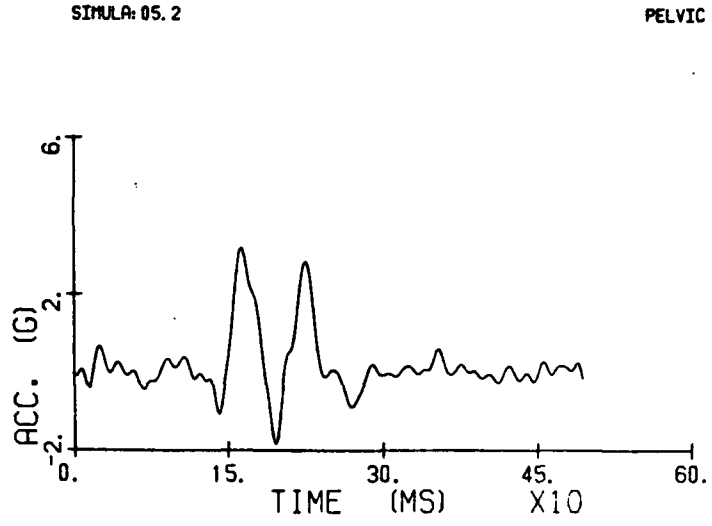

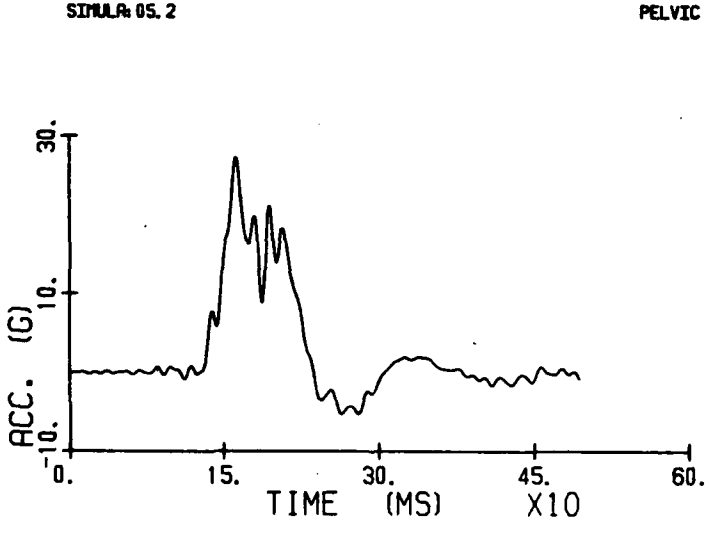

Pelvis acceleration.

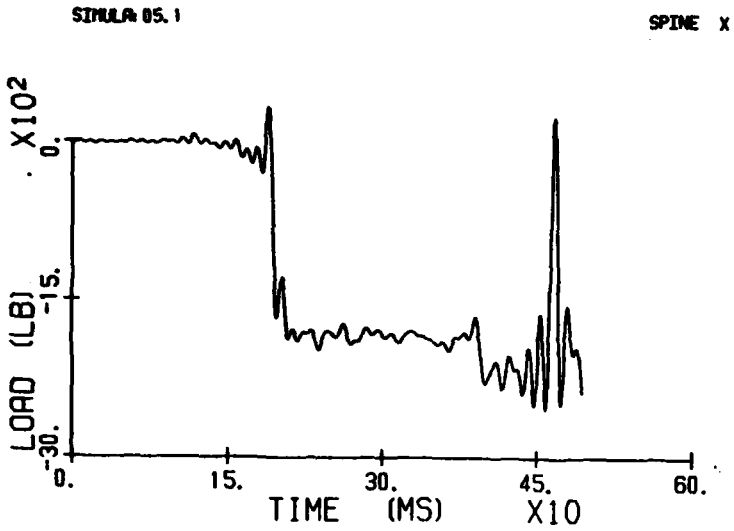

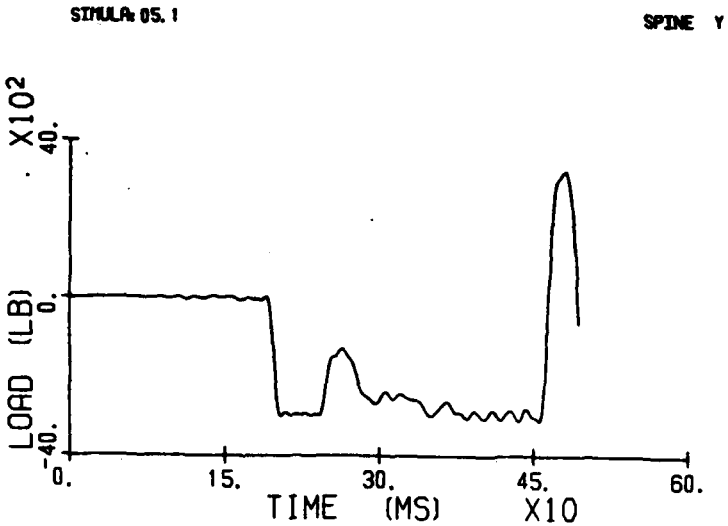

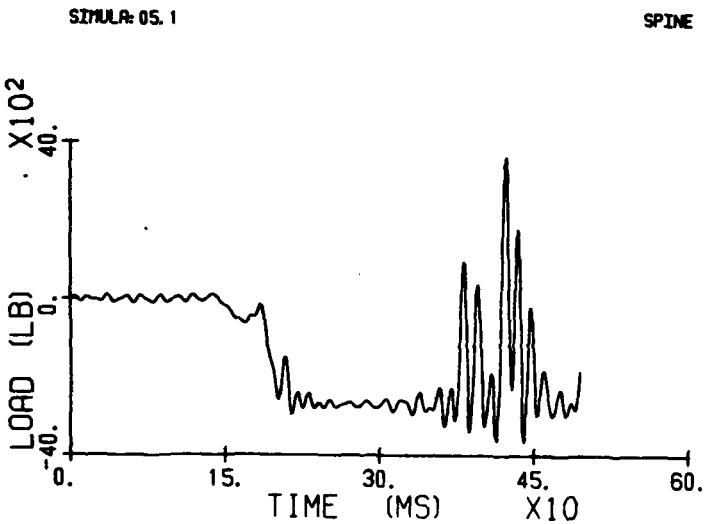

Lumbar force.

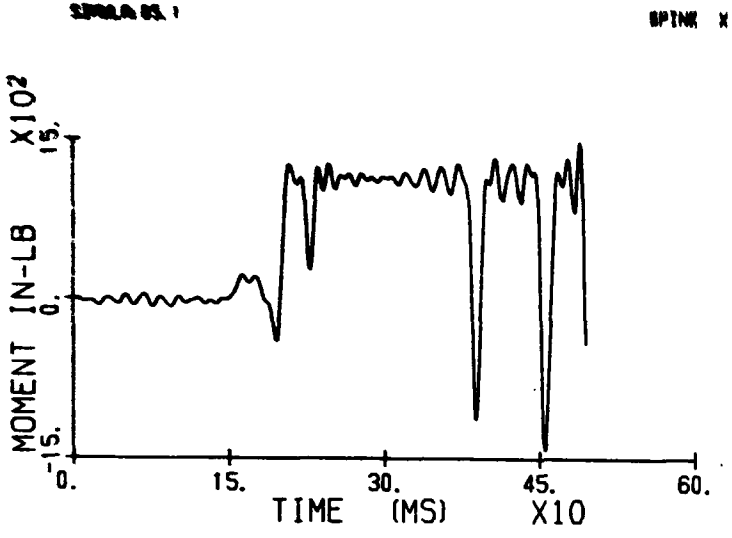

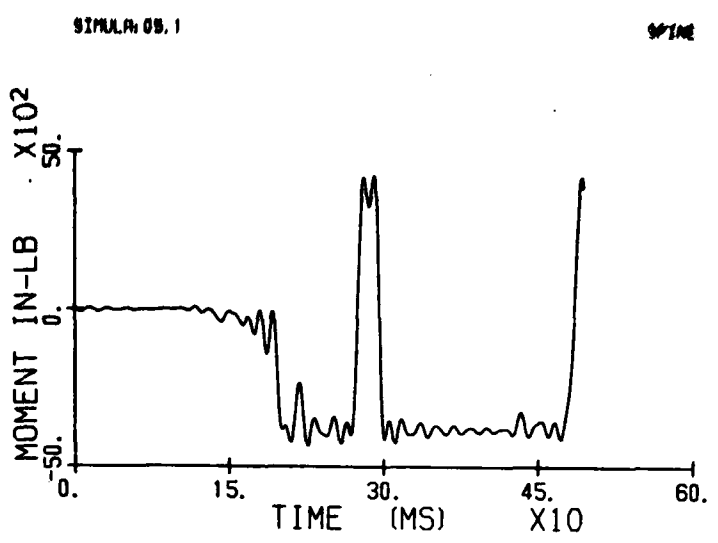

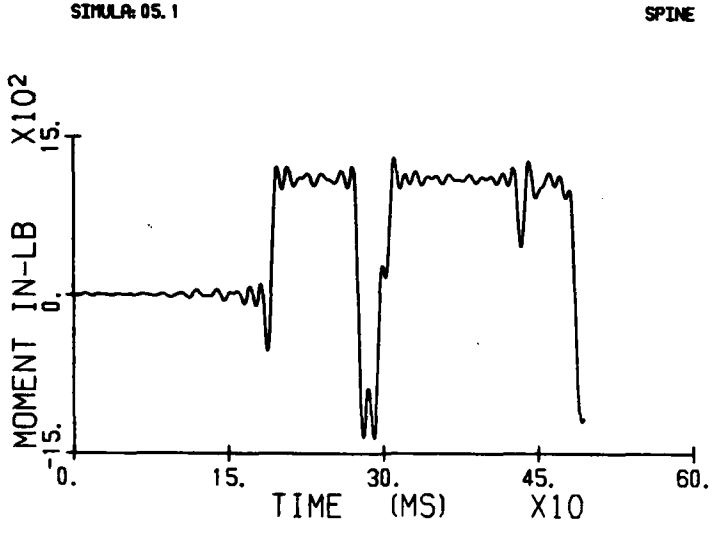

Lumbar moment.

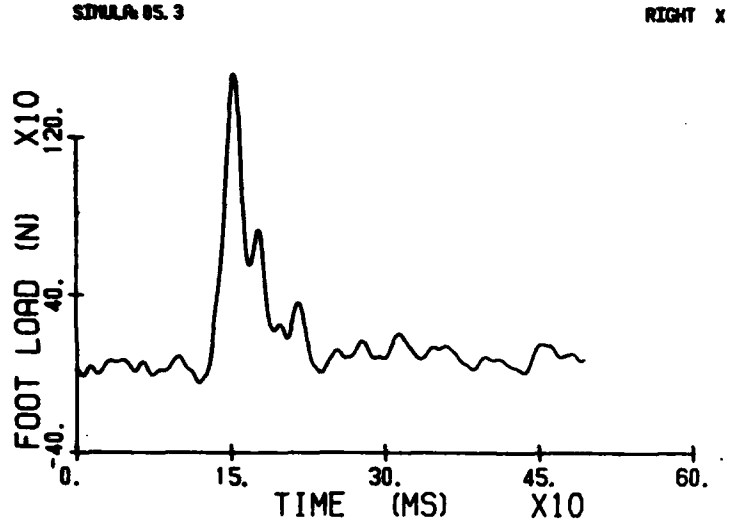

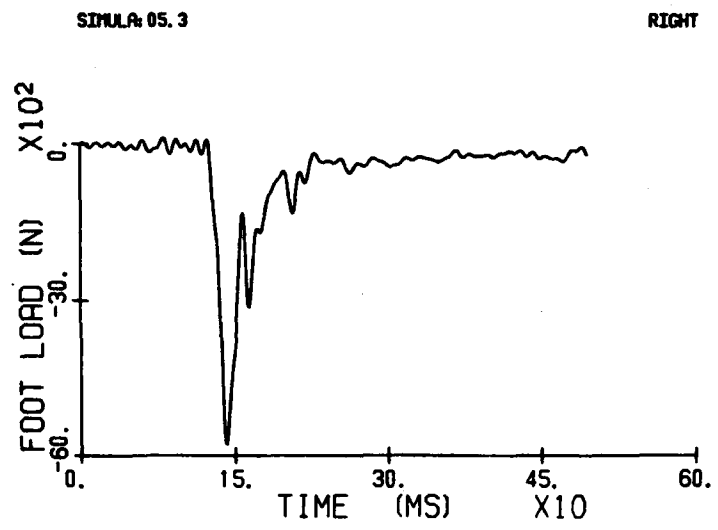

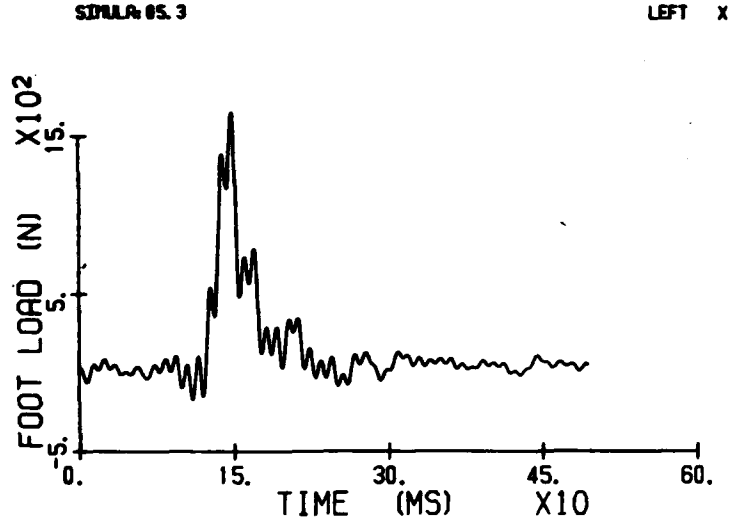

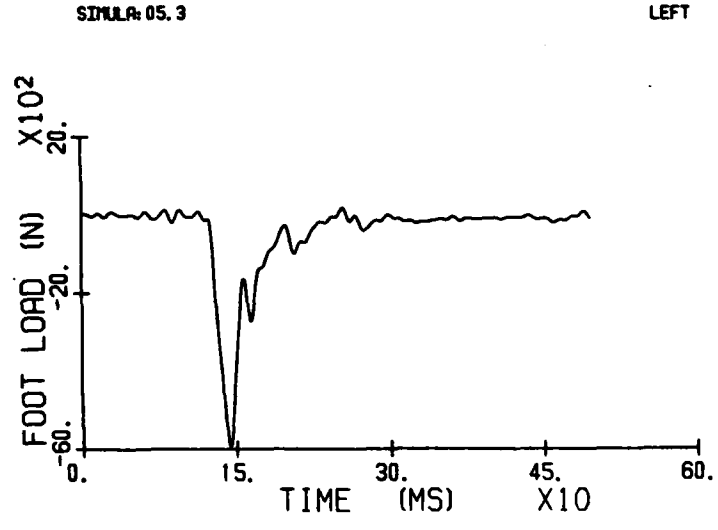

Footrest force.

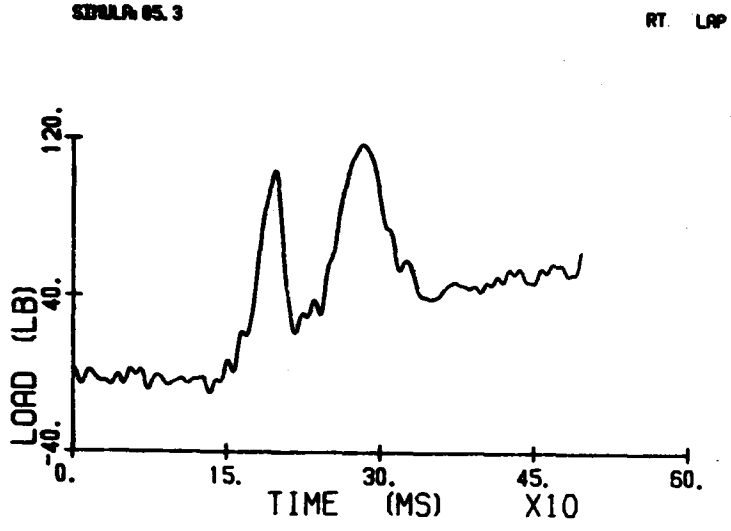

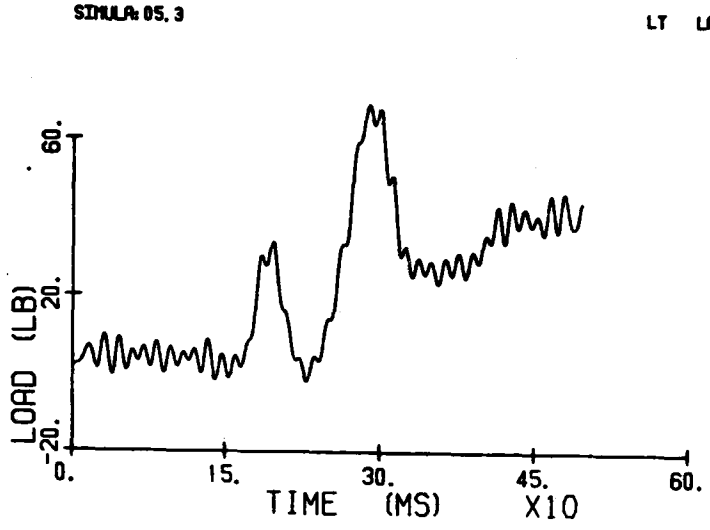

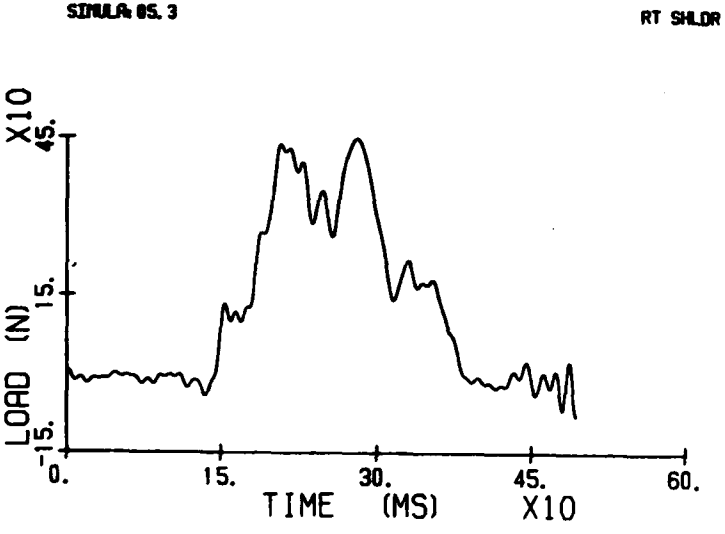

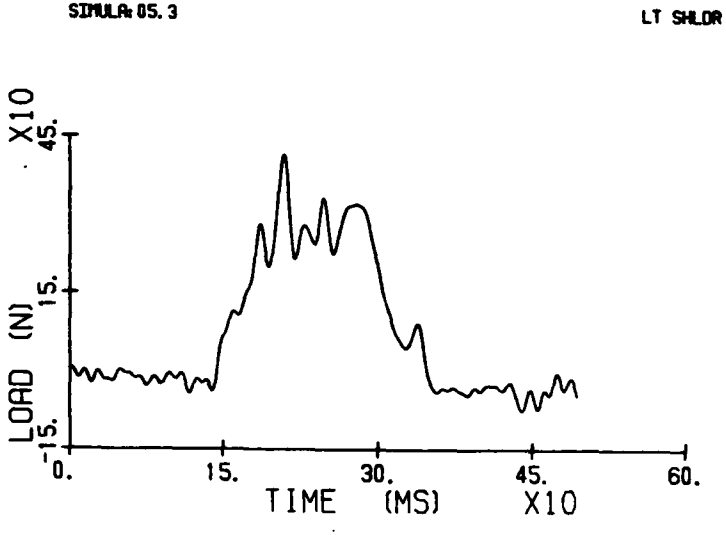

Lap and shoulder belt forces.

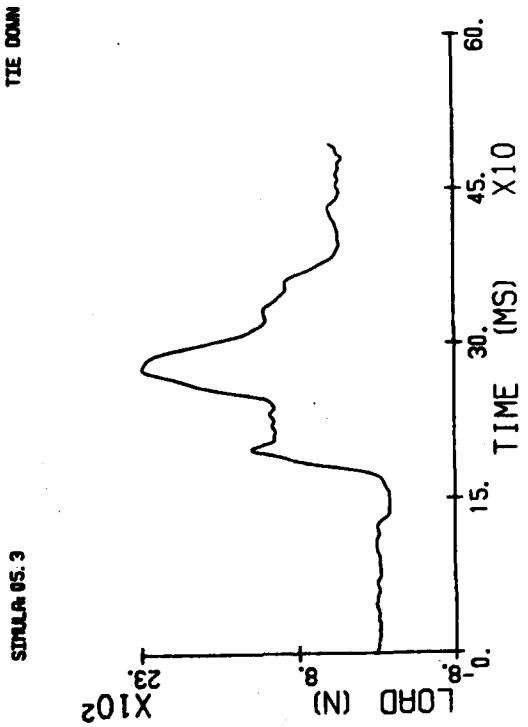

Tiedown strap.

END

FILMED

1-84

DTIC